PATHOGENIC MECHANISMS IN MULTIPLE SYSTEM ATROPHY: A STUDY OF OLIGODENDROGLIAL PATHOLOGY

Yasmine Taysir Asi

Institute of Neurology

UCL

Presented for the degree of Doctor of Philosophy

For my grandmother, Omi Lulwa, may her soul rest in peace.

إلى جدتي الغالية، أمي لولوة، الله يرحمها و يغمد روحها الجنة

Declaration

I, Yasmine Taysir Asi, confirm that the work presented in this thesis is my own. Where information has been derived from other sources, I confirm that this has been indicated in the thesis.

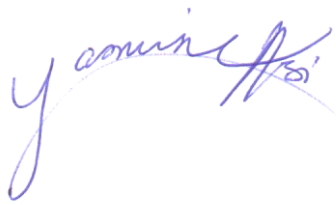

Signature

Acknowledgment

This PhD journey has been one of memorable encounters, valuable lessons, intellectual stimulation and self-discovery (or re-discovery I should say!). I would like to start off by thanking all those involved in the brain banking process – from donors and their families to the technical and administrative staff. Donating one's brain for the advancement of knowledge in neurological disorders is an act of selfless generosity and a gesture of trust and faith in the scientific community that is greatly appreciated and humbling. Joining the Queen Square Brain Bank (QSBB) for Neurological Disorders was my first encounter with the concept of brain banking and has inspired me and other neuroscience enthusiasts to establish brain banks in multiple Arab countries.

I am grateful to my supervisors – Dr. Janice Holton, Prof. Tamas Revesz and Prof. Henry Houlden – for their support and guidance throughout my PhD. I am especially grateful to Dr. Holton and Prof. Revesz for initially taking me on as a Master's student and then giving the opportunity to carry on with a PhD - I am fortunate to have been under the wing of two great neuropathologists. I will carry with me the wisdoms and knowledge gained through our various interactions – be it in private meetings, brain cut sessions, conferences and social events. Thank you again for the opportunity of joining your lab and I look forward to our paths crossing again in the future.

I am very thankful to the QSBB team for taking me in with open arms and hearts. Dr. Abi Li, Dr. Tammaryn Lashley, Catherine Strand, Christina Murray,

Dr. Sarah Pressey, Dr. Aoife Kiely, Dr. Adam Mammais, Dr. Stefen Brady, Robert Courtney, Hilary Ayling, Dr. Rina Bandopadhyay, Corinna Washbrook, Priya Gami, Linda Parsons, Susan Stoneham and Iliyana Komsiyska. I could not have asked for a better group of people to work (and party) with. Abi, thank you for always checking in on me (especially during my write up), for our culinary experiences and other adventures (what's next on the list, archery?). Tam thank you for giving me a shoulder to cry on and reassuring hugs that it will all be OK. Kate, thank you for showing us that it is just as exciting to challenge our other senses as it is our minds – looking forward to your next concoction! Christina, thank you for lending me your ear no matter how busy your schedule and for always making sure that we all have a good time. Aoife, thank you for taking a special interest in Arab culture and language. I enjoyed our tutorials and laughs and remember I am just an email away for any phrase you need! Dr. Daniah Trabzuni, I am delighted to have met a fellow Arab with similar ambitions for contributing to neuroscience research in the Middle East. I am very optimistic that our efforts to establish a brain bank in the region will be fruitful.

I am also thankful to the team at Sheffield Institute for Translational Neuroscience, especially Dr. Julie Simpson and Dr. Paul Heath, for their wonderful hospitality and assistance.

I am grateful to the Government of Kuwait for the scholarship that has allowed me to undertake both a MSc and PhD at UCL Institute of Neurology.

Last but not least – I would like to thank my family for their unwavering support. Thank you for believing in me and investing in me – it would have been impossible for me to be here without your support. I hope to make you all proud. I am also thankful, especially to my Mom, for enduring the colourful sides of my personality conjured up by this rollercoaster PhD ride! It was not always tolerable – but you hung in there.

ABSTRACTS

MSA WITH COGNITIVE IMPAIRMENT

Introduction: Multiple system atrophy (MSA) is a progressive neurodegenerative disease characterized by parkinsonism, cerebellar ataxia and autonomic dysfunction. According to the second consensus on MSA, a clinical diagnosis of MSA is excluded in the presence of cognitive impairment (CI). However, this view has been challenged by neuropsychological studies documenting CI in MSA patients and by some case studies of pathologically confirmed MSA patients reported to have CI. This study investigates the pathological substrates of CI in MSA by comparing the neuropathological profiles of MSA cases with documented CI (MSA-CI) and those with normal cognition (MSA-CN). *Methods:* Nine MSA-CI and nine MSA-CN cases were selected from the archive of the Queen Square Brain Bank (QSBB) for Neurological Disorders. Immunohistochemistry and routine histological techniques were employed to determine neuronal and glial α-synuclein pathology, Aβ deposition, tau pathology, gliosis, TDP-43 pathology and neuronal loss. These pathological changes were assessed using quantitative and semi-quantitative approaches. *Results*: No differences in the severity of neuronal or α-synuclein pathologies in any region were identified between the two MSA groups. Aβ deposits were more frequent in the CN group, while Alzheimer-type tau pathology was no greater the Braak and Braak stage II in either group. Other secondary pathologies (Lewy body, cerebral amyloid angiopathy, TDP-43 and small vessel disease) were

uncommon in this cohort. *Conclusions*: Brain regions important for cognition did not show more severe neuronal loss, α-synuclein pathology, Alzheimer or other secondary pathologies in MSA-CI as compared with MSA-CN. These findings indicate that CI is an inherent feature of MSA and is not due to concomitant pathologies or the load or distribution of α-synuclein pathology. Furthermore, the synergism displayed between α-synuclein, tau and Aβ in Parkinson's disease is not apparent in MSA. Further explorations into other substrates such as synaptic pathology, neurotransmitter abnormalities and subcortical deafferentation may have an impact on CI in MSA.

LONG DURATION AND MINIMAL CHANGE MSA

Introduction: Multiple system atrophy (MSA) is a progressive neurodegenerative disease characterized by parkinsonism, cerebellar ataxia and autonomic dysfunction. Widespread α-synuclein positive glial cytoplasmic inclusions (GCIs) found in oligodendrocytes and neuronal loss are two pathological features of MSA. The mean disease duration of MSA is 6-9 years, however, there are some patients that experience a longer disease course. Long duration (LD) and minimal change (MC) MSA are two unusual subtypes of the disease. LD-MSA exhibits a disease duration 15 years or longer, while in MC-MSA neuronal loss is largely restricted to the substantia nigra and locus coeruleus. The clinico-pathological profiles of these subgroups are explored in this study. *Methods***:** Immunohistochemical and routine histological staining were performed on tissue from LD-MSA (n=4), MC-MSA (n=6) and control (n=8) MSA cases. Neuronal loss, GCIs, neuronal cytoplasmic inclusions (NCIs) and gliosis were semi-quantitatively assessed in addition to investigation of concomitant pathologies. A review of the clinical records was also performed. *Results***:** GCI and NCI burden in LD-MSA was greater in the caudate compared to control MSA cases ($p \leq 0.002$). No statistical difference in GCI load was found between MC-MSA and control MSA in any region despite increased numbers of NCIs in the caudate and substantia nigra ($p \leq 0.002$). Regional neuronal loss was not statistically different between LD-MSA and control MSA cases and was not evident in the cortical and limbic regions of any of the three groups. *Conclusions***:** All cases showed typical neuropathological changes of MSA with widespread pathology in cortical, limbic, striatonigral and olivopontocerebellar regions. LD-

MSA may represent a benign disease variant with slower accumulation of GCIs and no increase in neuronal loss compared to control MSA. In contrast, MC-MSA may be a more aggressive form of the disease with a similar GCI load to control MSA despite the shorter disease duration. Delayed onset of autonomic dysfunction appears to be associated with the favourable clinical outcome in these cases. Further investigation of pathology in nuclei and connections associated with the autonomic system is warranted to determine their significance on clinical outcome.

GCIS IN THE OLIGODENDROGLIAL LINEAGE

Introduction: Glial cytoplasmic inclusion (GCI) in oligodendrocytes is the pathological hallmark of MSA. GCIs are composed of many proteins but with α-synuclein as the main constituent. GCIs are widespread in multiple brain regions and are hypothesized to play a primary role in the pathogenesis of MSA. Although GCIs have been determined to accumulate in oligodendrocytes, detailed characterization of their accumulation in different cells of the oligodendrocyte lineage has not been established. This study investigates the occurrence of GCIs in oligodendrocyte precursor cells ($NG2^+$ cells), premyelinating ($CNPase^-/MBP^+$) and mature myelinating ($CNPase^+/MBP^+$) oligodendrocytes in MSA. *Methods*: Double and triple immunofluorescence using anti-α-synuclein, NG2, CNPase and MBP antibodies were carried out on 8μm thick frozen sections from the posterior frontal cortex and cerebellum of 3 MSA cases. Qualitative analysis was conducted by systematically scanning the entire section for evidence of co-localisation using widefield and confocal fluorescence microscopy. *Results*: α-Synuclein accumulates in $CNPase^+/MBP^+$ cells but not in $NG2^+$ cells. $CNPase^-/MBP^+$ cells were unidentifiable in this cohort. *Conclusions*: GCIs occur within mature myelinating oligodendrocytes while oligodendrocyte precursor cells or immature oligodendrocytes are unaffected by α-synuclein pathology. These findings raise the possibility of interaction of α-synuclein with myelin and microtubules, rendering mature oligodendrocytes more susceptible to GCI formation than $NG2^+$ cells.

REGIONAL AND CELLULAR EXPRESSION OF *SNCA* IN MSA

Introduction: The pathological hallmark of MSA is the glial cytoplasmic inclusion (GCI) found in oligodendrocytes and composed of many proteins, but with α-synuclein as the main constituent. The mechanisms by which α-synuclein accumulates in oligodendrocytes as GCIs have not been established, but are crucial to understanding the molecular pathology of the disease. The aim of this study is to investigate alterations in regional and cellular *SNCA* mRNA expression in MSA as a possible substrate for GCI formation. *Methods*: Quantitative reverse transcription polymerase chain reaction (qPCR) was performed on post-mortem brain samples from 15 MSA, 5 PD and 5 control cases to investigate regional expression in the frontal region, occipital regions, dorsal putamen, pontine base and cerebellar white matter. For cellular expression analysis, neurons from the putamen and oligodendrocytes from the cerebellum were isolated by laser capture microdissection from 5 MSA and 5 control cases. *Results*: *SNCA* mRNA expression was not significantly different between the MSA, PD and control cases in all regions (multilevel statistical model, $p=0.14$). After adjusting for group effect, the highest expression was found in the occipital grey matter while the lowest was in the putamen (multilevel statistical model, $p<0.0001$). At the cellular level, both oligodendrocytes and neurons expressed *SNCA* mRNA. MSA oligodendrocytes expressed more *SNCA* than control oligodendrocytes and expression in MSA neurons was slightly lower than that in controls, however, these results did not reach statistical significance. *Conclusions*: There are regional variations in *SNCA* expression as it is higher in cortical than subcortical regions. Furthermore, *SNCA* mRNA expression was detected in

oligodendrocytes of control and MSA cases, with greater expression in MSA. This suggests that *SNCA* mRNA overexpression may be a possible mechanism for GCI formation.

THE ROLE OF EXTRACELLULAR ALPHA-SYNUCLEIN IN GCI FORMATION

Introduction: The pathological hallmark of MSA is the glial cytoplasmic inclusion (GCI) found in oligodendrocytes and composed of many proteins, but with α-synuclein as the main constituent. The mechanisms by which α-synuclein accumulates in oligodendrocytes as GCIs have not been established, but are crucial to understanding the molecular pathology of the disease. The aim of this study is to investigate internalization of extracellular α-synuclein by oligodendrocytes as a possible mechanism for GCI formation. *Methods*: C57BL/6JOlaHsd mice (Harlan, Bicester, UK) between 2-4 months of age were anesthetized using isoflurane. The mice were placed on the stereotaxic frame and injected in one hemisphere with MSA, PD, or control human brain lysates (5μg total protein). One set was sacrificed after 4 days post inoculation (dpi) and another after 30 dpi and the brains removed, fixed and processed. A total of six mice were injected for each lysate and time point. After serially sectioning the brain blocks (8μm), α-synuclein immunohistochemistry was performed. *Results*: The entire mouse brain was sectioned (~120 sections) and a battery of α-synuclein antibodies was tested on tissue sections at 40μm intervals. α-Synuclein positive staining was undetectable in neurons or glial cells in all sections and levels of the mouse brain inoculated with MSA, PD or control lysate. *Conclusions*: The *in vivo* model of this study was unsuccessful in determining internalization of extracellular α-synuclein by oligodendrocytes. The study needs to be taken forward by inoculating wild-type mice that express α-synuclein and transgenic mice with human MSA brain homogenate to look for evidence of α-synuclein uptake by oligodendrocytes. Also, other pathological changes such as myelin loss,

axonal damage, neuronal loss and gliosis may also be examined to determine if any correlations exist with α-synuclein pathology load and progression with time.

TABLE OF CONTENTS

LIST OF FIGURES

LIST OF TABLES

ABBREVIATIONS

αsyn	α-synuclein
ABA	Allen Brain Atlas
Aβ	B-Amyloid
ADL	Activities of daily living
B2M	Beta-2-microglobulin
CAA	Cerebral amyloid angiopathy
CBD	Corticobasal degeneration
CERAD	The Consortium to Establish a Registry for Alzheimer's disease
CI	Cognitive impairment
CN	Cognitively normal
CNPase	2',3'-Cyclic nucleotide-3'-phosphohydrolase
CNS	Central nervous system
CSPα	Cysteine string protein α
DevHBA	Developing Human Brain Atlas
DLB	dementia with Lewy bodies
EAE	Experimental allergic encephalomyelitis
EGFP	Enhanced green fluorescent protein
FFPE	Formalin – fixed paraffin embedded
GAPDH	Glyceraldehyde-3-phosphate dehydrogenase
GC	Galactocerebroside
GCI	Glial cytoplasmic inclusion
GFAP	Glial fibrillary acidic protein

GNI	Glial nuclear inclusions
HBA	Human Brain Atlas
ICC	Intrarater correlation coefficient
LD	Long duration
LCM	Laser capture microdissection
MBP	Myelin basic protein
MC	Minimal change
MCI	Mild cognitive impairment
MOG	Myelin/oligodendrocyte glycoprotein
MMSE	Mini mental state examination
MRI	Magnetic resonance imaging
MS	Multiple sclerosis
MSA	Multiple system atrophy
NCI	Neuronal cytoplasmic inclusion
NNI	Neuronal nuclear inclusions
OPC	Olivopontocerebellar
OPCA	Olivopontocerebellar atrophy
OSP	Oligodendrocyte-specific protein
PD	Parkinson's disease
PDGFα	Platelet-derived growth factor receptor α
PLP	Proteolipid protein
PMI	Post mortem interval
PSP	Progressive supranuclear palsy

qPCR	Quantitative polymerase chain reaction
QSBB	Queen Square Brain Bank
RPLP0	Ribosomal protein, large, P0
RT	Room temperature
SDHA	Succinate dehydrogenase complex, subunit A, flavoprotein
SDS	Shy-Drager syndrome
SNARE	Soluble NSF attachment protein receptor
SNCA	αSyn gene
SND	Striatonigral degeneration
SNP	Single nucleotide polymorphism
StrN	Striatonigral
SVD	Small vessel disease
TBP	TATA box binding protein
UBC	Ubiquitin C
UPR	Unfolded protein response
UPS	Ubiquitin-proteasome system
VBM	Voxel-based morphometry
YWHAZ	Tyrosine 3-Monooxygenase/Tryptophan 5-Monooxygenase Activation Protein, Zeta polypeptide

1

INTRODUCTION

1.1. MULTIPLE SYSTEM ATROPHY

1.1.1. Historical perspective

The term multiple system atrophy (MSA) was first introduced in 1969 by Graham and Oppenheimer to combine three disease entities with overlapping clinical and pathological pictures (Graham and Oppenheimer, 1969). The three neurodegenerative diseases considered were striatonigral degeneration (SND), olivopontocerebellar atrophy (OPCA) and Shy-Drager syndrome (SDS). Twenty years later, the discovery of glial cytoplasmic inclusions (GCIs) as a distinct pathological finding in all three conditions by Papp and colleagues gave further credence to the unified classification of MSA (Papp et al., 1989).

1.1.2. Clinical presentation

The clinical presentation of MSA includes parkinsonism, cerebellar ataxia, and autonomic dysfunction (Stefanova et al., 2009). Where parkinsonian features dominate, the condition is denoted as MSA-P, whereas MSA-C represents a clinical picture dominated by cerebellar features. The second consensus statement on MSA retains the categories of MSA-P and MSA-C in addition to definite, probable, and possible groups in the diagnosis of MSA (Gilman et al.,

2008). For a definite MSA diagnosis to be made, both clinical and neuropathological changes must be established. Probable MSA is defined as a sporadic, progressive adult onset disorder of autonomic failure and poorly levodopa responsive parkinsonism or cerebellar ataxia. A diagnosis of possible MSA is made where a sporadic, progressive adult onset disorder presents with parkinsonism or cerebellar ataxia in addition to at least one feature of autonomic dysfunction and another of clinical or neuroimaging abnormality. Table 1 outlines the consensus criteria for the categories of definite, probable, and possible MSA. The discovery of widespread GCIs with restricted neuronal loss in five autopsy cases without clinically documented neurological disorder (with the exception the one case of sporadic Creutzfeldt-Jakob disease but no clinical signs of MSA) suggests that MSA may exist in a preclinical or non-progressive form (Parkkinen et al., 2007; Fujishiro et al., 2008; Rodriguez-Diehl et al., 2012; Kon et al., 2013).

1.1.3. Pathological features

Macroscopic changes are evident in striatonigral (StrN) and/or olivopontocerebellar (OPC) regions of MSA cases. The striatonigral structures include the striatum and midbrain, where there is atrophy and dark discoloration of the putamen, most marked posteriorly, and pallor of the substantia nigra. The olivopontocerebellar regions include the medulla, pons and cerebellum. In the medulla, there may be blurring of the ribbon of the inferior olivary nucleus, while in the pons, there is pallor of the locus coeruleus. Furthermore, there is reduction in the size of the pontine base and middle and inferior cerebellar peduncles. In

the cerebellum, pathological changes affect both the grey and white matter. These changes present as cortical atrophy, narrowing of the folia, atrophy and dark discoloration of the white matter as is seen in Figure 1.1. (Quinn, 1989; Fearnley and Lees, 1990; Burn and Jaros, 2001; Greenfield, 2008)

Microscopically, the pathological hallmark of MSA is the GCI found in the cytoplasm of oligodendrocytes (Papp et al., 1989) (Figure 1.2). In addition to GCIs, neuronal cytoplasmic inclusions (NCIs), neuronal nuclear inclusions (NNIs), glial nuclear inclusions (GNIs) and threads are also observed in MSA cases (Wakabayashi and Takahashi, 2006). These inclusions are visualized by different staining techniques such as Gallays silver impregnation and ubiquitin and α-synuclein (αsyn) immunohistochemistry. Pathological changes are seen in both the grey and white matter in cortical and subcortical regions. In a study of cortical and subcortical regions (striatum, pons, medulla, and cerebellum), vacuolation and the presence of GCIs were observed in white matter tracts (Armstrong et al., 2007). GCIs are randomly distributed or occur in large clusters, with no apparent spatial correlation to abnormal neurons or neuronal inclusions (Armstrong et al., 2006). Neuronal inclusions, on the other hand, are found in regular clusters and are spatially correlated with abnormal neurons (Armstrong et al., 2006). Abnormal neurons were characterized as having enlarged cell bodies with displaced nuclei or distorted cell bodies due to shrunken, atrophic perikaryon (Armstrong et al., 2004, 2006). The random distribution of GCIs was interpreted as indicting that oligodendrocytes, rather than topographically

organized neurons, represent the cell population primarily affected in MSA (Armstrong et al., 2006).

In a review of 203 pathologically proven MSA cases, neuronal loss was most severe in the substantia nigra, locus coeruleus, putamen, inferior olives, pontine nuclei, Purkinje cells, and intermediolateral columns in the spinal cord (Wenning et al., 1997). The cerebral cortex, thalamus, subthalamic nucleus, caudate nucleus, globus pallidus, dentate nucleus, nucleus ambiguus, vestibular nuclei, anterior horn cells, and pyramidal tracts, on the other hand, are less affected (Wenning et al., 1997). Moreover, there is a positive correlation between GCI burden and neuronal loss and disease duration in both striatonigral and olivopontocerebellar regions (Inoue et al., 1997; Ozawa et al., 2004).

MSA pathological grading scales have been proposed to reflect the burden of pathology in StrN and OPC regions (Wenning et al., 2002; Ozawa et al., 2004; Jellinger et al., 2005). Based on semi-quantitative assessment of neuronal loss, astrogliosis and GCI burden in StrN and OPC regions, Jellinger and colleagues graded lesions on a four-point scale (SND 0-III and OPCA 0-III) thereby classifying cases as predominantly SND, OPCA or mixed (Jellinger et al., 2005). Ozawa and colleagues pathologically sub-typed MSA cases as SND, OPCA or mixed by only assessing neuronal loss on a four-point scale (0-3+) in the caudate, putamen, substantia nigra, pontine base, olive and cerebellum (Ozawa et al., 2004). SND subtype reflects predominant neuronal loss in StrN structures, OPCA reflects predominant neuronal loss in OPC structures while mixed reflects an equal neuronal loss score in both regions. Another MSA sub-type that

is classified according to pathological criteria is the 'minimal change' MSA group. The prominent defining feature of minimal change MSA in published literature is restricted neuronal loss to the substantia nigra and/or locus coeruleus (Wenning et al., 2002; Wakabayashi et al., 2005; Wenning et al., 1994 a; Huang et al., 2005).

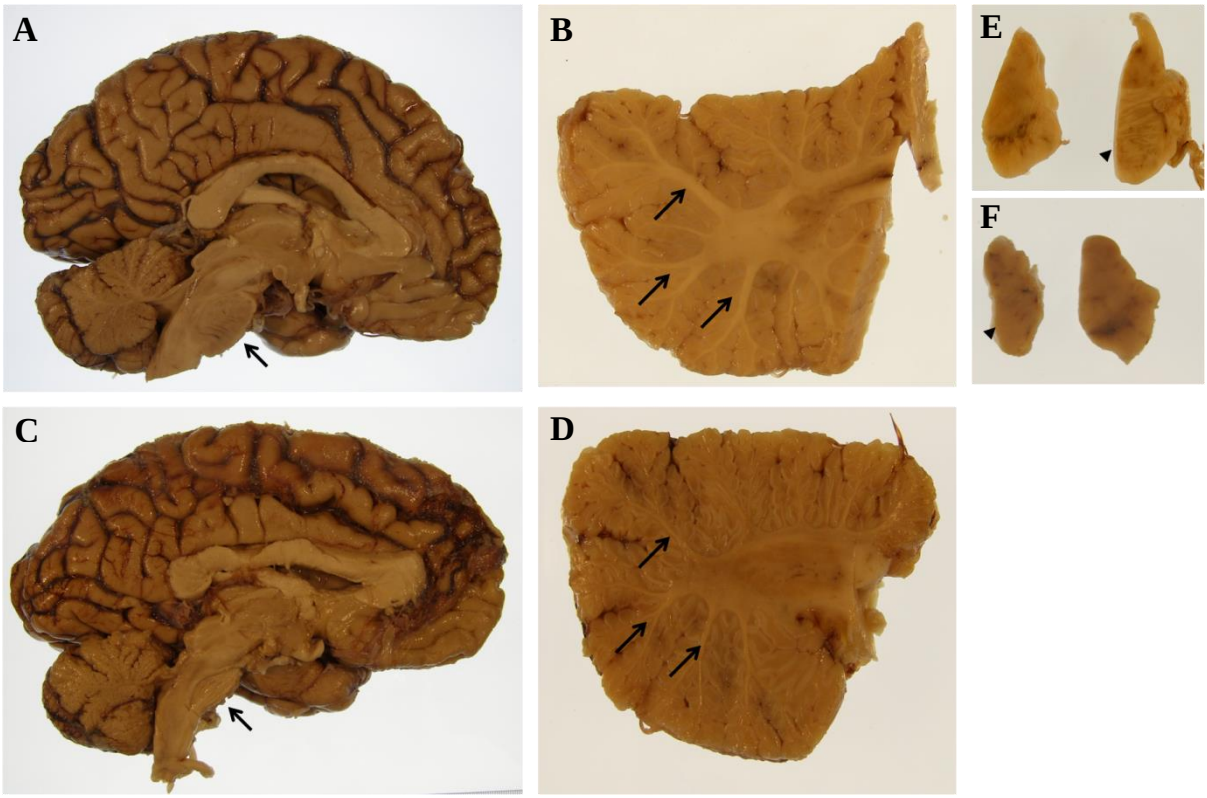

Figure 1.1. Macroscopic features in MSA

Normal control **(A)** & MSA **(B)** brain. Note pontine (arrows) atrophy in MSA brain. Normal control **(C)** MSA **(D)** cerebellum. Note narrowing of folia white matter (arrows) and discoloration of white matter in MSA.
Normal control **(E)** & MSA **(F)** pallor of the substantia nigra & pontine atrophy (arrow head).

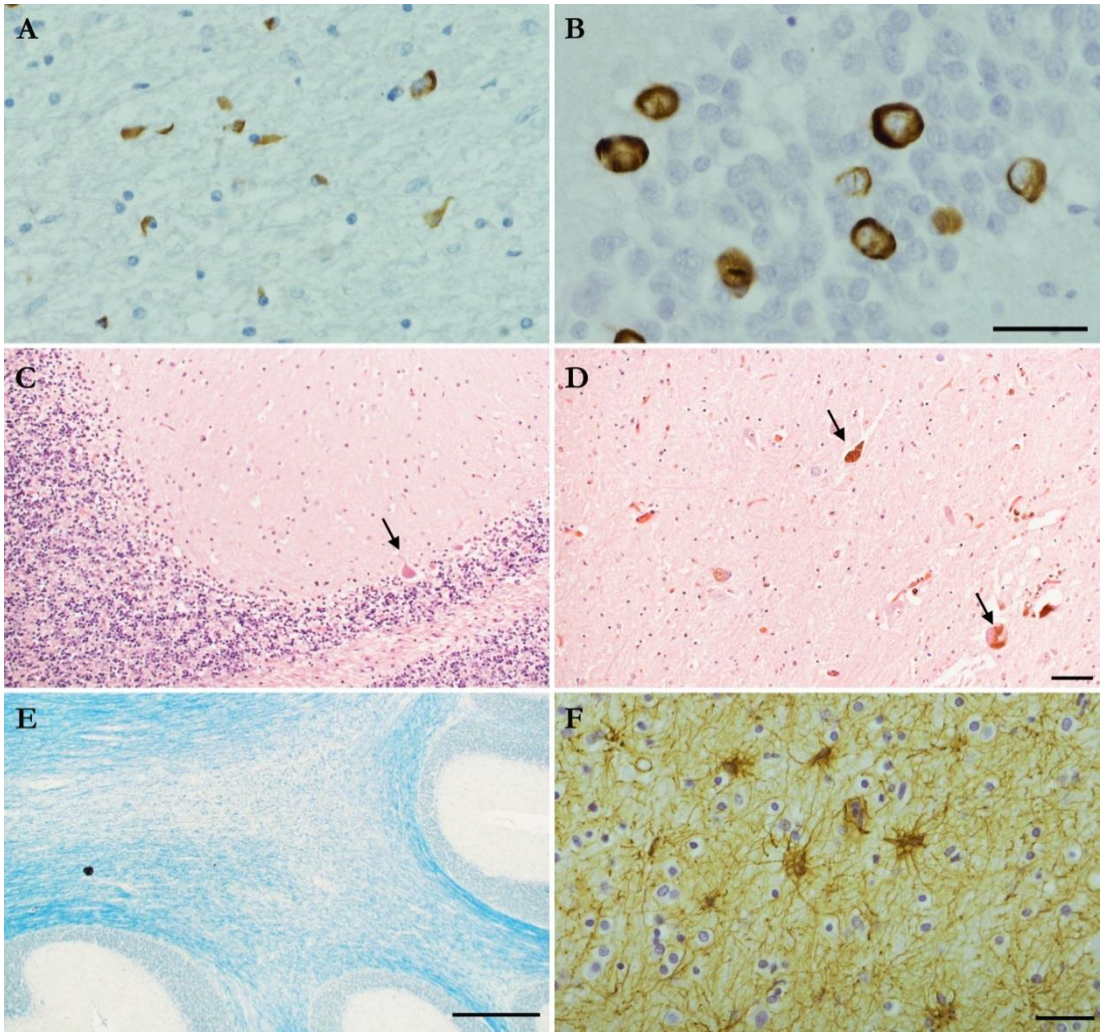

Figure 1.2. Typical neuropathological changes in MSA

Typical neuropathological changes in MSA include αsyn-positive inclusions, neuronal loss, myelin damage and gliosis. The pathological hallmark of MSA are αsyn-positive GCIs (A). αSyn-positive NCIs are also present as shown here in a severely affected dentate gyrus (B). Neuronal loss in the cerebellum (C) and substantia nigra (D) with few Purkinje cells and pigmented neurons remaining (arrows) as seen by H&E staining. LFB staining shows myelin damage in the cerebellum (E). Gliosis is demonstrated by GFAP immunohistochemistry (F).

H&E: Haematoxylin & Eosin. LFB: luxol-fast blue. GFAP: glial fibrillary acidic protein; asyn a-synuclein; GCIs: glial cytoplasmic inclusions; NCIs: Neuronal cytoplasmic inclusions.

Scale bar: A, B: 20μm; C,D: 50μm; E: 500μm; F: 20μm.

1.1.4. Pathogenesis

The pathogenesis of MSA is not well understood and the mechanisms leading to αsyn aggregation in neurons and oligodendrocytes and neuronal degeneration are yet to be established. MSA is largely regarded as a sporadic disease as to date there are only three reports suggesting inheritance of MSA in German and Japanese families (Wullner et al., 2004; Soma et al., 2006; Hara et al., 2007). Also, only a few groups identified single nucleotide polymorphism (SNP) in SNCA gene; rs11931074, rs3822086 and rs3775444, to be associated with increased risk for developing MSA, while others have failed to do so (Ozawa et al., 1999; Lincoln et al., 2007; Al-Chalabi et al., 2009; Scholz et al., 2009; Ross et al., 2010). Recent findings of the Multiple System Atrophy Research Collaboration have implicated mutations in *COQ2* to increased risk of MSA (Multiple-System Atrophy Research Collaboration, 2013). The levels of coenzyme Q10 (COQ10), an energy carrier and antioxidant in the mitochondria, were found to be decreased in MSA patients with mutations in *COQ2*. The implication therefore is that mutations in the enzyme encoded by *COQ2* hinder COQ10 biosynthesis leading to impairment of the mitochondrial respiratory chain and increased susceptibility to oxidative stress. Mitochondrial dysfunction is implicated in the pathogenesis of PD and may prove to play a significant role in MSA (Stefanova et al., 2005 a; Exner et al., 2012).

MSA is increasingly being regarded as a primary oligodendrogliopathy with secondary neurodegeneration due to myelin dysfunction, accumulation of αsyn, and axonal damage (Wenning et al., 2008; Jellinger and Lantos, 2010; Fellner et

al., 2011 b). An alternative hypothesis is that primary and secondary neurodegenerative processes occur synergistically in MSA, where primary neurodegeneration is due to accumulation of αsyn in neurons and secondary neurodegeneration results from the disruption of the oligodendroglial-myelin-axon-neuron axis due to αsyn accumulation in oligodendrocytes (Nishie et al., 2004; Yoshida, 2007). Subcellular mechanisms implicated in MSA pathogenesis include the unfolded protein response (UPR) which is part of the ER stress response system, the ubiquitin-proteasome system (UPS), autophagy and macroautophagy systems as protein components of each of these systems have been found to be present in GCIs (Makioka et al., 2010; Schwarz et al., 2012; Tanikawa et al., 2012; Tanji et al., 2013). This may imply that impairment in these systems has a role in GCI formation and MSA pathology. The vital issue in understanding the pathogenesis of MSA is determining the mechanisms by which αsyn accumulate in oligodendrocytes.

Table 1.1. Criteria for diagnosing MSA *(adapted from* (Gilman et al., 2008)*)*

Definite MSA

Features of probable or possible MSA in addition to neuropathological demonstration of CNS α-synuclein–positive glial cytoplasmic inclusions with neurodegenerative changes in striatonigral or olivopontocerebellar structures.

Probable MSA

A sporadic, progressive, adult (>30 y)–onset disease characterized by

- Autonomic failure involving urinary incontinence (inability to control the release of urine from the bladder, with erectile dysfunction in males) or an orthostatic decrease of blood pressure within 3 min of standing by at least 30 mm Hg systolic or 15 mm Hg diastolic *and*
- Poorly levodopa-responsive parkinsonism (bradykinesia with rigidity, tremor, or postural instability) *or*
- A cerebellar syndrome (gait ataxia with cerebellar dysarthria, limb ataxia, or cerebellar oculomotor dysfunction)

Possible MSA

A sporadic, progressive, adult (>30 y)–onset disease characterized by

- Parkinsonism (bradykinesia with rigidity, tremor, or postural instability) *or*
- A cerebellar syndrome (gait ataxia with cerebellar dysarthria, limb ataxia, or cerebellar oculomotor dysfunction) *and*
- At least one feature suggesting autonomic dysfunction (otherwise unexplained urinary urgency, frequency or incomplete bladder emptying, erectile dysfunction in males, or significant orthostatic blood pressure decline that does not meet the level required in probable MSA) *and*
- At least one of the additional features:

  Possible MSA-P or MSA-C

  - Babinski sign with hyperreflexia
  - Stridor

  Possible MSA-P

  - Rapidly progressive parkinsonism
  - Poor response to levodopa
  - Postural instability within 3 y of motor onset
  - Gait ataxia, cerebellar dysarthria, limb ataxia, or cerebellar oculomotor dysfunction
  - Dysphagia within 5 y of motor onset
  - Atrophy on MRI of putamen, middle cerebellar peduncle, pons, or cerebellum
  - Hypometabolism on FDG-PET in putamen, brainstem, or cerebellum

  Possible MSA-C

  - Parkinsonism (bradykinesia and rigidity)
  - Atrophy on MRI of putamen, middle cerebellar peduncle, or pons
  - Hypometabolism on FDG-PET in putamen
  - Presynaptic nigrostriatal dopaminergic denervation on SPECT or PET

1.2. OLIGODENDROCYTES AND GLIAL CYTOPLASMIC INCLUSIONS

1.2.1. Oligodendrocytes

Glial cells of the central nervous system include oligodendrocytes, astrocytes, radial glia, ependymal cells and microglia. The importance of oligodendrocytes resides in their ability to extend processes and form layers of myelin sheath around axons, thereby facilitating propagation of action potentials through saltatory conduction (Baumann and Pham-Dinh, 2001). In addition, oligodendrocytes produce neurotrophic factors that are essential in maintaining the integrity of axons (Ransom and Sontheimer, 1992; Nave, 2010). There are different subgroups of oligodendrocytes present in the central nervous system (CNS) as they undergo maturational changes. These subpopulations have been characterized both morphologically and antigenically (Baumann and Pham-Dinh, 2001).

Mature oligodendrocytes are known as myelinating (intrafasicular) or satellite (perineuronal) oligodendrocytes. Myelinating oligodendrocytes myelinate axons while satellite oligodendrocytes are found around neurons and are not in direct contact with the myelin sheath. Myelinating oligodendrocytes have been further divided according to their size and to the size and thickness of their myelin sheath from small to large. Furthermore, biochemical markers characterize oligodendrocytes at different maturational stages. A few markers may be present at one or more of the maturational stages, therefore, more than one marker is needed to better identify the maturational point of the cell. With that in mind, some of the markers used to identify oligodendrocyte precursor cells include

NG2, platelet-derived growth factor receptor α (PDGFRα), and A2B5; galactocerebroside (GC) and 2',3'-Cyclic nucleotide-3'-phosphohydrolase (CNP) for premyelinating oligodendrocytes; GC , CNP and myelin basic protein (MBP), for mature oligodendrocytes with the addition of myelin/oligodendrocyte glycoprotein (MOG) for myelinating oligodendrocytes. (Baumann and Pham-Dinh, 2001; Nishiyama et al., 2009). Oligodendrocytes may also be identified by their expression of the basic helix-loop-helix transcription factors olig1 and olig2. Characterization of the olig genes has shown their importance in the development of oligodendrocytes. Olig2, in turn, is used as a marker for oligodendrocytes. (Rowitch et al., 2002)

1.2.2. GCI discovery

In 1989, Papp and colleagues identified cells containing GCIs as the pathological hallmark of MSA (Papp et al., 1989). GCIs are present in oligodendroglia, however, a full profile of the subpopulations of oligodendroglia that contain GCIs has yet to be established (Wenning et al., 2008). Identifying these subpopulations may give further insight into the pathogenic mechanisms of MSA.

1.2.3. GCI antigenic characteristics

Extensive research has been conducted on profiling the content of GCIs. GCIs were found to be within oligodendrocytes and not neurons, astrocytes or microglia, as the cells containing GCIs were negative for the markers neurofilaments (neurons), glial fibrillary acidic protein (GFAP) (astrocytic) and Mac 387 (macrophage) (Papp et al., 1989). Furthermore, they were found to be

composed of multilayers of filaments, with α-synuclein at the core (Gai et al., 2003). Alpha-synuclein is a key component of GCIs and is the most sensitive marker for these inclusions (Gai et al., 1998; Tu et al., 1998; Wakabayashi et al., 1998; Wang et al., 2002). Other components of GCIs include ubiquitin, non-phosphorylated tau, α- and β-tubulin, 14-3-3 protein, aggresomal proteins, metallothionein (MT)-III, Rab5 and rababptin-5 (Papp et al., 1989; Gai et al., 1999; Nakamura et al., 2000; Kawamoto et al., 2002, 2007; Wakabayashi and Takahashi, 2006; Pountney et al., 2011; Chiba et al., 2012).

1.2.4. GCI morphology and distribution

GCIs portray various morphologies such as sickle-shaped, flame-shaped, ovoid, triangular and conical (Figure 1.3). Staining techniques that demonstrate GCIs include Gallyas silver impregnation and α-synuclein and ubiquitin immunohistochemistry (Castellani, 1998; Wakabayashi and Takahashi, 2006; Jellinger and Lantos, 2010).

GCIs are distributed throughout the CNS with varying frequencies according to brain region, disease severity and MSA pathological subtype. GCI density increases with disease severity, however, in very severe cases where there is great tissue damage, they are very few or absent. Areas mostly affected in MSA, and therefore where GCIs are present but not restricted to, include striatonigral and olivopontocerebellar structures. (Papp and Lantos, 1994; Inoue et al., 1997; Ozawa et al., 2004; Wakabayashi and Takahashi, 2006).

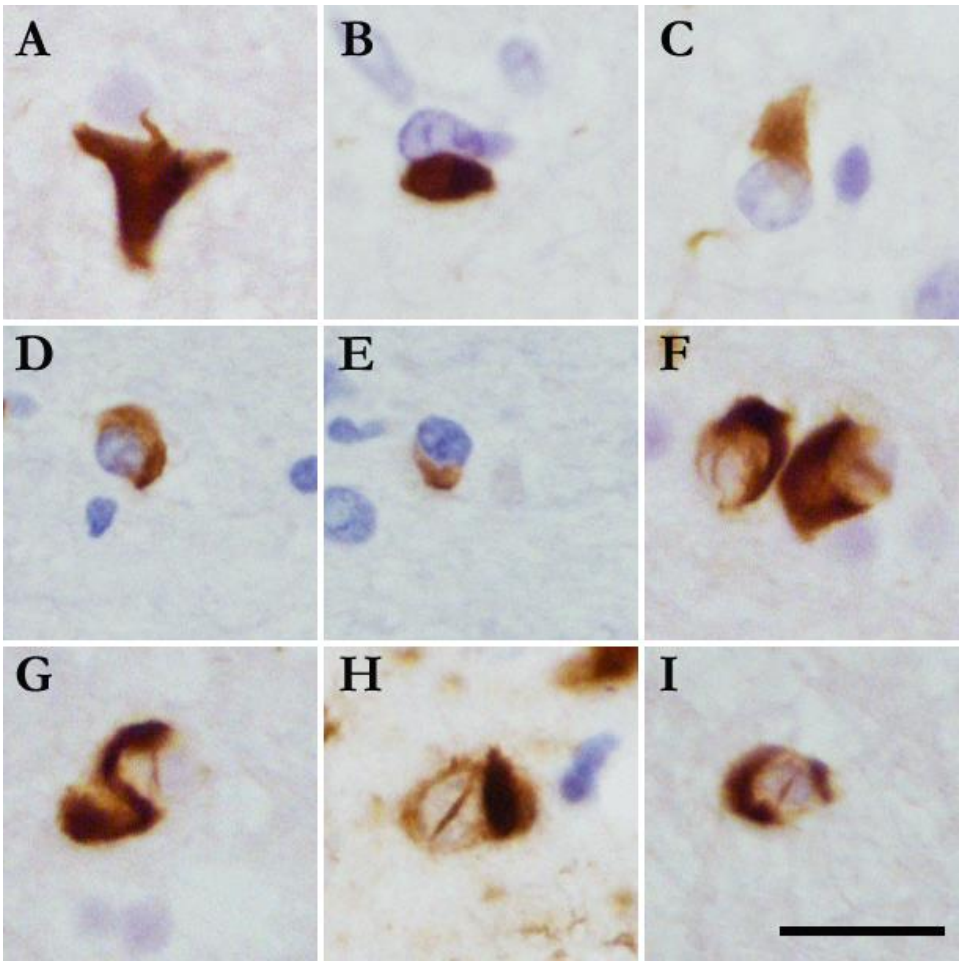

Figure 1.3. GCI and GNI morphology

GCIs occur in various shapes such as sickle-shaped, flame-shaped, ovoid, triangular and conical as shown by αsyn immunohistochemistry (A-G). GNIs are less common than GCIs and present as a filamentous line across the nucleus (H-I). *Scale bar: 10μm*

1.2.5. GCI significance

As mentioned previously, GCIs are the pathological hallmark of MSA. As an accumulation of misfolded proteins in oligodendrocytes, GCIs are believed to play a central role in the pathogenesis of MSA through dysfunction of oligodendrocytes, leading to impaired myelin formation and consequently neurodegeneration (Wenning et al., 2008). A correlation has been shown between GCI burden and neuronal loss and these pathological changes and disease duration in a large cohort of MSA cases (Ozawa et al., 2004). Furthermore, there seems to be a relationship between GCI distribution and clinical symptoms observed as cases with greater GCI burden in StrN regions presented with a predominant parkinsonian phenotype during life and those with greater GCI burden in OPC regions predominantly displayed cerebellar features (Ozawa et al., 2004; Jellinger et al., 2005). The contribution of GCI distribution to clinical phenotype is not straightforward as in a proportion of cases in one cohort, minimal pathology in StrN regions resulted in presence of parkinsonism (Ozawa et al., 2004) while in another parkinsonism was overshadowed by cerebellar signs (Jellinger et al., 2005).

1.3. ALPHA-SYNUCLEIN

1.3.1. Gene and protein

The synuclein family of proteins are natively unfolded and include α-, β- and γ-synuclein (Iwai et al., 1995; Weinreb et al., 1996; Eliezer et al., 2001; Uversky, 2007). αSyn is encoded by SNCA which has been mapped to chromosome 4q21 and consists of six exons five of which are transcribed (Spillantini et al., 1995). Alternative splicing of αsyn mRNA results in the production of four protein isoforms: αsyn 140, 126, 112, and 98; however, only isoforms 140 and 112 have been confirmed by consensus coding sequence (CCDS) project criteria (Pruitt et al., 2009; Harte et al., 2012). αSyn 140 is the transcript of the whole gene and is the most abundant isoform (Campion et al., 1995; Beyer et al., 2008 b). Isoforms 126 , 112, and 98 result from the in-frame deletion of exon 3, exon 5, and both exons 3 and 5, respectively (Uéda et al., 1994; Campion et al., 1995; Beyer, 2006; Beyer et al., 2008 b). As a result, the missing amino acid (AA) residues in αsyn 126 are AA 41-54 at the N-terminus and that in αsyn 112 are AA 103 – 130 at the C-terminus.

The full transcript results in a 140 amino acid protein (~14 kDa) with an amphipathic region at the N-terminus, a hydrophobic central region containing the non-amyloid- β (NAC) domain, and an acidic region at the C-terminal as shown in Figure 1.4 (Jo et al., 2000; Pettersen et al., 2004; Beyer, 2006). There are six imperfect repeats with a KTKEGV consensus sequence from amino acid residues 7 -87 spanning the amphipathic and central regions. As a natively unfolded protein, αsyn does not assume a specific secondary structure. In fact,

studies have shown that αsyn can adopt various conformational states as dictated by different environmental factors (Uversky, 2007; Silva et al., 2013), such as an α-helical membrane-bound structure or in a disordered free cytosolic state (Eliezer et al., 2001; Bussell et al., 2005).The N-terminal region is associated with lipid binding properties and assumes an α-helical conformation upon interaction with membranes (Eliezer et al., 2001; Jao et al., 2004). Point mutations found in familial Parkinson's disease (PD) are located in this region (Beyer, 2006). The hydrophobic core of αsyn plays a role in protein-protein interactions and filament assembly (Giasson et al., 2001; Miake et al., 2002; Beyer, 2006). The carboxyl end of the protein is rich with acidic and proline residues and interacts with metal and cationic compounds (Nielsen et al., 2001; Uversky et al., 2001; Beyer, 2006). The interaction of metals and cationic compounds induces α-synuclein oligomerisation (Nielsen et al., 2001; Uversky et al., 2001; Lowe et al., 2004). The consensus on the conformation of the C-terminal is that it is unfolded and unstructured even as other domains of the αsyn protein undergo changes (Eliezer et al., 2001; Beyer, 2006; Uversky, 2007). However, a study using limited proteolysis method demonstrated that the acidic C-terminal tail of αsyn is rigid and structured when micelle bound (de Laureto et al., 2006). More recent findings of the structure of αsyn suggest that it may exists physiologically as a helically folded tetramer, suggesting that αsyn aggregate formation is preceded by destabilization of this stable tetramer state. (Bartels et al., 2011; Wang et al., 2011; Silva et al., 2013).

1.3.2. Function

αSyn is a predominantly CNS protein, however, it is also found in peripheral tissue (Ltic et al., 2004). In the brain, its expression is evident in neurons and vascular endothelial cells, however, its expression in glial cells is still a matter of debate (Stefanova et al., 2001; Tamo et al., 2002; Cookson, 2009; Fellner et al., 2011 a). Expression of αsyn in oligodendrocytes has been demonstrated in rat and mouse oligodendrocytes (Richter-Landsberg et al., 2000; Culvenor et al., 2002; Nielsen et al., 2006) and in human tissue (Mori et al., 2002, 2003; Papadopoulos et al., 2006) despite the long standing notion that oligodendrocytes lack αsyn (Solano et al., 2000; Miller et al., 2005; Jin et al., 2008)

The exact function of αsyn is yet to be determined, however, possible roles have been deduced based on the protein's structure and localization in healthy and disease states. αSyn is located at the presynaptic terminal indicating a role in neuronal plasticity, vesicular transport, and membrane interaction (Iwai et al., 1995; Kahle et al., 2000; Reynolds et al., 2011). Findings of a single- and double-knockout study of αsyn and/or βsyn suggest that αsyn contributes to the long term regulation and/or maintenance of presynaptic function and its absence is not detrimental to brain function and survival (Chandra et al., 2004). The absence of αsyn is not lethal, however, its presence proved important in rescuing cysteine string protein α (CSPα), a synaptic vesicle protein and chaperone, null mice from lethality (Chandra et al., 2005). αSyn chaperone activity also extends to soluble N-ethylmaleimide-sensitive factor (NSF) attachment protein receptor (SNARE) proteins, which are central to the neurotransmitter release process, as αsyn

ensures continuous SNARE-complex assembly (Burré et al., 2010). The interaction of αsyn with the CSPα and SNARE proteins highlights the significance of αsyn as a chaperone and in the maintenance of the nerve terminal (Chandra et al., 2005; Burré et al., 2010). αSyn is also implicated in the nigrostriatal system as the levels of catecholamines, metabolites and tyrosine hydroxylase decreased in the absence of αsyn (Prasad et al., 2011). αSyn's interaction with the lipid bilayer may contribute to pathogenic mechanisms of disease as it results in disruption of the membrane and induction of αsyn helical conformation leading to the production of fibrils and aggregates (Zhu et al., 2003). In addition to presynaptic localization, αsyn has been shown to localize in the nucleus and interact with histones suggesting a role of αsyn in gene expression regulation (Goers et al., 2003)

1.3.3. Disease

αSyn is implicated in different neurological disorders such as neurodegenerative diseases, inflammatory demyelinating disease and psychiatric disorders (Krüger et al., 2000; Goedert, 2001; Papadopoulos et al., 2006; Kao et al., 2009). Neurodegenerative diseases where αsyn is thought to be the major protein contributing to the disease are known as α-synucleinopathies (Krüger et al., 2000; Goedert, 2001). PD, MSA, and dementia with Lewy bodies (DLB) are the most common α-synucleinopathies. αSyn positive inclusions accumulate mostly in neurons in PD and DLB in the form of Lewy bodies, while in MSA they are primarily found as cytoplasmic inclusions in oligodendrocytes. In all cases of MSA however, NCIs, NNIs, and threads are also present. The role which αsyn

plays in the pathogenesis of these diseases is the topic of extensive research and potential pathogenic mechanisms include synaptic damage, impairment of the vesicular transport system and proteasomal system, demyelination, axonal damage and neuronal death (Goedert, 2001; Wenning et al., 2008; Bate et al., 2010; Steiner et al., 2011). Furthermore, the biochemistry of αSyn is modified in neurodegenerative diseases. In PD, it is found to become increasingly phosphorylated and insoluble with the course of the disease (Zhou et al., 2011). In both PD and MSA, αsyn becomes increasingly insoluble, however, it is less protease-resistant in MSA than in PD and DLB (Campbell et al., 2001; Tong et al., 2010).

Mutations and multiplications in the SNCA gene have pathological consequences. A53T, A30P, and E46K are examples of mutations with confirmed association with PD (Polymeropoulos et al., 1996; Krüger et al., 1998; Athanassiadou et al., 1999; Zarranz et al., 2004; Michell et al., 2005). In MSA, however, the results are conflicting as some groups failed to detect mutations or multiplications in SNCA while other identified the SNPs rs11931074, rs3822086 and rs3775444 to be associated with increased risk for developing MSA (Ozawa et al., 1999; Lincoln et al., 2007; Al-Chalabi et al., 2009; Scholz et al., 2009; Ross et al., 2010). Mutations in SNCA gene may also lead to a pathological spectrum encompassing that seen in PD and MSA as seen in the case of G51D mutation which includes neuronal and oligodendroglial αsyn-positive inclusions (Kiely et al., 2013). Moreover, duplication and triplication of the SNCA gene leads to

variable parkinsonian phenotype, affecting age of onset and rate of deterioration (Fuchs et al., 2007; Ross et al., 2008).

A

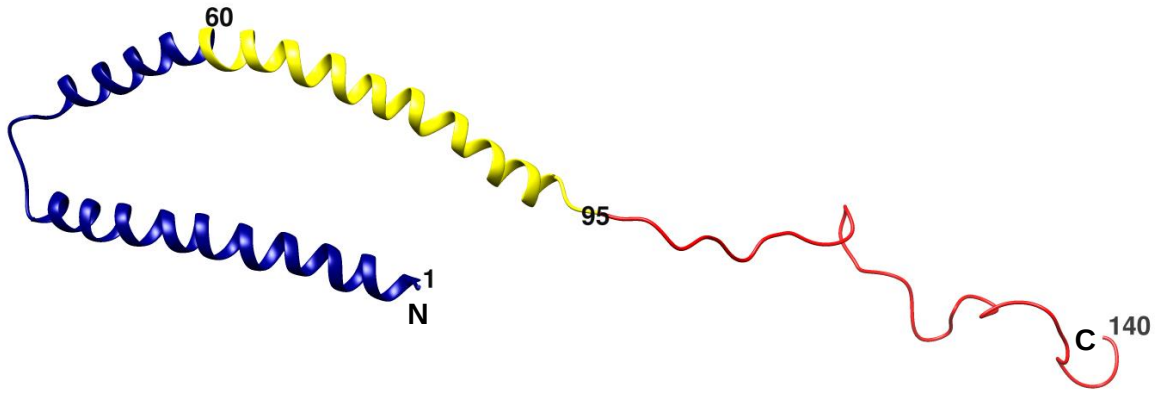

B

```
Homo sapiens          1   MDVFMKGLSKAKEGVVAAAEKTKQGVAEAAGKTKEGVLYVGSKTKEGVVHGVATVAEKTKEQVTNVGGAVVTGVTAVAQK  80
Rattus norvegicus     1   MDVFMKGLSKAKEGVVAAAEKTKQGVAEAAGKTKEGVLYVGSKTKEGVVHGVTTVAEKTKEQVTNVGGAVVTGVTAVAQK  80
Mus musculus          1   MDVFMKGLSKAKEGVVAAAEKTKQGVAEAAGKTKEGVLYVGSKTKEGVVHGVTTVAEKTKEQVTNVGGAVVTGVTAVAQK  80
Macaca mulatta        1   MRLRDPLFPGKREDAPWSFETYVLNVF----------VFVGSKTKEGVVHGVATVAEKTKEQVTNVGGAVVTGVTAVAQK  70

Homo sapiens         81   TVEGAGSIAAATGFVKKDQLGKNEEGAPQEGILEDMPVDPDNEAYEMPSEEGYQDYEPEA  140
Rattus norvegicus    81   TVEGAGNIAAATGFVKKDQMGKGEEGYPQEGILEDMPVDPSSEAYEMPSEEGYQDYEPEA  140
Mus musculus         81   TVEGAGNIAAATGFVKKDQMGKGEEGYPQEGILEDMPVDPGSEAYEMPSEEGYQDYEPEA  140
Macaca mulatta       71   TVEGAGSIAAATGFIKKDQLGKNEEGAPQEGILQDMPVDPDNEAYEMPSEEGYQDYEPEA  130
```

Figure 1.4. Alpha-synuclein protein structure

(A) Predicted lipid-bound αSyn structure. The N-terminal domain (aa 1-60; blue) is the amphipathic region with α-helical conformation and lipid –binding properties. The central domain spans aa 61-95 (yellow) and consists if the hydrophobic NAC domain believed to be aggregation-prone. The imperfect KTKEGV repeats are found across the N-terminal and central domains. The C-terminal domain (red) is rich in acidic, proline, and conserved tyrosine residues and is made up of aa 96-140. **(B)** Alpha-synuclein amino acid sequence alignment of *Homo sapiens, Rattus norvegicus, Mus musculus and Macaca mulatta* showing a highly conserved protein sequence across species. Red indicates highly conserved columns, blue indicates less conserved columns and grey a gap region.

Protein structure image produced using UCSF Chimera package and sequence alignment produced using the basic local alignment search tool (BLAST, http://blast.ncbi.nlm.nih.gov).

1.4. HYPOTHESIS

a. MSA patients with clinical evidence of cognitive impairment have more severe pathology in brain regions that are important for cognitive function.
b. The distribution and severity of pathology in patients with long disease duration and the minimal change group differ from the 'classic' MSA group.
c. αSyn accumulation as GCIs in oligodendrocytes occurs at different stages of oligodendrocyte maturation.
d. Accumulation of αsyn in oligodendrocytes in MSA is due to overexpression of αsyn mRNA in oligodendrocytes.
e. Accumulation of αsyn in oligodendrocytes in MSA is due to uptake of αsyn by oligodendrocytes from neurons and/or the surrounding environment.

1.5. AIMS OF RESEARCH PROJECTS

a. To determine if there is a difference in the distribution and burden of pathological changes in MSA patients with cognitive impairment compared with patients with normal cognition.

b. To determine the distribution and burden of pathological changes in long disease duration and minimal change MSA as compared to control MSA cases and to explore possible clinic-pathological correlations.

c. To investigate the involvement of $NG2^+$ cells, immature oligodendrocytes and mature oligodendrocytes by αsyn pathology in MSA.

d. To determine the regional and cellular expression profile of αsyn in MSA.

e. To assess whether exogenous αsyn can be internalized by oligodendrocytes and examine the pathological cascade of myelin and axonal damage due to accumulation of αsyn in oligodendrocytes using an *in vivo* model.

2

MATERIALS AND METHODS

2.1. CASE SELECTION

2.1.1. MSA with cognitive impairment

Nine MSA cases with documented cognitive impairment and nine with normal cognition were selected in a retrospective analysis of clinical data recorded during life. Cognitive impairment had been assessed by Mini-mental states examination (MMSE) by neurologists, and in some cases (n=5), formal neuropsychometry testing had been performed by a clinical psychologist. Neuropsychometry tests assess the following parameters: verbal memory, visual memory, working memory, visuospatial/constructive impairment, executive function, and language function (e.g. verbal fluency, comprehension, etc.). An MMSE score of 24-28 (out of 30) is suggestive of mild cognitive impairment (MCI) and ≤23 of dementia. Medical records were reviewed by a neurologist (Helen Ling). Patients with the pathological diagnosis of MSA were categorized as having cognitive impairment (MSA-CI) if their MMSE scores were consistently ≤ 28 and cognitive impairment was documented by a clinician on at least one occasion. The final MMSE score prior to death, presence of depression, hallucinations and the use of additional cognitive tests including formal neuropsychometry to confirm the

impairment of cognition were recorded. The control MSA group was matched for age (≤ 5 years difference), sex, disease duration (≤ 1 year difference), and had no documented cognitive impairment (MSA-CN) by clinician or care giver.

2.1.2. Long duration and minimal change MSA

Four cases in the long duration (one of which was provided by Toronto Western Hospital), six in the minimal change and eight control MSA cases were selected from the archives of QSBB. Cases were included into the long duration group if they had a disease duration ≥15 years. The minimal change group is a pathological characterization where cases have neuronal loss restricted to the substantia nigra and/or locus coeruleus. Patients in the control MSA group are those that have a more 'classical' presentation i.e. a disease duration of 5-10 years and neuronal loss not restricted to either the substantia nigra or locus coeruleus. The cases in the long duration and minimal change MSA were age (≤ 5 years difference) and sex – matched with the controls.

Table 2.1. Clinico-pathological studies cohort

No.	Study	Case	Diagnosis	Age	Sex	Disease duration
1	CI LDMC	CI-1 LD-MSA 1	MSA	77	F	16
2	CI	CI-2	MSA	75	M	9
3	CI	CI-3	MSA	82	F	9
4	CI	CI-4	MSA	54	M	7
5	CI	CI-5	MSA	74	F	8
6	CI	CI-6	MSA	60	M	6
7	CI	CI-7	MSA	57.8	M	12
8	CI	CI-8	MSA	56	M	7
9	CI LDMC	CI-9 LD-MSA 3	MSA	66.8	F	19
10	CI LDMC	CN-10 C-MSA 1	MSA	76	F	8
11	CI LDMC	CN-11 C-MSA 4	MSA	63.1	M	12
12	CI	CN-12	MSA	54	M	7
13	CI	CN-13	MSA	57	M	8
14	CI	CN-14	MSA	72	F	8
15	CI	CN-15	MSA	76	F	12
16	CI	CN-16	MSA	72	F	15
17	CI	CN-17	MSA	73	M	9
18	CI	CN-18	MSA	65	M	7
20	LDMC	LD-MSA 2	MSA	66	F	17
22	LDMC	LD-MSA 4	MSA	62	F	18
23	LDMC	MC-MSA 1	MSA	65	M	7.5
24	LDMC	MC-MSA 2	MSA	39	F	5.5
25	LDMC	MC-MSA 3	MSA	46	M	6.5
26	LDMC	MC-MSA 4	MSA	57	F	4
27	LDMC	MC-MSA 5	MSA	45	M	4
28	LDMC	MC-MSA 6	MSA	65	M	2.5
31	LDMC	C-MSA 2	MSA	56	F	10
32	LDMC	C-MSA 3	MSA	67	F	9
33	LDMC	C-MSA 5	MSA	82	F	5
34	LDMC	C-MSA 6	MSA	72	M	8
35	LDMC	C-MSA 7	MSA	58	F	5
36	LDMC	C-MSA 8	MSA	60	F	9

CI: cognitive impairment; CN: cognitively normal; LDMC: Long duration minimal change; LD: Long duration; MC: Minimal change; C: control; MSA: multiple system atrophy.

2.1.3. Regional and cellular expression of *SNCA* in MSA

MSA cases were pathologically typed according to published criteria (Ozawa et al., 2004) and grouped into mixed, SND and OPCA types as described in Chapter 2: Materials and methods section 2.4. Frozen tissue from 5 MSA-SND, 5 MSA-OPCA, 5 MSA-mixed types were selected and sex and age –matched to 5 PD and 4 normal control cases to study regional *SNCA* mRNA expression. The regions studied were the posterior frontal cortex (grey matter and white matter), occipital cortex (grey matter and white matter), dorsal putamen, pontine base and cerebellar white matter. For the cellular expression study, the pons of 5 MSA-mixed type and 6 normal controls was used to isolate neurons and oligodendrocytes. Cases that did not have frozen tissue available were excluded.

Table 2.2. *SNCA* mRNA expression study cohort

Study	Case	Diagnosis	MSA type	Age	Sex
Regional expression	1	MSA	Mixed	56	F
	2	MSA	Mixed	62	M
	3	MSA	Mixed	64	F
	4	MSA	Mixed	66	M
	5	MSA	Mixed	70	F
	6	MSA	SND	50	F
	7	MSA	SND	54	F
	8	MSA	SND	58	F
	9	MSA	SND	63	M
	10	MSA	SND	72	M
	11	MSA	OPCA	56	M
	12	MSA	OPCA	60	F
	13	MSA	OPCA	61	M
	14	MSA	OPCA	64	M
	15	MSA	OPCA	66	F
	16	PD	NA	61	F
	17	PD	NA	63	M
	18	PD	NA	65	M
	19	PD	NA	67	F
	20	PD	NA	70	M
	21	Control	NA	57	M
	22	Control	NA	69	M
	23	Control	NA	71	M
	24	Control	NA	73	F
Cellular expression	1	MSA	Mixed	50	M
	2	MSA	Mixed	70	F
	3	MSA	Mixed	56	M
	4	MSA	Mixed	64	F
	5	MSA	Mixed	64	M
	6	Control	NA	69	M
	7	Control	NA	82	F
	8	Control	NA	73	F
	9	Control	NA	85	M
	10	Control	NA	80	F
	11	Control	NA	83	M

MSA: multiple system atrophy; PD: Parkinson's disease; SND: striatonigral degeneration; OPCA: Olivopontocerebellar atrophy; NA: not applicable.

2.2. TISSUE PROCESSING

Samples were collected from brains donated to the Queen Square Brain Bank (QSBB) for Neurological Disorders, UCL Institute of Neurology, London. The donations were made according to ethically approved protocols and tissue is stored under a license issued by the Human Tissue Authority (No. 12198). One half of the brain is sliced in the coronal plane, flash frozen and stored at -80°C upon arrival to the QSBB, while the other half is fixed in 10% buffered formalin. Blocks are then sampled from the formalin fixed half brain, processed and embedded in paraffin wax using routine protocols.

2.3. IMMUNOHISTOCHEMISTRY ON FFPE

Eight-micrometre-thick section were cut, deparaffinised and placed in methanol/H_2O_2 (100:1) solution for 10 min to eliminate endogenous peroxidase activity. Following washes in PBS, pre-treatment was carried out with formic acid (98%) for 30 min for α-synuclein and Aβ immunohistochemistry and proteinase K for GFAP immunohistochemistry and then pressure cooking (10 min) in citrate buffer (0.1M) at pH 6.0 (except for GFAP immunohistochemistry). Sections were then placed in 10% non-fat milk for 30 min at room temperature (RT) to reduce non-specific binding, followed by incubation in the primary antibody for 1 hour at RT. After washes in PBS, the sections are incubated with biotinylated goat anti-rabbit IgG or biotinylated goat anti-mouse IgG (Vector Laboratories, Burlingame, CA) at a dilution of 1:200 for 30 min at RT. The secondary antibody was washed off then the sections were incubated in the avidin-biotin complex solution for 30 min at RT. After washes in PBS, they were

treated in the 3,3'-diaminobenzidine (DAB) solution for 3 min. The DAB solution was washed off and the tissues were counterstained in Mayer's haematoxylin for 10 sec. The tissue sections were then dehydrated in graded alcohol (70%, 90%, and absolute alcohol), cleared in three changes of xylene, and then mounted with DPX mounting medium.

Table 2.3. Primary and secondary antibodies

	Host	Dilution	Source (cat. no.)
Primary antibody			
α-synuclein	Mouse	1:50	Vector Laboratories, Burlingame, CA (VP A106)
α-synuclein	Mouse	1:1000	BD Transduction (610787)
GFAP	Rabbit	1:1000	DakoCytomation, Denmark (Z0334)
β-Amyloid (Aβ)	Mouse	1:100	DakoCytomation, Denmark (M0872)
Tau (AT8)	Mouse	1:600	Source Bioscience, UK (90206)
TDP – 43	Rabbit	1:2000	ProteinTech, Chicago, IL (12892-1-AP)
Secondary antibody			
Biotinylated rabbit anti-mouse IgG	Mouse	1:200	DakoCytomation , Denmark (E0354)
Biotinylated swine anti-rabbit IgG	Rabbit	1:200	DakoCytomation , Denmark (E0353)

2.4. EVALUATION OF IMMUNOHISTOCHEMISTRY

2.4.1. MSA cognitive impairment group

GCI burden was assessed in the anterior frontal (Brodmann area 6), posterior frontal (Brodmann area 4), parietal (Brodmann areas 5&7), temporal (Brodmann area 19), occipital (Brodmann area 17), and cingulate (Brodmann areas 24,32 &33) cortices, hippocampus, amygdala, caudate, putamen, substantia nigra, pons, medulla and cerebellum in a quantitative manner using the image analysis software, ImagePro Plus 7.0. A systematic uniform random distribution was used to generate 20 counting frames. Using the systematic uniform random distribution, allows for coverage of the entire region of interest and generation of random counting frames without any overlap (Fig. 2.1). GCI and NCI inclusions were visually identified and counted at 400x magnification and the counting frame was set at 125μm x 125μm. The density of inclusions was then calculated by dividing the total number of inclusions or cells counted by the total number of counting frames (cells/125μm^2). The counting criteria are presented in Table 2.2.

Table 2.4. GCI counting criteria

Inclusion criteria	Exclusion criteria
• **Flame-shaped, sickle-shaped, ovoid** • **α –synuclein positive** • **presence of nucleus not essential as long as morphology is characteristic**	• If the inclusion is of thin or reduced bulk that it could be confused for threads.

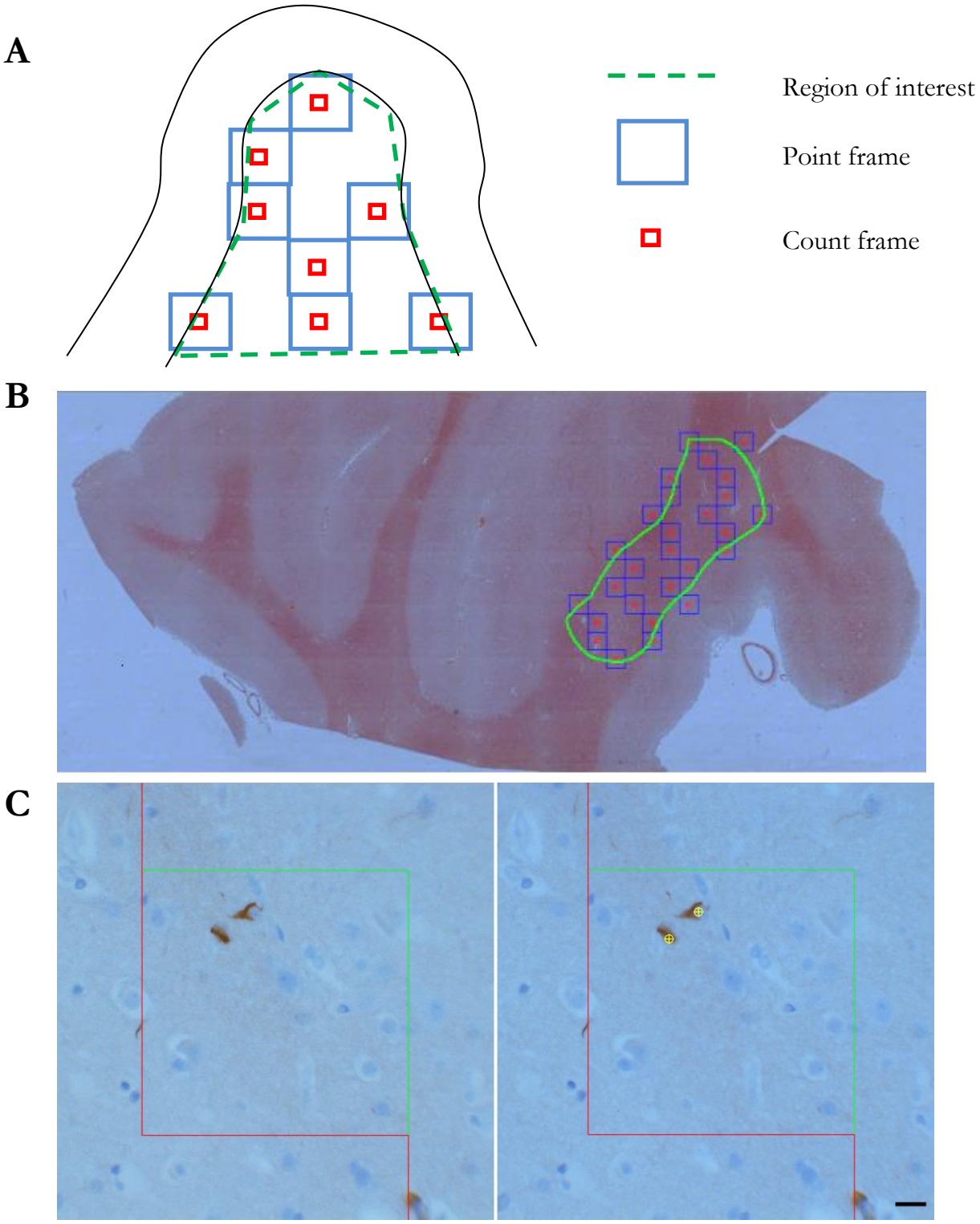

Figure 2.1. ImagePro Plus 7.0 analysis

Schematic representation (A) and representative image (B) of ImagePro Plus 7.0 analysis. Analysis was carried out using systematic uniform random distribution to generate counting frames set at 125µm x 125µm Using the systematic uniform random distribution, allows for coverage of the entire region of interest and generation of random counting frames without any overlap. Only GCIs or NCIs that fell within or on the green border of the counting frame were manually counted (C). *Scale bar: 20µm.*

Neuronal loss, gliosis and concomitant pathologies (Aβ, CAA, tau, TDP-43, Lewy bodies, and SVD) were assessed in a semi-quantitative manner according to published criteria (Mirra et al., 1991; Braak et al., 2003, 2006; Ozawa et al., 2004; Williams et al., 2007; Lashley et al., 2008; Mackenzie et al., 2010, 2011). A score scale of 0 - +3 was used to indicate increasing pathology as seen in Table 2.3. Furthermore, Aβ semi-quantitative scores for diffuse and mature Aβ plaques were each summated in the regions analysed to give a sub-total score (range 0 to 13) and a total score (diffuse + mature; range 0 to 21) in cortical regions.

2.4.2. MSA long duration/ minimal change group

Neuronal loss, GCIs, neuronal cytoplasmic inclusions, and gliosis were assessed in a semi-quantitative manner and MSA pathological type was determined based on a published method (Ozawa et al., 2004). Concomitant pathologies (Aβ, CAA, tau, TDP-43, Lewy bodies, and SVD) were also assessed according to published criteria (Mirra et al., 1991; Braak et al., 2003, 2006; Williams et al., 2007; Lashley et al., 2008) and summarized in Table 2.3. Diffuse and mature Aβ plaque semi-quantitative scores were each summed up to give a subtotal score (range 0 to 13) and then calculated together to give a total score (range 0 to 21) in cortical regions analysed as above.

Table 2.5. Semi-quantitative scale

Parameter	Scale		Objective magnification
GCI & NCI burden	**0**	No GCIs present	x20 objective of mean of five random fields
	+1	1-5 inclusions	
	+2	6 - 19 inclusions	
	+3	≥ 20 inclusions	
Neuronal loss	**0**	No neuronal loss	x10 – x40
	+1	Slight neuronal loss	
	+2	Moderate neuronal loss	
	+3	Severe neuronal loss	
Gliosis	**0**	Gliosis absent	x10 – x20
	+1	Astrocytes around blood vessels and sub-pial	
	+2	Astrocytes around blood vessels, sub-pial and extending into intervening parenchyma	
	+3	Greater burden than +2	
CAA	**0**	No amyloid	x10 – x40
	+1	Scattered vessels in leptomeninges or cortex with patchy deposition	
	+2	As +1 with occasional vessels having circumferential deposition	
	+3	Widespread circumferential deposition	
	+4	Severe deposition of amyloid accompanied by projection of amyloid into the adjacent parenchyma	
SVD	**0**	Vessels normal	x10 – x40
	+1	Occasional vessels affected	
	+2	A significant proportion of small vessels affected with few or no sequelae noted	
	+3	A significant proportion of the small vessels affected with obvious sequelae	

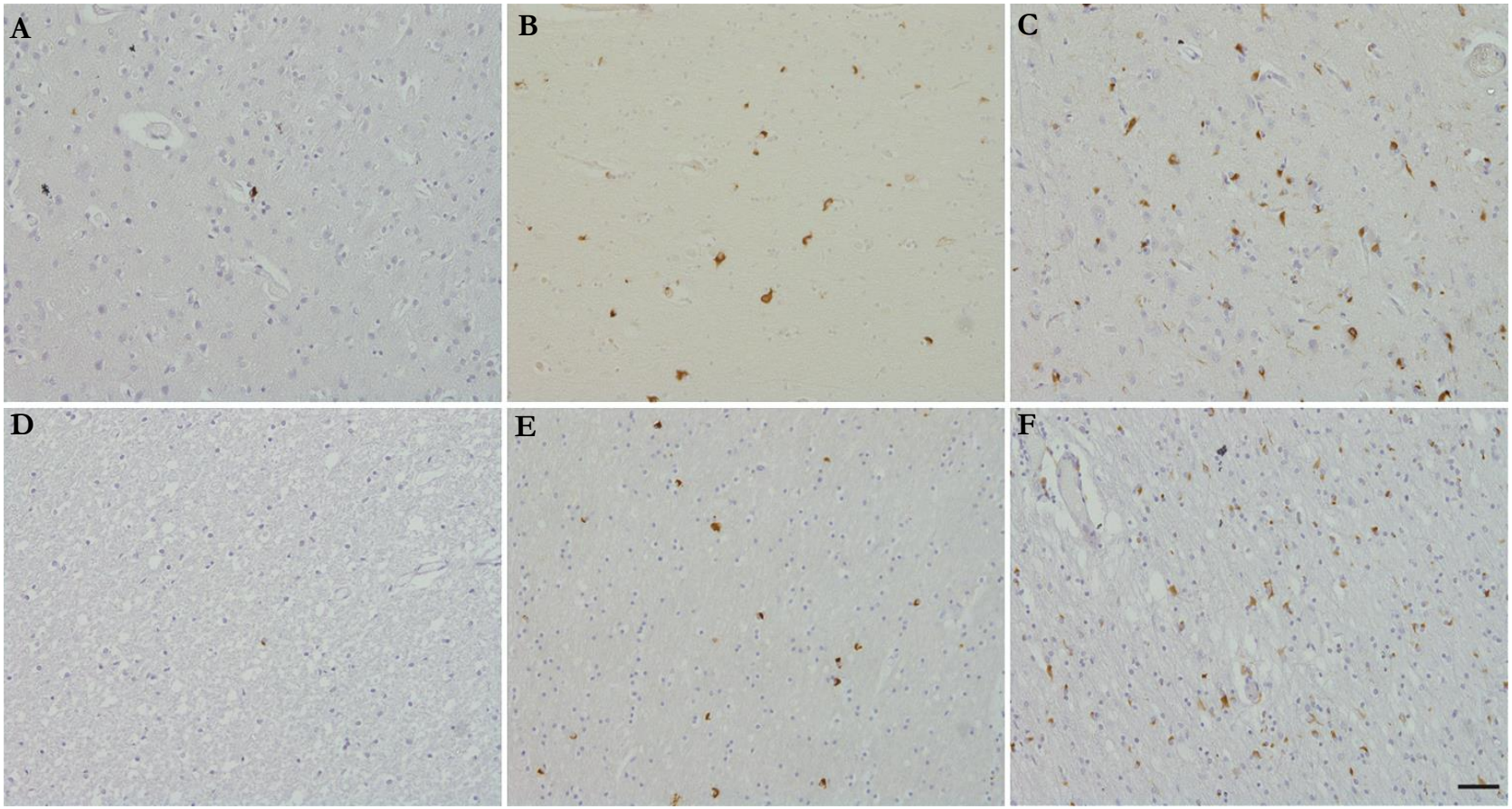

Figure 2.2. GCI semi-quantitative scale.

GCI grading scale in grey (A-C) and white (D-F) matter as assessed using αSyn immunohistochemistry. A score of '+1' was denoted to fields that contained 1-5 inclusions (A, D), '+2' 6 - 19 inclusions (B, E) and '+3' where there were ≥ 20 inclusions (C, F). *Scale bar: 50μm*

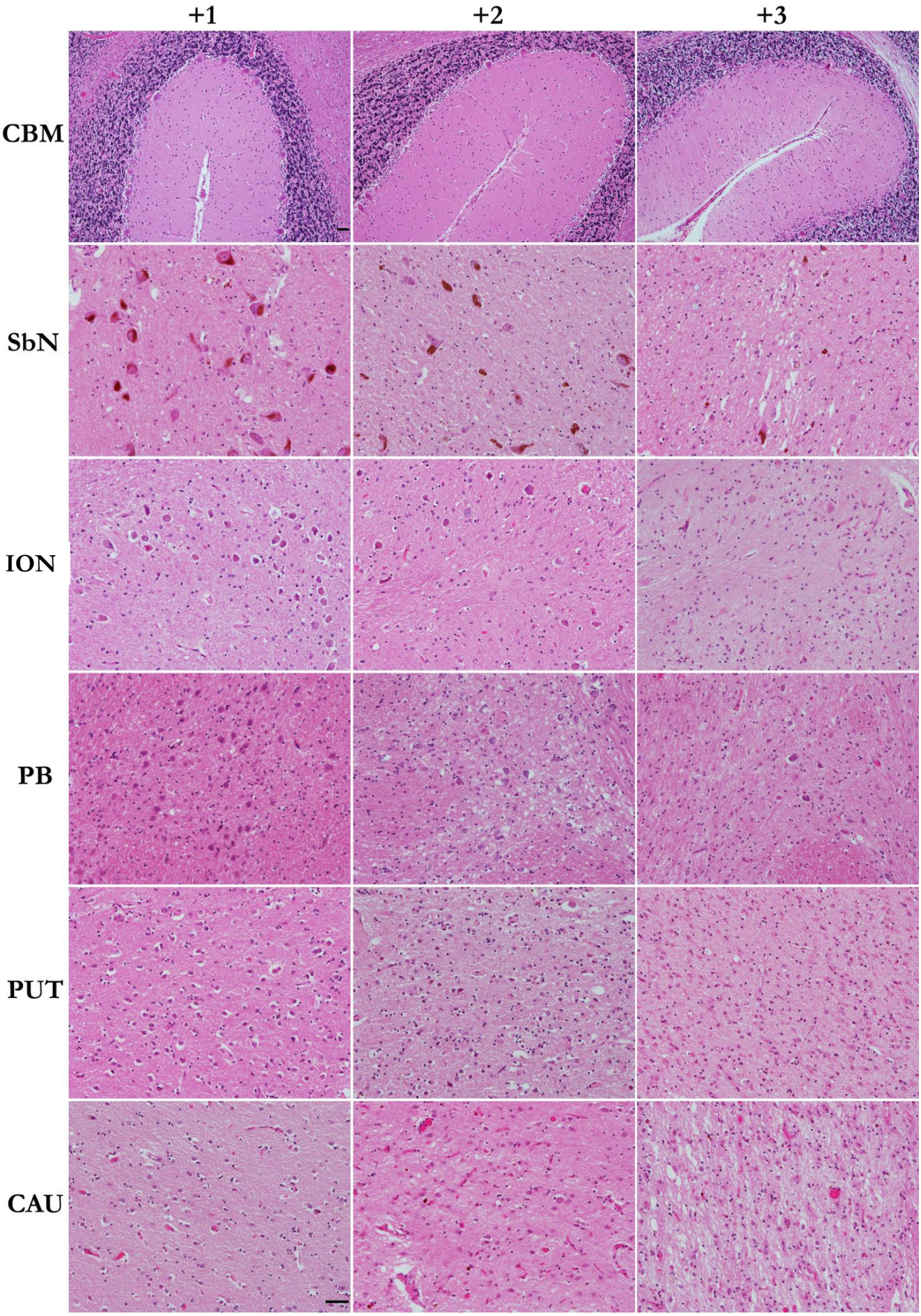
+1
+2
+3
CBM
SbN
ION
PB
PUT
CAU

Figure 2.3. Neuronal loss grading scheme

Neuronal loss semi-quantitative grading scale where '+1' denotes mild, '+2' moderate and '+3' severe neuronal loss in the cerebellum, substantia nigra, olivary nucleus, pontine base, putamen and caudate.

CBM: cerebellum; SbN: substantia nigra; ION: inferior olivary nucleus; PB: pontine base; PUT: putamen; CAU: caudate. Scale bar: 50μm (SbN, ION, PB, PUT & CAU at same magnification).

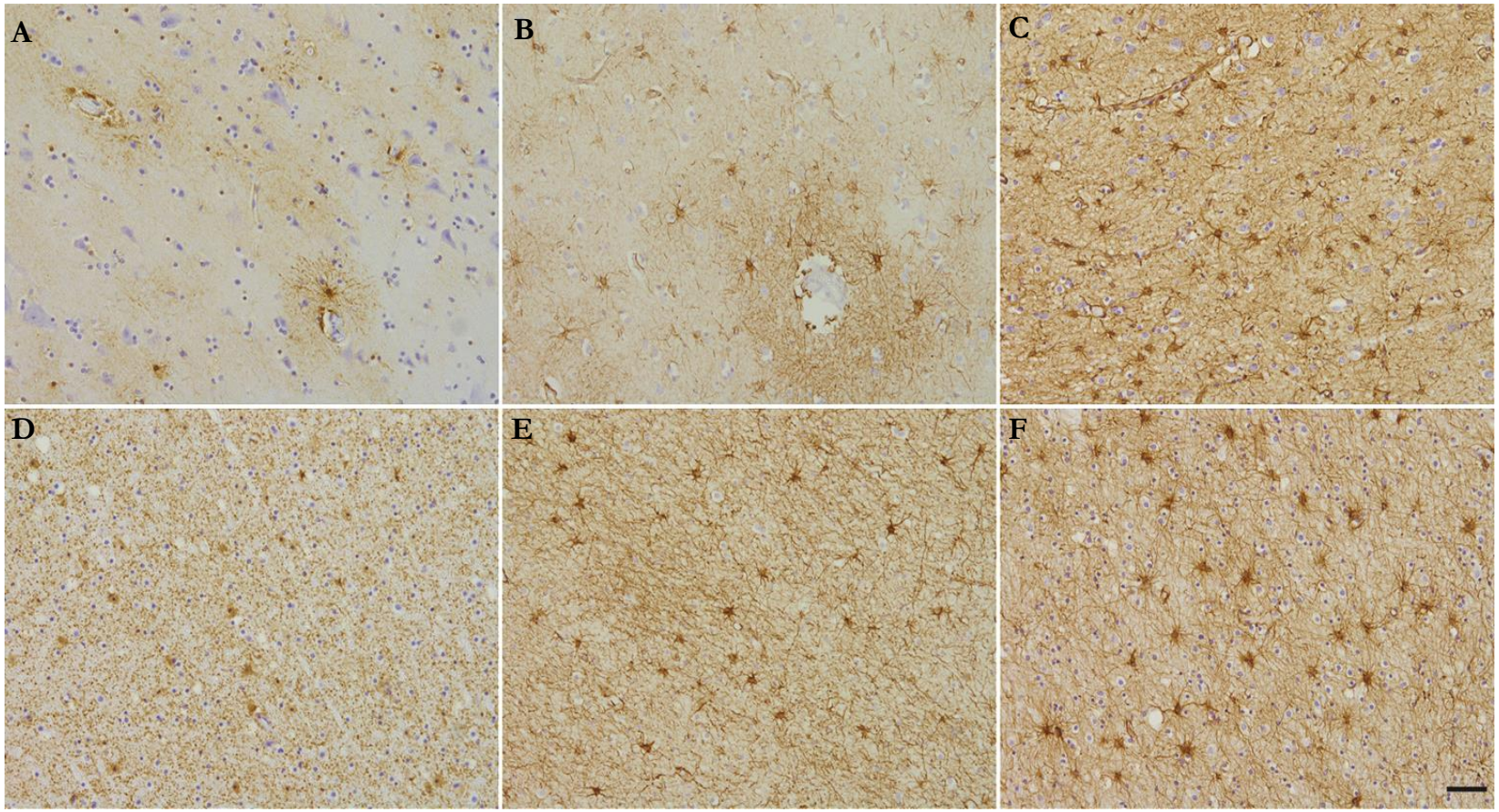

Figure 2.4. Gliosis semi-quantitative scale.

Astrogliosis grading scale in grey (A-C) and white (D-F) matter as assessed using GFAP immunohistochemistry. A score of '+1' was denoted to fields where astrocytes were found around blood vessels and sub-pial (A, D), '+2' where astrocytes were around blood vessels, sub-pial and extended into intervening parenchyma (B, E) and '+3' to fields where there was greater burden than +2 fields (C, F). *Scale bar: 50μm*

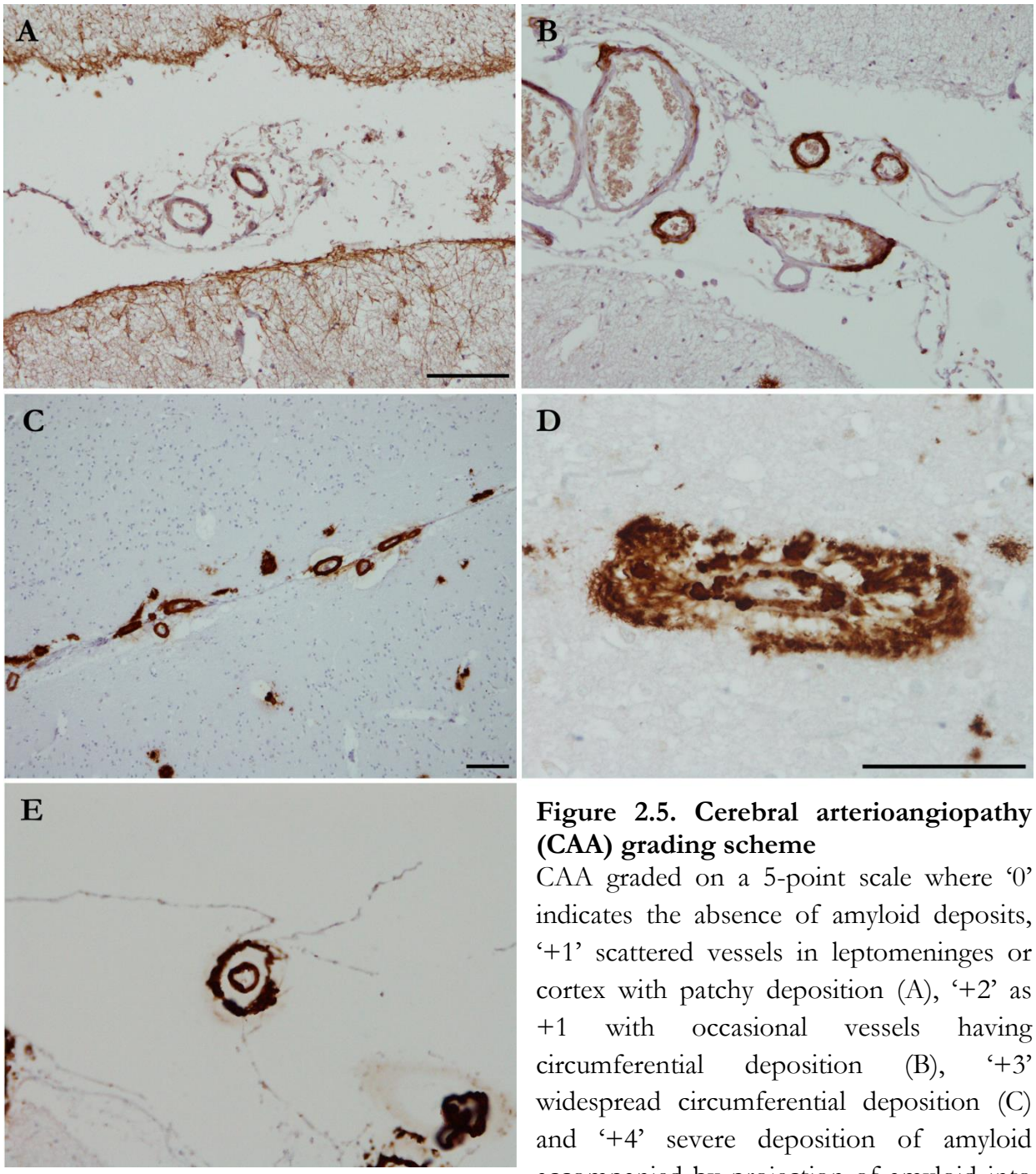

Figure 2.5. Cerebral arterioangiopathy (CAA) grading scheme
CAA graded on a 5-point scale where '0' indicates the absence of amyloid deposits, '+1' scattered vessels in leptomeninges or cortex with patchy deposition (A), '+2' as +1 with occasional vessels having circumferential deposition (B), '+3' widespread circumferential deposition (C) and '+4' severe deposition of amyloid accompanied by projection of amyloid into adjacent parenchyma (D) or vessel wall degeneration with 'double barrel' appearance (E) as shown by Aβ-immunohistochemistry. *Scale bar: 100μm (A, B, E same magnification)*

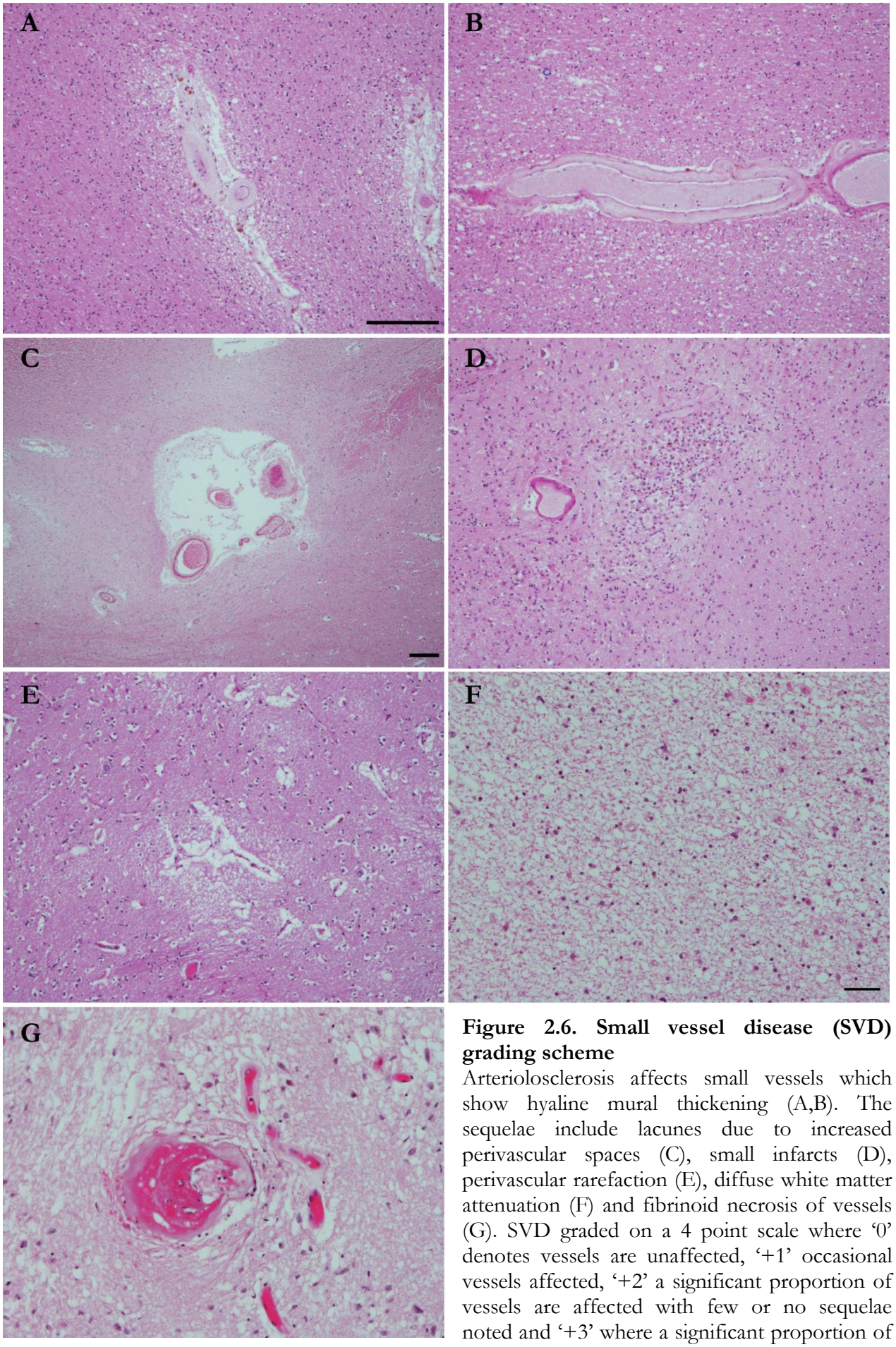

Figure 2.6. Small vessel disease (SVD) grading scheme
Arteriolosclerosis affects small vessels which show hyaline mural thickening (A,B). The sequelae include lacunes due to increased perivascular spaces (C), small infarcts (D), perivascular rarefaction (E), diffuse white matter attenuation (F) and fibrinoid necrosis of vessels (G). SVD graded on a 4 point scale where '0' denotes vessels are unaffected, '+1' occasional vessels affected, '+2' a significant proportion of vessels are affected with few or no sequelae noted and '+3' where a significant proportion of vessels are affected with obvious sequelae. *Scale bar: 200μm (A, B, D, E same magnification); 50μm (F,G same magnification); 200μm (C).*

2.5. PATHOLOGICAL SUB-TYPING ANALYSIS

MSA cases were assigned a pathological sub-type of SND, OPCA or mixed according to a modification of the published scheme by Ozawa et al. (14) by only assessing the caudate (Cau 3 & 4), putamen (Put 3 & 4), substantia nigra (SbN 4,5,6), pontine base (Pons 2), olive (Olive 1) and cerebellum (CBH) (Fig. 2.2). Neuronal loss is assessed in the above mentioned regions and given a grade of 0 to +3 depending on the severity of cell loss. Neuronal cell loss scores are recorded for each structure and an overall score is given to denote the grade of pathology in StrN and OPC regions (Table 2.4). The combination of StrN and OPC pathology grades is used to assign the case as SND, OPCA or mixed sub-type (Table 2.5). The MSA case is sub-typed as SND if neuronal loss is predominant in the StrN regions, OPCA if neuronal loss is predominant in the OPC regions, and mixed if the neuronal loss score is equal in both regions.

Figure 2.7. Regions for MSA pathological typing analysis
(adapted from Ozawa et al 2004)

Table 2.6. StrN and OPC grading

StrN Grade	
StrN 1	SbN + or ++ with 0 **OR** + in caudate, GP or Putamen
StrN 2	SbN and Putamen ++ **OR** +++ with + **OR** ++ in caudate and GP
StrN 3	SbN and putamen +++
OPC Grade	
OPC 1	Olive, pons or cerebellum 0 or + **OR** only one structure with ++ and others 0
OPC 2	Olive, pons or cerebellum ++ **OR** one area +++ with <++ in remaining 2 areas
OPC 3	Olive, pons or cerebellum +++ in more than 2 regions **OR** +++ in one region and ++ in 1 or 2 other regions

Table 2.7. Assignment of MSA pathological type

Pathological phenotype	Grade of StrN pathology	Grade of OPC pathology	Name of combination
SND type	3	2	SND 3–OPC 2
	3	1	SND 3–OPC 1
	2	1	SND 2–OPC 1
OPCA type	2	3	SND 2-OPC 3
	1	3	SND 1–OPC 3
	1	2	SND 1–OPC 2
Mixed type	3	3	SND 3–OPC 3
	2	2	SND 2–OPC 2
	1	1	SND 1–OPC 1

2.6. DOUBLE/TRIPLE IMMUNOFLUORESCENCE

Double and triple immunofluorescence labelling was carried out using sequential labelling protocol. The antibodies used are presented in

Table 2.8.

aSyn and NG2

Frozen tissue sections were acclimatised to RT before incubating in normal goat serum at a dilution of 1:100 in PBS (Vector Laboratories, Burlingame, CA) for 20 min at RT. They were incubated in the first primary antibody, NG2 (R&D Systems, Minneapolis, MN), at a dilution of 1:200 for 1 hour at RT. After washes in PBS, the tissue sections were incubated with biotinylated goat anti-mouse IgG (Vector Laboratories, Burlingame, CA) at a dilution of 1:200 for 30 min at RT. The sections were incubated in the avidin/biotin (ABC) solution (Vector Laboratories, Burlingame, CA) for 30 min at RT. After washing off the ABC solution, the sections were incubated in fluorophore tyramide amplification reagent working solution of the TSA Plus Fluorescence Systems kit (PerkinElmer, Massachusetts, USA) for 15 min. After washes in PBS, the second primary antibody, αSyn (1:800; Abcam, Cambridge, UK), was then added and incubated for 1 hour at RT. Washing off the primary antibody was followed by incubation in Alexa Fluor® 568 goat anti-rabbit IgG secondary antibody (1:1000; Invitrogen, Paisley, UK) for 1 hour at RT. The secondary antibody was then washed off and the slides were mounted with VECTASHIELD Mounting Medium with DAPI (Vector Laboratories, Burlingame, CA). Autofluorescence

was not dramatically reduced after treatment with Sudan Black, therefore, this step was not further pursued.

aSyn, MBP and CNPase

Frozen tissue sections were acclimatised to RT before incubating in normal goat serum (NGS) for 20 min at RT. The first primary antibody, CNPase (1:100; R&D Systems, Minneapolis, MN), was added for 1 hour RT. After washes in PBS, sections were incubated in Alexa Fluor® 488 goat anti-chicken IgG secondary antibody (1:1000; Invitrogen, Paisley, UK) for 1 hour at RT. The second primary antibody, MBP (1:500; Convance, Cambridge, UK), was then added for 1 hour at RT after washing off the secondary antibody. This was followed by 1 hour incubation at RT in Alexa Fluor® 680 goat anti-mouse IgG secondary antibody (1:1000; Invitrogen, Paisley, UK). After washes in PBS, sections were incubated in the third primary antibody, αSyn (1:800; Abcam, Cambridge, UK). The final secondary antibody, Alexa Fluor® 568 goat anti-rabbit IgG secondary antibody (1:1000; Invitrogen, Paisley, UK), was then added to the sections for 1 hour at RT. After washing in PBS, the sections were mounted with VECTASHIELD Mounting Medium with DAPI (Vector Laboratories, Burlingame, CA).

Qualitative analysis was conducted by systematically scanning the entire section for evidence of co-localisation using widefield and confocal fluorescence microscopy (Leica DM550 and Leica SPE, Leica Microsystems, Milton Keynes, UK).

Table 2.8. Antibodies used in double/triple immunofluorescence

	Host	Dilution	Source (cat. no.)
Primary antibody			
α-synuclein	Rabbit	1:800	Abcam, Cambridge, UK (ab15530)
NG2	Mouse	1:200	R&D Systems, Minneapolis, MN (MAB2585)
CNPase	Chicken	1:100	Abcam, Cambridge, UK (ab50739)
MBP	Mouse	1:500	Convance, Cambridge, UK (SMI-94)
Secondary antibody			
Alexa Fluor® 568 goat anti-rabbit IgG	Rabbit	1:1000	Invitrogen, Paisley, UK (A11011)
Alexa Fluor® 488 goat anti-chicken IgG	Chicken	1:1000	Invitrogen, Paisley, UK (A11039)
Alexa Fluor® 647 goat anti-mouse IgG	Mouse	1:1000	Invitrogen, Paisley, UK (A21235)

2.7. FROZEN TISSUE SAMPLING FOR REGIONAL EXPRESSION STUDIES

Frozen tissue sample (~100mg) were collected from the posterior frontal region (PF; Brodmann area 4), occipital region (OC; Brodmann area 17), dorsal putamen, pontine base and cerebellar white matter of MSA, PD, and control cases. Grey and white matter were separately sampled from the PF and OC. The following landmarks were used to ensure consistency of sampling between the different cases: PF at the level of the pulvinar, OC at the calcarine fissure, putamen at the level of the thalamus, pons at the level of the locus coeruleus and cerebellum at the level of the dentate. The sample were collected in sterile microcentrifuge tubes and stored at -80°C until use.

2.8. STAINING PROTOCOL FOR USE IN LASER CAPTURE MICRODISSECTION

2.8.1. Rapid immunohistochemistry

Frozen sections from the cerebellum (at the level of the dentate nucleus) were cut at 7 μm, collected on uncharged, sterile glass slides and warmed to RT for 30 seconds. They sections were then fixed in ice-cold acetone for 3 min and immunostained using oligodendrocyte-specific protein (OSP) primary antibody (Abcam, UK, ab7474) and VECTASTAIN Elite ABC kit (Vector labs, Burlingame, CA, PK-6101). Sections were blocked with normal goat serum (2%) for 3 min then incubated in OSP (1:10) for 3 min at RT. After a brief rinse with tris-buffered saline (TBS), sections were incubated in 5% biotinylated secondary antibody for 3 min at RT, then rinsed again with TBS. The avidin-biotin complex

solution was then added to the section for 3 min at RT then rinsed off. DAB peroxidase substrate kit (Vector labs, Burlingame, CA, SK-4100) was used to visualise the reaction by incubating section for 3 min at RT. The sections were rinsed with TBS, dehydrated in graded alcohol (70%, 95%, 100%, 100% for 1 min each), cleared in two changes of xylene and allowed to air dry in an air-flow hood for an hour prior to LCM. This rapid IHC protocol was carried out under sterile conditions and using DEPC-treated water.

2.8.2. Toluidine blue nuclear staining

Frozen sections from the pons (at the level of the locus coeruleus) were cut at 7 μm, collected on uncharged, sterile glass slides and warmed to RT for 30 seconds. They sections were then fixed in ice-cold acetone for 3 min and placed in Toluidine blue stain for 1 min at RT. After careful washes in DEPC-water, the sections were dehydrated in graded alcohol (70%, 95%, 100%, 100% for 1 min each), cleared in two changes of xylene and allowed to air dry in an air-flow hood for an hour prior to LCM.

2.9. LASER CAPTURE MICRODISSECTION

PixCell II laser capture microdissection system (Arcturus Engineering, Mountain View, CA, USA) and Arcturus CapSure Macro caps (Applied Biosystems, UK, LCM0211) were used to perform LCM. The following parameters were used to isolate neurons: 7.5 μm spot size, 30 mW power and 20x objective and oligodendrocytes: 7.5 μm spot size, 20 mW power and 20x objective. A CapSure Macro cap was placed on the air-dried, stained section then the infrared laser was fired causing the thermoplastic film of the cap to melt and adhere to the cells of

interest. After microdissection, the film was separated from the cap using sterile tweezers and transferred to a sterile 0.5 mL Eppendorf tube for RNA extraction.

2.10. RNA EXTRACTION OF REGIONAL BRAIN SAMPLES

RNA extraction was carried out using RNeasy Mini Kit (Qiagen). 700 µL of QIAzol to the sample, which was then disrupted and homogenized using TissueRuptor (Qiagen). The homogenized sample was left at RT for 5 min. To the homogenized sample, 140 µL of chloroform was added and the sample vortexed for 30 sec and incubated at RT for 2-3 min. The sample was then centrifuged at 12000 x*g* at 4°C for 15 min. After centrifugation, the aqueous phase (upper layer) was transferred to a sterile 2 mL RNase free tube to which 100% ethanol (1.5x the volume of the aqueous phase) was added and mixed with the pipette to precipitate the RNA. Up to 700 µL of the sample was added into the spin column (including any precipitate) and centrifuged at 10000 rpm at RT for 1 min. Discard flow-through and wash the samples of salt traces and impurities by adding 700µL of the RWT solution and spin the column at 10000 rpm at RT for 1 min. Discard flow-through then add 500µL RPE solution and spin the column at 10000 rpm at RT for 1 min. Discard flow-through and repeat the washing step. Discard flow-through then add 500µL RPE solution and spin the column at 10000 rpm at RT for 2 min. Transfer the column to a new 1.5 mL RNase free tube. Add 25 µL RNase-free water to the column. Let stand for 5 min at RT, then spin at 10000 rpm at RT for 1 min. The elute contains the extracted RNA. RNA quality and concentration was then assessed using the

Nanodrop and Agilent Bioanalyser 2100. The RNA sample may be stored at -80°C.

2.11. RNA EXTRACTION OF LCM SAMPLES

RNA extraction of LCM samples was carried out using the Arcturus PicoPure RNA isolation kit (Applied Biosystems, UK, KIT0204). 50 μL Extraction buffer was added to the sterile tube containing the film with microdissected cells and incubated for 30 min at 42°C. After centrifugation at 800x*g* for 2 min at RT, the film was discarded and the cell extract saved. The RNA Purification Column had to be pre-conditioned by adding 250 μL Conditioning buffer to it, incubating for 5 min at RT then centrifuging at 16000x*g* for 1 min at RT. RNA was precipitated by adding 70% Ethanol to the cell extract and mixed by pipetting. The cell extract/ethanol solution was then transferred to the pre-conditioned column and centrifuged at 100 x*g* for 2 min then 16000 x*g* for 1 min at RT. The column was then subjected to a series of washing steps as follows: 100 μL wash buffer (W1) and centrifuge at 8000 x*g* for 1 min, 100 μL was buffer (W2) and centrifuge at 8000 x*g* for 1 min then 100 μL wash buffer (W2) and centrifuge at 16000x*g* for 2 min at RT. The column was then transferred to a new sterile 1.5 mL Eppendorf tube and 13 μL Elution buffer was added to the column. After a 1 min incubation at RT, the column was centrifuged at 1000 x*g* for 1 min then at 16000x*g* for 1 min at RT. The elute contains the extracted RNA. RNA quality and concentration was then assessed using the Nanodrop and Agilent Bioanalyser 2100. The RNA sample may be stored at -80°C.

2.12. REVERSE TRANSCRIPTION

RNA is reverse transcribed to form cDNA using SuperScript® VILO™ cDNA Synthesis Kit (Invitrogen, UK). According to manufacturer's instructions, the following components are mixed in a tube for a single reaction. For multiple reactions, prepare a master mix without RNA.

Contents	Volume (μL)
5X VILO Reaction Mix	4
10X SuperScript Enzyme Mix	2
RNA (up to 2.5μg)	x
DEPC-treated water	to 20

After gently mixing tube contents, incubate at 25°C for 10 min. After that, incubate at 42°C for 60 min and terminate with a 5 min incubation at 85°C. Store at -20°C until use. cDNA may be used diluted or undiluted for PCR reaction.

2.13. AGAROSE GEL ELECTROPHORESIS

A 2% agarose gel was prepared by adding 2g of agarose to 100mL 1X TAE buffer in a flask and mixed by swirling the flask. This was then heated in the microwave for about 1 min to dissolve the agarose. The flask was then removed from the microwave and allowed to cool down for about a minute at RT after which 5 μL SafeView (NBS-SV1, NBS Biologicals) into gel to help visualize the bands. The gel was then poured into the gel frame and place at 4°C for about 30 min so that it may set.

Once the gel has set, it was placed in the electrophoresis tank containing 1X TAE buffer. Into the first well 4 µL of HyperLadder IV or V (Bioline, UK) was added. Samples were mixed with 5x Orange G and 15µL were loaded into the other wells. The gel was run at 100V for 30 - 45 min. An image of the gel was taken using the Gel capture software.

2.14. QUANTITATIVE PCR (QPCR)

2.14.1. Primers

Primers for the genes of interest (SNCA and SNCA112) were designed in house (Table 2.9). Where the isoform had an exon spliced out, the primer was designed across an exon-exon boundary, reducing contamination through amplification of genomic DNA. Reference genes (*TBP*, *UBC*, *GAPDH*) were designed using RTprimerDB (Table 2.8).

2.14.2. Real-time PCR

Real-time PCR was performed on Stratagene MX3000p (Agilent technologies, CA) using Power SYBR Green Master Mix (Applied Biosystems). According to manufacturer's instructions, a master mix for each gene was prepared by mixing the following components in sterile tubes. The volumes presented are for a single reaction.

Contents	Volume (µL)
Power SYBR Green PCR Master Mix	10
Forward primer (500nM)	1
Reverse primer (500nM)	1
Molecular biology grade water	3

Table 2.9. Alpha-synuclein primer information

Gene	**SNCA**
Gene name	synuclein, alpha (non A4 component of amyloid precursor)
RefSeq no.	NM_001146055.1
Primer sequence	**F:** CAACAGTGGCTGAGAAGACCA **R:** GCTCCTTCTTCATTCTTGCCCA
Alignment	**F:** base 228 to 249 **R:** base 369 to 390
Amplicon sequence	**CAACAGTGGCTGAGAAGACCA**AAGAGCAAGTGACAAA TGTTGGAGGAGCAGTGGTGACGGGTGTGACAGCAGT AGCCCAGAAGACAGTGGAGGGAGCAGGGAGCATTGC AGCAGCCACTGGCTTTGTCAAAAAGGACCAGT**TGGGC AAGAATGAAGAAGGAGC**
Exon	3-5
Amplicon length (bp)	163
Splice variant	Full transcript
Organism	Homo sapiens
Source	In house design

Table 2.10. Reference genes primer information

Gene	TBP	UBC	GAPDH
Gene name	TATA box binding protein	Ubiquitin C	Glyceraldehyde-3-phosphate dehydrogenase
RefSeq no.	NM_003194	NM_021009	NM_002046
Primer sequence	**F:** TGCACAGGAGCCAAGAGTGAA **R:** CACATCACAGCTCCCCACCA	**F:** ATTTGGGTCGCGGTTCTTG **R:** TGCCTTGACATTCTCGATGGT	**F:** GAAATCCCATCACCATCTTCCAGG **R:** GAGCCCCAGCCTTCTCCATG
Alignment	**F:** base 892 to 913 **R:** base 1004 to 1024	**F:** base 399 to 418 **R:** base 511 to 532	**F:** base 313 to 337 **R:** base 413 to 433
Amplicon sequence	TGCACAGGAGCCAAGAGTGAAGAACAGTC CAGACTGGCAGCAAGAAAATATGCTAGAG TTGTACAGAAGTTGGGTTTTCCAGCTAAGT TCTTGGACTTCAAGATTCAGAATATGGTGG GGAGCTGTGATGTG	ATTTGGGTCGCAGTTCTTGTTTGTGGATCG CTGTGATCGTCACTTGACAATGCAGATCTT CGTGAAGACTCTGACTGGTAAGACCATCAC CCTCGAGGTTGAGCCCAGTGACACCATCGA GAATGTCAAGCA	GAAATCCCATCACCATCTTCCAGGAG CGAGATCCCTCCAAAATCAAGTGGG GCGATGCTGGCGCTGAGTACGTCGT GGAGTCCACTGGCGTCTTCACCACC ATGGAGAAGGCTGGGGCTC
Amplicon length (bp)	132	133	120
Organism	Homo sapiens	Homo sapiens	Homo sapiens
Source	RTPrimerDB (ID: 2630)	RTPrimerDB (ID: 8)	RTPrimerDB (ID: 1108)

To 96-well PCR plates, 15μL of the master mix was added to each well. Add 5 μL of diluted sample (1:10) or standards to the wells. The plates were covered using cover strips, placed into the Stratagene and run at the following profile:

Hot start	1 cycle	95°C	10 min
2-step PCR	40 cycles	95°C	15 sec
		60°C	1 min

2.14.3. Reference genes

The number and choice of reference genes was determined using the Stratagene (Agilent Technologies, California) and qBase (Biogazelle, Belgium) softwares. Initial quality control check of the reference genes primers was assessed by melt curve analysis and agarose gel electrophoresis. Only primers that produced a single peak on the melt curve graph and a band at the predicted size on the agarose gel were included in the qBase analysis. A qPCR experiment was set up on the Stratagene using standards and unknown samples for each reference gene. The standard curve produced provides information on the efficiency and dynamic range of the primers. The expression data is then entered into the qBase software. The output of qBase provides gNormM and gNormV values. The gNormM value is indicative of the average expression stability of the gene, while the gNormV value reflects the optimal number of reference genes that need to be used for the experiment. The candidate reference genes tested were

TBP, *UBC*, *GAPDH*, *RPLP0*, *YWHAZ*, *B2M* and *SDHA* and were chosen based on published literature (Vandesompele et al., 2002; Coulson et al., 2008; Trabzuni et al., 2011).

2.14.4. Standards preparation

Pooled cDNA samples from the posterior frontal cortex, pons, and cerebellar white matter of control cases were used to prepare the standards. After running a PCR for each gene, part of the PCR product was run on an agarose gel to check that the predicted product size was obtained. The rest of the PCR product was then cleaned up using the MicroClean kit (Microzone ltd, UK) according to manufacturer's instructions to remove buffers, enzymes, primers, primer dimers and dNTPs. Briefly, an equal volume of microClean solution is added to the PCR product, mixed by pipetting and incubated at RT for 5 min. The mixture is then centrifuged at maximum speed (10 – 13000 rpm) at RT for 7 min. After centrifugation, the supernatant is carefully removed. Another brief spin is required to remove any remaining liquid. The pellet is resuspended in 15µL of TE (10/1 Tris-EDTA) buffer and incubated at RT for 5 min to rehydrate the PCR product. The concentration of the cleaned up PCR product is obtained using the Nanodrop. The number of copies/µL is then calculated using the concentration, molecular weight and product size for each gene. This usually results in an original stock concentration of 10^{10} or 10^{11} copies/µL. From this original stock, the first working dilution (10^8) is prepared in tRNA water (5µg/mL), then serially diluted 10-fold to a final dilution of 10^1. Standards are stored at -20°C until use.

2.14.5. Expression calculation

Real-time qPCR data is analysed using absolute or relative quantification method. The absolute quantification method was adopted for this thesis, where copy number of unknown samples was derived from standard curves for each gene of interest (GOI) and reference genes. The standard curves were produced from a starting material with known copy number as described in section 2.14.4. The GOI was then normalized to the geometric mean of the reference genes as recommended by Vandesompele et al (2002). The mean normalized copy number was then calculated for each region within each disease and control group. Statistical analysis was performed on the mean normalized copy number to extrapolate expression differences.

2.14.6. Statistical analysis

A multilevel statistical model was used for regional expression analysis using STATA 12 software. Data were first controlled for regions to determine expression differences in the different groups and then controlled for groups to determine expression pattern in the different regions and in both cases the significance levels set at 0.05. The Mann-Whitney U test was used to analyse cellular expression data and the significance levels set at 0.05.

2.15. IN-VIVO STEREOTAXIC EXPERIMENTS

2.15.1. Lysate preparation

Inoculation material for mice stereotaxic experiments from MSA, PD and control cases were prepared according to a previously published protocol (Luk et al., 2012 a). About 100 mg of brain tissue from the pontine base of MSA and control cases and cingulate cortex from PD cases were homogenised in 1mL sterile PBS. The homogenate was centrifuged at 3000*g* for 5 min at 4°C. The supernatant is then collected and protein assay run to determine total protein concentration of the sample. The sample is stored at -80°C until use for surgery.

The protocol of Masuda-Suzukake and colleagues (Masuda-Suzukake et al., 2013) was also used to prepare sarkosyl-insoluble lysate only from MSA pontine base for inoculation. Firstly, 1g of tissue is homogenized in 5mL of Buffer A (10mM Tris-HCL pH 7.4, 0.8M NaCl, 1mM EGTA & 10% sucrose). After adding sarkosyl at a concentration of 2% to the homogenate, incubate for 30 min at 37°C. Sonicate then centrifuge the sample at 9100*g* for 10 min at 25°C. Transfer the supernatant to another tube and further centrifuge at 113000g for 20 min at 25°C. this fraction is designated as the sarkosyl-soluble fraction. Wash the pellet with Buffer A then resuspend in saline. After centrifugation at 800g for 5 min, transfer the supernatant to a new tube and designate as sarkosyl-insoluble fraction. A protein assay is run on this fraction to determine the concentration of total protein and then the sample is stored at -80°C until use for surgery.

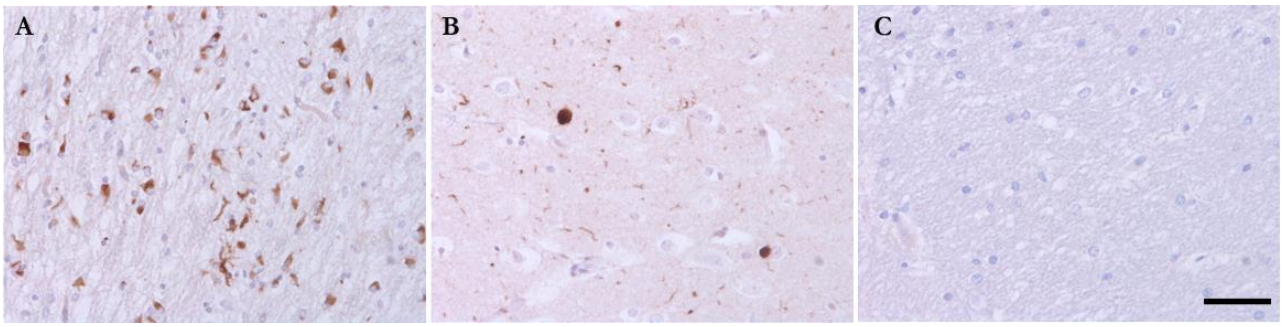

Figure 2.5. Intracerebral inoculation material

Lysates for intracerebral inoculation were prepared from MSA (A), PD (B), and normal control (C) human brain tissue. αSyn-positive GCIs from MSA pontine base and LB from PD cingulate cortex are evident while the normal control brain does not show any αsyn pathology.

asyn: a-synuclein; GCIs: glial cytoplasmic inclusions; LB: Lewy bodies; MSA: multiple system atrophy; PD: Parkinson's disease. Scale bar: 50μm

2.15.2. Protein assay

Pierce BCA Kit (Thermo Scientific) was used to determine total protein concentration. Firstly, standard dilutions were prepared according to manufacturer's instructions as follows, using RIPA buffer as the diluent:

Vial	Volume of Diluent (µL)	Volume & Source of BSA (µL)	Final BSA Concentration (µg/mL)
A	0	300 of Stock	2000
B	125	375 of Stock	1500
C	325	325 of Stock	1000
D	175	175 of vial B dilution	750
E	325	325 of vial C dilution	500
F	325	325 of vial E dilution	250
G	325	325 of vial F dilution	125
H	400	100 of vial G dilution	25
I	400	0	0=Blank

The working reagent was prepared by mixing reagents A and B at a ratio of 50:1. The required volume of working reagent was calculated using the following formula: *(# standards + # unknowns) x (# replicates) x (volume of working reagent per sample; 200µL)*. To a flat-bottomed 96 well plate, 200µL working reagent and 25µL sample are added. After incubation for 30 min at 37°C in the dark, the plate is measured at 562nm (540-590nm acceptable range).

2.15.3. Stereotaxic surgery

C57BL/6JOlaHsd mice (Harlan, Bicester, UK) between 2-4 months of age were anesthetized using isoflurane. The mice were placed on the stereotaxic frame and injected in one hemisphere with either MSA, PD, or control human brain lysates

(5μg total protein). Using a single needle insertion at +0.2mm relative to Bregma and +2.0 from midline, 2.0μL of the inoculum was introduced into the dorsolateral striatum (2.6 beneath the dura) and somatosensory cortex (0.8 beneath the dura) at a rate of 0.15μL/min. The mice were monitored carefully during surgery and after recovery and were then sacrificed at the pre-determined time points of 4 and 30 dpi with a dose of Lethobarb 20% w/v Solution (Ayrton Saunders Limited, UK). After transcardial perfusion with PBS, the brains were removed, fixed in formalin for at least 24 hours, then processed and embedded in paraffin.

3

CLINICO-PATHOLOGICAL STUDIES IN MSA

3.1. COGNITIVE IMPAIRMENT

3.1.1. Introduction

Cognitive impairment (CI) is considered as a non-supporting feature in the diagnosis of MSA according to the second consensus statement on MSA (Gilman et al., 2008). Recent clinical studies, however, have revealed that a proportion of MSA patients do suffer from some degree of cognitive dysfunction (Robbins et al., 1992; Testa et al., 1993; Meco et al., 1996; Wenning et al., 2000; Berent et al., 2002; Bak et al., 2005; Kawai et al., 2008; O'Sullivan et al., 2008; Kao et al., 2009; Kitayama et al., 2009; Brown et al., 2010; Colosimo et al., 2010; Siri et al., 2013). A large prospective study on cognitive function in MSA and PSP estimates that 11-32% of MSA patients are affected by some form of cognitive impairment (Brown et al., 2010). Testa and colleagues found that MSA-P patients performed poorly in visuospatial organization tests and the constructive and visuomotor ability tests in a study comparing the neuropsychological profiles of MSA-P and PD patients (Testa et al., 1993). In a study by Meco and colleagues, MSA-P cases displayed more severe attentional deficits as compared to both PD and normal controls, while long term memory

and verbal fluency were intact (Meco et al., 1996). Comparing cognitive dysfunction across PD, MSA, and DLB disease groups, the greatest impairment was found in the DLB group and the least in the PD group, while the MSA group displayed a range of impairment between those two (Kao et al., 2009). The deficits found in differing degrees across those disease groups include executive and visuospatial functions and memory, but not language. Attention and memory deficits were found in 67.7% of MSA patients in a study of non-motor symptoms in atypical and secondary parkinsonism (Colosimo et al., 2010). Poor performance in spatial short term memory, spatial working memory, planning, and attention set shifting tasks by MSA, PD, and Steele-Richardson-PSP (PSP-RS) patients demonstrates that these three disease groups exhibit frontal lobe dysfunction (Robbins et al., 1994).

In addition to the comparison of cognitive profiles of MSA patients with other disease groups, comparisons between the different MSA subtypes have also been made. Chang and colleagues used voxel-based morphometry of magnetic resonance imaging (VBM-MRI) and neuro-psychological tests to evaluate the relationship between cognitive impairment and brain atrophy in MSA cases (Chang et al., 2009). Both MSA-P and MSA-C patients exhibited diminished cognitive abilities as compared to controls and this correlated with frontal atrophy and disease duration. Also, of the two subtypes, the executive function deficits and dementia were worse in the MSA-C subtype. Similarly, in a cohort of 58 MSA patients, cerebral atrophy and white matter lesions detected by MRI

scans were found in those that showed signs of frontal executive dysfunction and dementia (Kitayama et al., 2009). Ten patients of the 58 showed CI with the impairment developing after the onset of ataxia in seven and before ataxia onset in the other three and all ten patients with CI were of the MSA-C subtype. It must be noted that there were only nine MSA-P patients included in this study, therefore, the predominance of cognitive impairment in the MSA-C subtype does not necessarily suggest that this subtype is more vulnerable to cognitive deficits, rather it may be attributed to a better representation of the MSA-C group as it is the dominant subtype in Asian population. The susceptibility of either MSA subtype to CI is further supported by another study where a greater degree of cognitive dysfunction was evident in MSA-P patients compared to MSA-C (Kawai et al., 2008). MSA-P patients exhibited deficits in visuospatial and constructional function, verbal fluency and executive function while the factors affected in MSA-C were visuospatial and constructional function. The authors suggest that the MMSE is not the most sensitive scale to differentiate MSA cases from others, as MSA patients had similar scores to those of normal controls. Furthermore, there was significant hypoperfusion in the dorsolateral prefrontal cortex, frontal and parietal lobe in MSA cases suggesting a role of these structures in the CI seen in MSA. (Kawai et al., 2008)

These neuropsychometry and neuroradiological studies on MSA indicate that MSA patients exhibit signs cognitive impairment and that it should no longer be considered an exclusion criterion for diagnosis. Neuropathological examination

of MSA patients with signs of cognitive impairment will prove valuable in further understanding the pathogenic mechanisms leading to such deficits. To date there are only three published case reports from Japan detailing the macroscopic and microscopic features of MSA patients with documented cognitive impairment (Wakabayashi et al., 1998; Konagaya et al., 1999; Shibuya et al., 2000). This chapter addresses the issue of limited published clinic-pathological reports on MSA patients with cognitive impairment by assessing the clinical and pathological profile of MSA patients with cognitive impairment as compared to MSA patients with normal cognition.

3.1.2. Hypothesis

MSA patients with clinical evidence of cognitive impairment have more severe pathology in brain regions that are important for cognitive function.

3.1.3. Aim

The aim of this study is to determine if there is a difference in the distribution and burden of pathological changes in MSA patients with cognitive impairment compared with MSA patients with normal cognition. The contribution of concomitant pathologies to cognitive impairment in MSA will also be assessed.

3.1.4. Case selection

Nine MSA cases with documented cognitive impairment and nine with normal cognition were selected in a retrospective analysis of clinical data recorded during life. Cognitive impairment had been assessed by Mini-mental states examination

(MMSE) by neurologists, and in some cases (n=5), formal neuropsychometry testing had been performed by a clinical psychologist. Neuropsychometry tests assess the following parameters: verbal memory, visual memory, working memory, visuospatial/constructive impairment, executive function, and language function (e.g. verbal fluency, comprehension, etc.). An MMSE score of 24-28 (out of 30) is suggestive of mild cognitive impairment (MCI) and ≤23 of dementia. Medical records were reviewed by a neurologist (Helen Ling). Patients with the pathological diagnosis of MSA were categorized as having cognitive impairment (MSA-CI) if their MMSE scores were consistently ≤ 28 and cognitive impairment was documented by a clinician on at least one occasion. The final MMSE score prior to death, presence of depression, hallucinations and the use of additional cognitive tests including formal neuropsychometry to confirm the impairment of cognition were recorded. The control MSA group was matched for age (≤ 5 years difference), sex, disease duration (≤ 1 year difference), and had no documented cognitive impairment (MSA-CN) by clinician or care giver. Patient demographics are displayed in Table 3.1.

3.1.5. Methods

Formalin-fixed paraffin-embedded blocks from the following 14 brain regions were used: anterior frontal, posterior frontal, parietal, temporal, occipital, and cingulate cortices, hippocampus, amygdala, striatum, substantia nigra, pons, medulla and cerebellar hemisphere. Immunohistochemical and routine histological staining techniques were used to assess neuronal loss, GCIs, NCIs

and concomitant pathologies (Aβ, CAA, tau, TDP-43, Lewy bodies, and SVD) as described in Chapter 2: Materials and methods, sections 2.3.

GCI and NCI burden was quantitatively assessed using ImagePro Plus 7.0 software. The systematic uniform random sampling was used to generate 20 counting frames in the regions of interest. Using the systematic uniform random sampling, allows for coverage of the entire region of interest and generation of random counting frames without any overlap. Counting was carried out at x400 magnification and the counting frame was set at 125μm x 125μm. The total number of inclusions counted was divided by the total number of counting frames to give the density measure in 125 μm^2. 'Total cortical load' is the sum of GCI or NCI counts in the neocortical regions (anterior frontal, posterior frontal, parietal, temporal, and occipital cortices) and the 'total limbic load' is the sum of counts of the cingulate cortex, amygdala and hippocampus.

Neuronal loss and concomitant pathologies were assessed in a semi-quantitative manner. The regional severity of neuronal loss was graded on a 0 to +3 scale (Ozawa et al., 2004). Aβ deposition in the form of diffuse and mature plaques was semi-quantitatively assessed in the frontal, temporal, parietal, occipital and entorhinal cortices according to the principles of 'The Consortium to Establish a Registry for Alzheimer's disease' (CERAD) (Mirra et al., 1991; Lashley et al., 2008). Diffuse and mature Aβ plaque semi-quantitative scores in all cortical region were each summed to give a subtotal score (score range 0 to 15) and then

the total diffuse and mature plaque scores were added together to give a total score (score range 0 to 30). Other concomitant pathologies including cerebral amyloid angiopathy (CAA), tau, TDP-43, Lewy bodies, and small vessel disease (SVD) were assessed according to published criteria (Mirra et al., 1991; Braak et al., 2003, 2006; Williams et al., 2007; Lashley et al., 2008; Mackenzie et al., 2010, 2011). Neuropathological assessments were conducted blind to cognitive status by J.L.H and Y.T.A.

Statistical analysis

Statistical analysis was performed using SPSS PASW Statistics 18 software. The Mann-Whitney U test was used to compare GCI and Aβ plaque burden between groups. The significance level for GCI burden was set at $p < 0.004$ after Bonferroni correction for multiple comparisons (0.05/14) and $p < 0.01$ for Aβ plaque burden (0.05/5). The Wilcoxon Mann-Whitney U test or the Student's t test was used to compare semi-quantitative grading or clinical data using p value of 0.05. Intra-rater reliability was assessed by repeating GCI burden quantification in 10% of the cases resulting in an intraclass correlation coefficient (ICC) of 0.989 ($p<0.001$) indicating high reproducibility the analysis.

3.1.6. Results

Demographic and clinical data

There were 12 cases with MSA-P and 6 cases with MSA-C; 5 MSA-P and 4 MSA-C in the CI group and 7 MSA-P and 2 MSA-C in the CN group. The mean age at death was 67 years in the MSA-CI and 67.6 years in the MSA-CN subgroups (Student's t test, p=0.90). The disease duration was 10.2 years in the MSA-CI and 9.6 years in the MSA-CN subgroups (Student's t test, p=0.70). Among the 9 MSA-CI cases, 2 cases had at least one episode of hallucination, which was unrelated to infection or medications. The median score of the final MMSE was 25.8 out of 30 in the MSA CI group, and these scores were tested on average 2.7 years prior to death (Table 3.1).

Table 3.1. Demographic data of the MSA-cognitively impaired (CI) and the MSA-cognitively normal (CN) groups

No.	CI/CN	MSA type	Age	Sex	Disease duration	Cognitive assessment			Depression	Hallucinations
						MMSE (score)	MMSE* (years)	Neuropsychometry test		
1	CI	MSA-P	77	F	16	26	0.9	ND	No	No
2	CI	MSA-P	75	M	9	19	0.3	ND	Yes	Yes
3	CI	MSA-P	82	F	9	26	2.2	ND	No	No
4	CI	MSA-C	54	M	7	25	2	Yes	No	No
5	CI	MSA-P	74	F	8	28	0.5	Yes	Yes	No
6	CI	MSA-C	60	M	6	28	3.9	Yes	No	No
7	CI	MSA-C	57.8	M	12	28	4	Yes	Yes	No
8	CI	MSA-C	56	M	7	26	6.1	ND	No	No
9	CI	MSA-P	66.8	F	19	27	4	Yes	Yes	Yes
10	CN	MSA-P	76	F	8	ND	ND	ND	ND	No
11	CN	MSA-P	63.1	M	12	ND	ND	ND	ND	No
12	CN	MSA-P	54	M	7	ND	ND	ND	ND	No
13	CN	MSA-C	57	M	8	ND	ND	ND	ND	No
14	CN	MSA-P	72	F	8	29	1.7	ND	ND	No
15	CN	MSA-P	76	F	12	ND	ND	ND	ND	No
16	CN	MSA-C	72	F	15	ND	ND	ND	ND	No
17	CN	MSA-P	73	M	9	ND	ND	ND	ND	No
18	CN	MSA-P	65	M	7	ND	ND	ND	ND	No

* No. of years before death at which last MMSE score was taken. *CI: cognitively impaired; CN: cognitively normal; ND: none* documented

Comparison of pathologies between MSA-P and MSA-C

GCI, NCI, neuronal loss and Aβ- pathologies were compared between MSA-P and MSA-C group to determine if any differences exist irrespective of CI status. A statistically significant difference was not established between the two groups in the tested pathologies (Table 3.2). Accordingly, the cases were stratified by presence of CI so that the CI and CN groups were each comprised of both MSA-P and MSA-C cases.

Table 3.2. Comparison of pathologies between MSA-P and MSA-C

Pathology	MSA-P vs. MSA-C (*p*-value)
GCI	0.17
NCI	0.43
Neuronal loss	0.94
Aβ plaques	
Diffuse	0.01
Mature	0.11
Total	0.03

GCI, NCI and neuronal loss: Mann-Whitney U test Bonferroni correction for multiple comparisons at significance level $p<0.004$. Aβ plaques: Mann-Whitney U test Bonferroni correction for multiple comparisons at significance level $p<0.01$.

Glial cytoplasmic inclusions and neuronal cytoplasmic inclusions

GCI burden was quantitatively assessed in all 14 regions (Figure 3.1). Although minor differences were found in the regional GCI load between the MSA-CI and MSA-CN groups these did not reach statistical significance in any region (Mann-Whitney U test after Bonferroni correction, $p>0.004$). Similarly, when the total GCI load in neocortical and limbic regions was calculated in the two groups the small increase in load in the CN group was not found to be statistically significant (Mann-Whitney U test after Bonferroni correction, $p>0.004$). GCIs were abundant in StrN (caudate, putamen, substantia nigra) and OPC (inferior olivary nucleus, pontine nuclei, cerebellar white matter) regions but there was no difference in the total GCI burden in these regions between the CN and CI patients (Mann-Whitney U test after Bonferroni correction, $p>0.004$). NCI burden was quantitatively assessed in the same manner as GCIs, however, none were detected in either MSA-CI or MSA-CN cases.

Neuronal loss

Neuronal loss in the neocortical and limbic regions in the MSA-CI and MSA-CN groups was not detected using semi-quantitative analysis. Both groups demonstrated neuronal loss in the StrN and OPC regions, however, a statistically significant difference was only observed in the cerebellar Purkinje cells where there was greater neuronal loss in MSA-CI (Mann-Whitney U test after Bonferroni correction, $p=0.001$) (Figure 3.2).

Concomitant pathologies

Assessment of Aβ-pathology revealed that, although both diffuse and mature Aβ deposits were more abundant in the MSA-CN group than the MSA-CI group, these did not individually, or in combination, reveal a statistical difference between the two groups (Figure 3.3). Tau-positive neurofibrillary tangles and neuropil threads were observed in cases from both groups (Figure 3.4). Using Braak and Braak staging for Alzheimer disease-associated neurofibrillary pathology (Braak et al., 2006), the degree of pathology in both groups reached a maximum of Braak & Braak stage II. The severity of Braak stages did not differ between the MSA-CI and MSA-CN groups (Wilcoxon rank-sum test, $p=0.78$) (Table 3.3). There was no difference between the proportion of cases with SVD (Wilcoxon rank-sum test, $p=1.00$) between the two groups. CAA was not present in the CI group, while there were two cases with mild and two cases with moderate CAA in the CN group (Mann-Whitney U test, $p=0.03$). Sparse Lewy body pathology was present in only two MSA-CI cases, in the substantia nigra of one case and in the substantia nigra and locus coeruleus of the other. TDP-43 inclusions were not detected in either MSA-CI or MSA-CN cases.

Figure 3.1 A

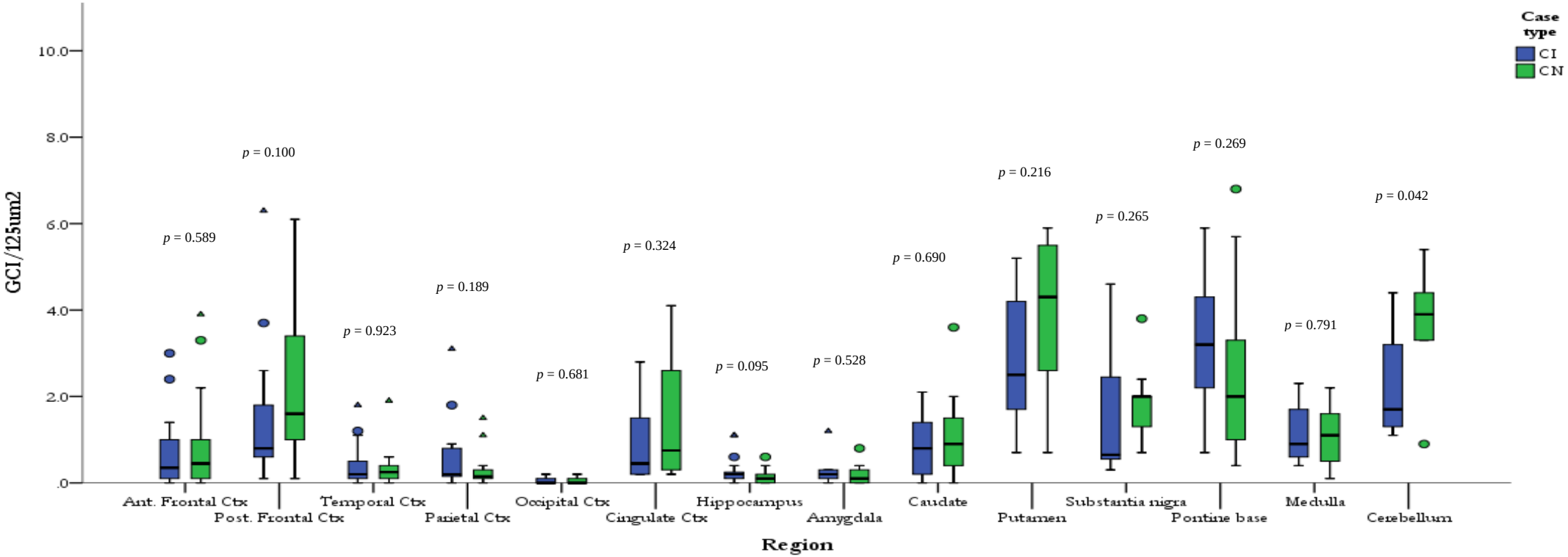
Case type
CI
CN
GCI/125um2
10.0
8.0
6.0
4.0
2.0
.0
p = 0.589
p = 0.100
p = 0.923
p = 0.189
p = 0.681
p = 0.324
p = 0.095
p = 0.528
p = 0.690
p = 0.216
p = 0.265
p = 0.269
p = 0.791
p = 0.042
Ant. Frontal Ctx
Post. Frontal Ctx
Temporal Ctx
Parietal Ctx
Occipital Ctx
Cingulate Ctx
Hippocampus
Amygdala
Caudate
Putamen
Substantia nigra
Pontine base
Medulla
Cerebellum
Region

Figure 3.1. B

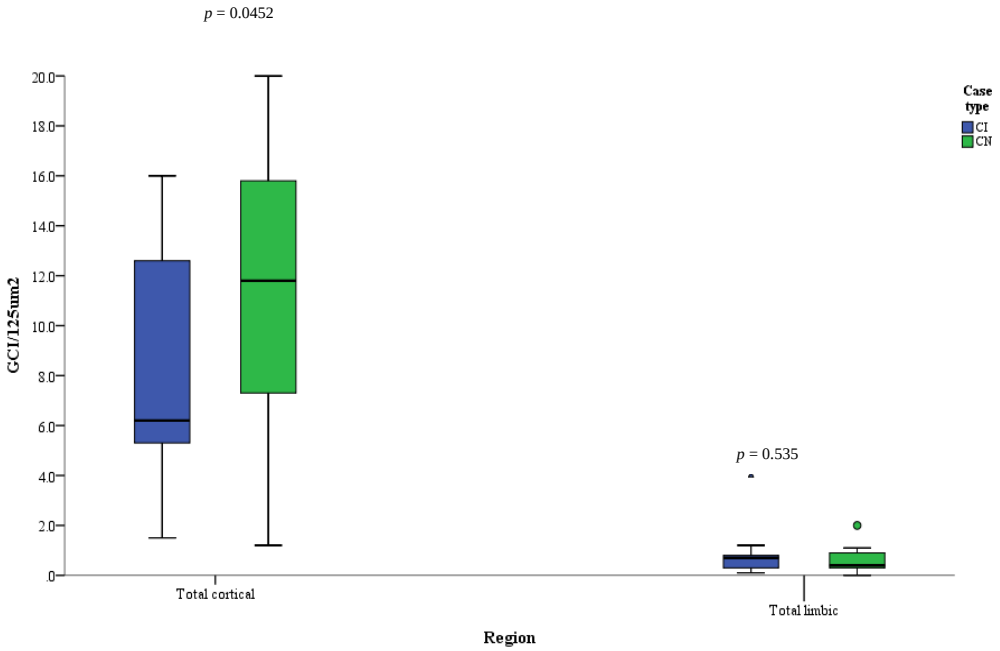

Figure 3.1. GCI burden in MSA patients with CI and normal cognition

GCI load in all regions (A) and total cortical and limbic region counts (B). There was greater GCI load in the MSA-CN than MSA-CI groups however these results did not reach statistical significance (Mann-Whitney U test, $p>0.004$). *The plots show median values as the line within the box, the box reflects the interquartile range and the whiskers the range of the values. Mann-Whitney U test with Bonferroni correction for multiple comparisons was used and significance level set at p <0.004. CI: cognitively impaired; CN: cognitively normal; ∘outliers; ▲extreme outliers.*

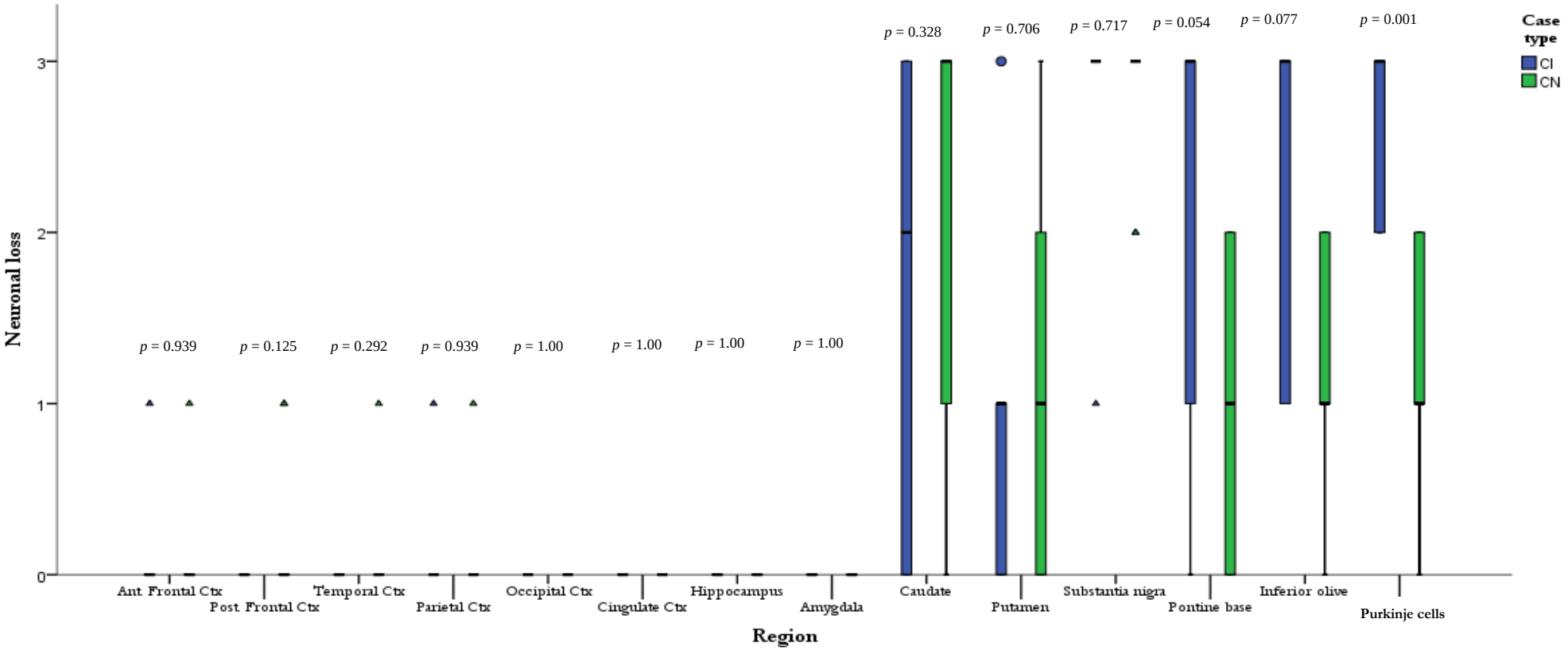

Figure 3.2. Neuronal loss in MSA patients with CI and normal cognition

Neuronal loss was most evident in the striatonigral and olivopontocerebellar regions, however, a statistically significant difference was only observed in the cerebellum where there was greater neuronal loss in MSA-CI. *The plots show median values as the line within the box, the box reflects the interquartile range and the whiskers the range of the values. Mann-Whitney U test with Bonferroni correction for multiple comparisons was used and significance level set at p <0.004. CI: cognitively impaired; CN: cognitively normal; ●outliers; ▲extreme outliers*

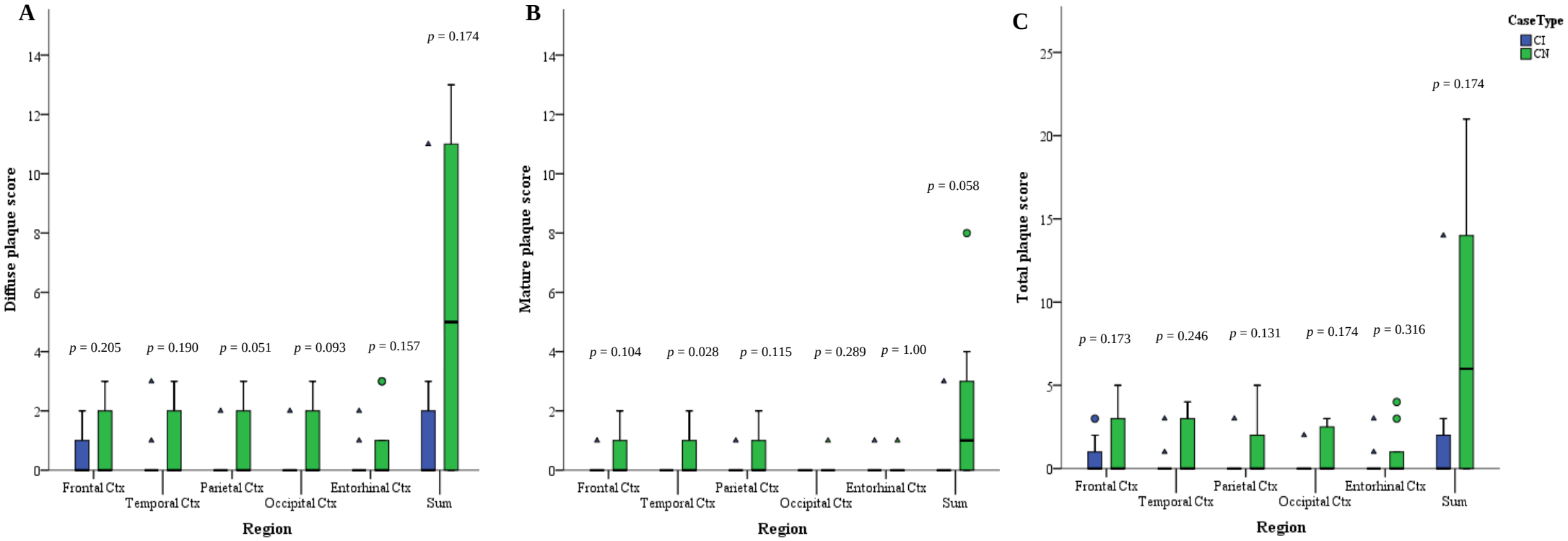

Figure 3.3. Aβ plaque burden in MSA patients with CI and normal cognition

Regional and total amyloid-β diffuse (A), mature (B), and diffuse + mature (C) plaque scores in MSA patients with CI (n=9) and normal cognition (n=9). The burden of Aβ pathology is greater in MSA patients with normal cognition than those with CI, however, these findings did not reach statistical significance (Mann-Whitney U test with Bonferroni correction for multiple comparisons at significance level p <0.01). The plots show median values as the line within the box, the box reflects the interquartile range and the whiskers the range of the values. *CI: cognitively impaired*; •*outliers;* ⋆*extreme outliers*

	Braak & Braak AD tau stage						CAA grade				SVD grade			
	0	**I**	**II**	**III**	**IV**	**V**	**0**	**1**	**2**	**3**	**0**	**1**	**2**	**3**
CI *(n=9)*	3 (33.3%)	3 (33.3%)	3 (33.3%)	0	0	0	9 (100%)	0	0	0	7 (77.8%)	1 (11.1%)	0	1 (11.1%)
CN *(n=9)*	2 (22.2%)	4 (44.4%)	3 (33.3%)	0	0	0	5 (55.6%)	2 (22.2%)	2 (22.2%)	0	7 (77.8%)	1 (11.1%)	0	1 (11.1%)
***p*-value**	0.78						0.03				1.00			

Table 3.3. Concomitant pathology in MSA patients with cognitive impairment and normal cognition

Braak & Braak Alzheimer's disease (AD) tau staging, cerebral amyloid angiopathy (CAA) and small vessel disease (SVD) were analysed in each case. No statistically significant difference was observed in the Braak and Braak stage or grade of small vessel disease between the MSA groups (Wilcoxon rank-sum test, p=0.78 and p=1.00). CAA was only observed in four MSA-CN cases which had mild to moderate CAA pathology (Wilcoxon rank-sum test, $p=0.03$).

CI: cognitively impaired; CN: cognitively normal; AD: Alzheimer's disease; CAA: cerebral amyloid angiopathy; SVD: small vessel disease.

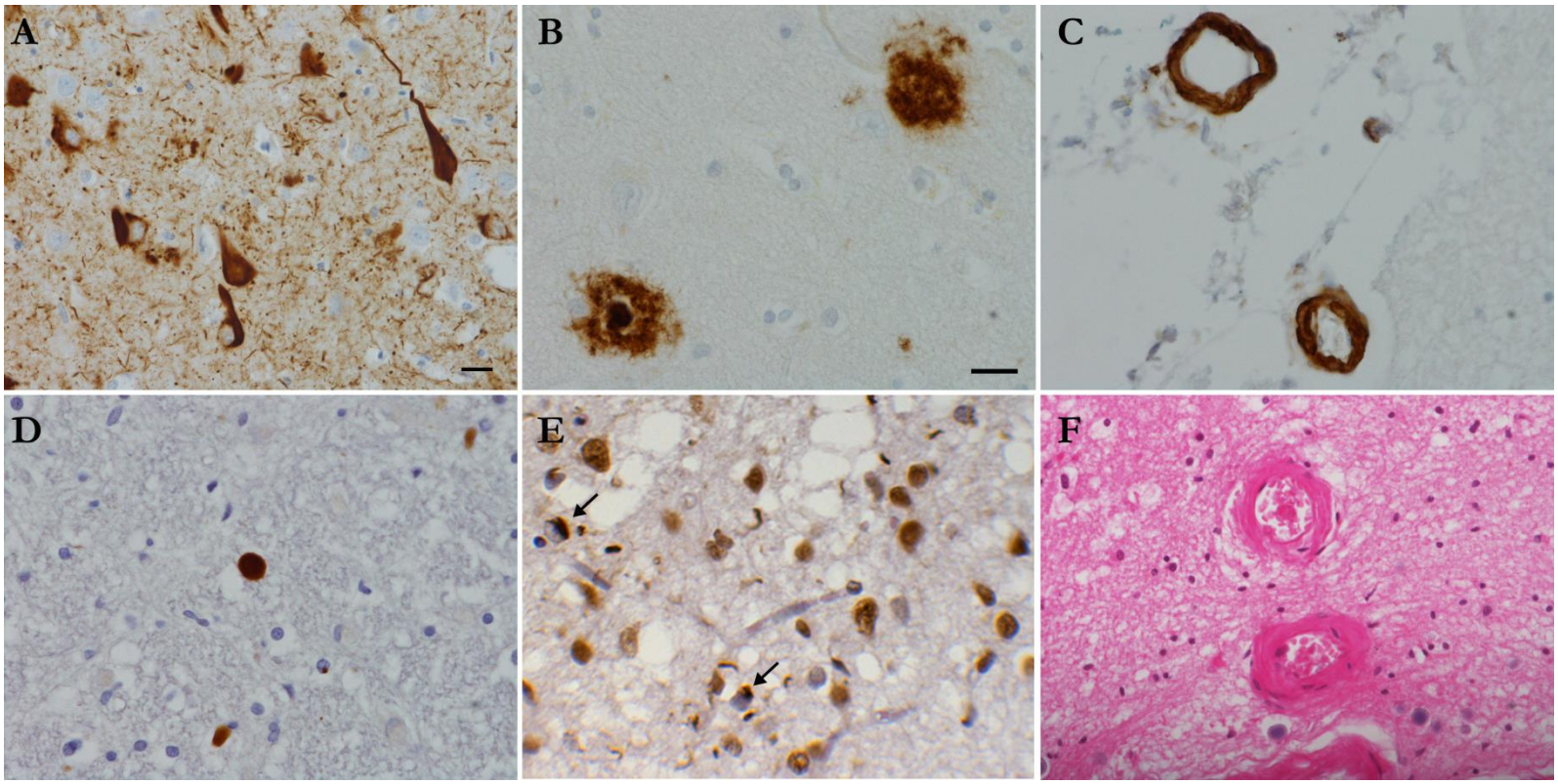

Figure 3.4. Concomitant pathologies

Concomitant pathologies screened for include tau, parenchymal Aβ deposition, cerebral amyloid angiopathy (CAA), TDP-43, Lewy bodies, and small vessel disease (SVD). Tau pathology is demonstrated by NFT and threads using AT8 immunohistochemistry (A; case 5, hippocampus). Mature and diffuse Aβ plaques are markers of Aβ pathology (B; case 14, frontal cortex), while Aβ deposition around blood vessels is indicative of CAA (C; case 12, occipital cortex). Lewy body as demonstrated by αSyn immunohistochemistry (D; case 2, locus coeruleus). TDP-43 normal and pathological (arrows) staining demonstrated with TDP-43 immunohistochemistry, however, TDP-43 pathology was not present in the cohort of this thesis. (E). Thickened walls of blood vessels is a sign of SVD (F; case 5, striatum). *Scale bar: A, F: 20μm; B-E: 20μm*

3.1.7. Discussion

The second consensus on MSA states that signs of impaired cognition are grounds for disregarding a diagnosis of MSA. However, this view has been challenged by neuropsychological studies documenting CI in MSA patients and by some case studies of pathologically confirmed MSA patients reported to have CI (Testa et al., 1993; Wakabayashi et al., 1998; Konagaya et al., 1999; Shibuya et al., 2000; Soliveri et al., 2000; Lange et al., 2003; Krishnan et al., 2006; Kawai et al., 2008; O'Sullivan et al., 2008; Brown et al., 2010). The most common presentation of cognitive abnormality in MSA is fronto-subcortical executive dysfunction followed by memory and visuospatial impairment (Testa et al., 1993; Robbins et al., 1994; Meco et al., 1996; Kao et al., 2009; Colosimo et al., 2010). Functional imaging studies demonstrated fronto-striatal dysfunction (Kawai et al., 2008) and hypoperfusion in prefrontal, frontal, temporal and parietal regions, which are probably the consequence of subcortical deafferentation of the cortical regions (De Volder et al., 1989; Gilman et al., 1994; Otsuka et al., 1996; Lee et al., 2008 b). In this study, the pathological profiles of MSA patients with documented cognitive impairment and those with normal cognition were evaluated to elucidate possible mechanisms leading to diminished cognitive function. Regional GCI burden and neuronal loss were analysed in addition to Alzheimer's pathology and other additional pathological changes.

Cortical and limbic regions play an important role in cognitive function, therefore, pathology in these structures may lead to CI. In this study, a statistically significant difference in the GCI burden in cortical or limbic regions

between the MSA-CI and MSA-CN groups was not established. Despite the presence of GCIs in these regions, neuronal loss was minimal. The microscopic findings of the cohort of this thesis are similar to three Japanese case reports of MSA patients with cognitive impairment showing widespread GCIs and minimal neuronal loss in cortical regions (Wakabayashi et al., 1998; Konagaya et al., 1999; Shibuya et al., 2000). The macroscopical findings, however, were unremarkable in both the CI and CN groups of the cohort of this thesis, unlike the Japanese case reports where frontal or temporal lobe atrophy was reported. The minimal difference in GCI and neuronal pathology between these two groups demonstrated in the current study may suggest that they do not play a primary role in the development of cognitive dysfunction in MSA.

The concept of subcortical dementia refers to cognitive disturbances caused by primary pathology in the basal ganglia, brainstem and cerebellum (Turner et al. 2002). Therefore, greater subcortical pathology in the CI group may contribute to their altered cognitive profiles. There was widespread GCI pathology and neuronal loss in the StrN and OPCA regions in this cohort, however, a statistically significant difference was not observed between CI and CN group. As such, CI in MSA may not be contributed to by GCI and neuronal subcortical pathology.

MMSE scores were used to categorise MSA cases into the cognitively impaired and normal groups. MMSE is widely used to assess cognitive impairment both as a screening tool and for purposes of diagnosis, however, its reliability has been challenged in the literature (Lopez et al., 2005; Mitchell, 2009; Nieuwenhuis-

Mark, 2010). The MMSE detects global cognitive impairment and has been shown to not be very reliable in distinguishing MCI in normal aging population and those with early dementia (Mitchell, 2009). As a test of global cognitive impairment, the MMSE is not informative on the specific domain affected and does not detect impairment in executive function (Lopez et al., 2005). This calls into question the usefulness of the MMSE on patients with MSA whose leading cognitive impairment is fronto-subcortical executive dysfunction (Testa et al., 1993; Robbins et al., 1994; Meco et al., 1996; Kao et al., 2009). Therefore, using neuropsychometry tests designed to detect executive dysfunction maybe better suited for classifying MSA patients with cognitive impairment. Despite its limitations, the wide use of the MMSE renders it the most common measure of cognition in medical records and that is why it was employed as one measure to assess the cognitive state of the cohort of this study by retrospective analysis of clinical notes. The neurologists' and carers' judgement of cognitive decline which was significant enough to affect the patient's activities of daily living was also included in the inclusion criteria in this study to improve sensitivity.

Concomitant involvement of Alzheimer's pathology in the form of Aβ plaques and tau pathology could also contribute to the cognitive impairment observed in MSA. Aβ plaques and tau load were analysed in this cohort. Aβ diffuse and mature plaques were quantified in the frontal, temporal, parietal, occipital and entorhinal cortices. Both diffuse and mature Aβ plaques were more abundant in the CN group. In addition, no cases scored above a Braak and Braak stage II for Alzheimer's disease tau staging and the proportion of cases with tau pathology in

the CI group is similar to that in the CN group. These findings are interesting as a synergistic relationship between αsyn and Alzheimer's pathology has been demonstrated in PD, the most common α-synucleinopathy (Masliah et al., 2001; Lashley et al., 2008; Compta et al., 2013). Furthermore, a detailed study of PD cases with and without documented dementia showed that a combination of the degree of αsyn, tau and Aβ pathology best predicted the occurrence of dementia (Compta et al., 2011). This synergistic relationship was not observed in MSA patients of this cohort, suggesting αsyn pathology in MSA is not associated with an increase in tau or Aβ aggregation suggesting differences in the properties of αsyn in MSA and PD. Additional pathological changes were also assessed. Lewy body pathology, TDP-43 pathology, CAA and SVD were uncommon in this cohort, and therefore, are unlikely to contribute to CI in MSA.

Future studies to address the mechanism of cognitive impairment in MSA may investigate loss of synaptic connectivity and neurotransmitter abnormalities. There is evidence in the literature that synaptic pathology plays a role in psychiatric and neurological disorders (Blanpied and Ehlers, 2004; Gouras et al., 2010; van Spronsen and Hoogenraad, 2010). Alterations in the synaptic connections and proteins due to αsyn accumulation has been demonstrated in DLB, PD and PD with dementia patients and in cell culture models (Schulz-Schaeffer, 2010; Scott et al., 2010). These studies justify the examination of synaptic pathology in MSA as it may prove to be the determining factor for cognitive impairment.

Neurotransmitter (acetylcholine, serotonin, noradrenaline, and/or dopamine) depletion has been shown in AD, vascular dementia and PD and is suggested as a contributing factor, if not the major factor, in the development of dementia (Perry et al., 1987; Court and Perry, 2003; Alisky, 2006; Hirano et al., 2012). Loss of cholinergic, catecholaminergic and serotonergic neurons have been demonstrated in MSA (Kato et al., 1995; Benarroch et al., 1998, 2001, 2002, 2004; Tada et al., 2009). Therefore it is possible that the loss of these neurons results in reduced neurotransmitter levels, which in turn, affects the function of their target sites, which include cortical regions. Radiological, biochemical and neuropathological testing of these neurotransmitters in addition to correlations with neuropsychological tests will shed light into the extent of involvement of neurotransmitter depletion to cognitive impairment in MSA.

Conclusion and further directions

CI may be intrinsic to the MSA disease process as it is independent of Alzheimer's pathology and other concomitant pathologies. Increased GCI load and neuronal loss in cortical, limbic and subcortical structures are not however related to CI in MSA. Further investigation of synaptic pathology, neurotransmitter abnormalities, subcortical deafferentation and correlating of neuropsychological, radiological and neuropathological findings are warranted to elucidate the pathogenic substrates leading to cognitive impairment in MSA.

3.2. LONG DURATION AND MINIMAL CHANGE MSA

3.2.1. Introduction

MSA is an adult onset disease usually presenting in the fifth decade of life and with a mean disease duration of 6-9 years (Wenning et al., 1994 b; Ben-Shlomo et al., 1997; Watanabe et al., 2002; Gilman et al., 2008; Schrag et al., 2008). It is clinically diagnosed as MSA-P or MSA-C based on predominant parkinsonian or cerebellar presentations respectively, in addition to definite, probable, and possible with regards to certainty of the diagnosis (Gilman et al., 2008). Neuropathological confirmation is needed for a definite diagnosis. MSA is pathologically subtyped as SND, OPCA or mixed type reflecting the degree of neuronal loss in StrN and OPC structures (Ozawa et al., 2004). As with other diseases, there are MSA patients who do not follow the 'classical' presentation of the disease as they display variations in neuropathological and/or clinical profiles. It is important to note these 'non-classical' MSA patient groups and explore any clinico-pathological correlations that may exist in them. Long disease duration and the minimal change MSA are two examples of such groups.

Long disease duration MSA refers to patients who experience a disease course that can last over 10 years (Wenning et al., 1994 b; Masui et al., 2011; Piao et al., 2001; Wakabayashi et al., 1998; Konagaya et al., 1999). Due to the rarity of such patients, there are few published reports detailing the clinical and pathological presentation of long duration MSA (Wakabayashi et al., 1998; Konagaya et al., 1999; Piao et al., 2001; Masui et al., 2011; Petrovic et al., 2012). Factors contributing to speed of deterioration and survival in MSA are unclear, however,

autonomic failure and early respiratory irregularities have been shown to be poor prognostic factors (Watanabe et al., 2002; O'Sullivan et al., 2008; Tada et al., 2009). The leading causes of mortality in MSA are sudden unexpected death (SUD) and infection (Munschauer et al., 1990; Sadaoka et al., 1996; Wakabayashi et al., 2005; Papapetropoulos et al., 2007; Shimohata et al., 2008; Tada et al., 2009).

Minimal change MSA is a pathological characterisation reflecting restricted neuronal loss to the substantia nigra and locus coeruleus, unlike the typical distribution in MSA where neuronal loss is evident in multiple structures of the StrN and OPC pathways (Wenning et al., 2002; Wakabayashi et al., 2005; Wenning et al., 1994 a; Huang et al., 2005). In the cases described by Wenning and colleagues (Wenning et al., 1994 a), the neuropathological examination of two patients who presented with parkinsonism and autonomic failure revealed neuronal loss that was confined to the substantia nigra and locus coeruleus while GCIs were found in abundance throughout the brain. Neuronal loss limited to OPC regions in addition to widespread GCIs was reported by Wakabayashi and colleagues (Wakabayashi et al., 2005) in a patient who presented with cerebellar signs, dysarthria, and saccadic eye movement.

This section focuses on assessing neuropathological changes in long duration and minimal change MSA and to compare these with MSA cases having a typical disease duration and spectrum of neuronal loss to uncover substrates that may contribute to the different clinico-pathological presentation of these sub-groups.

3.2.2. Hypothesis

The distribution and severity of pathological changes in patients with long disease duration or minimal change MSA differs from typical MSA group.

3.2.3. Aim

The aim of this study is to determine the distribution and burden of pathological changes in long disease duration and minimal change MSA as compared to control (typical) MSA cases and to explore possible clinico-pathological correlations.

3.2.4. Case selection

Four cases in the long duration (one of which was provided by Toronto Western Hospital), six in the minimal change and eight control MSA cases were selected from the archives of QSBB. Cases were included into the long duration group if they had a disease duration ≥15 years. The minimal change group is a pathological characterization where cases have neuronal loss restricted to the substantia nigra and/or locus coeruleus. Patients in the control MSA group are those that have a more 'classical' presentation i.e. a disease duration of 5-10 years and neuronal loss not restricted to either the substantia nigra or locus coeruleus. The cases in the long duration and minimal change MSA were age (≤ 5 years difference) and sex – matched with the controls. The demographics of this cohort are presented in Table 3.5.

3.2.5. Methods

Formalin-fixed paraffin-embedded (FFPE) blocks from the following regions were used: anterior frontal, posterior frontal, parietal, temporal, occipital and cingulate cortices, hippocampus, amygdala, basal ganglia, substantia nigra, pons, medulla and cerebellum. Immunohistochemical and routine histological staining techniques were used to assess neuronal loss, GCIs, NCIs, gliosis, and concomitant pathologies (Aβ, CAA, tau, TDP-43, Lewy bodies, and SVD) as described in 2 Materials and methods, sections 2.3.

Neuronal loss was assessed in haematoxylin and eosin stained sections. Gliosis was determined using immunohistochemical staining for glial fibrillary acidic protein (GFAP) and both GCIs and NCIs were visualized using αsyn immunohistochemistry. The following regions were investigated: neocortex (anterior frontal, posterior frontal, temporal, parietal, occipital, cingulate), hippocampus, amygdala, caudate, putamen, globus pallidus, substantia nigra, pontine nuclei, inferior olivary nucleus and Purkinje cell layer. MSA subtype was determined by semi-quantitative assessment of neuronal loss in the caudate, putamen, globus pallidus, substantia nigra, pontine nuclei, inferior olivary nucleus and Purkinje cell layer based on a published method (Ozawa et al., 2004). GCIs, NCIs, neuronal loss and gliosis were graded on a 0 to +3 scale to reflect the severity of pathology as described (Ozawa et al., 2004). Concomitant pathologies: cortical Aβ deposition (neuritic plaque frequency), cerebral amyloid angiopathy (CAA), tau deposition, TDP-43 immunoreactive inclusions, Lewy bodies, and small vessel disease (SVD) were assessed according to published criteria as

described previously (Mirra et al., 1991; Braak et al., 2003, 2006; Williams et al., 2007; Lashley et al., 2008; Mackenzie et al., 2010, 2011). Neuropathological assessments were conducted by J.L.H and Y.T.A. Intra- and inter-rater reliability was assessed by re-analysing 10% of slides.

Statistical analysis

Statistical analysis was performed using SPSS PASW Statistics 18 software. Intra-rater reliability was assessed by intraclass correlation coefficient (ICC) and inter-rater reliability by using Cohen's Kappa. Comparisons between groups were performed using the Mann-Whitney U test and the level of statistical significance was set at $p < 0.05$. Where Bonferroni's correction for multiple testing was applied, the significance level was set at $p<0.003$. $\chi 2$ / Fisher's exact test was used to compare gender groups (significance level set at $p < 0.05$).

3.2.6. Results

Demographic and clinical data

Details of age and gender of the 3 patient groups are provided in Table 3.4. There was no significant difference in the distribution of gender and age of disease onset between the groups. A statistically significant difference was found in the duration of disease between the groups with the long duration cases having a longer disease duration than control MSA (Mann-Whitney U, p=0.006) while the minimal change MSA group had a shorter disease duration than control MSA (Mann-Whitney U, p=0.037). The clinical details of the cases are presented in Table 3.5.

Minimal change MSA

Three out of six patients presented with parkinsonism while the remaining presented with autonomic features. Mean disease duration was 5 years and all patients fulfilled clinical criteria for MSA diagnosis after a mean interval from first symptom onset of 18.7 months. Cerebellar ataxia, pyramidal signs and cognitive impairment were not present in this group of patients. All cases developed significant respiratory symptoms most frequently inspiratory stridor and episodes of unprovoked or exertional dyspnea. The cause of death was SUD in three patients while others succumbed because of pulmonary embolism, suicide and multiple myeloma respectively. All cases reached at least one disease disability milestone after a mean of 3.2 years from disease onset and 1.8 years

before death. The subgroup of SUD cases reached the majority of disability milestones, specifically all cases reached wheelchair or gait tool use state. Those cases dying due to concurrent disease reached only one disability milestone and all of them were ambulatory in the period near to death. More precisely, only one patient from this subgroup reached the frequent falls state 6 years after disease onset. In addition, recurrent postural faintness or syncope was present in all patients succumbing from SUD after a mean latency of 7.3 months.

Long duration MSA

All 4 patients presented with the cardinal signs of parkinsonism. The mean interval from first symptom onset to evolution to criteria-defined MSA was 11.3 years. Recurrent postural faintness or syncope was present in two patients after a mean latency of 12.5 years. Initial levodopa response was considered good in one, moderate in two, and poor in one patient. All patients developed dyskinesia after a mean duration of levodopa treatment of 4.3 years. Two patients (one of which corresponds to case 9 in CI cohort) had MMSE of less than 26 out of 30, 12 and 15 years after first symptom onset; one of whom developed visual hallucinations and dementia 17 years after the first motor symptom in the final year of her life. Frequent falling was the first activities of daily living (ADL) milestone to occur in all patients with a mean latency of 12 years. Mean latencies to wheelchair dependence, unintelligible speech and urinary catheterisation were between 12 to 13 years.

Glial and neuronal cytoplasmic inclusions

GCI burden was assessed using a semi-quantitative method in all groups and comparisons were made between the following pairs: long duration and control MSA group; minimal change and control MSA group; long duration and minimal change group (Figure 3.5). GCI score was greater in the striatum and substantia nigra in the long duration group as compared to control MSA, while it was similar in both groups in the pons, inferior olivary nucleus and cerebellum. A greater GCI burden in long duration cases was also seen in cortical and limbic regions with the exception of the occipital cortex and amygdala where they were similar. The cingulate cortex had a higher GCI burden in controls. However, statistical significance was only reached in the caudate which showed greater numbers of GCIs than control MSA cases (Mann-Whitney U, p=0.002).

In the minimal change group the GCI burden in the striatum, substantia nigra, cerebellum and hippocampus was greater than in the control MSA cases. In contrast with the long duration group, the minimal change cases showed a lesser degree of GCI pathology in the cortical regions as compared to control MSA. However, statistical significance was not reached in any of these regions (Mann-Whitney U, p>0.003). Microscopic findings of a representative case of minimal change MSA is shown in Figure 3.9.

Comparisons between the long duration and minimal change groups indicated that the long duration group shows a higher burden of GCI pathology in all of the regions analysed with the exception of the putamen, globus pallidus and

cerebellum, but statistical significance was only reached in the anterior frontal and temporal cortices (Mann-Whitney U, p=0.001).

NCIs were most abundant in the inferior olivary nucleus and least frequent in the occipital cortex in all groups (Figure 3.6). With the exception of the cingulate cortex, putamen and pons, NCI burden was greater in long duration cases than control MSA cases in StrN and OPC regions as well as in the frontal cortex, hippocampus and amygdala but statistical significance was only reached in the caudate (Mann-Whitney U, p=0.00).The StrN and OPC regions of the minimal change group had a greater NCI burden than controls, with a statistical significance reached in the caudate and substantia nigra where there was an increased NCI burden compared with control MSA cases (Mann-Whitney U, p=0.002 and p=0.00 respectively) but no statistical difference was found between minimal change and long duration cases in these regions.

Neuronal loss

In keeping with the selection criteria neuronal loss in the minimal change group was restricted to the substantia nigra with the exception of one case with +1 loss in posterior putamen (Figure 3.7). A statistically greater degree of neuronal loss in control MSA compared with the minimal change group was confirmed in the caudate, putamen, globus pallidus and pons (Mann-Whitney U, p<0.003)

Neuronal loss in cortical and limbic regions of long duration and minimal change cases was not detected and was only mild in control MSA cases in the frontal and

parietal cortices (Figure 3.7). The long duration cases showed no statistical difference in neuronal loss compared with the control cases in any of the regions examined.

Gliosis

Gliosis assessed using GFAP immunohistochemistry was present in all of the regions assessed in all cases (Figure 3.8). There was no statistically significant difference in the degree of gliosis between the control MSA and the long duration MSA. When comparing the minimal change and control MSA groups gliosis was significantly increased in the control MSA group the putamen, caudate, pons and cerebellar white matter (Mann-Whitney U, $p<0.003$).

Concomitant pathologies

The cases were examined for Alzheimer tau pathology and Braak and Braak staging was determined. Tau pathology was observed in long duration and control MSA cases only reached a maximum of Braak and Braak stage II. Neuritic Aβ plaques were also restricted to long duration and control groups. CAA and SVD were only observed in five cases in the control MSA group, with one case having severe CAA and SVD while the others were mildly affected. Lewy bodies were not identified in brain stem nuclei in any of the cases and none had TDP-43 pathology (Table 3.6).

Table 3.4. Patient demographics for MSA subgroups

	Long duration MSA	**Control MSA**	***P*-value**
n	4	8	
Gender (%)	4 (100) female	6 (75) female	0.515
Age of onset (years)	50.8 ± 8.1	58.8 ± 10.9	0.126
Disease duration (years)	17.3 ± 1.7	8 ± 2.9	0.006

	Minimal change MSA	**Control MSA**	***P*-value**
n	6	8	
Gender (%)	1 (16.7) female	6 (75) female	0.103
Age of onset (years)	47.8 ± 11.5	58.8 ± 10.9	0.137
Disease duration (years)	5 ± 1.8	8 ± 2.9	0.037

Data expressed as ± SD except for gender as *n* (percentage) female. Mann-Whitney test was applied except for gender where the chi-square test was used.

Table 3.5. Clinical details of long duration, minimal change, and control MSA cases

	Age at onset	Disease duration (years)	Initial presentation	Second system involvement (latency in months)	Additional autonomic symptoms (latency in months)	Cerebellar signs	Pyramidal signs	Respiratory symptoms	Cause of death	Concomitant diseases	MSA pathological type
LD-MSA 1	62	15	Parkinsonism	Autonomic UI (132)	No	No	No	No	Bronchopneumonia	ND	SND
LD-MSA 2	50	17	Parkinsonism	Autonomic UI (108)	Postural faintness and syncope (120)	No	Yes	IS	Bronchopneumonia	ND	SND
LD-MSA 3	48	19	Parkinsonism	Autonomic UR (132)	No	No	No	No	Bronchopneumonia	ND	Mixed
LD-MSA 4	43	18	Parkinsonism	Autonomic OH (168)	Postural faintness (168)	Yes	Yes	IS		ND	OPCA
MC-MSA 1	57.5	7.5	Autonomic (OH)	Parkinsonism (12)	Nocturia (18) Erectile dysfunction (18) Urinary retention	No	Yes	Acute unprovoked dyspnoea; IS	Pulmonary embolism and infarct	Prostatic hyperplasia	SND
MC-MSA 2	33.5	5.5	Parkinsonism	Autonomic UR; UF (12)	OH (14)	No	Yes	IS	Sudden death	ND	SND
MC-MSA 3	39.5	6.5	Autonomic UI; OH	Parkinsonism (36)	Constipation (40)	No	No	Obstructive sleep apnoea; IS	Sudden death	Depression	SND
MC-MSA 4	53	4	Parkinsonism	Autonomic UI (2)	OH (4)	No	Yes	Dyspnoea on exertion; IS	Suicide	Depression	SND
MC-MSA 5	41	4	Parkinsonism	Autonomic OH (26)	No	No	Yes	Dyspnoea on exertion	Sudden death	ND	SND
MC-MSA 6	62.5	2.5	Autonomic UF; OH	Parkinsonism (24)	Nocturia (18)	No	No	Acute unprovoked dyspnoea, Obstructive sleep apnoea	Possible multiple myeloma	Possible multiple myeloma	Mixed

ND: non documented; OH: orthostatic hypotension; IS: inspiratory stridor; UI: urinary incontinence; UR: urinary retention; UF: urinary frequency; SD: sexual dysfunction; SND: striatonigral degeneration;

OPCA: olivopontocerebellar atrophy

Table 3.4. Clinical details of long duration, minimal change, and control MSA cases (cont.)

	Age at onset	Disease duration (years)	Initial presentation	Second system involvement (latency in months)	Additional autonomic symptoms (latency in months)	Cerebellar signs	Pyramidal signs	Respiratory symptoms	Cause of death	Concomitant diseases	MSA pathological type
C-MSA 1	67	8	Parkinsonism	Autonomic bradycardia (72)	Breathing problems (86)	No	No	Breathing problems	Pneumonia	ND	Mixed
C-MSA 2	47	9	Autonomic UI	Parkinsonism (36)	Autonomic OH (84)	Yes	Yes	Irregular breathing rate	Pneumonia	ND	Mixed
C-MSA 3	58	9	Parkinsonism	Autonomic UI (48)	Constipation	No	No	ND	Pneumonia	ND	SND
C-MSA 4	51	12	Autonomic SD & urinary symptoms	Parkinsonism (120)	Autonomic OH (132)	Yes	Yes	Sleep apnoea	Respiratory failure	ND	Mixed
C-MSA 5	80	2	Ataxia	Autonomic OH (24)	ND	Yes	No	Aspiration pneumonia	Pneumonia	ND	OPCA
C-MSA 6	63	9	Autonomic UI	Ataxia (48)	Autonomic SD (24)	Yes	No	Bronchopneumonia	Pneumonia	ND	OPCA
C-MSA 7	53	6	Autonomic UI	Parkinsonism (6)	ND	No	Yes	ND	Respiratory failure	ND	OPCA
C-MSA 8	51	9	Ataxia	Autonomic UF (67)	ND	Yes	Yes	ND	Pneumonia	ND	Mixed

ND: non documented; OH: orthostatic hypotension; IS: inspiratory stridor; UI: urinary incontinence; UR: urinary retention; UF: urinary frequency; SD: sexual dysfunction; SND: striatonigral degeneration;

OPCA: olivopontocerebellar atrophy

Table 3.6. Concomitant pathology in MSA sub-groups

	LD *(n=4)*	MC *(n=6)*	Control *(n=8)*
CERAD neuritic plaque score			
Negative	1	6	4
Infrequent	3	0	3
Moderate	0	0	1
Frequent	0	0	0
CAA	0	0	3 (mild, case 1 & 4; severe, case 6)
Tau-pathology (maximum Braak & Braak stage II)	3	0	7
Lewy body pathology	0	0	0
TDP-43 pathology	0	0	0
SVD	0	0	3 (mild, case 5 & 8; severe, case 6)

Figure 3.5 A

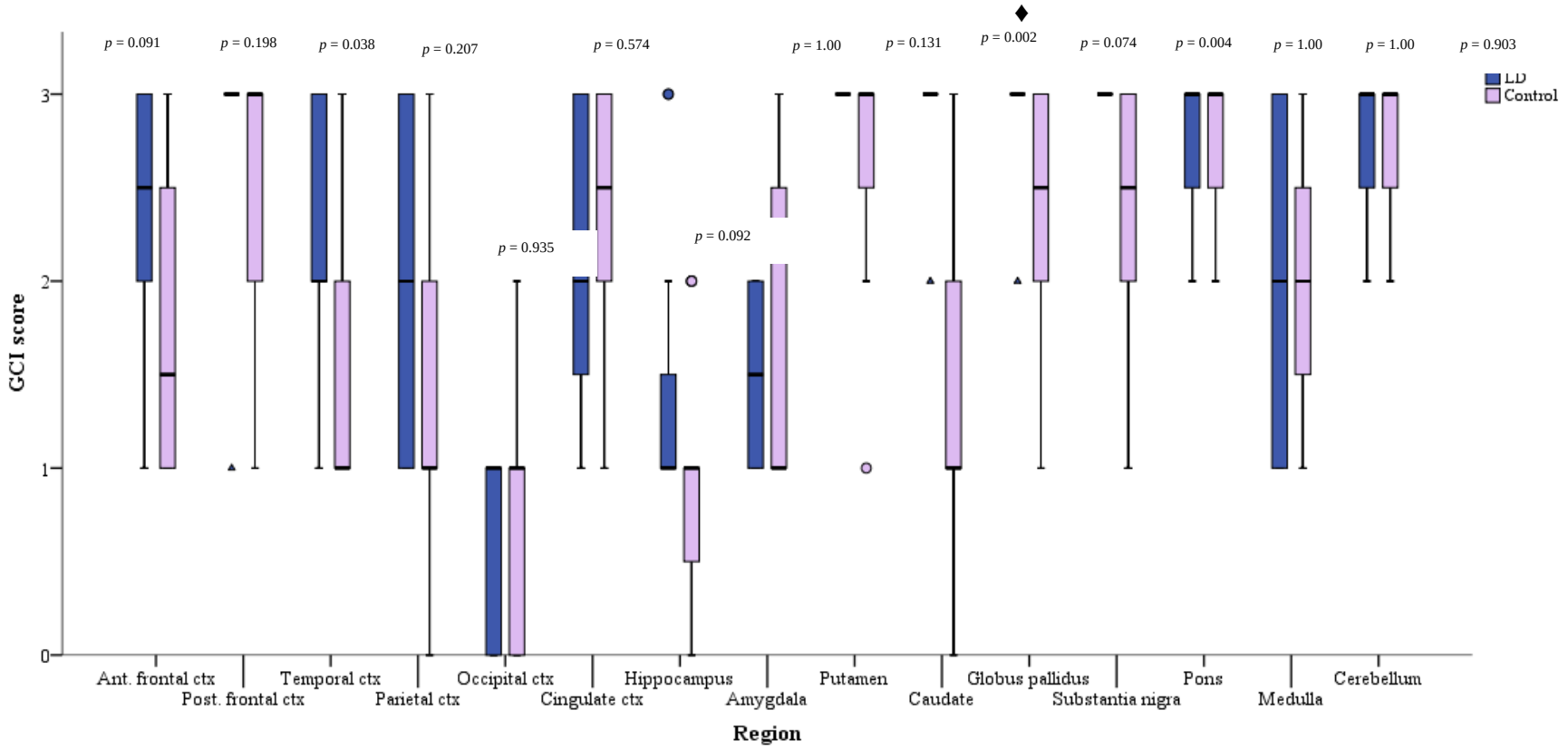
p = 0.091
p = 0.198
p = 0.038
p = 0.207
p = 0.935
p = 0.574
p = 0.092
p = 1.00
p = 0.131
p = 0.002
p = 0.074
p = 0.004
p = 1.00
p = 1.00
p = 0.903
LD
Control
GCI score
0
1
2
3
Ant. frontal ctx
Post. frontal ctx
Temporal ctx
Parietal ctx
Occipital ctx
Cingulate ctx
Hippocampus
Amygdala
Putamen
Caudate
Globus pallidus
Substantia nigra
Pons
Medulla
Cerebellum
Region

Figure 3.5 B

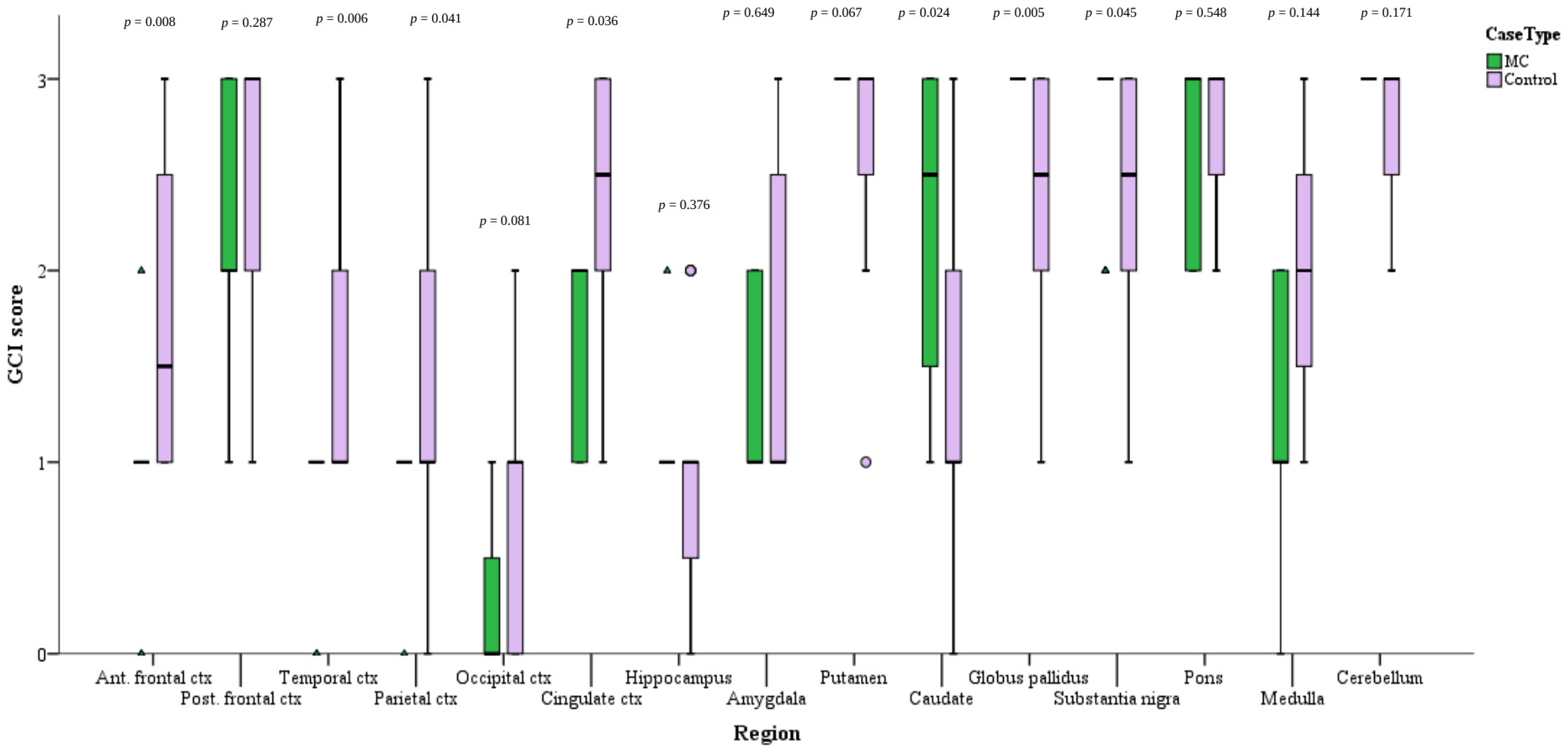
p = 0.008
p = 0.287
p = 0.006
p = 0.041
p = 0.081
p = 0.036
p = 0.376
p = 0.649
p = 0.067
p = 0.024
p = 0.005
p = 0.045
p = 0.548
p = 0.144
p = 0.171
CaseType
MC
Control
GCI score
0
1
2
3
Ant. frontal ctx
Post. frontal ctx
Temporal ctx
Parietal ctx
Occipital ctx
Cingulate ctx
Hippocampus
Amygdala
Putamen
Caudate
Globus pallidus
Substantia nigra
Pons
Medulla
Cerebellum
Region

Figure 3.5 C

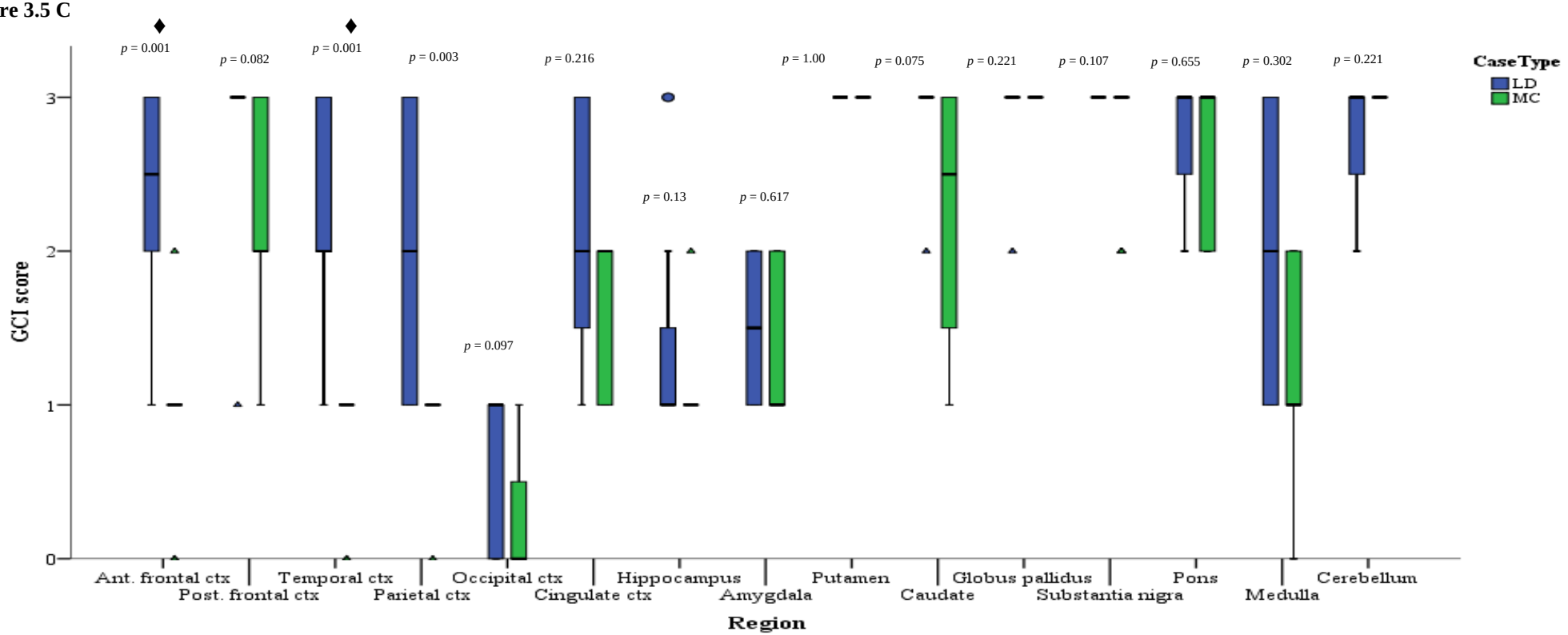

Figure 3.5. GCI burden in long duration, minimal change and control MSA groups

Semi-quantitative analysis of GCI burden in long duration (n=4) (A) and minimal change (n=6) (B) MSA as compared to the control MSA group (n=8) and long duration MSA compared to minimal change MSA (C). GCI burden was significantly higher in the caudate of the long duration cases as compared to control MSA cases. When comparing long duration and minimal change MSA cases, a statistical significance was only found in the anterior frontal and temporal cortices, where GCI burden was higher in the long duration cases. The plots show median values as the line within the box, the box reflects the interquartile range and the whiskers the range of the values.

Figure 3.6 A

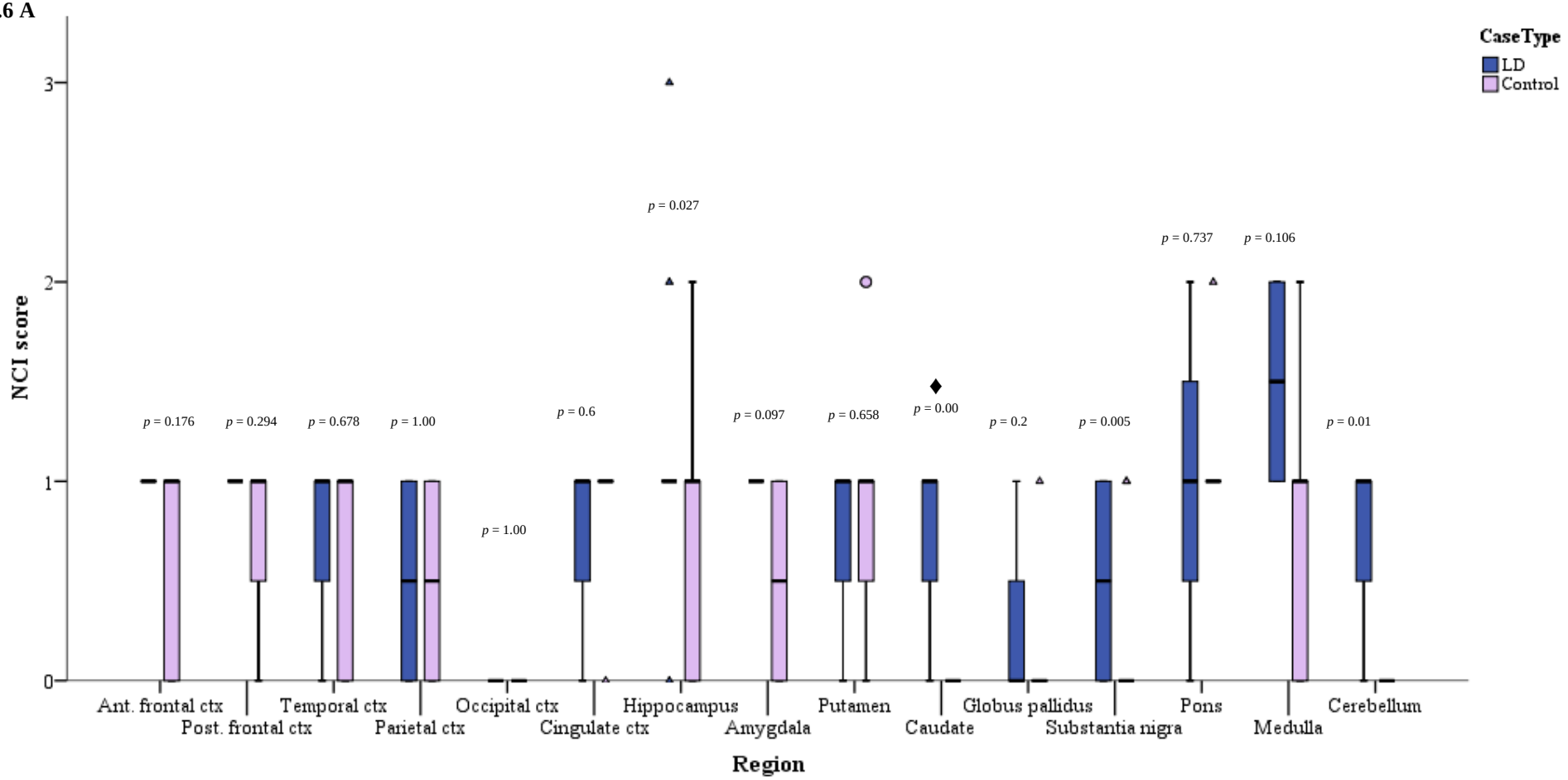
CaseType
LD
Control
NCI score
0
1
2
3
p = 0.176
p = 0.294
p = 0.678
p = 1.00
p = 1.00
p = 0.6
p = 0.027
p = 0.097
p = 0.658
p = 0.00
p = 0.2
p = 0.005
p = 0.737
p = 0.106
p = 0.01
Ant. frontal ctx
Post. frontal ctx
Temporal ctx
Parietal ctx
Occipital ctx
Cingulate ctx
Hippocampus
Amygdala
Putamen
Caudate
Globus pallidus
Substantia nigra
Pons
Medulla
Cerebellum
Region

Figure 3.6 B

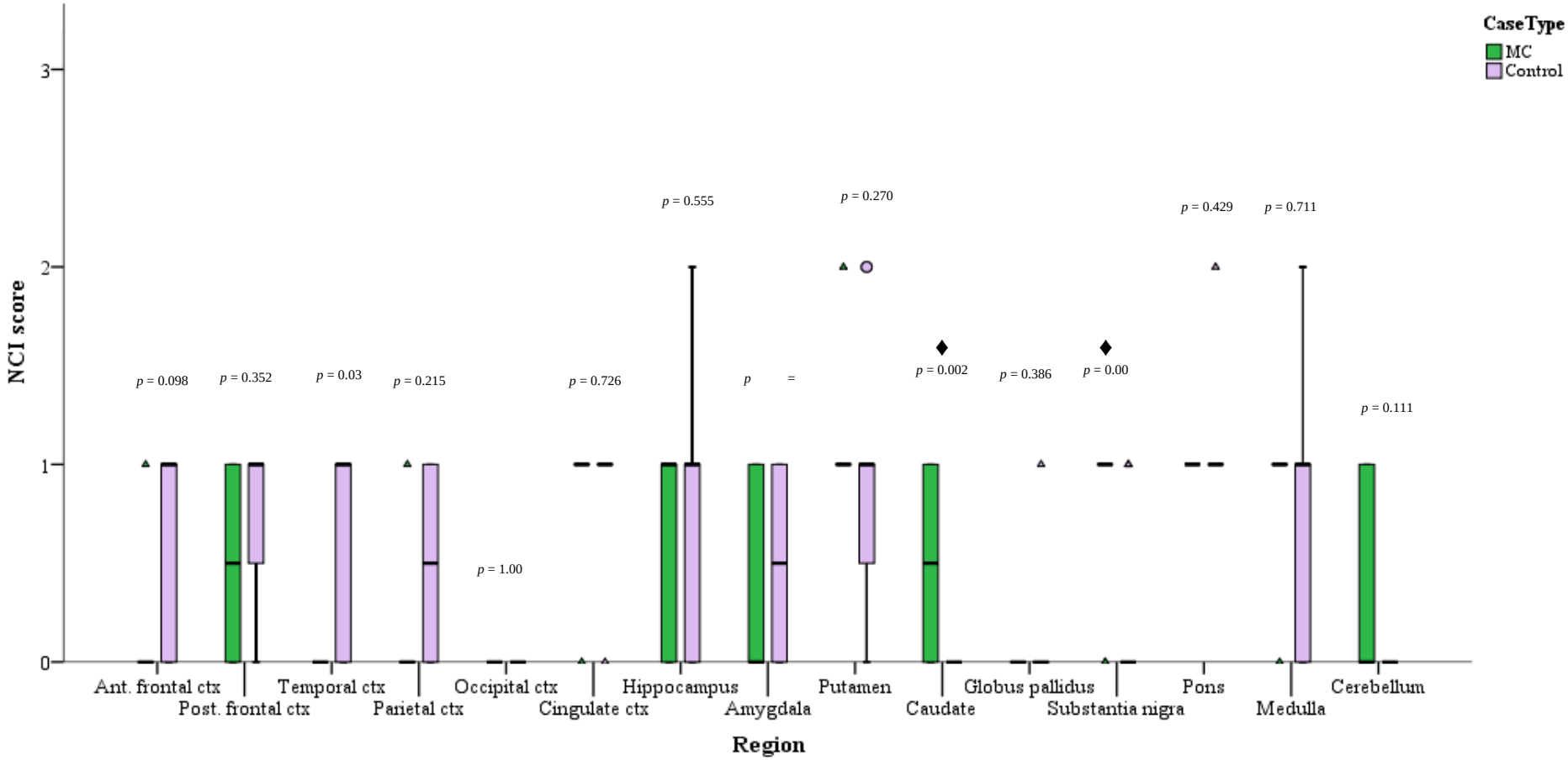
CaseType
MC
Control
NCI score
3
2
1
0
p = 0.098
p = 0.352
p = 0.03
p = 0.215
p = 1.00
p = 0.726
p = 0.555
p
=
p = 0.270
p = 0.002
p = 0.386
p = 0.00
p = 0.429
p = 0.711
p = 0.111
Ant. frontal ctx
Post. frontal ctx
Temporal ctx
Parietal ctx
Occipital ctx
Cingulate ctx
Hippocampus
Amygdala
Putamen
Caudate
Globus pallidus
Substantia nigra
Pons
Medulla
Cerebellum
Region

Figure 3.6 C

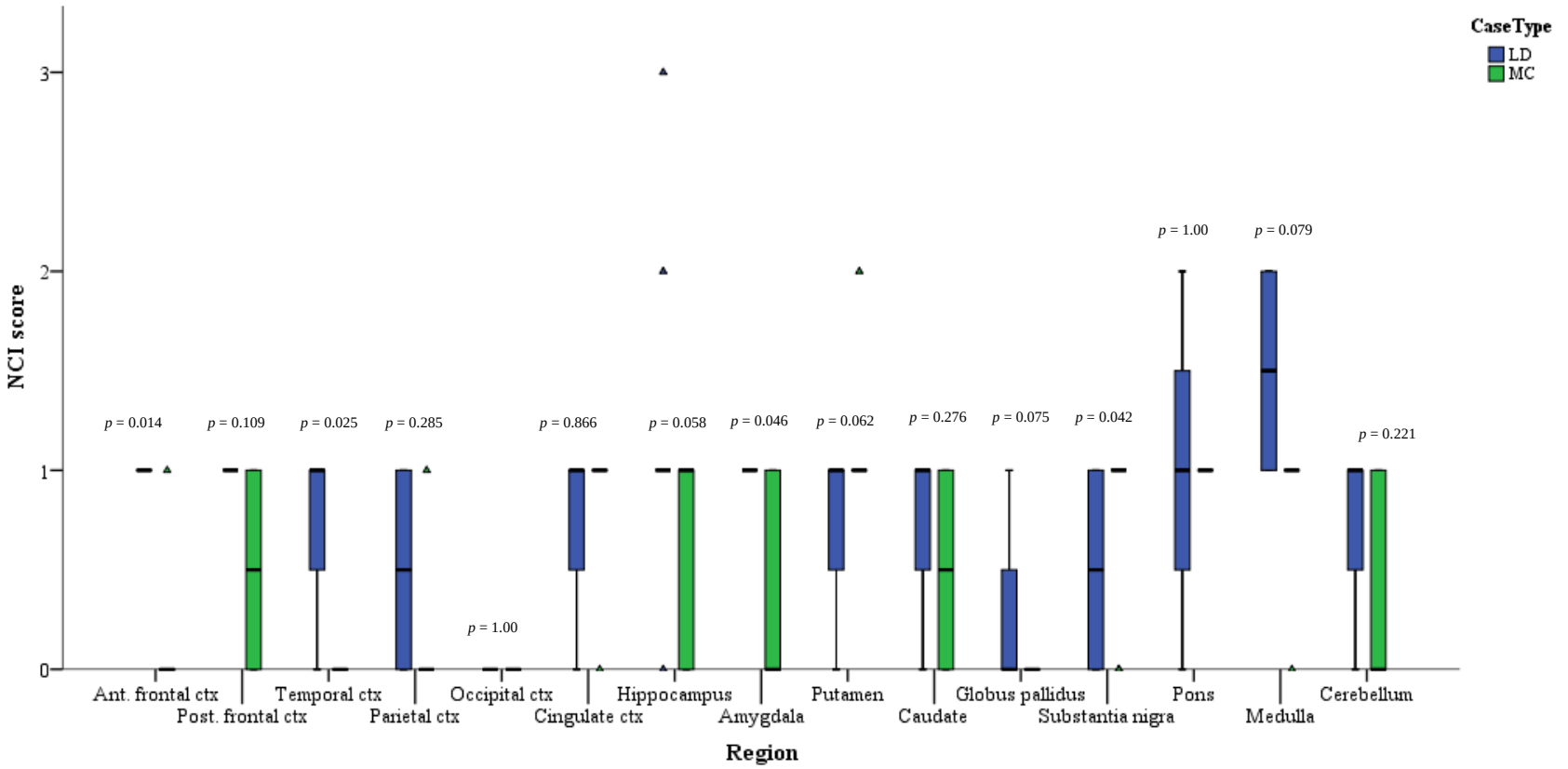

Figure 3.6. NCI burden in long duration, minimal change and control MSA groups

Semi-quantitative analysis of NCI burden in long duration (n=4) (A) and minimal change (n=6) (B) MSA as compared to the control MSA group (n=8) and long duration MSA compared to minimal change MSA (C). NCI burden was significantly higher in the caudate of the long duration MSA group as compared to controls. The caudate and substantia nigra of the minimal change MSA group displayed significantly greater numbers of NCIs compared with the control MSA group. The plots show median values as the line within the box, the box reflects the interquartile range and the whiskers the range of the values (Mann-Whitney U test with Bonferroni correction for multiple comparisons at significance level $p < 0.003$). *•outliers; ★extreme outliers; ◆p <0.003. Ctx: cortex.*

Figure 3.7 A

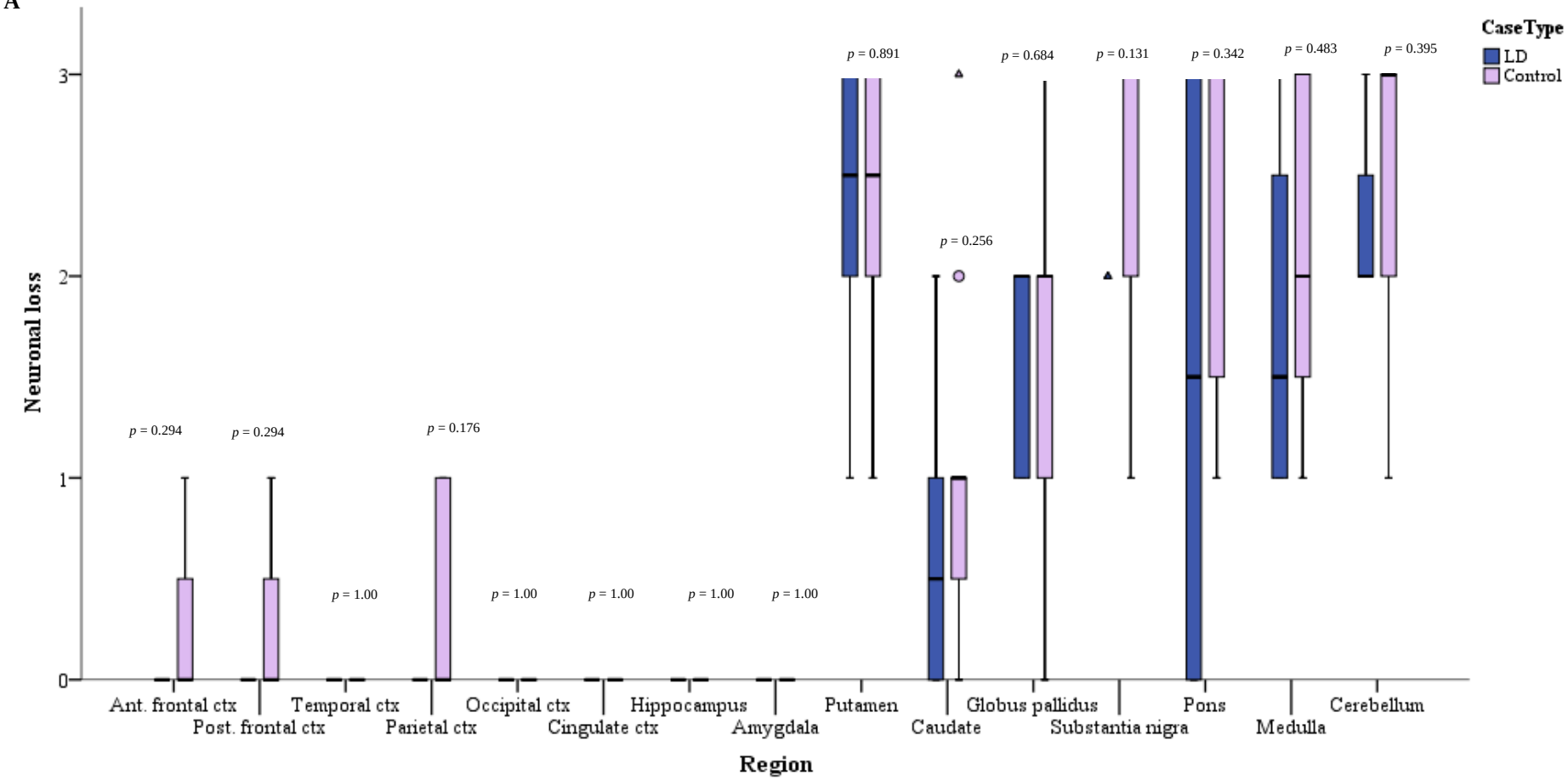
CaseType
LD
Control
Neuronal loss
0
1
2
3
p = 0.294
p = 0.294
p = 1.00
p = 0.176
p = 1.00
p = 1.00
p = 1.00
p = 1.00
p = 0.891
p = 0.256
p = 0.684
p = 0.131
p = 0.342
p = 0.483
p = 0.395
Ant. frontal ctx
Post. frontal ctx
Temporal ctx
Parietal ctx
Occipital ctx
Cingulate ctx
Hippocampus
Amygdala
Putamen
Caudate
Globus pallidus
Substantia nigra
Pons
Medulla
Cerebellum
Region

Figure 3.7 B

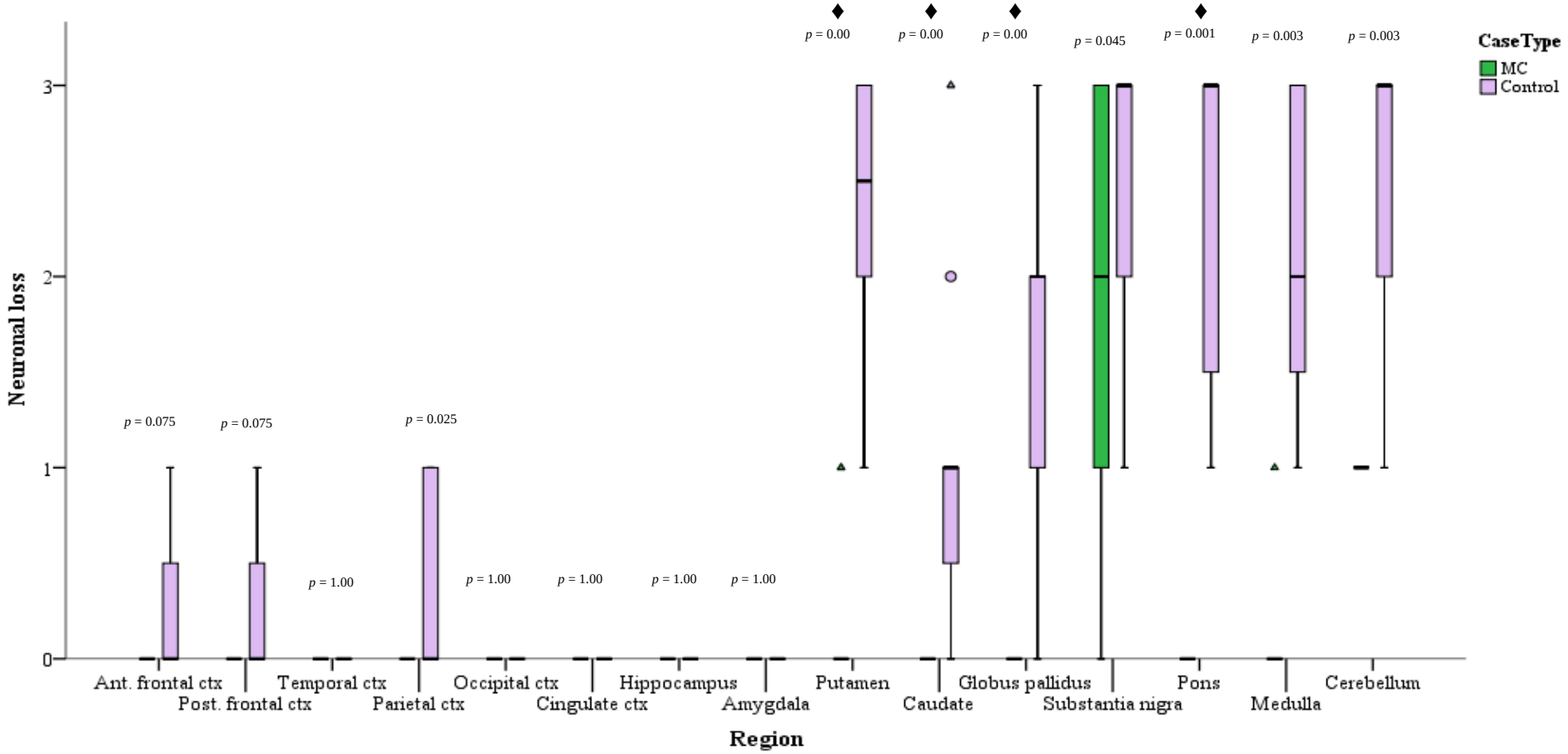
p = 0.00
p = 0.00
p = 0.00
p = 0.045
p = 0.001
p = 0.003
p = 0.003
CaseType
MC
Control
Neuronal loss
3
2
1
0
p = 0.075
p = 0.075
p = 0.025
p = 1.00
p = 1.00
p = 1.00
p = 1.00
p = 1.00
Ant. frontal ctx
Post. frontal ctx
Temporal ctx
Parietal ctx
Occipital ctx
Cingulate ctx
Hippocampus
Amygdala
Putamen
Caudate
Globus pallidus
Substantia nigra
Pons
Medulla
Cerebellum
Region

Figure 3.7 C

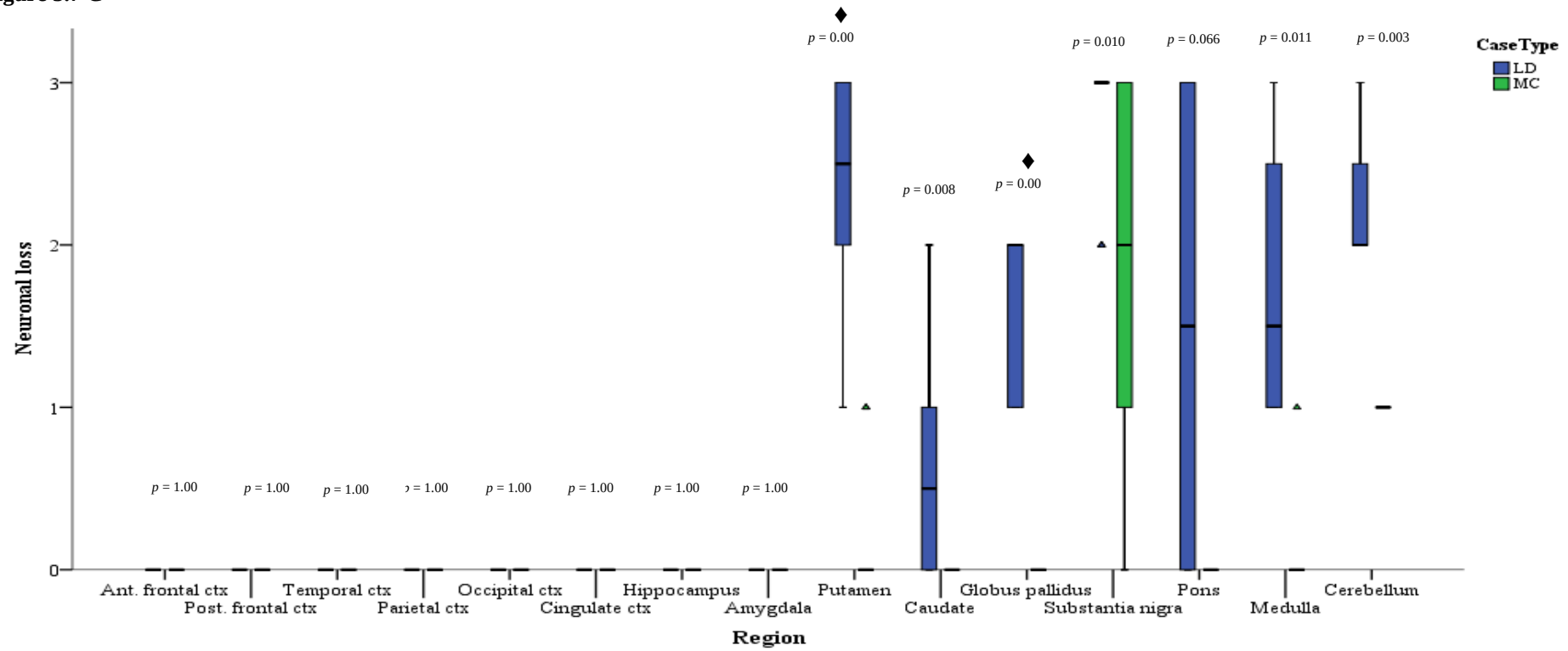

Figure 3.7. Neuronal loss in long duration, minimal change and control MSA groups

Semi-quantitative analysis of neuronal loss in long duration (n=4) (A) and minimal change (n=6) (B) MSA as compared to the control MSA group (n=8) and long duration MSA compared to minimal change MSA (C). Neuronal loss was not evident in the cortical and limbic regions of the long duration and minimal change MSA cases. Neuronal loss in minimal change MSA was significantly less in the putamen, caudate, globus pallidus and pontine base as compared to 'classical MSA' cases ($p<0.003$) thus satisfying selection criteria of neuronal loss restricted to substantia nigra and locus coeruleus. A statistical difference between long duration and control MSA cases was not found. The plots show median values as the line within the box, the box reflects the interquartile range and the whiskers the range of the values. *(Mann-Whitney U test with Bonferroni correction for multiple comparisons at significance level p <0.003).* ◦*outliers;* ★*extreme outliers;* ♦*p <0.003.*

Figure 3.8 A

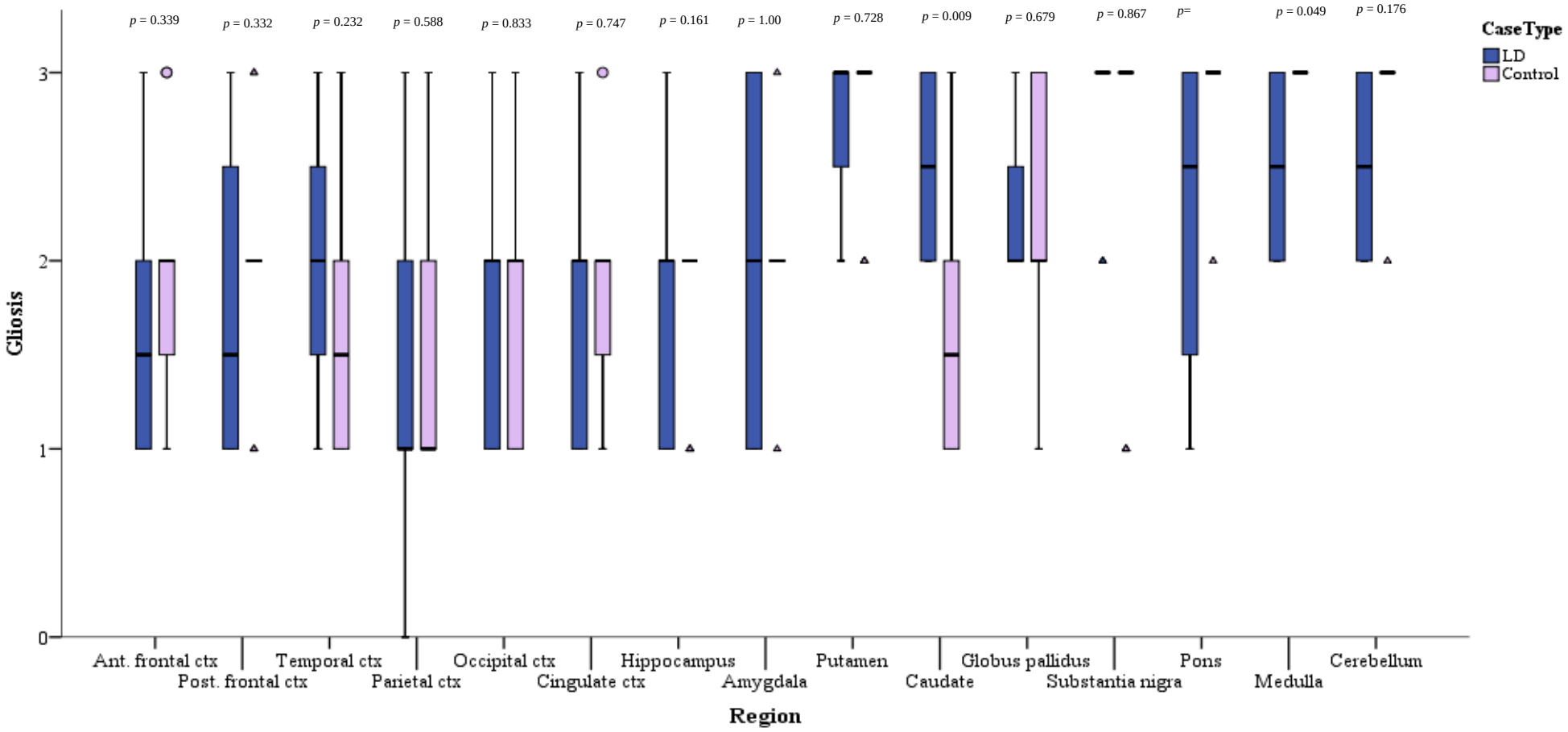
p = 0.339
p = 0.332
p = 0.232
p = 0.588
p = 0.833
p = 0.747
p = 0.161
p = 1.00
p = 0.728
p = 0.009
p = 0.679
p = 0.867
p=
p = 0.049
p = 0.176
CaseType
LD
Control
Gliosis
3
2
1
0
Ant. frontal ctx
Post. frontal ctx
Temporal ctx
Parietal ctx
Occipital ctx
Cingulate ctx
Hippocampus
Amygdala
Putamen
Caudate
Globus pallidus
Substantia nigra
Pons
Medulla
Cerebellum
Region

Figure 3.8 B

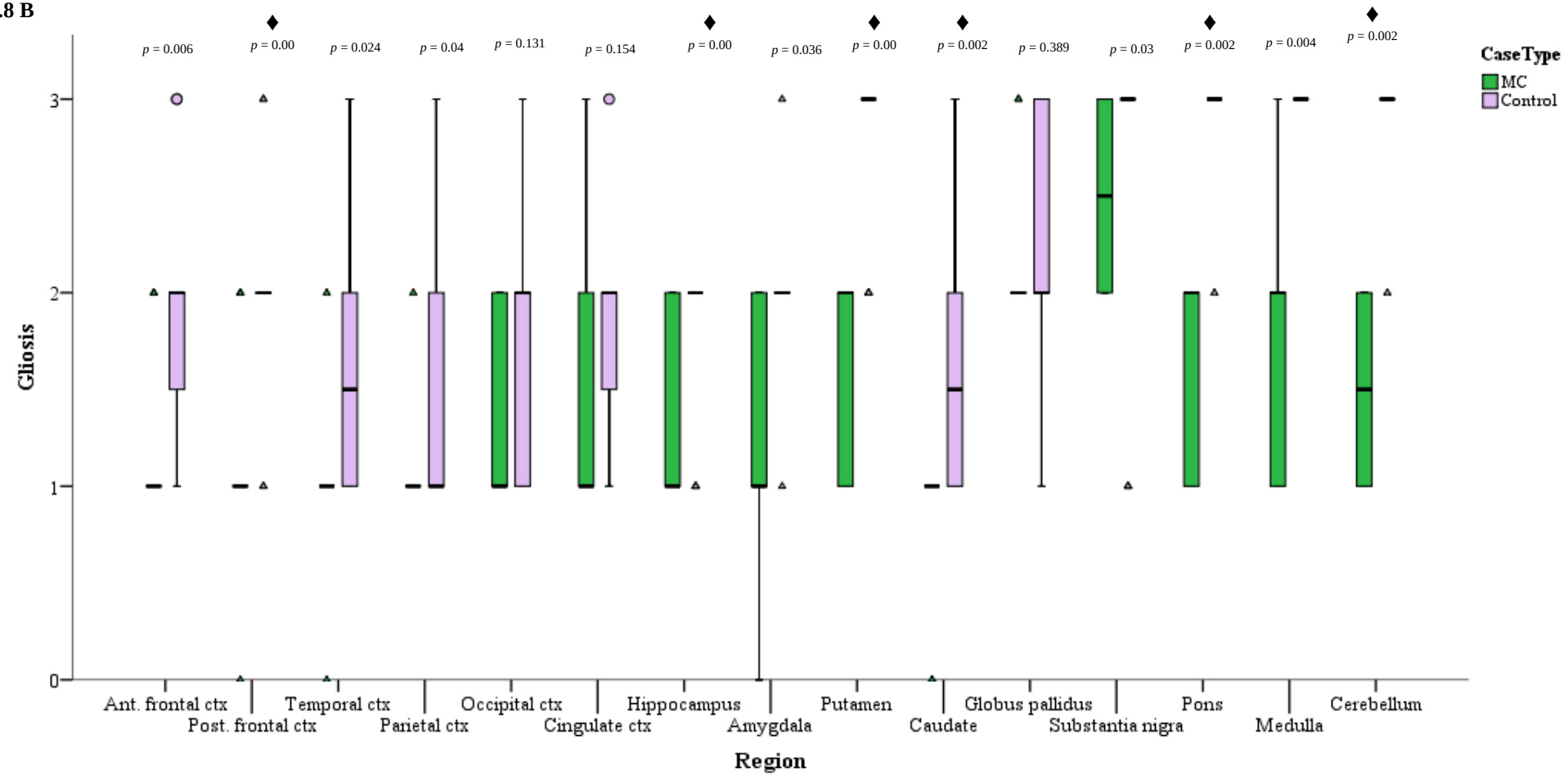
p = 0.006
p = 0.00
p = 0.024
p = 0.04
p = 0.131
p = 0.154
p = 0.00
p = 0.036
p = 0.00
p = 0.002
p = 0.389
p = 0.03
p = 0.002
p = 0.004
p = 0.002
CaseType
MC
Control
Gliosis
0
1
2
3
Ant. frontal ctx
Post. frontal ctx
Temporal ctx
Parietal ctx
Occipital ctx
Cingulate ctx
Hippocampus
Amygdala
Putamen
Caudate
Globus pallidus
Substantia nigra
Pons
Medulla
Cerebellum
Region

Figure 3.8 C

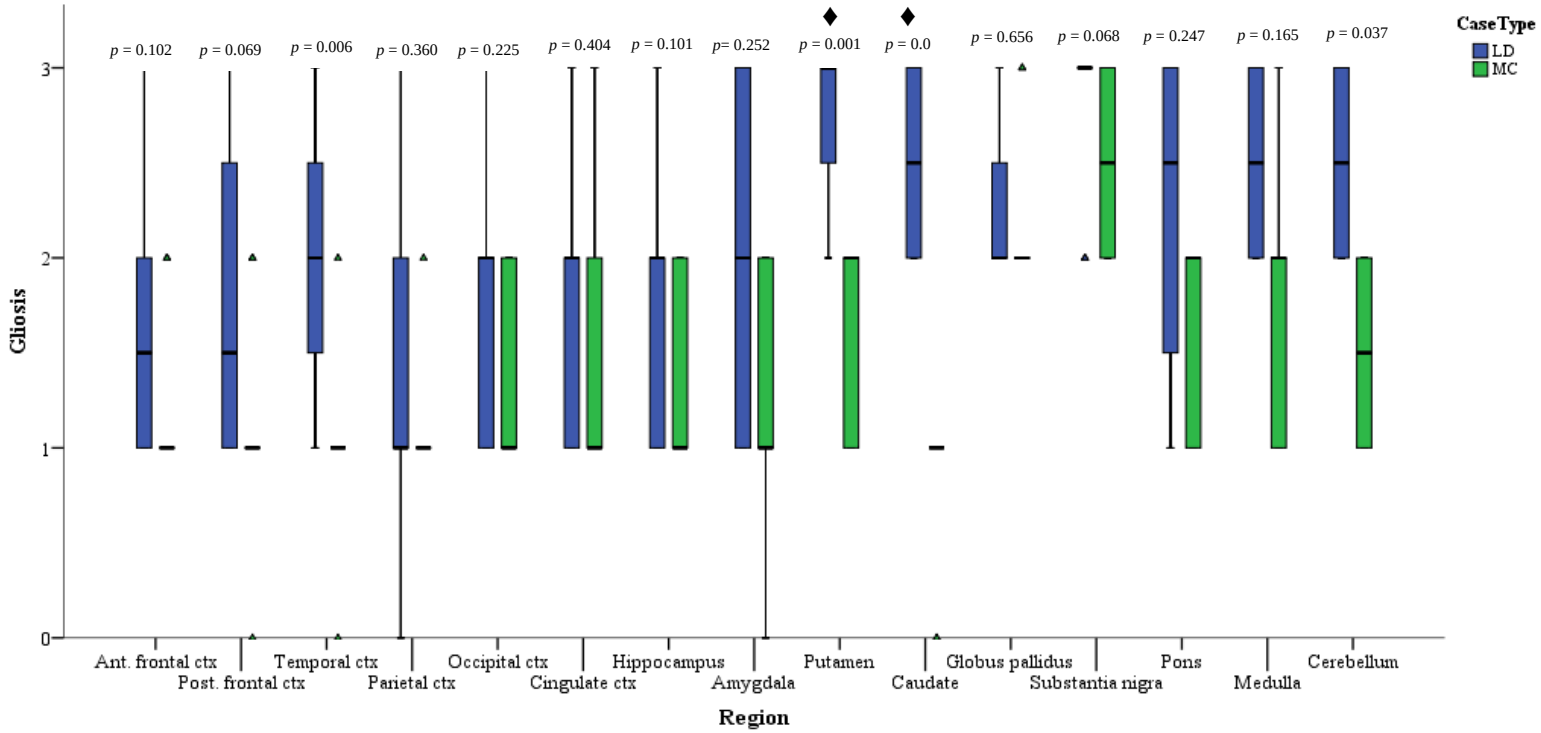

Figure 3.8. Gliosis in long duration, minimal change and control MSA groups

Semi-quantitative analysis of gliosis in long duration (n=4) (A) and minimal change (n=6) (B) MSA as compared to the control MSA group (n=8) and long duration MSA compared to minimal change MSA (C). Gliosis was abundant in all cases. A statistically significant difference was found between minimal change MSA and the control MSA group in the putamen, caudate, pontine base and cerebellum, where the level was higher in the control group. The plots show median values as the line within the box, the box reflects the interquartile range and the whiskers the range of the values (Mann-Whitney U test with Bonferroni correction for multiple comparisons at significance level $p < 0.003$). *°outliers; *extreme outliers; ♦$p < 0.003$. Ctx: cortex.

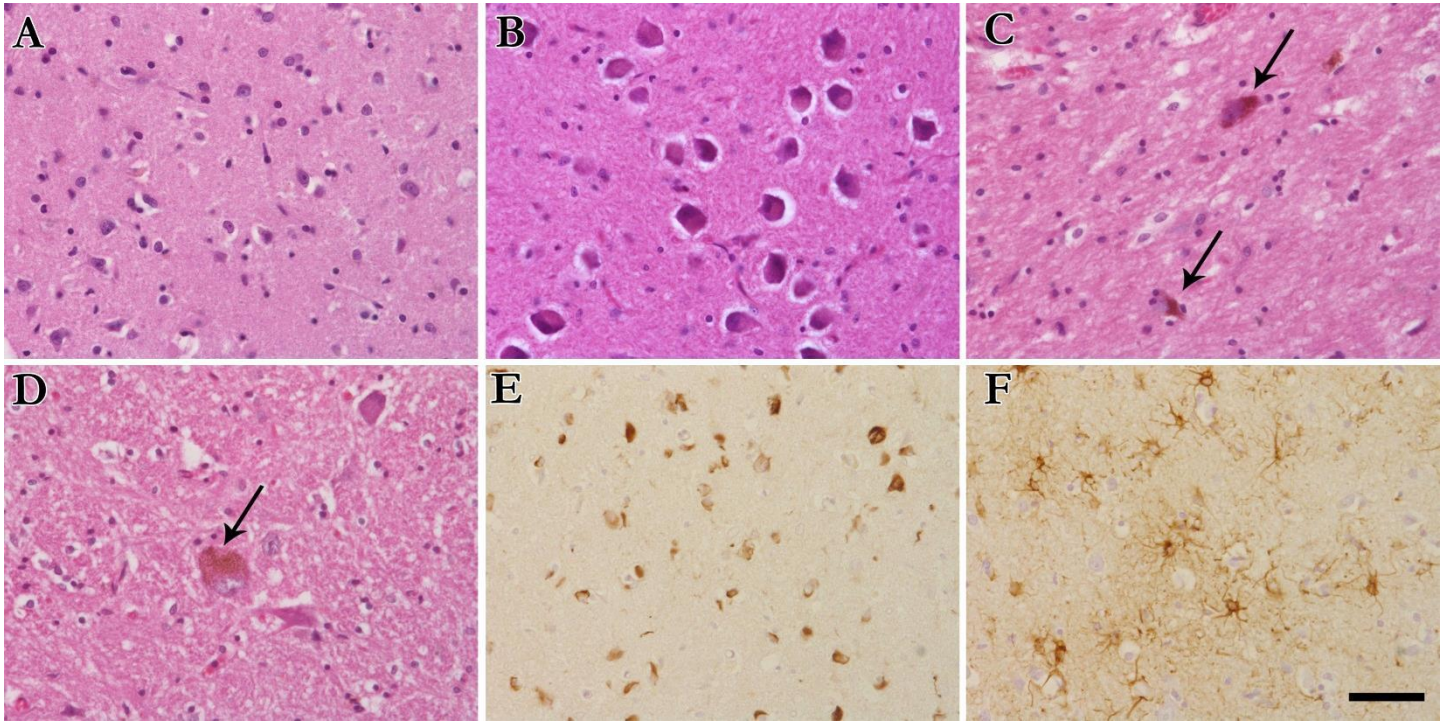

Figure 3.9. Minimal change MSA profile

A representative case of minimal change MSA, where neurons are well preserved in the putamen (A) and inferior olivary nucleus (B). The substantia nigra (C) and locus coeruleus (D) are severely affected by neuronal loss with few remaining pigmented neurons (arrows). Despite absence of neuronal loss in the putamen, this region has a heavy burden of GCIs (E) and astrogliosis (F). *A-D: haematoxylin and eosin; E: alpha-synuclein immunohistochemistry; F: GFAP immunohistochemistry. Scale bar: 50 μm in all panels.*

Table 3.7. Summary of significant findings

	LD-MSA vs. Control MSA	**MC-MSA vs. Control MSA**	**LD-MSA vs. MC MSA**
GCI	Caudate: LD-MSA> Control MSA, *p=0.002*	No significant differences	Anterior frontal cortex: LD-MSA> MC-MSA, *p=0.001* Temporal cortex: LD-MSA> MC-MSA, *p=0.001*
NCI	Caudate: LD-MSA> Control MSA, *p<0.001*	Caudate: MC-MSA > Control MSA, *p=0.002* Substantia nigra: MC-MSA > Control MSA, *p<0.001*	No significant differences
Neuronal loss	No significant differences	Caudate, putamen, globus pallidus and pons: Control MSA > MC-MSA, *p≤0.001*	Caudate and globus pallidus: LD-MSA > MC-MSA, *p<0.001*
Gliosis	No significant differences	Posterior frontal cortex, hippocampus, putamen, caudate, pons and cerebellar white matter: Control MSA > MC-MSA, *p≤0.002*	Putamen and caudate: LD-MSA > MC-MSA, *p≤0.001*

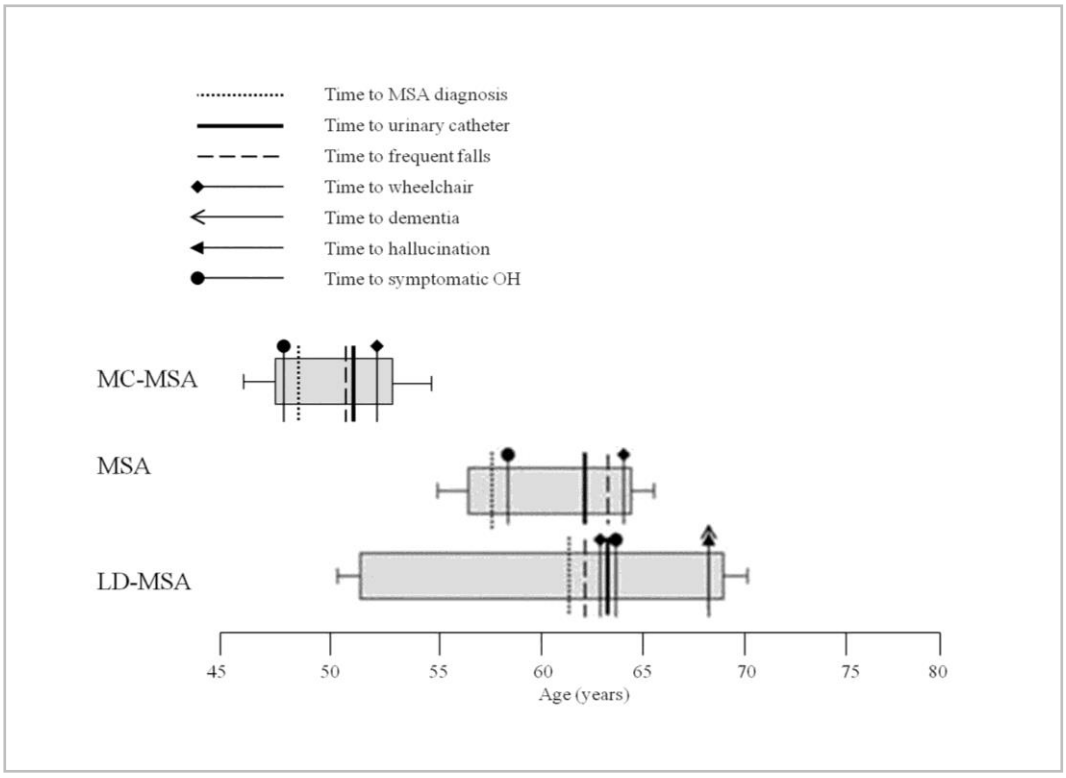

Figure 3.10. Clinical profile in long duration, minimal change and control MSA groups

Clinical disease milestones and disease course in long duration, minimal change and control MSA group. Gray rectangles represent mean duration of disease course starting from mean age of onset until mean age of death. Rapid disease progression ensued after onset of autonomic symptoms.

3.2.7. Discussion

The clinical and pathological profiles of the long duration and minimal change MSA subgroups were reviewed and compared to a control MSA group with classical clinical presentation and pathological findings. A common pathological observation of all groups was absent or minimal neuronal loss in the cortical and limbic regions despite the presence of widespread GCIs and NCIs. All groups showed widespread gliosis in cortical, limbic, StrN and OPC regions. Significant findings are summarised in Table 3.7.

Long duration MSA

GCI and NCI pathology was greater in the long duration MSA group when compared with control MSA but statistical significance was only reached in the caudate. This increased severity of pathology in the caudate, a structure that is usually mildly affected, may be an indication of anatomical disease progression with time. Despite widespread αsyn pathology in the regions evaluated, neuronal loss was undetectable in the cortical and limbic regions and was limited to the StrN and OPC regions, where it showed no difference in severity compared with control MSA. These findings are in keeping with the published literature on long duration MSA cases, with the exception of one case, which exhibited severe neuronal loss in cortical and limbic regions (Wakabayashi et al., 1998; Konagaya et al., 1999; Piao et al., 2001; Masui et al., 2011). Similarity in the distribution and severity of pathological changes in long duration MSA and the control MSA

group may imply that the pathology progresses at a slower rate over a longer duration in this clinical subgroup, making it a relatively 'benign' variant with a disease duration lasting for almost twice as long as classical MSA. Slowly progressive MSA has been suggested to be associated with minimal change pathology (Yoshida, 2007). However, this was not the observation in the long duration cases studied in this thesis as none of them had neuronal loss restricted to the substantia nigra or locus coeruleus. The long disease duration is more likely to be due to the late onset of autonomic symptoms as discussed below.

Minimal change MSA

Minimal change MSA has previously been defined as showing restricted neuronal loss in the substantia nigra and/or the locus coeruleus (Wenning et al., 1994 a; Huang et al., 2005; Wakabayashi et al., 2005). Careful evaluation of neuronal loss the minimal change cases in this thesis (of which cases MC-MSA 2 & 3 were previously described by Wenning and colleagues, 1994) using published assessment criteria (Ozawa et al., 2004) and a review of the published literature suggests that the definition of minimal change MSA may be revised as follows: Macroscopically, pallor of the substantia nigra and locus coeruleus. Microscopically, neuronal loss (+1 to +3) in the substantia nigra and locus coeruleus with not more than +1 in the cerebellar Purkinje cells and a maximum of +1 in one other structure.

Despite the restricted neuronal loss, GCI burden in these minimal change cases did not differ significantly from the control group and was abundant in all

regions. The presence of αsyn pathology in areas where neuronal loss was not observed adds strength to the argument that oligodendroglial pathology plays a significant, and most likely primary, role in the pathogenic mechanism of MSA (Inoue et al., 1997; Wenning et al., 2008; Jellinger and Lantos, 2010). NCI burden was greater in the substantia nigra and caudate of the minimal change group than controls. Previous studies have suggested that NCIs represent early pathology in MSA and that NCI pathology decreases in quantity as the disease progresses as a result of neuronal cell loss (Yokoyama et al., 2001; Nishie et al., 2004; Yoshida, 2007). The greater load of NCIs observed in patients with minimal change MSA may reflect that they have died at an earlier stage in the evolution of disease.

Out of 135 MSA cases analysed from the QSBB collection, only six were identified as 'minimal change' cases. All these cases fulfilled clinical criteria for MSA during life. Three of the six died from causes other than MSA and it is reasonable to assume that they would have fulfilled criteria for 'typical' MSA had the disease not been interrupted. The other three minimal change MSA cases died of SUD and in this subgroup the disease progression was notably more rapid than control MSA, the patients' disability reached all clinical milestones within three years of initial presentation (O'Sullivan et al., 2008) and that they seem to have had a short duration of disease (mean 5 years; SD 1.8 years). A mean survival of 2.5 years was previously reported in 6 minimal change cases (Yoshida, 2007). Interestingly, all minimal change cases were diagnosed clinically as MSA-P and cerebellar features were not reported but this may just reflect the predominance of MSA-P in Western populations.

The leading causes of death in MSA are SUD, as a result of central brain stem autonomic failure and death due to infection (urinary tract infection or aspiration pneumonia) (Papapetropoulos et al., 2007). Proposed mechanisms leading to SUD include dysphagia, stridor, acute airway obstruction, and vocal cord abductor paralysis (Isozaki et al., 1996; Sadaoka et al., 1996; Silber and Levine, 2000; Papapetropoulos et al., 2007; Shimohata et al., 2008). All six minimal change MSA cases had inspiratory stridor. Other prominent respiratory symptoms including dyspnea on exertion, episodes of acute unprovoked dyspnea and sleep apnea have also been noted. This shows that these respiratory symptoms may arise early in MSA even in cases with limited neuronal loss. In addition to early respiratory symptoms the three minimal change MSA cases with SUD had prominent symptomatic orthostatic hypotension and reached the majority of disease disability milestones (O'Sullivan et al., 2008), especially frequent falls and wheelchair dependant state within the first three years of clinical presentation (Figure 3.10).

The importance of autonomic system involvement and the prognostic value of autonomic symptoms implies that the pathological involvement of brain stem nuclei plays an important role in disease progression in MSA (Watanabe et al., 2002; Benarroch et al., 2004; O'Sullivan et al., 2008; Tada et al., 2009). This is reflected in the cohort of this thesis as a favourable outcome and prolonged disease duration associated with late onset of autonomic symptoms was seen in the long duration cases, while the minimal change cases, especially in those with SUD, had early onset of autonomic symptoms and shorter survival. The three

SUD minimal change cases also had an unusually early age of onset in their 30's and early 40's. It might be possible that these three cases represent an 'aggressive' variant of MSA with early onset and early sudden death due to early pathological involvement of vital cardiovascular and respiratory functions.

Conclusion and further directions

GCIs and NCIs were greater in the caudate of long duration MSA, while in the minimal change cases NCIs were more abundant in the caudate and substantia nigra. Other than those changes, there was no significant difference in the pathologies of these groups as compared to the group of control MSA patients in cortical, limbic, StrN and OPC region examined in this study. In contrast to previous findings (Ozawa et al., 2004), the results of this study suggest that the GCI burden in these disease subgroups does not correlate with the clinical outcome in either long duration and minimal change groups nor does it correlate with the neuronal loss which is restricted in the minimal change group. Widespread GCIs in all subgroups of MSA and in areas of no, or minimal, neuronal loss adds strength to the argument that MSA is a primary oligodendrogliopathy. Furthermore, the significance of onset of autonomic symptoms to disease progression warrants exploration of nuclei or connections associated with the autonomic system, including the intermediolateral column spinal cord, dorsal motor nucleus of vagus, medullary serotonergic and catecholaminergic neurons, as pathology in those regions may help identify significant pathological differences between the groups and better correlation between neuronal loss and GCI burden.

Declaration:

Clinical data for this chapter was compiled by Dr. Helen Ling and Dr. Igor Petrovic.

This chapter contributed to the following papers:

Asi, Y.T.[*], Ling H[*], Ahmed, Z, Lees, A.J., Revesz, T, Holton, J.L. *Pathological changes in multiple system atrophy with cognitive impairment*. Submitted.

Asi, Y.T, Ling, H. [*], Petrovic, I.N. [*], Ahmed, Z., Prashanth, L.K.., Hazrati, L.-N., Nishizawa, M, Ozawa, T, Lang, A.E., Lees, A.J., Revesz, T. and Holton, J.L. *Long duration and minimal change MSA: benign and aggressive variants?* Submitted.

Petrovic, I.N., Ling, H., **Asi, Y.**, Ahmed, Z., Prashanth, L.K.., Hazrati, L.-N., Lang, A.E., Revesz, T., Holton, J.L. and Lees, A.J., 2012. *Multiple system atrophy-parkinsonism with slow progression and prolonged survival: a diagnostic catch*. Mov. Disord. 27, 1186–1190.

4

GCIs IN THE OLIGODENDROGLIAL LINEAGE

4.1. INTRODUCTION

Oligodendrocytes are the cell type most vulnerable to inclusion formation in MSA. Oligodendrocytes are one class of central nervous system (CNS) glial cells. Important functions of oligodendrocytes include forming myelin sheaths around axons thus facilitating propagation of action potentials through saltatory conduction and production of neurotrophic factors (Baumann and Pham-Dinh, 2001). Neural stem cells undergo a number of proliferative and differentiation stages in the production of oligodendrocytes resulting in fully differentiated, mature myelin producing oligodendrocytes at the final stage. At different maturation stages cells in the oligodendrocyte lineage exhibit a number of different markers. Cues from neurons and astrocytes may play an important role in the process of maturation (Baumann and Pham-Dinh, 2001). As such, these cells have different morphological and antigenic characteristics as they mature (Figure 4.1) (Baumann and Pham-Dinh, 2001; Zhang, 2001; Buchet and Baron-Van Evercooren, 2009; Espinosa-Jeffrey et al., 2009; Nishiyama et al., 2009).

Olig2, a basic helix-loop-helix transcription factor, is important for the development of oligodendrocytes (Rowitch et al., 2002). Olig2 expression occurs

in pre-oligodendrocytes and persists throughout the lineage and is therefore used as a marker for oligodendrocytes. Identifying oligodendrocytes at different maturational stages is a challenging task as certain markers may be present in more than one stage, requiring the use of multiple markers for characterisation of a maturational state. Oligodendrocyte precursor cells may be identified by the markers NG2, PDGFRα, and A2B5; premyelinating oligodendrocytes by galactocerebroside (GC) and 2',3'-Cyclic nucleotide-3'-phosphohydrolase (CNPase); mature oligodendrocytes by GC, CNPase and myelin basic protein (MBP) with the addition of myelin oligodendrocyte glycoprotein (MOG) for myelinating oligodendrocytes (Baumann and Pham-Dinh, 2001; Zhang, 2001; Buchet and Baron-Van Evercooren, 2009; Espinosa-Jeffrey et al., 2009; Nishiyama et al., 2009).

$NG2^+$ cells are an abundant population of cells in the adult CNS (Levine et al., 1993; Dawson et al., 2003). Though there is consensus that $NG2^+$ cells are oligodendrocyte precursor cells, debate in the literature suggests that they are not limited to this function (Berry et al., 2002; Butt et al., 2002; Nishiyama et al., 2009). In fact, the high density and distinct electrophysiological profile of some $NG2^+$ cells resulted in calls for classifying $NG2^+$ cells as a fourth glial type (Butt et al., 2002; Mallon et al., 2002; Nishiyama et al., 2009). $NG2^+$ cells have been hypothesized to play a part in remyelination and monitoring of CNS integrity as studies have shown them to respond to demyelinating insults (Franklin, 2002; Franklin and ffrench-Constant, 2008).

The presence of GCIs in oligodendrocytes is essential for a definite diagnosis of MSA. Cells containing GCIs were characterized as mature oligodendrocytes according to morphological features and for their negative staining of neuronal (neurofilament), astrocytic (GFAP) and microglial (Mac 387) markers (Papp et al., 1989). Accumulation of GCIs in different oligodendrocyte maturational stages, however, has not been studied and is the focus of this chapter. Establishing the oligodendrocyte maturational stage at which GCIs begin to form will provide greater insight into the pathogenic mechanism of MSA.

4.2. HYPOTHESIS

αSyn accumulation as GCIs in oligodendrocytes occurs at different stages of oligodendrocyte maturation.

4.3. AIM

To investigate the involvement of $NG2^+$ cells, immature oligodendrocytes and mature oligodendrocytes by αsyn pathology in MSA.

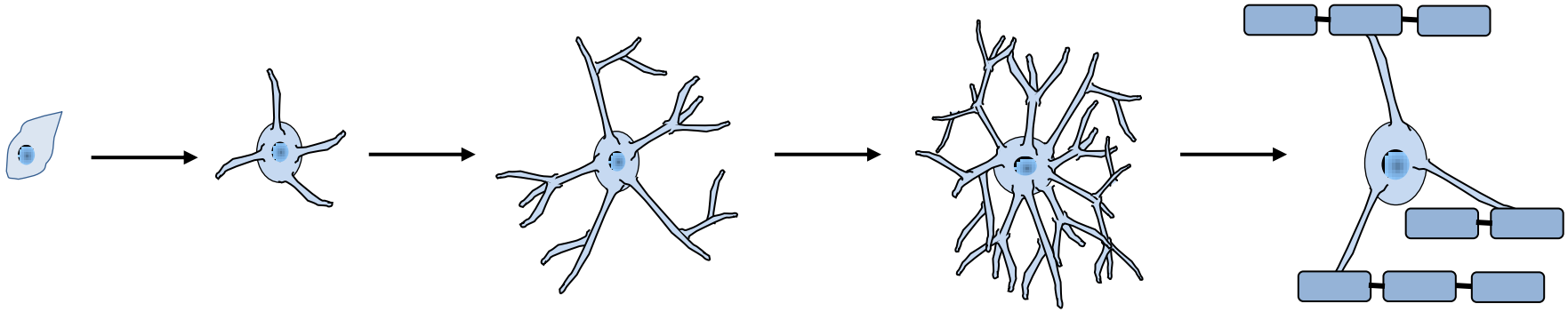

Neural stem cell	**Oligodendrocyte progenitor cell**	**Pre-oligodendrocyte**	**Immature pre-myelinating oligodendrocyte**	**Myelinating mature oligodendrocyte**
Nestin	A2B5	A2B5	OLIG2	OLIG2
Vimentin	PDGFRα	PDGFRα	O4	O4
Sox2	Nestin	NG2	GalC	GalC
	NG2	OLIG2	CNPase	CNPase
	OLIG2	O4		PLP
				MBP
				MOG

Figure 4.1. Oligodendrocyte maturational stages

Oligodendrocytes undergo proliferation and differentiation from the stem cell stage to the mature myelinating stage, where the appearance and disappearance of certain markers dictates the fate of the cells. Above are some markers expressed during each developmental stage of the oligodendrocyte lineage.

PDGFRa: platelet-derived growth factor receptora; GalC: galactocerebroside; CNPase: 2',3'-cyclic nucleotide 3'-phosphodiesterase; MAG: myelin-associated glycoprotein; MBP: myelin basic protein; PLP: proteolipid protein.

4.4. METHOD

Double and triple immunofluorescence was carried out as described in Chapter 2 Materials and methods section 2.6. Briefly, 8μm thick frozen sections were cut from the posterior frontal cortex and cerebellum of 3 MSA cases. Sections were incubated in two or three successive rounds of primary antibody followed by secondary antibody incubation. The primary antibodies include NG2 (1:200; R&D Systems, Minneapolis, MN), CNPase (1:100; Abcam, Cambridge, UK), MBP (1:500; Convance, Cambridge, UK) and αsyn (1:800; Abcam, Cambridge, UK). Alexa Fluor® secondary antibodies (1:1000; Invitrogen, Paisley, UK) were used for detection of CNPase, MBP and αsyn while the TSA Plus Fluorescence Systems kit (PerkinElmer, Massachusetts, USA) was used for NG2 detection. Qualitative analysis was conducted by systematically scanning the entire section for evidence of co-localisation using widefield and confocal fluorescence microscopy (Leica DM550 and Leica SPE, Leica Microsystems, Milton Keynes, UK).

αSyn, NG2 and MBP immunohistochemistry were incubated in the primary antibody as above. The Vector stain Elite ABC Kit (Vector Laboratories, Burlingame, CA) was used as the detection system for αSyn and MBP, while the Dako REAL™ EnVision™ Detection System (Dako, Cambridgeshire, UK) was used for NG2. Therefore after washes in PBS, the tissues were incubated with biotinylated goat anti-rabbit IgG or biotinylated goat anti-mouse IgG (Vector Laboratories, Burlingame, CA) at a dilution of 1:200 for 30 min at RT. After washing off the secondary antibody, the sections were incubated in the avidin-

biotin complex solution for 30 min at RT. For the NG2 antibody however, the Dako REAL™ EnVision™ Detection System (Dako, Cambridgeshire, UK) was used. The tissues were incubated in the Dako REAL™ EnVision™/HRP, Rabbit/Mouse reagent for 30 min at RT. After washes in PBS, they were treated in the diaminobenzidine (DAB) solution for 3 min. The DAB solution was washed off and the tissues were counterstained in Mayer's haematoxylin for 3 min. The tissue sections were then dehydrated in graded alcohol (70%, 90%, and absolute alcohol), cleared in three changes of xylene, and then mounted with DPX mounting medium.

4.5. RESULTS

Double and triple immunofluorescence microscopy was carried out to identify co-localisation of αsyn positive GCIs with positive (+) or negative (−) immunoreactivity of a cell marker(s) of interest for each maturational stage. Oligodendrocyte precursor cells were identified with $NG2^+$ immunoreactivity, immature oligodendrocytes as $CNPase^+/MBP^-$ and mature oligodendrocytes as $CNPase^+/MBP^+$.

$NG2^+$ cells (Figure 4.2) commonly exhibit stellate, multi-branching morphology, although some cells may appear bipolar and more polarized. The long delicate processes of $NG2^+$ cells may also display a "beads and swellings" morphology. $NG2^+$ cells and GCIs were widespread in the frontal cortex (Figure 4.3) and cerebellum (Figure 4.4). They were found in close proximity to each other in

some areas, however, did not co-localise. These results indicate that GCI do not accumulate in $NG2^+$ cells.

Immature oligodendrocytes, indicated by $CNPase^+/MBP^-$ staining, were undetectable in tissue sections, while mature oligodendrocytes ($CNPase^+/MBP^+$) were present in great abundance. αSyn co-localised with $CNPase^+/MBP^+$ cells confirming that GCIs are present in mature oligodendrocytes (Figure 4.5).

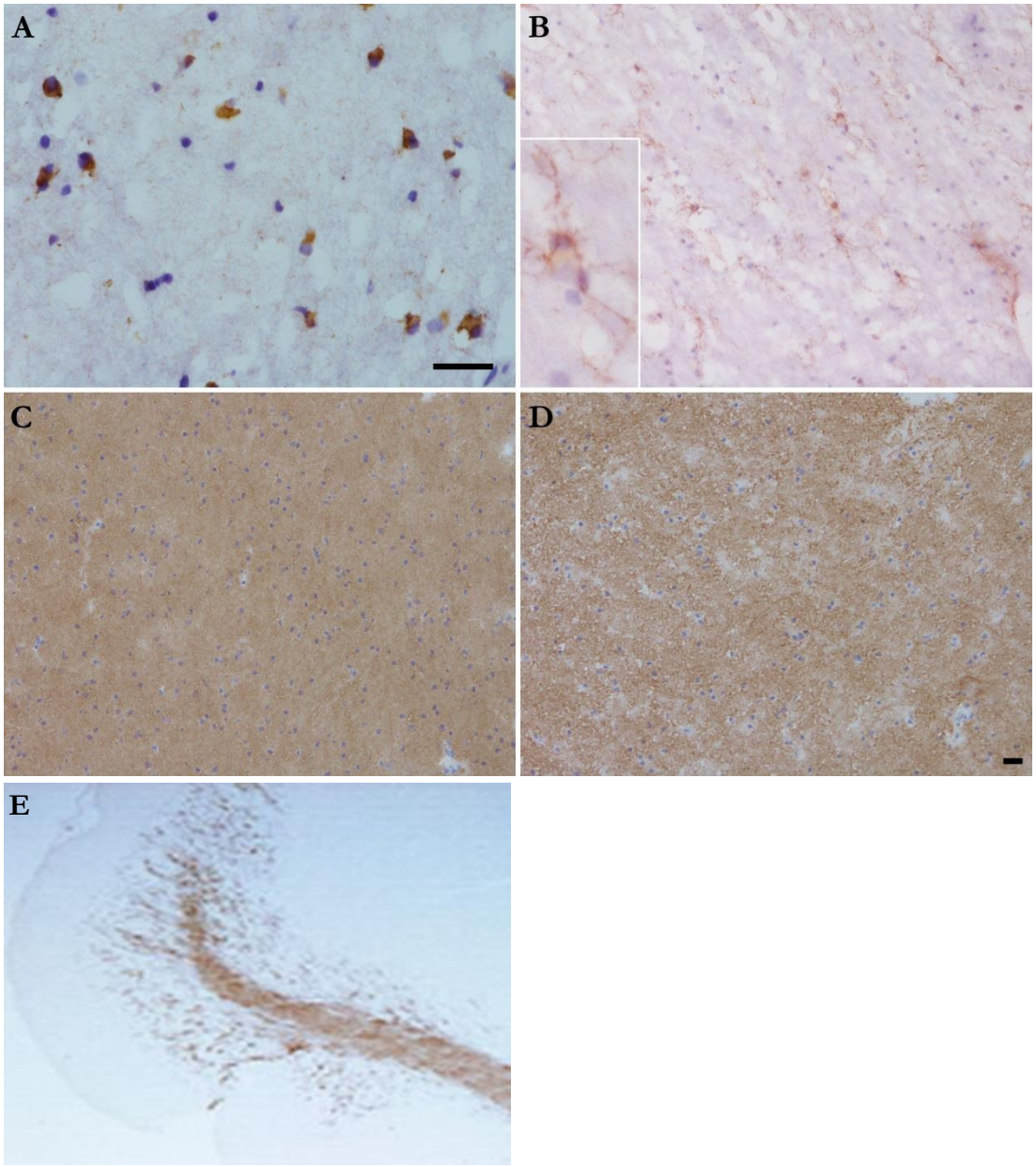

Figure 4.2. Cell and inclusions in MSA

Immunohistochemistry of αsyn-positive GCIs **(A)**, NG2+ cells **(B)** and MBP positive staining in the frontal cortex **(C)** and cerebellar white matter **(D)** of MSA. CNPase-positive staining in white matter tracts and the granule cell layer of the cerebellum an adult mouse brain as illustrated by the manufacturer **(E)**.

asyn: a-synuclein; GCIs: glial cytoplasmic inclusions; MBP: myelin basic protein; Scale bar: 20μm

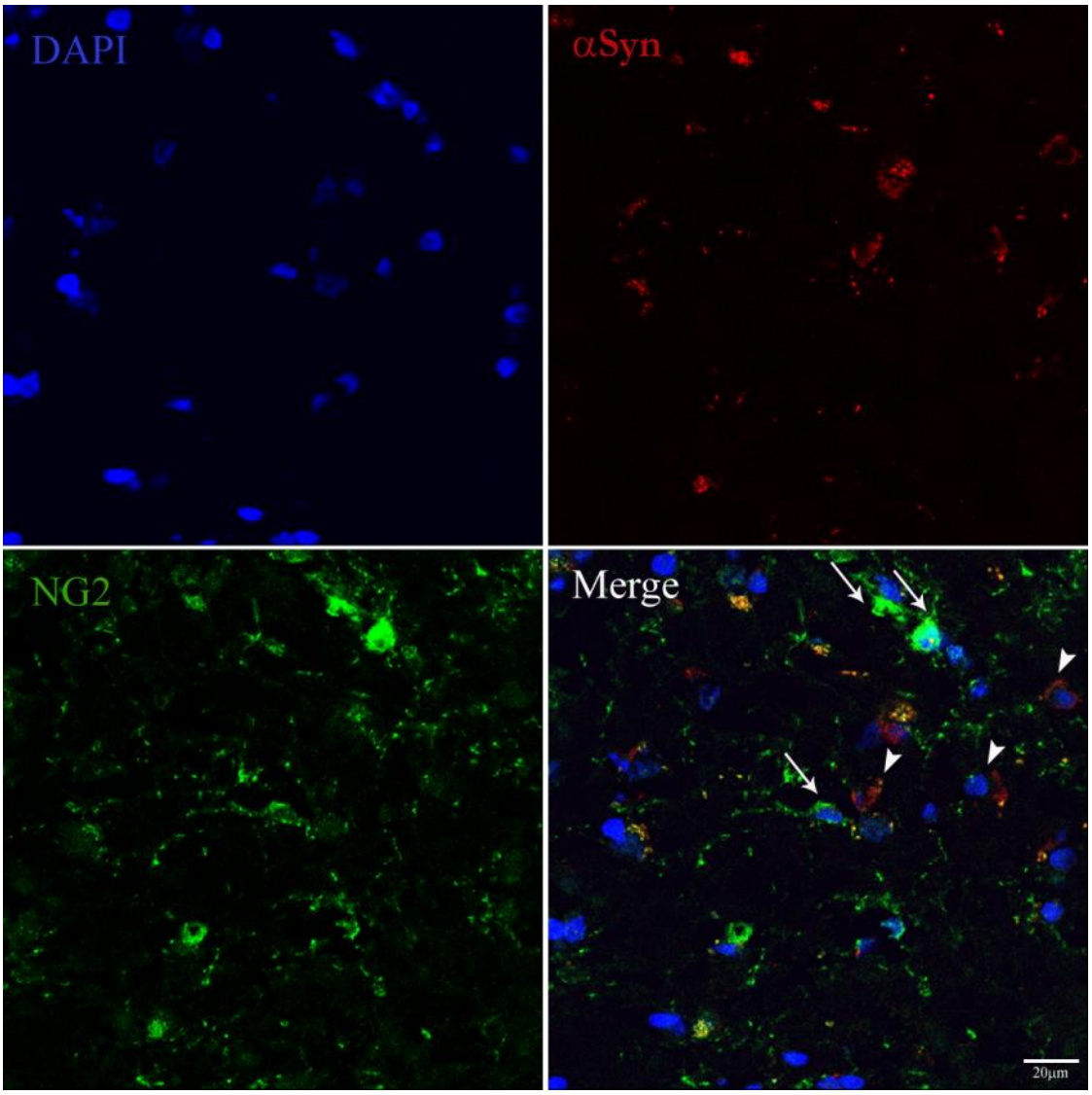

Figure 4.3. GCIs and NG2$^+$ cells in frontal white matter

Double immunofluorescence microscopy of frozen human MSA cortical sections (8μm) for αSyn (red), and NG2 (green) with nuclear DAPI stain (blue). GCIs (red, arrowheads) identified by αSyn immunoreactivity around glial nuclei (DAPI, blue) and NG2$^+$ cells (green, arrows) are both present in frontal cortex white matter. Some GCIs and NG2$^+$ cells are located in close proximity, however, they do not co-localize indicating that GCIs are not found in NG2$^+$ cells. Lipofuscin (lipid-containing granules) are fluorescent at any excitation wavelength and are seen in the merged image as yellow-orange deposits.

GCIs: glial cytoplasmic inclusions; DAPI: 4',6-Diamidino-2-Phenylindole.

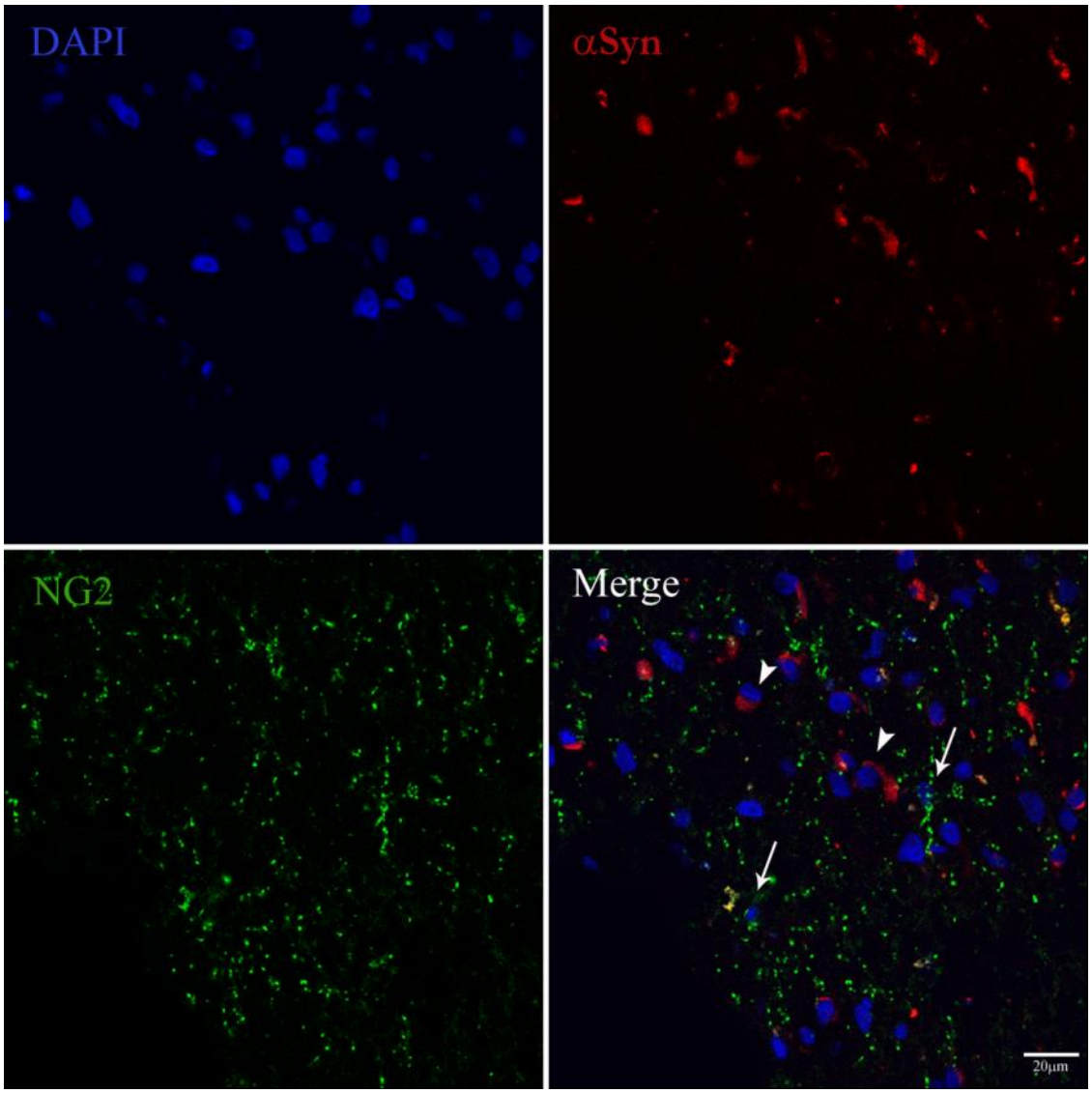

Figure 4.4. GCIs and NG2$^+$ cells in cerebellar white matter

GCIs (red, arrowheads) and NG2$^+$ cells (green, arrows) in human MSA cerebellar white matter sections (8μm). Thus GCIs were not identified in NG2$^+$ oligodendrocyte precursor cells. Lipofuscin (lipid-containing granules) fluoresce at any excitation wavelength and are seen in the merged image as yellow-orange deposits.

GCIs: glial cytoplasmic inclusions; DAPI: 4',6-Diamidino-2-Phenylindole.

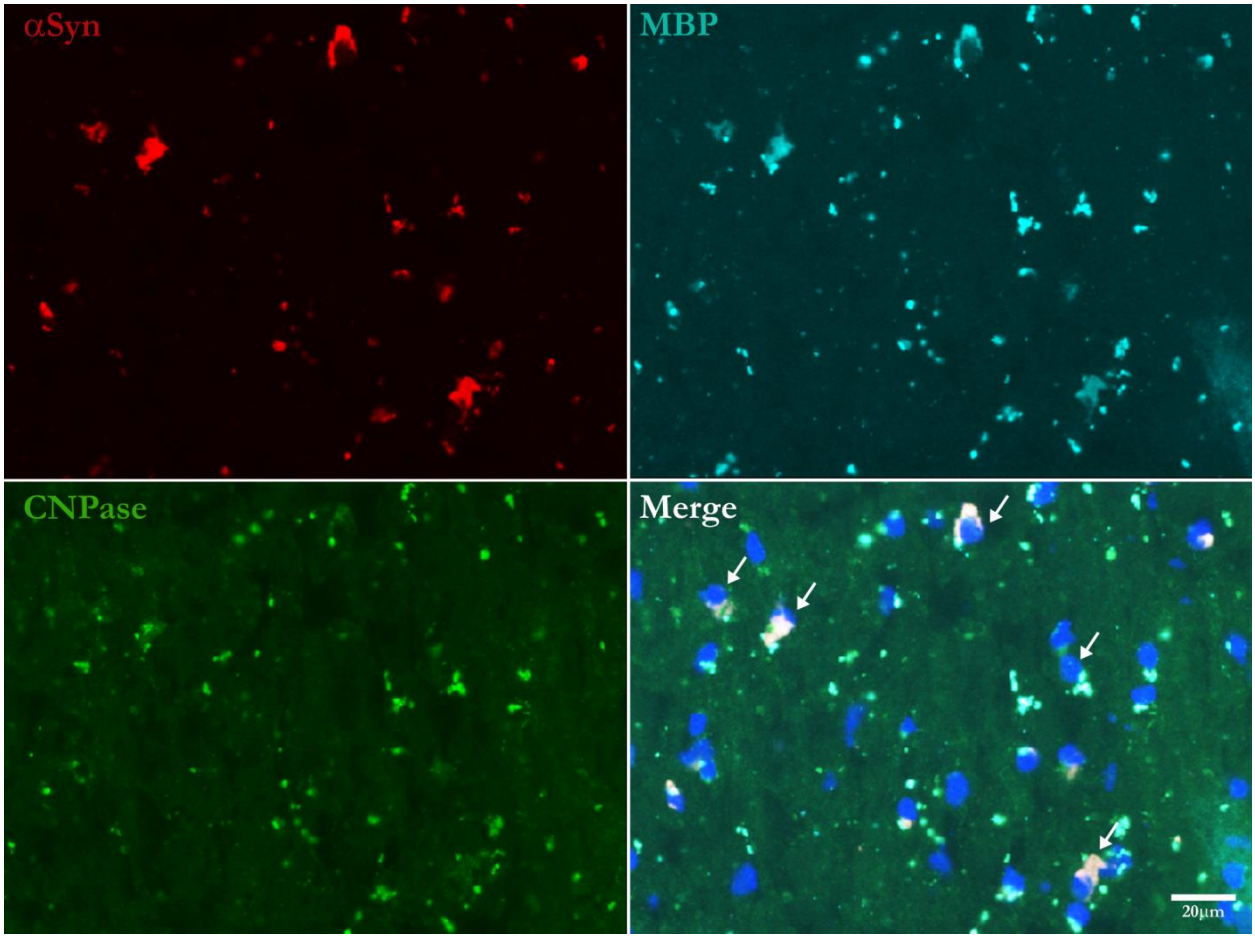

Figure 4.5. GCIs and mature oligodendrocytes in cerebellar white matter

MBP (light blue) and CNPase (green) are both present in mature myelinating oligodendrocytes in MSA cerebellar white matter sections (8µm). The merged image shows that GCIs (red, arrow head) co-localize with MBP and CNPase (white, arrow) indicating that GCIs accumulate in mature myelinating oligodendrocytes. Nucleus is represented by dark blue DAPI staining.

aSyn: a-synuclein; CNPase: 2',3'-cyclic nucleotide 3'-phosphodiesterase; MBP: myelin basic protein; DAPI: 4',6-Diamidino-2-Phenylindole.

4.6. DISCUSSION

GCIs are the hallmark of MSA and their morphologic characteristics coupled with antigenic characterisation of cell type indicate that they accumulate in oligodendrocytes (Papp et al., 1989). Despite the discovery of GCIs in 1989, the mechanisms leading to their formation remain unclear (Papp et al., 1989; Ubhi et al., 2011). Understanding at which oligodendrocyte maturational stage GCIs accumulate is one line of research that can bring us closer to understanding the mechanism of GCI formation and is the focus of this chapter.

Oligodendrocyte progenitor cells which are $NG2^+$ do not co-localize with αsyn which suggests that GCIs do not accumulate in these cells. Confirming previous studies (Papp et al., 1989), the inclusions were found in mature oligodendrocytes as indicated by αsyn co-localisation with $CNPase^+/MBP^+$ cells. The presence of GCIs in $CNPase^+/MBP^+$ cells but not in $NG2^+$ cells indicates that only mature oligodendrocytes are susceptible to GCI formation. These findings parallel those found in an multiple sclerosis (MS) rat model where αsyn protein was not found in $NG2^+$ cells but was present in $CNPase^+$ oligodendrocytes in the spinal cord of myelin oligodendrocyte glycoprotein (MOG)-induced experimental autoimmune encephalomyelitis (EAE) rats (Papadopoulos et al., 2006). What are the reasons behind $NG2^+$ cells' resistance and mature oligodendrocytes' vulnerability to GCI formation? One speculation is a role for myelin in this process as $NG2^+$ cells lack myelin proteins and an extensive microtubule network (Richter-Landsberg, 2000). Myelin formation is a dynamic process involving interaction and transport of lipids and proteins with the aid of the

microtubule network (Pfeiffer et al., 1993). In addition to acting as a highway for lipid and protein transport, the oligodendrocyte microtubule network plays a role in myelin compaction and stabilization (Richter-Landsberg, 2000). Disruption of the oligodendrocyte microtubule network inhibits the translocation of essential proteins and mRNA to the myelin compartment which eventually leads to myelin damage (Carson et al., 1997). αSyn has been shown to interact with membranes, vesicular transport and microtubule associated proteins (MAP) in neurons (Iwai et al., 1995; Kahle et al., 2000; Riedel et al., 2009; Reynolds et al., 2011) but its role in oligodendrocytes is unknown especially while a consensus is yet to be reached on whether oligodendrocytes are capable of producing αsyn (Mori et al., 2002, 2003; Miller et al., 2005). However, similar roles for αsyn may be inferred in mature oligodendrocytes in light of the fact that mature oligodendrocytes contain microtubules and MAP also found in neurons such as tau and MAP2 (LoPresti et al., 1995; Müller et al., 1997; Richter-Landsberg, 2000) in addition to the synergistic relationship found between αsyn and tau (Muntane et al., 2008; Riedel et al., 2009; Clinton et al., 2010; Badiola et al., 2011). Aberrant changes in αsyn, through oligomerisation and fibrillization, may lead to inclusion formation and alter the interaction of αsyn with microtubules and MAP recruiting them into the inclusion and disrupting the microtubule network. Cell culture evidence suggests that αsyn functions as a MAP and that loss of αsyn microtubule-assembly activity induces tubulin aggregation (Alim et al., 2004). Tubulin oligomers, in turn, seed αsyn fibrillogenesis creating a cycle where αsyn and tubulin both induce and exacerbate aggregate formation (Alim et al., 2002, 2004). GCIs have been shown to contain αsyn, tau, α- and β-tubulin in addition to other

proteins (Papp et al., 1989; Gai et al., 1999; Nakamura et al., 2000; Kawamoto et al., 2002, 2007; Pountney et al., 2011; Chiba et al., 2012). Therefore, it may be hypothesized that the interaction of αsyn with myelin and microtubules renders mature oligodendrocytes more susceptible to GCI formation than $NG2^+$ cells.

Determining presence of GCIs in immature pre-myelinating oligodendrocytes, an intermediate phase between $NG2^+$ cells and mature oligodendrocytes, proved to be a more challenging task. Immature oligodendrocytes, identified as $CNPase^+/MBP^-$ cells, are non-myelinating oligodendrocytes and were undetectable in the frontal cortex and cerebellum of this cohort. The lack of immature oligodendrocytes may be explained by the age of the cases studied and the transient nature of this oligodendrocyte maturational stage. The number of immature oligodendrocytes peaks around 28 – 41 gestational weeks and myelination begins at around 30 gestational weeks and progress over several decades (Hasegawa et al., 1992; Back et al., 2001; Jakovcevski et al., 2009). In addition, there is a caudal to rostral pattern where myelination begins in the spinal cord, followed by the brainstem and subcortical structures then finally cortical structures after birth (Hasegawa et al., 1992; Back et al., 2001; Jakovcevski et al., 2009). Transition of immature oligodendrocytes to mature myelinating oligodendrocytes is a regulated process with a narrow window of differentiation and myelination - transitioning from immature oligodendrocytes to myelinating oligodendrocytes within 2 days and myelinating axons within 12-18 hours (Pfeiffer et al., 1993; Bradl and Lassmann, 2010). It is therefore not surprising that immature oligodendrocytes are sparse or not found by the fifth

decade of life, the mean age of onset of MSA, and when myelination is complete and oligodendrocytes fully differentiated.

A further possible source of immature oligodendrocytes would be those that arise due to activation of oligodendrocyte precursor cells ($NG2^+$ cells) as part of the disease process. Myelin loss is a pathological event in MSA and $NG2^+$ cells have been shown to respond to demyelinating events by exiting their quiescent state and populating demyelinated lesions as demonstrated in MS studies (Franklin, 2002; Franklin and ffrench-Constant, 2008). Though some degree of remyelination does occur in MS, it is a suboptimal process resulting in thinner, disproportionate myelin to axon diameter (Franklin and ffrench-Constant, 2008). One hypothesis for the failure of remyelination in MS is inadequate differentiation of oligodendrocyte precursor cells (Franklin, 2002). Therefore even if it were proposed that similar remyelination events occur in MSA, the inadequate differentiation of oligodendrocyte precursor cells and transient presence of immature oligodendrocytes suggest that this maturational stage does not play a vital role in the pathogenesis of MSA.

Conclusion

GCIs occur within mature myelinating oligodendrocytes while oligodendrocyte precursor cells or immature oligodendrocytes are unaffected by αsyn pathology. Understanding the reasons for this preferential accumulation of GCIs could be vital in understanding disease propagation in MSA. It may be hypothesized that a

possible interaction of αsyn with myelin and microtubules renders mature oligodendrocytes more susceptible to GCI formation than $NG2^+$ cells.

This chapter contributed to the following paper:

Ahmed, Z., **Asi, Y.T.**, Lees, A.J., Revesz, T. and Holton, J.L., 2013. *Identification and quantification of oligodendrocyte precursor cells in multiple system atrophy, progressive supranuclear palsy and Parkinson's disease*. Brain pathology, 23(3), pp.263–273.
(Contribution to paper: execution of experiments, data collection and analysis and drafting and review of manuscript).

5

REGIONAL AND CELLULAR EXPRESSION OF *SNCA* IN MSA

5.1. INTRODUCTION

Much information on transcriptional regulation and mutations of the αsyn gene (*SNCA*) has been contributed from PD studies, due to the longer history of research and resources available to the PD field. PD and MSA are α-synucleinopathies and so lessons learned from PD studies may be used as leads or guides for research in MSA. PD exists in inherited and sporadic forms while MSA is largely regarded as a sporadic disease as genetic clues to prove otherwise remain to be discovered and validated. To date, there are three reports suggesting inheritance of MSA in German and Japanese families (Wullner et al., 2004; Soma et al., 2006; Hara et al., 2007). A dosage effect of *SNCA* has been identified where duplication and triplication of the gene leads to different parkinsonian phenotypes (Fuchs et al., 2007; Ross et al., 2008). *SNCA* mutations known to have cause PD were used as a guide for candidate examination in MSA cases, however, there is conflicting evidence for the effect of *SNCA* mutations and multiplication in MSA. While some groups failed to detect mutations or multiplications of *SNCA* in pathologically confirmed MSA cases, other studies

identified single nucleotide polymorphism (SNP) in *SNCA*; rs11931074, rs3822086 and rs3775444, to be associated with increased risk for developing MSA (Ozawa et al., 1999; Lincoln et al., 2007; Al-Chalabi et al., 2009; Scholz et al., 2009; Ross et al., 2010). Mutations in *SNCA* may also lead to a pathological spectrum encompassing that seen in PD and MSA as seen in the case of G51D mutation which includes neuronal and oligodendroglial αsyn-positive inclusions (Kiely et al., 2013).

In addition to examining mutations and multiplications of *SNCA*, there has been some attempt to examine *SNCA* mRNA expression in MSA. Variations in *SNCA* mRNA expression using *in situ* hybridization (ISH) were found in different regions of the normal human brain (Solano et al., 2000). Strong expression was detected in the substantia nigra, entorhinal cortex, granule cell layer of the dentate gyrus, intralaminar nuclei, locus coeruleus, basis pontis, granule cell layer of cerebellum, and inferior olive. In the same study, *SNCA* mRNA expression was not detected in the globus pallidus, dorsal medial nucleus, subthalamic nucleus, superior colliculus, red nucleus, crus cerebri, periaqueductal gray, pontine tegmentum, and molecular layer of cerebellum. Ozawa and colleagues (2001) found that *SNCA* mRNA levels in cortical regions (frontal, temporal or occipital) of MSA brains did not differ from those in controls using quantitative PCR (qPCR). Cortical areas are less severely affected than subcortical regions in MSA and that may be a possible explanation for the similar *SNCA* levels between MSA and controls. It may be plausible that expression differences are more likely to arise in areas more severely affected in MSA such

as the pons and cerebellum. However, as with the evidence for *SNCA* mutations, there are conflicting results with regards to *SNCA* expression in the pons. Jin and colleagues (2008) observed no difference in *SNCA* copy number and mRNA expression in the pons of MSA and control cases, while down-regulation in MSA cases was reported by Langerveld and colleagues (2007). Alternative splicing of *SNCA* mRNA results in the production of different isoforms of the protein, and changes in the mRNA expression level of these isoforms were evident in PD, DLB, and MSA (Beyer et al., 2008 a). The mRNA expression level of isoform *SNCA* 98 was found to be up regulated in the frontal cortices of MSA, PD, and DLB patients. Unlike PD and DLB however, there was no significant difference in the level of *SNCA* 126 mRNA in MSA (Beyer et al., 2008 a).

The previous studies focused on understanding *SNCA* mRNA expression in MSA at the regional level. However, since the pathological hallmark of MSA is αsyn accumulation in oligodendrocytes, a more pertinent question is what is the expression profile of *SNCA* at the cellular level? To date, there is one published study addressing this question (Miller et al., 2005) in which double-labelling ISH for αsyn and proteolipid protein (PLP), an oligodendrocyte marker was performed. The findings of this revealed that *SNCA* is not expressed in oligodendrocytes of MSA or control brains. αSyn is regarded as a pre-synaptic neuronal protein and so understanding its origins in oligodendrocytes in MSA is important to unravelling the pathogenic mechanisms of this disease.

5.2. HYPOTHESIS

a. *SNCA* mRNA expression in MSA is altered and is greater in brain regions with greater αsyn pathology.

b. Accumulation of αsyn in oligodendrocytes in MSA is due to overexpression of *SNCA* mRNA in oligodendrocytes.

5.3. AIM

To determine the regional and cellular expression profile of *SNCA* mRNA in MSA.

5.4. CASE SELECTION

MSA cases were pathologically typed according to published criteria (Ozawa et al., 2004) and grouped into mixed, SND and OPCA types as described in Chapter 2: Materials and methods section 2.4. Frozen tissue from 5 MSA-SND, 5 MSA-OPCA, 5 MSA-mixed types were selected and sex and age –matched to 5 PD and 4 normal control cases to study regional *SNCA* mRNA expression (Table 5.1). The regions studied were the posterior frontal cortex (grey matter and white matter), occipital cortex (grey matter and white matter), dorsal putamen, pontine base and cerebellar white matter. For the cellular expression study, the pons of 5 MSA-mixed type and 6 normal controls was used to isolate neurons and oligodendrocytes. Cases that did not have frozen tissue available were excluded. The demographics of this cohort are presented in Table 5.2.

Table 5.1. Regional expression cohort demographics

Case	Age	Sex	Diagnosis	MSA Pathological Type	PMI (hrs)
1	56	F	MSA	Mixed	28
2	62	M	MSA	Mixed	20
3	64	F	MSA	Mixed	52
4	66	M	MSA	Mixed	105
5	70	F	MSA	Mixed	65
6	50	F	MSA	SND	4
7	54	F	MSA	SND	47
8	58	F	MSA	SND	11
9	63	M	MSA	SND	27
10	72	M	MSA	SND	50
11	56	M	MSA	OPCA	37
12	60	F	MSA	OPCA	62
13	61	M	MSA	OPCA	ND
14	64	M	MSA	OPCA	35
15	66	F	MSA	OPCA	74
16	61	F	PD	NA	26
17	63	M	PD	NA	37
18	65	M	PD	NA	43
19	67	F	PD	NA	108
20	70	M	PD	NA	75
21	57	M	Control	NA	79
22	69	M	Control	NA	ND
23	71	M	Control	NA	39
24	73	F	Control	NA	24

MSA: multiple system atrophy; PD: Parkinson's disease; SND: striatonigral degeneration; OPCA: Olivopontocerebellar atrophy; NA: not applicable; ND: not documented.

Table 5.2. Cellular expression cohort demographics

Case	Age	Sex	Diagnosis	MSA Pathological Type	PMI (hrs)	RIN before LCM	RIN after LCM
1	50	M	MSA	Mixed	30	4.8	2.6
2	70	F	MSA	Mixed	65	5.8	ND
3	56	M	MSA	Mixed	75	4.7	ND
4	64	F	MSA	Mixed	99	4.4	2.8
5	64	M	MSA	Mixed	100	5.1	3.1
6	69	M	Control	NA	ND	4.4	ND
7	82	F	Control	NA	ND	4.8	3.6
8	73	F	Control	NA	24	5.3	2.0
9	85	M	Control	NA	78	4.2	2.2
10	80	F	Control	NA	49	3.9	2.5
11	83	M	Control	NA	63	4.2	2.3

MSA: multiple system atrophy; NA: not applicable; ND: not documented.

5.5. METHOD

5.5.1. Reference genes

The candidate reference genes tested were *TBP*, *UBC*, *GAPDH*, *RPLP0*, *YWHAZ*, *B2M* and *SDHA* and were chosen based on published literature (Vandesompele et al., 2002; Coulson et al., 2008; Trabzuni et al., 2011). The number and choice of reference genes was determined using the Stratagene (Agilent Technologies, California) and qBase (Biogazelle, Belgium) softwares as described in Chapter 2: Materials and methods, section 2.13.3.

5.5.2. Regional expression study

Frozen tissue samples for regional expression study were collected as described in, section 2.6. Tissue was homogenized, RNA extracted and reverse transcription were carried out using TissueRuptor (Qiagen), RNeasy Mini Kit (Qiagen) and SuperScript® VILO™ cDNA Synthesis Kit (Invitrogen, UK) according to manufacturer's instructions and as described in Chapter 2: Materials and methods, sections 2.10 and 2.12. qPCR was performed on Stratagene MX3000p (Agilent technologies, CA) using Power SYBR Green Master Mix (Applied Biosystems) and detailed in Chapter 2: Materials and methods, section 2.14.2.

5.5.3. Cellular expression study

Neurons from the pontine base (~1000 cells) and oligodendrocytes from cerebellar white matter (~1000 cells) of MSA and control cases were isolated using PixCell II laser capture microdissection system (Arcturus Engineering,

Mountain View, CA, USA) and Arcturus CapSure Macro caps (Applied Biosystems, UK, LCM0211) as described in Chapter 2: Materials and methods, section 2.9 and based on a published protocol (Waller et al., 2012). Neurons were identified using Toluidine blue nuclear stain (Chapter 2: Materials and methods, section 2.8.2) and oligodendrocytes using Anti-OSP in a rapid IHC protocol (Chapter 2: Materials and methods, section 2.8.1). RNA extraction was carried out using Arcturus PicoPure RNA isolation kit (Applied Biosystems, UK, KIT0204) and reverse transcription using SuperScript® VILO™ cDNA Synthesis Kit (Invitrogen, UK) according to manufacturer's instructions and as described in Chapter 2: Materials and methods, sections 2.11 and 2.12. qPCR was performed on Stratagene MX3000p (Agilent technologies, CA) using Power SYBR Green Master Mix (Applied Biosystems) and detailed in Chapter 2: Materials and methods, section 2.14.2.

5.5.4. Allen Brain Atlases

The Allen Brain Atlas (ABA) is a resource that provides gene expression data from human, mouse and rhesus macaque brains using ISH and/or microarray techniques. The atlases utilized for the purposes this thesis are the Human Brain Atlas (HBA) and Developing Human Brain Atlas (DevHBA) (Hawrylycz et al., 2012). These atlases are found at the following website http://www.brain-map.org.

5.6. RESULTS

5.6.1. Reference gene analysis

Seven genes – TATA box binding protein (*TBP*), ubiquitin C (*UBC*), glyceraldehyde-3-phosphate dehydrogenase (*GAPDH*), ribosomal protein large P0 (*RPLP0*), tyrosine 3-monooxygenase/tryptophan 5-monooxygenase activation protein, zeta polypeptide (*YWHAZ*), β_2 microglobulin (*B2M*) and succinate dehydrogenase complex, subunit A, flavoprotein (*SDHA*) - were chosen based on published literature (Vandesompele et al., 2002; Coulson et al., 2008; Trabzuni et al., 2011) and analysed to determine which are the most suitable as reference genes for this study. Initial quality control check of the reference genes primers was assessed by melt curve analysis (Figure 5.1) and agarose gel electrophoresis. Multiple peaks on a melting curve plot and bands on an agarose gel indicate the production of non-specific products such as primer-dimers in addition to the desired product rendering the primer set unsuitable for qPCR experiments (Ririe et al., 1997). One set of primers for each gene was assessed except for *UBC* and *TBP*, where two sets of primers were assessed. More than one peak was detected for primers *UBC*-2, *SDHA* and *RPLP0* and therefore they were excluded as candidate reference genes. Only primers that produced a single peak on the melt curve graph and a band at the predicted size on the agarose gel were included for gNorm analysis using qBase plus (qBase+) software (Vandesompele et al., 2002). This analysis allows the determination of the most suitable reference genes (according to the stability of their expression in disease and normal conditions) and the number of reference genes recommended to carry out the desired qPCR assay.

A qPCR experiment on MSA and controls using the primers *TBP*-1, *TBP*-2, *UBC*-1, *GAPDH*, *YWHAZ* and *B2M* was conducted for gNorm analysis. The output of gNorm analysis provides gNorm M and gNorm V values (Figure 5.2). The gNorm M value is indicative of the average expression stability of the gene and a value of 0.5 or less is an indication of greater stability. The most stable genes were *TBP*-1 (gNorm M = 0.329), *TBP*-2 (gNorm M = 0.422), *UBC*-1 (gNorm M = 0.397) and *GAPDH* (gNorm M = 0.498). The gNormV value (<0.15) reflects the optimal number of reference genes that need to be used for the experiment and in this experiment the recommended number of reference genes was set at three. As such, *TBP*-1, *UBC*-1 and *GAPDH* were selected as appropriate reference genes (Table 5.3). Standard curve analysis of these reference genes indicates that they have comparable efficiencies and parallel slopes and are therefore suitable for experimental use (Figure 5.3).

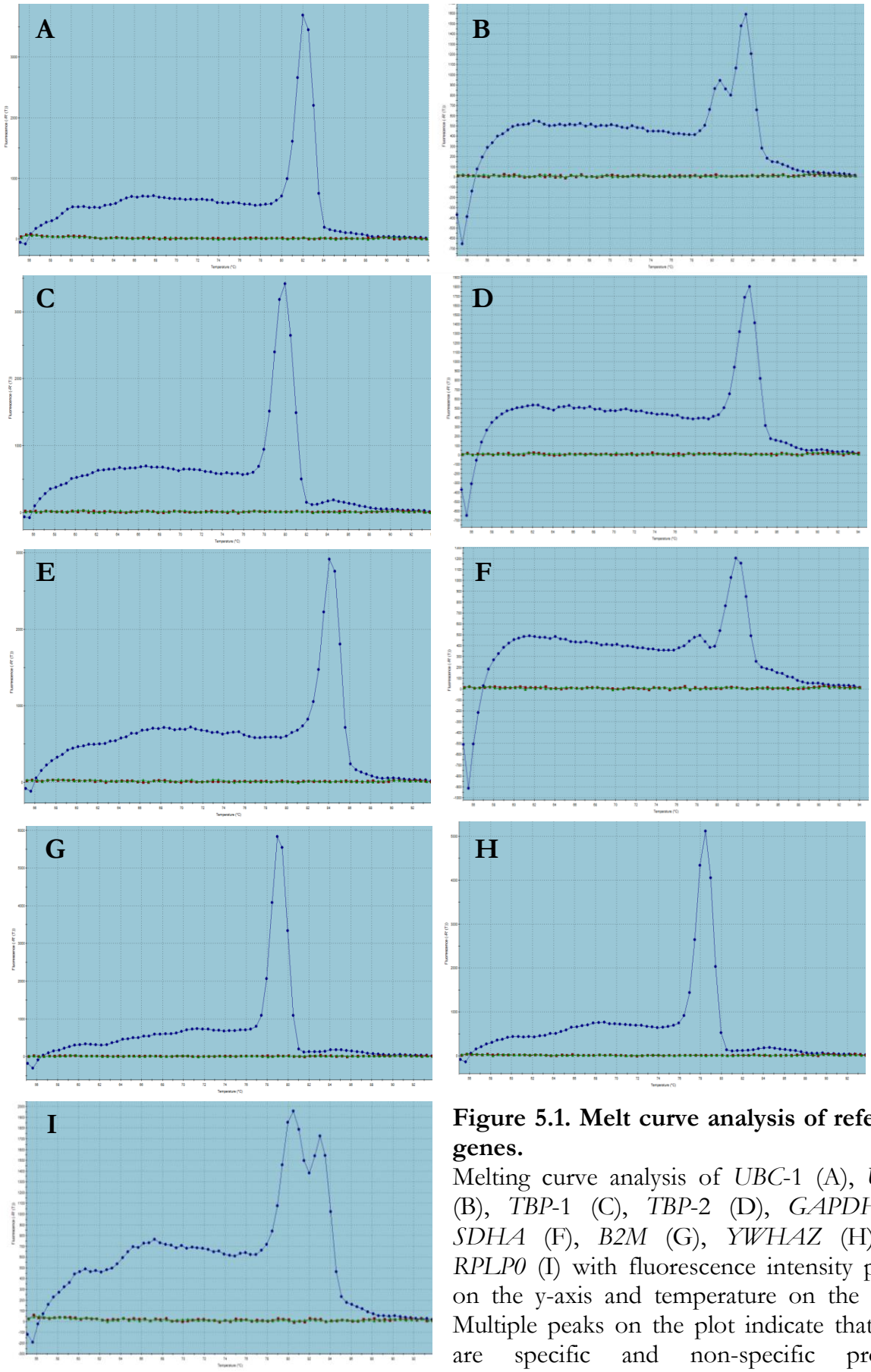

Figure 5.1. Melt curve analysis of reference genes.
Melting curve analysis of *UBC*-1 (A), *UBC*-2 (B), *TBP*-1 (C), *TBP*-2 (D), *GAPDH* (E), *SDHA* (F), *B2M* (G), *YWHAZ* (H), and *RPLP0* (I) with fluorescence intensity plotted on the y-axis and temperature on the x-axis. Multiple peaks on the plot indicate that there are specific and non-specific products produced by the primer set. Therefore, only those primer sets with single peaks (*UBC*-1, *TBP*-1, *TBP*-2, *GAPDH*, *B2M* and *YWHAZ*) were included for further analysis.

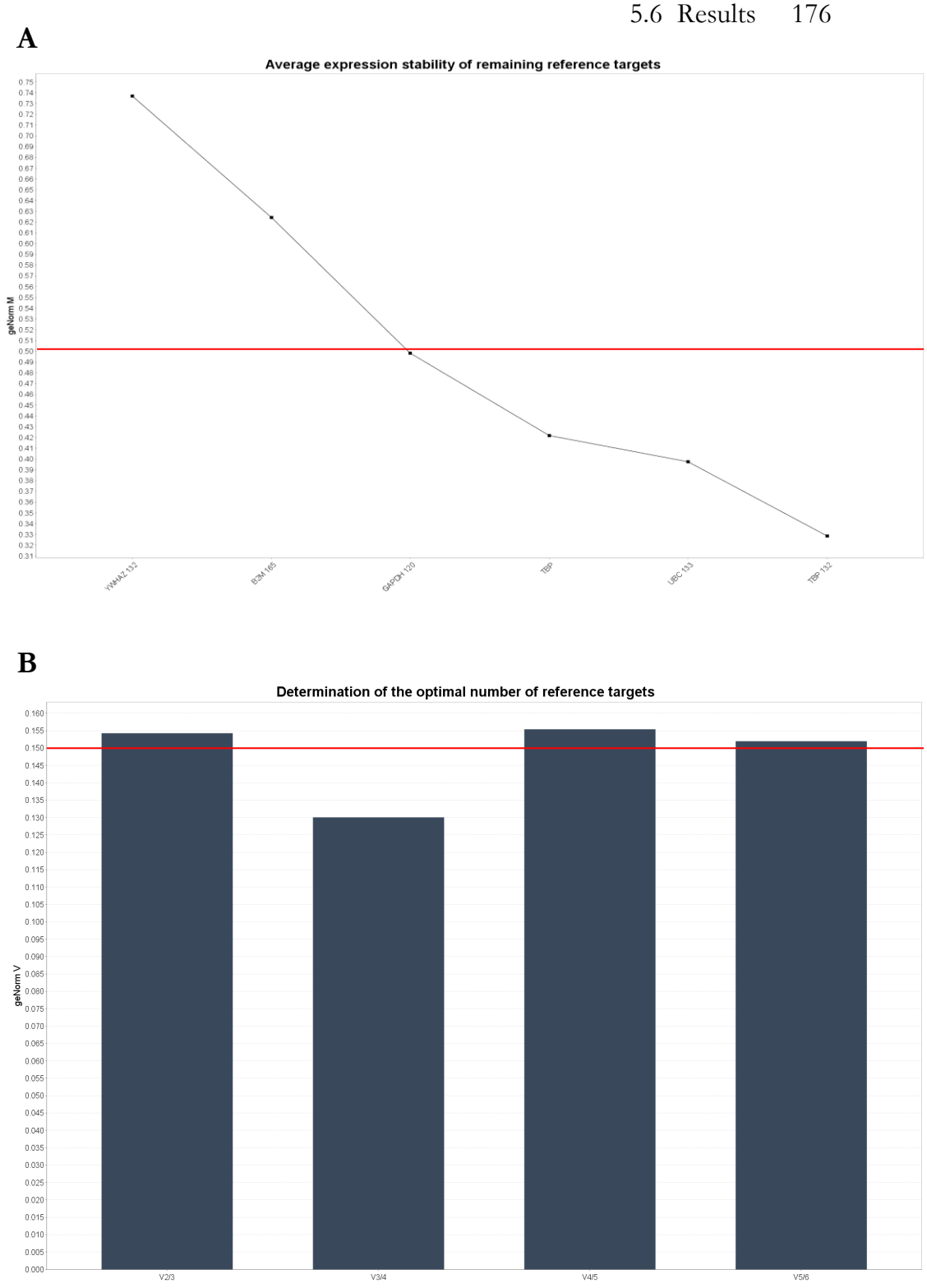

Figure 5.2. gNorm reference gene analysis.

gNormM (A) and gNormV (B) results of gNorm analysis. gNorm M values ≤ 0.5 indicate stability of expression. TBP-1 (0.329), TBP-2 (0.422), UBC-1 (0.397) and GAPDH (0.498) were more stably expressed than B2M (0.624) and YWHAZ (0.737). A gNorm V value of <0.15 was reached at 3 genes indicating that the optimal number of reference genes needed for analysis is three.

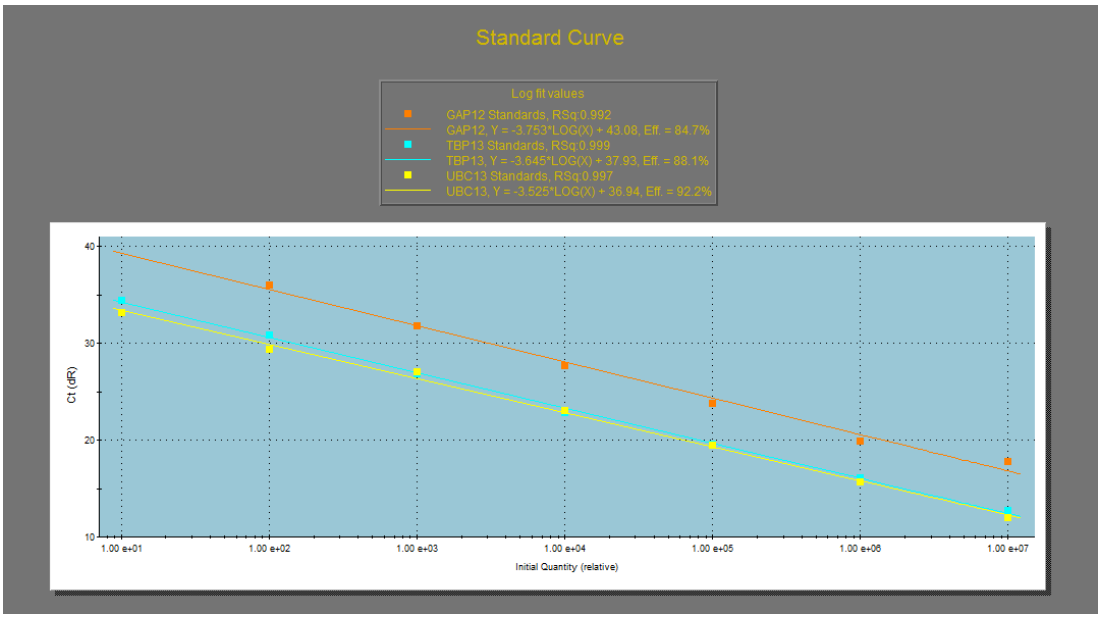

Figure 5.3. Standard curve of reference genes.

Standard curve of the reference genes *UBC* (yellow), *TBP* (blue), and *GAPDH* (orange). These reference genes have parallel slopes and therefore are suitable for use in qPCR experiments. The efficiencies of these genes are 92.2% for *UBC*, 88.1% for *TBP* and 84.7% for *GAPDH*.

Table 5.3. Primer information

Gene	***SNCA***	***TBP***	***UBC***	***GAPDH***
Gene name	synuclein, alpha (non A4 component of amyloid precursor)	TATA box binding protein	Ubiquitin C	Glyceraldehyde-3-phosphate dehydrogenase
RefSeq no.	NM_001146055.1	NM_003194	NM_021009	NM_002046
Primer sequence	**F:** CAACAGTGGCTGAGAAGACCA **R:** GCTCCTTCTTCATTCTTGCCCA	**F:** TGCACAGGAGCCAAGAGTGAA **R:** CACATCACAGCTCCCCACCA	**F:** ATTTGGGTCGCGGTTCTTG **R:** TGCCTTGACATTCTCGATGGT	**F:** GAAATCCCATCACCATCTTCCAGG **R:** GAGCCCCAGCCTTCTCCATG
Alignment	**F:** base 228 to 249 **R:** base 369 to 390	**F:** base 892 to 913 **R:** base 1004 to 1024	**F:** base 399 to 418 **R:** base 511 to 532	**F:** base 313 to 337 **R:** base 413 to 433
Amplicon length (bp)	163	132	133	120
Organism	Homo sapiens	Homo sapiens	Homo sapiens	Homo sapiens
Source	In house design	RTPrimerDB (ID: 2630)	RTPrimerDB (ID: 8)	RTPrimerDB (ID: 1108)

5.6.2. Regional expression

SNCA mRNA expression level was examined in the posterior frontal region, occipital region, dorsal putamen, pontine base and cerebellar white matter of MSA, PD and control cases. MSA cases were further divided into the three pathological subgroups: Mixed, SND and OPCA. *TBP*, *UBC-1* and *GAPDH* were the reference genes used to obtain normalized expression values. A multilevel statistical model was applied in analysing the data whereby the data was first adjusted for regional effect and then adjusted to control for group effect (Figure 5.4).

The mean level of *SNCA* mRNA expression was highest in PD and lowest in MSA-SND, however, there was no overall statistically significant difference in expression between the groups (p=0.14; Figure 5.4 A). After adjusting for group effect, the highest expression was found in the occipital cortex while the lowest was in the putamen. The differences between regions was found to be statistically significant (p<0.0001; Figure 5.4 B). This regional difference in *SNCA* mRNA expression has also been demonstrated in other databases where higher expression was also found in cortical regions compared to subcortical and cerebellar regions (Figure 5.5).

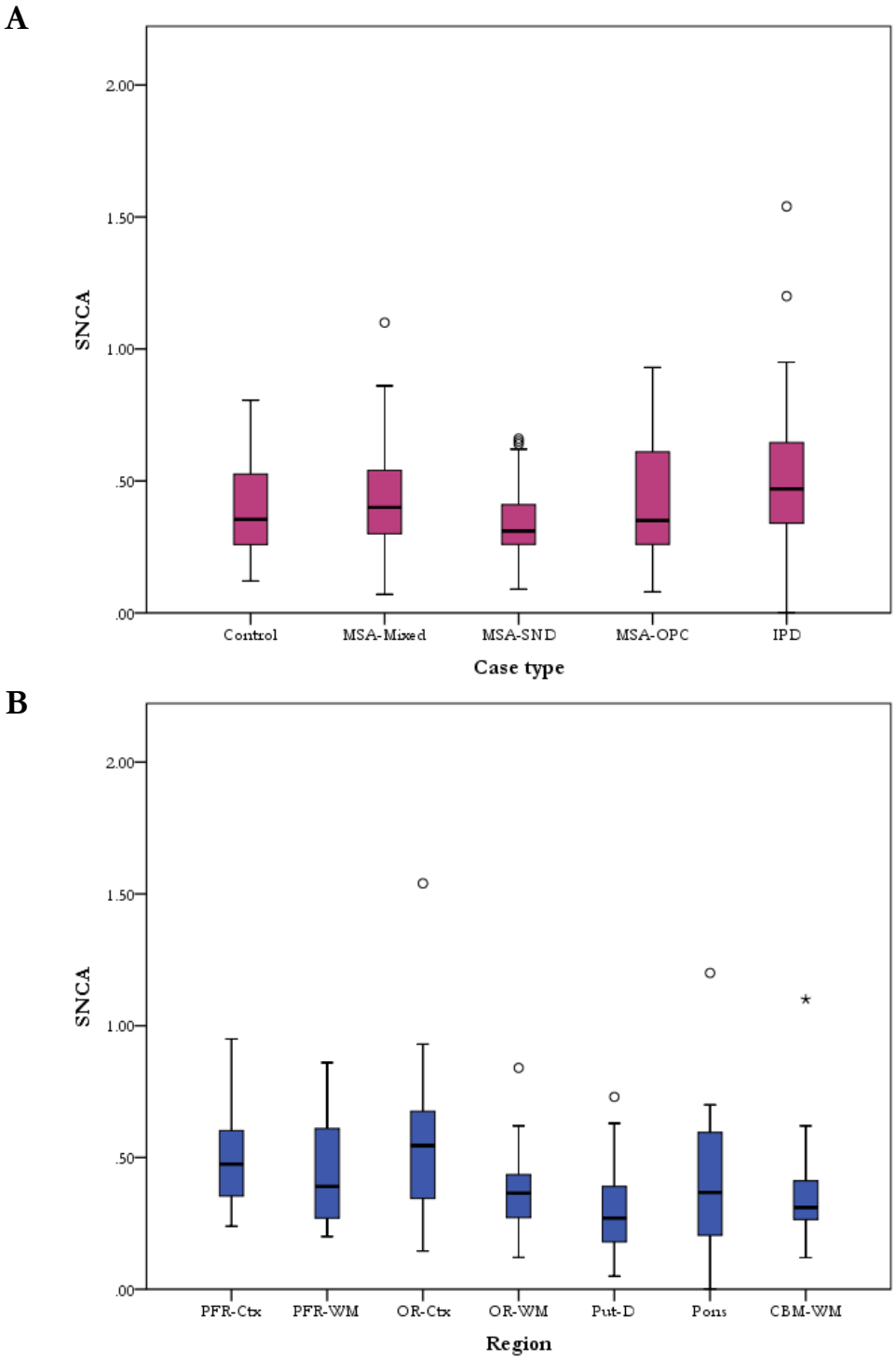

Figure 5.4. *SNCA* mRNA regional expression

Expression of *SNCA* in different groups after adjusting for regional effect indicate that the lowest level of expression is in the MSA-SND group while the highest was in the PD group (A), however, these findings did not reach statistical significance (p=0.14). Comparing expression in different regions while adjusting for group effect (B), shows that there is a statistically significant difference in *SNCA* expression between regions (p<0.0001). The lowest expression was found in the dorsal putamen and the highest in the occipital cortex. *Multilevel model test with significance level set at p=0.05. The boxplot show median values as the line within the box, the box reflects the interquartile range and the whiskers the range of the values.*

PFR: posterior frontal region; OR: occipital region; Put-D: dorsal putamen; CBM: cerebellum; Ctx: cortex; WM: white matter; MSA: multiple system atrophy; SND: striatonigral degeneration; OPC: olivopontocerebellar; PD: idiopathic Parkinson's disease.

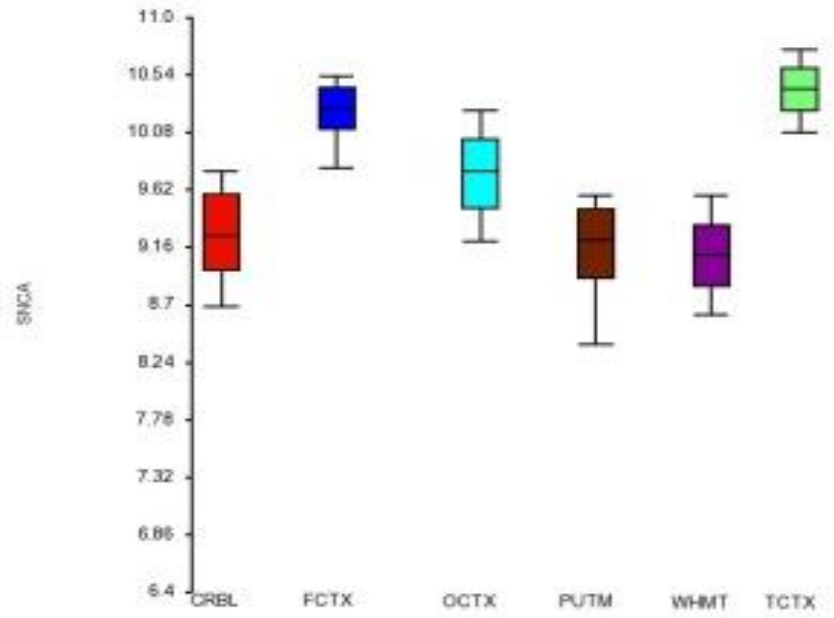

Figure 5.5. *SNCA* mRNA expression from UKBEC dataset

Microarray analysis of *SNCA* mRNA expression in different regions of normal control brains from UKBEC dataset showing greater expression in cortical regions than subcortical and cerebellar.

CRBL: cerebellum; FCTX: frontal cortex; OCTX: occipital cortex; PUTM: putamen; WHMT: white matter; TCTX: temporal cortex; SNCA: a-synuclein

5.6.3. Cellular expression

5.6.3.1. LCM DATA

Neurons and OSP-positive oligodendrocytes were isolated from both MSA-mixed and control brain tissue sections by LCM (Figure 5.6). *SNCA* mRNA expression was detected in neurons and oligodendrocytes of both MSA and control cases, with the highest level of expression found in MSA oligodendrocytes (Figure 5.7 A).

The fold changes in *SNCA* mRNA expression between the different cell types and groups were also calculated (Figure 5.7 B). There was a slight increase in expression in MSA oligodendrocytes as compared to control oligodendrocytes (fold change = 0.7, Mann Whitney U test, $p=0.18$). Expression in MSA neurons, on the other hand, was slightly decreased as compared to control neurons (fold change = -0.4, Mann Whitney U test, $p=0.46$). Comparing the different cell types within the same groups reveals that control oligodendrocytes express 0.3 times (Mann Whitney U test, $p=0.92$) more *SNCA* than control neurons. The greatest difference was seen between MSA oligodendrocytes and neurons as expression in MSA oligodendrocytes is 3.1 times higher than MSA neurons (Mann Whitney U test, $p=0.16$).

RNA quality was assessed using the Agilent Bioanalyser 2100. Maintenance of RNA quality was adequate as assessed by the RIN of samples before and after LCM was carried out and this is in keeping with previous findings (Waller et al., 2012). Prior to LCM, samples had a mean RIN of 4.7 (range 4.2-5.8) declining to 2.6 (range 2.0-3.1) after LCM.

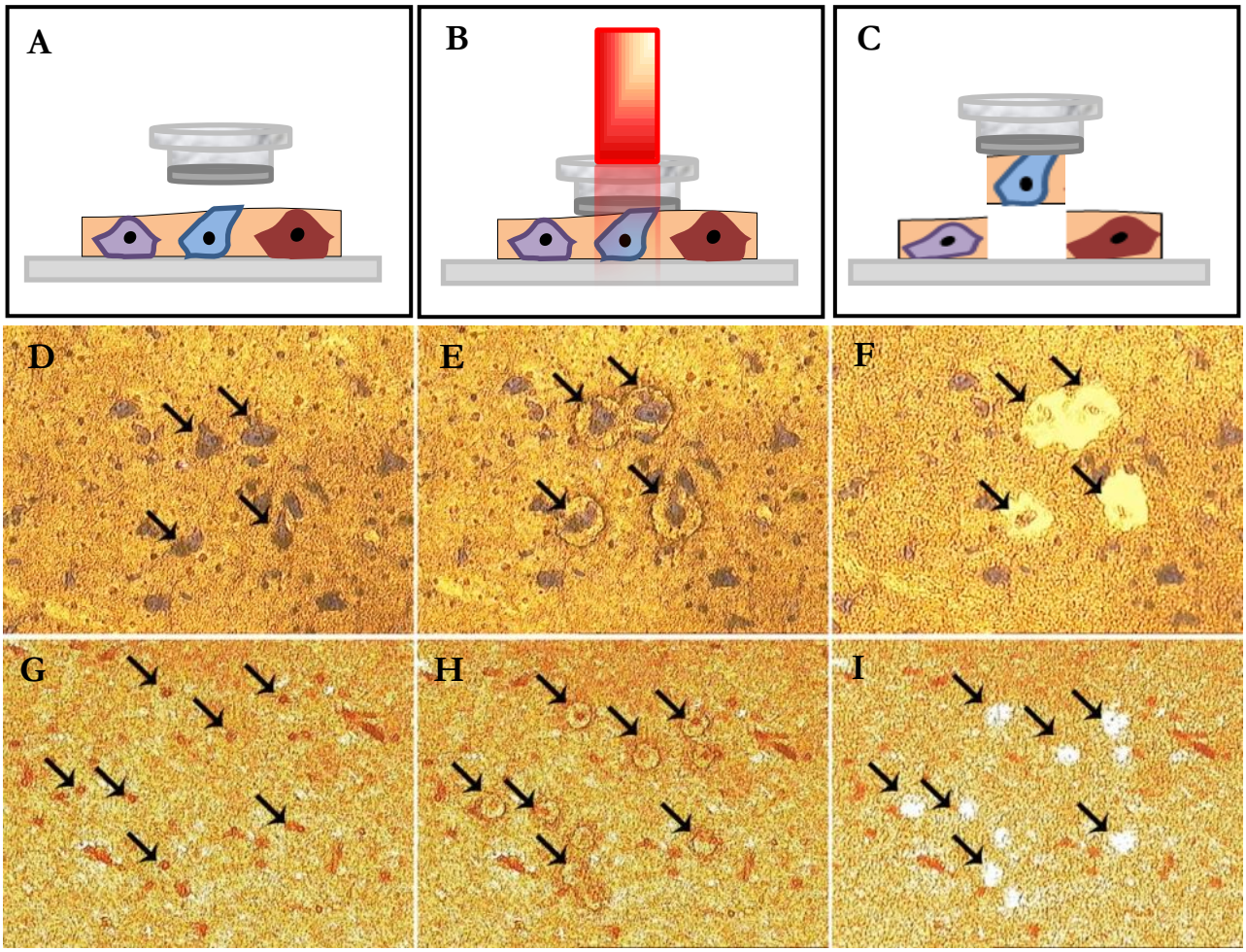

Figure 5.6. LCM of neurons and oligodendrocytes

Schematic of LCM (A-C) and LCM of neurons identified by Toluidine nuclear stain (D-F) and oligodendrocytes identified by OSP-immunohistochemistry (G-I) from frozen post-mortem human brain tissue. Once cells of interest were identified in the tissue section (A,D,G), the laser was fired on those cells causing the thermoplastic film on the cap to melt and the cells to adhere to the film (B,E,H). The cap was then lifted carrying with it the targeted cells and leaving behind unwanted cells (C,F,I).

OSP: oligodendrocyte specific protein

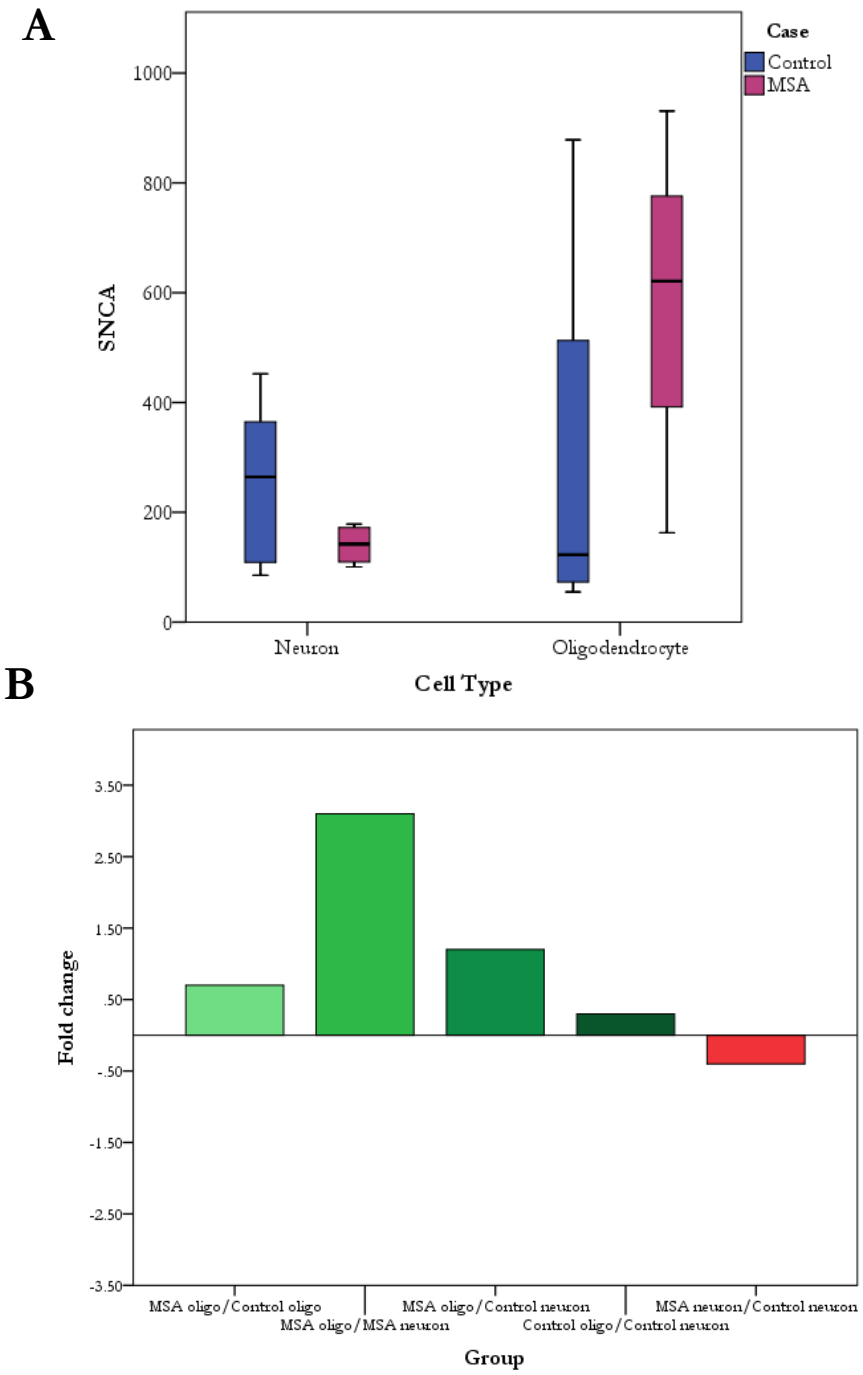

Figure 5.7. *SNCA* mRNA cellular expression

SNCA is expressed in neurons and oligodendrocytes of both MSA and control cases. Expression in neurons is greater in controls as compared to MSA (*p=0.47*), in contrast to oligodendrocytes where expression is greater in MSA (*p=0.18*), however, these results did not reach statistical significance (A). The bar graph represents fold change of expression values between the different cases and cell types (B). Although none of the differences reached statistical significance, the bar graph shows increased expression in MSA oligodendrocytes when compared to control oligodendrocytes (*p=0.18*), MSA neurons (*p=0.16*) and control neurons (*p=0.18*).

In contrast, there was a slight decrease in αSyn expression in MSA neurons as compared to control neurons (*p=0.46*). *Mann-Whitney U test with significance level set at p=0.05. The boxplot shows median values as the line within the box, the box reflects the interquartile range and the whiskers the range of the values.*

Oligo: oligodendrocytes; MSA: multiple system atrophy.

5.6.3.2. HUMAN BRAIN ATLAS (HBA) AND DEVELOPING HUMAN BRAIN ATLAS (DEVHBA)

There is a clear demarcation between grey and white matter in cortical areas, as such, data from cortical areas were chosen to assess *SNCA* mRNA expression from the HBA and DevHBA. Neuronal *SNCA* mRNA expression was assessed in grey matter as this area is enriched in neurons. White matter, on the other hand, is an oligodendrocyte enriched region and is therefore taken as a proxy for oligodendrocyte *SNCA* mRNA expression. The cortical regions available in the HBA include the temporal and visual cortices, while, the prefrontal and visual cortices were part of the DevHBA dataset. The data reviewed is *SNCA* ISH from normal, adult brain.

Neurons in the grey matter of prefrontal, temporal and visual cortices show strong expression of *SNCA* mRNA (Figure 5.8). *SNCA* mRNA expression is not evident in the white matter of the same cortical regions which may indicate that it is not expressed by oligodendrocytes or present in axons (Figure 5.9).

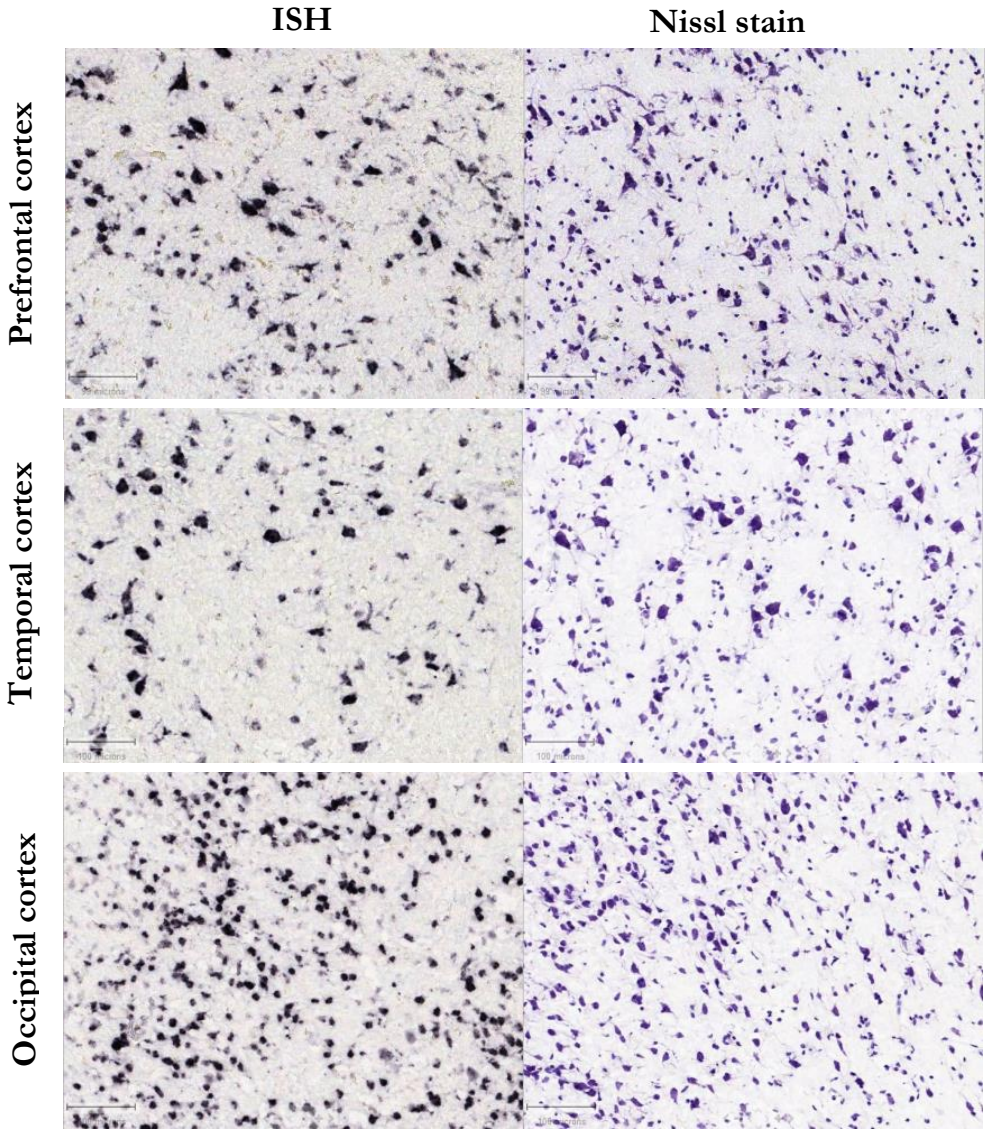

Figure 5.8. *SNCA* ISH in cortex of human brain

The cortex is a neuron-rich area of the brain. It is evident here that there is strong *SNCA* mRNA expression in neurons of the prefrontal, temporal and occipital cortices. The left column represents the ISH sections and the right column is the corresponding Nissl stain sections to help visualize cells.
ISH data from the Allen Brain Atlas (Hawrylycz et al., 2012) http://www.brain-map.org.

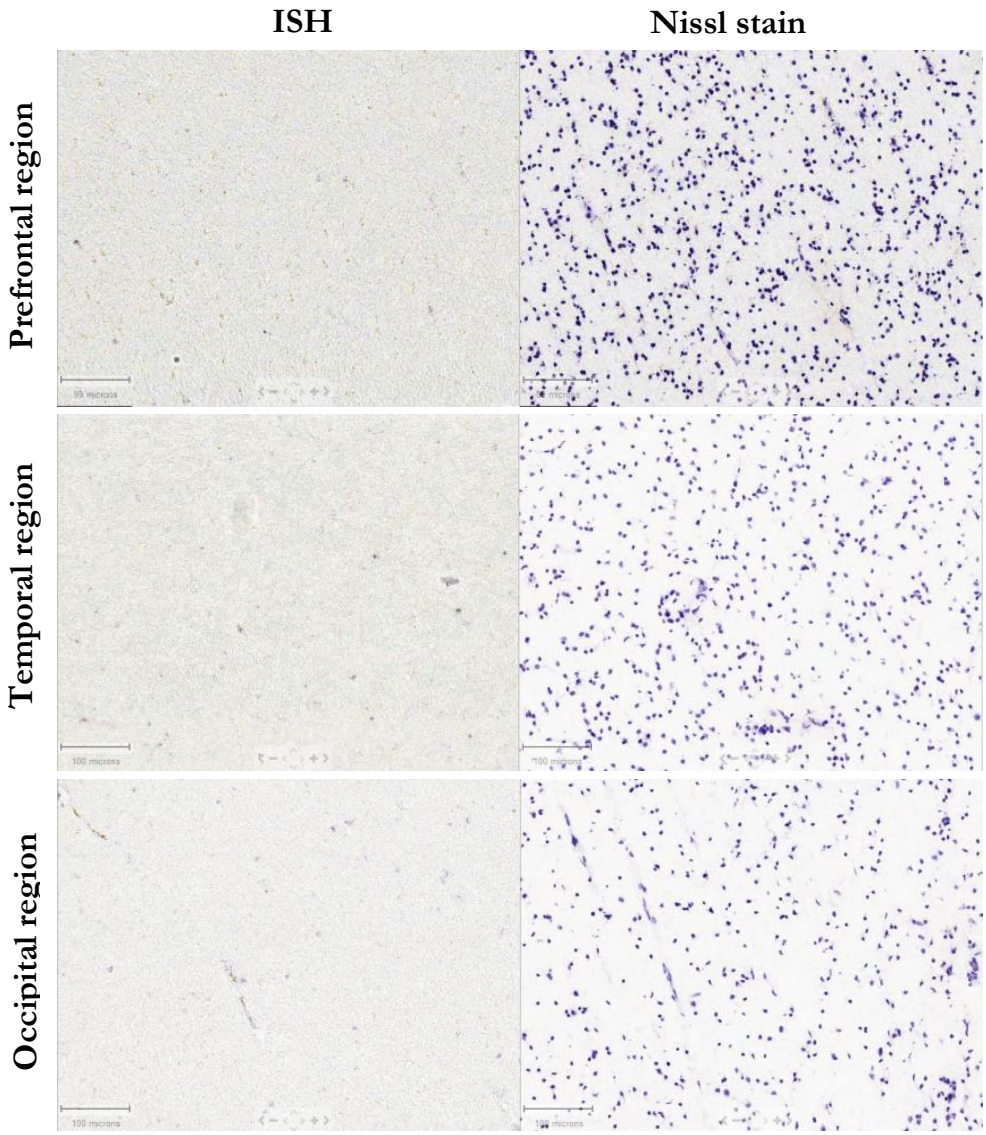

Figure 5.9. *SNCA* ISH in subcortical white matter of human brain

White matter is an oligodendrocyte-rich area of the brain. *SNCA* mRNA expression in oligodendrocytes is not evident in these sections of white matter from the prefrontal, temporal and visual cortices. The left column represents the ISH sections and the right column is the corresponding Nissl stain sections to help visualize cells.

ISH data from the Allen Brain Atlas (Hawrylycz et al., 2012) http://www.brain-map.org.

5.7. DISCUSSION

αSyn has been localized in the brain to neuronal presynaptic terminals and is thought to play a role in neuronal plasticity, vesicular transport and membrane interaction (Iwai et al., 1995; Kahle et al., 2000; Reynolds et al., 2011). There has been great interest in αsyn in MSA since its identification as one of the main constituents of GCIs. Understanding the expression pattern of *SNCA* mRNA in MSA at both the regional and cellular levels is essential to determine if changes in expression play a role in MSA pathogenesis and whether this influences regional vulnerability to disease. The regional expression analysis demonstrates that *SNCA* expression level varies across different brain regions in control, MSA and PD groups. The greatest expression is found in the occipital cortex and the lowest level in the putamen. However, *SNCA* mRNA expression is not significantly different between the MSA subgroups, PD and control cases in all regions. The expression trend found in MSA and control cases of this cohort is similar to that found in other expression databases such as UKBEC (Trabzuni et al., 2011) and Allen Brain Atlas (Hawrylycz et al., 2012) which analyze gene expression in control human brains (Figure 5.5). The similarity in trend, where *SNCA* is generally expressed more in cortical regions than subcortical and cerebellar regions, has two main implications. The first is that the vulnerability of StrN and OPC regions is not associated with a higher baseline expression level of *SNCA*. It could be hypothesized that the abundance of GCIs in specific regions is due to higher expression levels of *SNCA* in the normal condition in those regions that is exacerbated by disease. The findings of this study, however, do not support this hypothesis as *SNCA* mRNA levels are higher in cortical than

subcortical regions in both normal and disease cases, while GCI pathology is greater in StrN and OPC regions in MSA. This also indicates that the disease has not caused an alteration in expression levels in areas of greater vulnerability. The undetectable difference in *SNCA* expression level between the different MSA groups, PD and controls may imply that factors contributing to pathogenic mechanisms of MSA may be further downstream and not at the transcriptional level and may suggest that impaired αsyn degradation may contribute to the disease.

Another possibility is that any differences at the transcriptional level are masked by the cellular heterogeneity of the samples. The major cell type of white matter is oligodendrocytes, but this region also contains axons, astrocytes and microglia. Therefore, it may be inferred that the *SNCA* expression found in white matter samples is contributed to by axons, oligodendrocytes and other glial cells. Although it has long been suggested that mature oligodendrocytes lack *SNCA* (Solano et al., 2000; Miller et al., 2005; Jin et al., 2008), cell-culture evidence indicates that rat and mouse oligodendrocytes express *SNCA*, and in some cases this expression is transient, appearing in precursor cells and declining as they mature (Richter-Landsberg et al., 2000; Culvenor et al., 2002; Nielsen et al., 2006). The contribution of axons to expression values of white matter samples is a valid argument especially that axons have been shown to have a local repository of mRNA and that *SNCA* has been shown to be transported down axons in hippocampal cultures (Withers et al., 1997). There have been attempts to identify and characterize the axonal transcriptome and the source of this local repository

has been shown to be from neuronal as well as glial nuclei (Cutillo et al., 1983; Giuditta et al., 2008).

To overcome this problem of cellular heterogeneity, LCM was used to obtain samples highly enriched in neurons and oligodendrocytes as LCM isolation of OSP-positive oligodendrocytes has been shown to provide an oligodendrocyte-enriched sample (Waller et al., 2012). Using this approach this study has unmasked interesting findings in *SNCA* expression profile in neurons and oligodendrocytes of MSA and control cases. Firstly, *SNCA* expression was detected in oligodendrocytes of both control and MSA cases confirming the findings in white matter samples in the regional analysis of this and other cohorts. Secondly, the highest *SNCA* expression was found in MSA oligodendrocytes as compared to control oligodendrocytes, MSA neurons and control neurons. Therefore, not only has *SNCA* been found to be expressed by oligodendrocytes, but in the disease condition, this expression seems to be increased. This overexpression in MSA parallels findings in MS studies which show an increase in *SNCA* mRNA and protein expression in the presence of inflammatory and cell stress signals (Tanji et al., 2001; Papadopoulos et al., 2006; Lu et al., 2009).

The overexpression of *SNCA* mRNA in MSA oligodendrocytes may be a mechanism contributing to the accumulation of the αsyn protein in MSA oligodendrocytes as GCIs. In addition to overexpression by oligodendrocytes, the fold change difference between neurons and oligodendrocytes may also be a contributing factor. There is a subtle fold change difference between neurons

and oligodendrocytes of controls, where it is slightly higher in oligodendrocytes. In MSA, however, this fold difference is ten times higher. This may suggest that there is an expression equilibrium between neurons and oligodendrocytes and a disruption in this equilibrium could be a disease modifying factor. Though speculative, MSA oligodendrocytes may be overexpressing to compensate for a possible shortage caused by the slight down regulation by MSA neurons and aiding in replenishing αsyn pool in neurons. The cellular expression of *SNCA* in MSA may also explain the pathological profile of the disease. GCIs are found in greater abundance than NCIs in MSA, and this greater susceptibility of oligodendrocytes to inclusion formation may be a reflection of overexpression of *SNCA* by oligodendrocytes in MSA.

SNCA mRNA expression in oligodendrocyte-rich white matter areas and LCM-oligodendrocytes samples, of both normal and disease groups adds further evidence to the on-going debate in the literature on whether *SNCA* mRNA and/or protein is present in oligodendrocytes of normal and disease cases. Microarray data of databases such as UKBEC and Allen Human Brain Atlas have shown similar findings in their cohorts as found in the cohort of this thesis indicating the reproducibility of *SNCA* mRNA expression detection by qPCR and microarray techniques. Unlike qPCR and microarray, there is undetectable *SNCA* expression in white matter areas in ISH experiments. The undetectable signal using ISH may not necessarily indicate an absence of expression but rather the resolution limitation of the technique (Miller et al., 2005; Deglincerti and Jaffrey, 2012). This is a more plausible explanation as *SNCA* was clearly detected

by qPCR and microarray. The higher sensitivity power of qPCR and microarray techniques comes at the expense of losing anatomical localization of expression in different cells and regions in intact tissue, as is feasible by ISH. However, using LCM to isolate specific cell types is one way of overcoming this impediment. LCM is a powerful tool so long as one is aware of its limitations, especially when using human post mortem tissue. LCM allows single cell isolation, however, there will always be some minor degree of contamination from the area surrounding the cell that falls within the laser spot. Another caveat is that with every additional processing step the likelihood of further RNA degradation is increased and in LCM those extra steps are the staining of the cells followed by laser capture. Furthermore, this is a time consuming process where hours may be spent on one sample to collect an adequate number of cell that would result in a substantial RNA yield.

Another technique for isolating single-cell populations is fluorescence-activated cell sorting (FACS). FACS may be employed to separate specific cell types from brain homogenates which may then be used for molecular analysis (Schwartz et al., 2003; Nielsen et al., 2006; Olah et al., 2012; Dammer et al., 2013). It would be beneficial to compare the results and quality of LCM- and FACS- isolated cells of post-mortem tissue as sampling from human cases rather than animal and cell models is the most accurate representation of disease-related changes. Expression of genes in LCM- or FACS- isolated samples may then be conducted using qPCR and microarray or using new technologies such as Nanostring – a

multiplex digital gene expression platform analysing up to 800 genes (Morrow and Donaldson, 2011; Cajigas et al., 2012; Northcott et al., 2012).

The promising findings of the LCM experiment of this thesis open the door to further exploration into the molecular pathogenesis of MSA. The first step would be to repeat and expand the experiment on a different, larger cohort to ensure reproducibility of the findings. Inclusion of unaffected brain regions may help to elucidate the selective vulnerability of StrN and OPC regions. In addition to affected and unaffected brain regions, examination of expression in MSA cases with short disease duration and long disease duration may provide further insight into the role of *SNCA* mRNA expression on clinical outcome. A further step would be to characterize *SNCA* mRNA expression at different stages of oligodendrocyte maturation. The oligodendrocyte lineage comprises precursor, immature, mature non-myelinating and mature myelinating cells and αsyn protein in GCIs has been found in mature but not precursor oligodendrocytes in MSA (Papp et al., 1989; Ahmed et al., 2012). Therefore, determining *SNCA* mRNA expression in the different maturation stages may provide further insight into any underlying vulnerability of cells of oligodendrocytes lineage. Furthermore, expression analysis on FACS-isolated cells using the same markers as those of the LCM experiment is warranted to determine the feasibility of this technique. If adequate RNA quality and quantity are obtained using FACS, then it may prove as a useful alternative or complimentary tool to LCM analysis. Studying the transcriptome and proteome of single cell populations from control and disease

human post-mortem tissue will provide greater insight into the molecular mechanisms leading to disease

Conclusion and future directions

SNCA mRNA overexpression in mature oligodendrocytes in MSA is a possible mechanism by which GCIs form. Further exploration of *SNCA* mRNA expression in affected and unaffected brain regions and in MSA patients with different clinico-pathological profiles will provide further insight into the contribution of cellular *SNCA* mRNA expression to regional vulnerability and clinical outcome in MSA.

This chapter contributed to the following paper:

Asi, Y.T, Simpson, J.E., Heath, P.R., Wharton, S.B., Lees, A.J., Revesz, T, Houlden, H, Holton, J.L. *Alpha-synuclein mRNA expression in oligodendrocytes in MSA*. Accepted *GLIA*.

6

THE ROLE OF EXTRACELLULAR ALPHA-SYNUCLEIN IN GCI FORMATION

6.1. INTRODUCTION

MSA is proposed to be a primary oligodendrogliopathy with secondary neurodegeneration due to myelin dysfunction, accumulation of αsyn, and axonal damage (Wenning et al., 2008; Jellinger and Lantos, 2010). Abnormal accumulation of αsyn in oligodendrocytes as GCIs is the pathological hallmark of MSA, however, the mechanism of this accumulation is yet to be established. Candidate hypotheses to the mechanisms of inclusion body formation in oligodendrocytes cells are overexpression of the protein by oligodendrocytes, oligodendrocytes internalization of the protein from the external environment, and compromised efficacy of the protein degradation system.

In vitro models utilizing oligodendroglial cells rather than other glial cells are better suited as MSA models as inclusions in other glial cells have not been detected in MSA, however, there are few studies addressing the mechanism for αsyn accumulation in oligodendroglial cells. Stefanova and colleagues used astrocytoma cells and found that overexpression of αsyn has detrimental effects on the cells that are exacerbated by the presence of oxidative stress (Stefanova et

al., 2001, 2005 b). Overexpression of αsyn in the oligodendroglial cell line OLN-93 results in disorganization of the microtubule network but does not cause cell death as it does in the astrocytoma cells (Scholz et al., 2007). These studies overexpressed αsyn in glial cell cultures as a means of recapitulating inclusion body formation and the pathological consequences that follow. Although these studies provide insight into the sequelae of abnormal protein accumulation, they do not address the question of how the inclusion bodies initially form. In addition to overexpression of *SNCA* in oligodendroglial cell lines, these cell lines were used to examine the mechanism of αsyn internalization (Kisos et al., 2012; Konno et al., 2012). Oli-neu, OLN-93, KG1C, MO3.13 oligodendroglial cell lines were used to demonstrate that oligodendroglia are capable of internalizing exogenous αsyn present in the media and that the uptake proceeded in a time- , concentration- and endocytotic- dependant manner (Kisos et al., 2012; Konno et al., 2012). In addition to oligodendrocytes, endocytotic internalization of extracellular αsyn by astrocytes and microglia has also been demonstrated (Lee et al., 2008 a, 2010).

In vivo models provide evidence for the capacity of neuron-to-neuron αsyn transmission (Desplats et al., 2009; Hansen et al., 2011). GFP-labelled mouse neuronal stem cells grafted into the hippocampus of transgenic mice expressing human αsyn were immunopositive for human αsyn as early as one week after post transplantation (Desplats et al., 2009). Similarly, mouse embryonic mesencephalic neurons transplanted into the striatum of transgenic mice expressing human αsyn developed human αsyn-positive puncta (Hansen et al.,

2011). Transmission of αsyn from host to grafted neurons in PD patients with the development of LB in the grafted neurons provides further evidence of the pathological spread of αsyn (Kordower et al., 2008; Li et al., 2008; Angot and Brundin, 2009).

Moving to a different approach, the effect of intracerebral inoculation of αsyn into mutant and wild-type mice was investigated (Luk et al., 2012 a; b; Masuda-Suzukake et al., 2013). The inoculated αsyn initiated LB/LN-like inclusions, cell-to-cell transmission of inclusions, neuronal loss and motor deficits. These studies indicate that similar neuropathological changes may be induced in both mutant and wild-type mice.

Although *in vitro* studies suggest that oligodendrocytes are capable of internalizing αsyn, this has not been shown *in vivo*. *In vivo* evidence of αsyn transmission have provided confirmation for neuron-to-neuron transfer but has not established uptake of αsyn by glia. The focus of this chapter is to investigate whether uptake of extracellular αsyn by oligodendrocytes represents a possible mechanism for inclusion formation.

6.2. HYPOTHESIS

a. αSyn accumulation in oligodendrocytes in MSA as GCIs is due to internalization of αsyn derived from neurons or the surrounding environment by oligodendrocytes.
b. Accumulation of αsyn in oligodendrocytes affects myelin sheath integrity, axonal integrity, and neuronal survival in a time dependant manner.

6.3. AIM

To determine if αsyn is taken up by oligodendrocytes as a possible mechanism for the formation of GCIs in MSA using an *in vivo* model.

6.4. METHOD

C57BL/6JOlaHsd mice (Harlan, Bicester, UK) between 2-4 months of age were anesthetized using isoflurane. The mice were placed on the stereotaxic frame and injected in one hemisphere with either MSA, PD, or control human brain lysates (5μg total protein). Lysate preparation was as described in Chapter 2: Materials and methods, section 2.14.1. Using a single needle insertion at +0.2mm relative to Bregma and +2.0mm from midline, 2.0μL of the inoculum was introduced into the dorsolateral striatum (2.6mm beneath the dura) and somatosensory cortex (0.8mm beneath the dura) at a rate of 0.15μL/min. The mice were monitored carefully during surgery and after recovery and were then sacrificed at the pre-determined time points of 4 and 30 days post inoculation (dpi) with a dose of Lethobarb 20% w/v Solution (Ayrton Saunders Limited, UK). After transcardial perfusion with PBS, the brains were removed, fixed in formalin for at least 24 hours, then processed and embedded in paraffin. A total of six mice were injected for each lysate and time point. This protocol was initially carried out using fluorescent microbeads (FluoSpheres, Invitrogen) to verify correct injection site.

Eight-micrometre-thick serial section were cut, deparaffinised and placed in methanol/H_2O_2 (100:1) solution for 10 min to eliminate endogenous peroxidase

activity. Following washes in PBS, pre-treatment was carried out by pressure cooking in citrate buffer at pH 6.0. Sections were then placed in 10% non-fat milk for 30 min at room temperature (RT) to reduce non-specific binding, followed by incubation in the primary antibody for 1 hour at RT. After washes in PBS, the sections are incubated with primary antibody at a dilution of 1:200 for 30 min at RT. The secondary antibody was washed off then the sections were incubated in the avidin-biotin complex solution for 30 min at RT. After washes in PBS, they were treated in the 3,3'-diaminobenzidine (DAB) solution for 3 min. The DAB solution was washed off and the tissues were counterstained in Mayer's haematoxylin for 10 sec. The tissue sections were then dehydrated in graded alcohol (70%, 90%, and absolute alcohol), cleared in three changes of xylene, and then mounted with DPX mounting medium.

Table 6.1. Antibodies used in *in vivo* study

	Host	Reactivity	Dilution	Source (cat. no.)
Primary antibody				
αSyn	Mouse	Human, mouse	1:50	Vector Laboratories, Burlingame, CA (VP A106)
αSyn	Mouse	Human, mouse	1:1000	BD Transduction (610787)
LB509	Mouse	Human, mouse	1:500	Abcam (ab27766)
αSyn	Rabbit	Human, mouse	1:800	Abcam (ab15530)
αSyn	Sheep	Human, mouse	1:800	Chemicon (AB5334P)
αSyn	Mouse	Mouse	1:200	Cell signalling (4179)
Secondary antibody				
Biotinylated rabbit anti-mouse IgG	Rabbit	Mouse	1:200	DakoCytomation , Denmark (E0354)
Biotinylated swine anti-rabbit IgG	Swine	Rabbit	1:200	DakoCytomation , Denmark (E0353)
Biotinylated rabbit anti-sheep IgG	Rabbit	Sheep	1:200	Vector Laboratories, Burlingame, CA (BA-600)

6.5. RESULTS

6.5.1. Intracerebral inoculation of fluorescent microbeads

Fluorescent microbeads (FluoSpheres, Invitrogen) were initially inoculated into the mice at the desired coordinates to ensure inoculation into the cortex and striatum as indicated in Figure 6.1.

6.5.2. αSyn pathology

The entire mouse brain was sectioned (~120 sections) and a battery of αsyn antibodies (Table 6.1) was tested on tissue sections at 40μm intervals. αSyn positive staining was undetectable in neurons or glial cells in all sections and levels of the mouse brain inoculated with MSA, PD or control lysate.

A

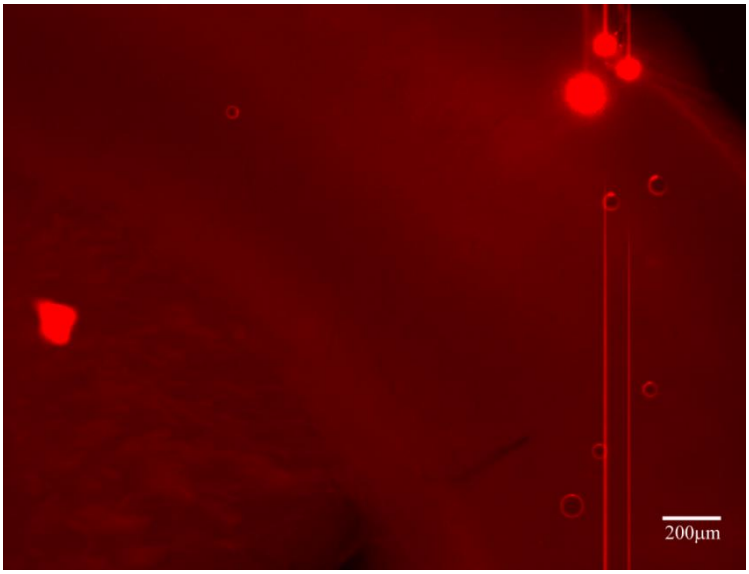

B

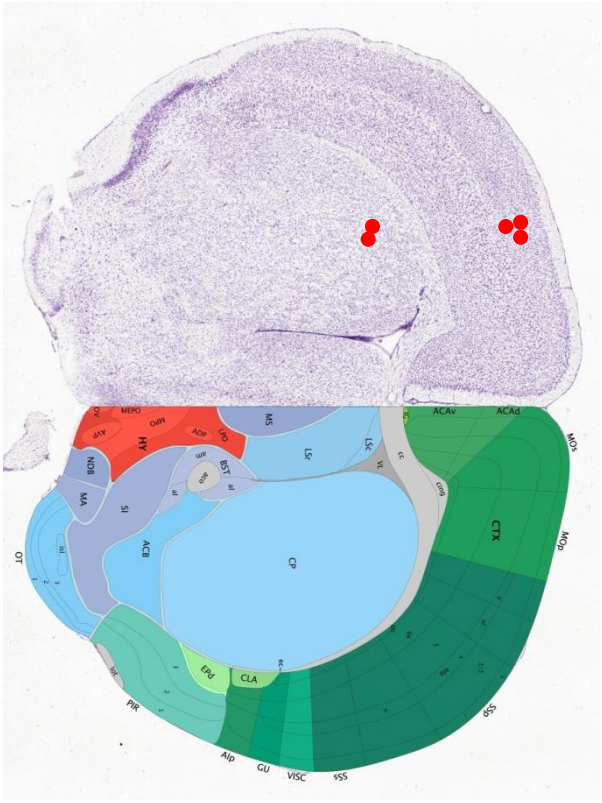

Figure 6.1. Fluorescent beads inoculation

Fluorescent beads were intracerebrally inoculated at the specified coordinates to ensure that the cortex and striatum are successfully targeted (A). A schematic representation of fluorescent beads location. Coronal brain image obtained from Allen Brain Atlas (B).

6.6. DISCUSSION

GCIs found in oligodendrocytes in MSA is the pathological hallmark of the disease. αSyn is the main constituent of GCIs, however, the mechanisms by which it accumulates are poorly understood. The hypothesis tested in this chapter is that internalization of extracellular αsyn is one mechanism by which GCIs form. Luk and colleagues demonstrated that unilateral intracerebral inoculation of pathological αsyn into transgenic mice overexpressing human A53T and C57BL6/C3H wild-type mice resulted in uptake of αsyn by neurons to form LB-like pathology and that the pathology spread to the contralateral side (Luk et al., 2012 a; b). Masuda-Suzukake and colleagues performed a similar experiment, however, using lysates from human DLB brain as the inoculum. The C57BL/6J wild-type mice recapitulated pathology seen in DLB as LB-like inclusions formed in neurons and spread to multiple regions of the brain (Masuda-Suzukake et al., 2013).

Informed by the methods and findings of these studies, lysates from MSA, PD and control human brains were inoculated intracerebrally into C57BL/6JOlaHsd wild-type mice to test the hypothesis that oligodendrocytes internalize extracellular αsyn. MSA, PD and control human brains were used to investigate whether the uptake of αsyn, if successful, is selective to the source of αsyn species and it is postulated that different strains of αsyn may exist (Bousset et al.; Guo et al., 2013). C57BL/6JOlaHsd are a subline of the C57BL/6 mice that lack the *SNCA* gene (Specht and Schoepfer, 2001) and were chosen so that uptake of

αsyn from the human brain lysates may be examined without any interference from endogenous mouse αsyn.

αSyn immunoreactivity was not observed in neurons or glia of mice inoculated with MSA, PD or control human brain lysates at both the 4 and 30 dpi time-points. The lack of αsyn immunoreactivity has several implications. Firstly, that neurons and glia are incapable of internalizing αsyn from MSA, PD or control human brain lysates. This is highly unlikely as previous studies with human DLB or AD brain lysate in to mice were successful in recapitulating the pathology (Kane et al., 2000; Borlikova et al., 2013; Masuda-Suzukake et al., 2013). A second implication is that the cells did take up the protein, however, the amount taken up may have been below the detection limit of the assay. Thirdly, the lack of pathology may also have been due to the relatively short incubation time warranting further assessments of time-points longer than 30 dpi. Furthermore, that the lack of endogenous αsyn may have affected the successful uptake of the injected αsyn. Therefore, this study needs to be taken further by inoculating C57BL/6 mice that express αsyn and transgenic mice (e.g. mice overexpressing A53T mutant human αsyn) with MSA, PD or control human brain lysates and to examine any pathology that may ensue. Only then will it be possible to state with greater confidence that oligodendrocytes do not internalize extracellular αsyn in an *in vivo* model. The evidence in the literature demonstrates that oligodendrocytes are capable internalising αsyn by endocytosis *in vitro*, however, *in vivo* confirmation of these findings has yet to be established.

Conclusion and future directions

Internalization of extracellular αsyn by oligodendrocytes is a possible mechanism by which GCIs form in MSA. Evidence from *in vitro* studies indicates that this mechanism takes place, however, *in vivo* confirmation of these findings has yet to be established. An *in vivo* model would be to inoculate wild-type and transgenic mice with human MSA brain homogenate and look for evidence of αsyn uptake by oligodendrocytes and the resultant load of αsyn pathology at the different time-points. Taking the study further, other pathological changes such as myelin loss, axonal damage, neuronal loss and gliosis may also be examined to determine if any correlations exist with αsyn pathology load and progression with time.

7

CONCLUSIONS AND FUTURE DIRECTIONS

7.1. CLINICO-PATHOLOGICAL STUDIES SUMMARY AND FUTURE DIRECTIONS

MSA is an adult onset neurodegenerative disease where patients clinically present with varying degrees of parkinsonism, cerebellar ataxia and autonomic dysfunction. The pathological manifestations of this disease are most severely seen in the StrN and OPC structures and include GCIs, NCIs, myelin damage, neuronal loss and gliosis. GCIs are the pathological hallmark of MSA and are required for a definite diagnosis. MSA patients are clinically subtyped into MSA-P and MSA-C reflecting a predominance for parkinsonian and cerebellar features respectively. Pathological subtyping into SND, OPC or mixed is made post-mortem indicating predominant neuronal loss in StrN and OPC structures of the brain. These clinical and pathological groups of MSA are the most noted, however, other subtypes of MSA do exist such as MSA with CI, long duration MSA and minimal change MSA. Exploring the relationships between the clinical and pathological profiles of these subtypes allows better understanding of the evolution of the disease and opportunities for therapeutic interventions.

Cognitive impairment is regarded as an exclusion criterion for a diagnosis of MSA, however, this view has been challenged by neuropsychological studies documenting CI in MSA patients and by some case studies of pathologically confirmed MSA patients reported to have CI (Testa et al., 1993; Wakabayashi et al., 1998; Konagaya et al., 1999; Shibuya et al., 2000; Soliveri et al., 2000; Lange et al., 2003; Krishnan et al., 2006; Kawai et al., 2008; O'Sullivan et al., 2008; Brown et al., 2010). CI seems to be inherent to the disease as concomitant pathologies associated with CI were uncommon in MSA in the cohort studied in this thesis and factors other than GCI load and neuronal loss may influence the cognitive decline. The synergistic relationship between αsyn, tau and Aβ pathology seen in PD (Masliah et al., 2001; Lashley et al., 2008; Compta et al., 2011, 2013) was not recapitulated in MSA suggesting αsyn pathology in MSA is not associated with an increase in tau or Aβ aggregation and this may be due to possible differences in the properties of αsyn in MSA and PD. Therefore, future directions for this study would be to characterize the biochemical properties of αsyn in cognitively impaired MSA and PD cases. Also, exploring other substrates associated with CI such as synaptic pathology, neurotransmitter abnormalities and subcortical deafferentation is warranted to understand their contribution to cognitive impairment in MSA.

Long duration and minimal change MSA are two rare subtypes where the former have an unusually long survival period of more than 10 years and the later have restricted neuronal loss to the substantia nigra and/or locus coeruleus. The clinico-pathological profiles of these subtypes provide further insight into the

evolution of the disease. Widespread GCI pathology in areas that exhibit no, or minimal, neuronal loss adds further credence to the hypothesis that MSA is a primary oligodendrogliopathy. Furthermore, these cases highlight the significance of the involvement of the autonomic system as cases rapidly declined upon onset of autonomic symptoms. Therefore, carrying this study forward warrants exploration of nuclei and connections associated with the autonomic system, including the intermediolateral column spinal cord, dorsal motor nucleus of vagus, medullary serotonergic and catecholaminergic neurons, to uncover the contribution of pathology in these structures to the clinico-pathological profiles of long duration, minimal change and typical MSA.

Clinico-pathological studies are important to understanding the evolution of disease. The limitations of the clinico-pathological studies of this thesis are inherent to retrospective review of medical records when reconstructing the clinical profiles of the cases. The studies are also limited by the small number of cases and so interpretations must be made with caution. The strength of the studies includes the use of detailed neuropathological assessment according to published criteria.

7.2. ALPHA-SYNUCLEIN ORIGIN IN OLIGODENDROCYTES

SUMMARY AND FUTURE DIRECTIONS

GCIs in oligodendrocytes are found in greater abundance than other types of inclusions (GNIs, NCIs, NNIs and inclusions in other glia) in MSA. The abundant presence of these αsyn-positive oligodendroglial inclusions in numerous brain structures in MSA indicates the important role they play in the pathogenesis of the disease. αSyn is mainly found in neurons in the CNS, while its presence in oligodendrocytes remains a matter of debate. As the main constituent of GCIs, it is important to understand the origin of αsyn in oligodendrocytes in order to establish the step-by-step mechanisms by which GCIs form. To address this, the expression profile of *SNCA* mRNA and αsyn protein in the different cells of the MSA brain were explored in this thesis. αSyn-positive GCIs are found to occur within mature myelinating oligodendrocytes but not within oligodendrocyte precursor cells or immature oligodendrocytes. This indicates that oligodendrocytes are vulnerable to GCI formation at the mature myelinating stage. Furthermore, *SNCA* mRNA was detected by qPCR in LCM-isolated mature oligodendrocytes of both MSA and normal control cases and expression was greater in MSA. The implication here is that overexpression of *SNCA* mRNA leads to increased *de novo* production of αsyn protein in oligodendrocyte which contributes to the formation of GCIs. This is a significant finding and prompts re-evaluation of the position that there is an absence of *SNCA* mRNA in oligodendrocytes of normal and MSA cases (Miller et al., 2005). The study by Miller and colleagues is only study in the literature to date that addresses the question of *SNCA* mRNA expression in oligodendrocytes in

MSA using human post-mortem tissue, however, the detection limit of *in situ* hybridization technique may explain their negative findings (Miller et al., 2005). The findings of the cellular expression study of this thesis need to be replicated and validate in a different cohort, but preliminarily highlight the importance of the contribution of *SNCA* mRNA overexpression in oligodendrocytes to inclusion formation in MSA. *SNCA* mRNA expression in oligodendrocyte precursor cells could be a point for future consideration, however, it would be a very challenging task due to the difficulty of immunohistochemical detection of these cells. However, future success in isolating and analysing *SNCA* mRNA expression in these oligodendrocyte precursor cells may provide further insight into the pattern of *SNCA* transcription and translation in the oligodendrocyte lineage in MSA and explain why αsyn is found in mature oligodendrocytes but not in the precursor cells.

In addition to *de novo* production, an alternative hypothesis to the origin of αsyn in oligodendrocytes is internalization of extracellular αsyn by oligodendrocytes. There is cell culture evidence that this may occur, however, *in vivo* confirmation is lacking and was sought in this thesis. The findings of this study were inconclusive and warrant further investigations using multiple strains of wild-type and transgenic mice to determine the capability of oligodendrocytes in internalizing αsyn and to elucidate the contribution of endogenous αsyn to the uptake process. In addition, the use of MSA, PD and control human brain homogenates will further clarify if the uptake of αsyn is dependent on its source. Different protein strains resulting in different phenotypic traits in the host have been demonstrated

in prion diseases (Aguzzi et al., 2007) and recent studies propose that different αsyn strains may exist with different propensities to form aggregates, recruit other proteins and penetrate into cells (Bousset et al.; Guo et al., 2013). Therefore, the hypothesis of different αsyn strains may be further supported if the mice exhibit varying pathologies, where mice inoculated with PD homogenates exhibit greater neuronal pathology while those inoculated with MSA homogenates exhibit greater oligodendroglial pathology.

The main limitation of using post-mortem human tissue for expression analysis is preservation of RNA quality. Additional processing steps required for isolating cells by LCM further compromises RNA quality. LCM allows single cell isolation, however, there will always be some minor degree of contamination from the area surrounding the cell that falls within the laser spot. Furthermore, this is a time consuming process where hours may be spent on one sample to collect an adequate number of cell that would result in a substantial RNA yield.

The main limitation of the *in vivo* study was time constraint. The methodology has been previously published and shown to produce results, however, the results of this thesis are inconclusive as additional strains of wild-type and transgenic mice need to be added to the study.

A hypothetical model of the molecular pathogenesis of MSA based on the findings of this thesis and that of published literature is summarised in Figure 7.1.

Caption ▶

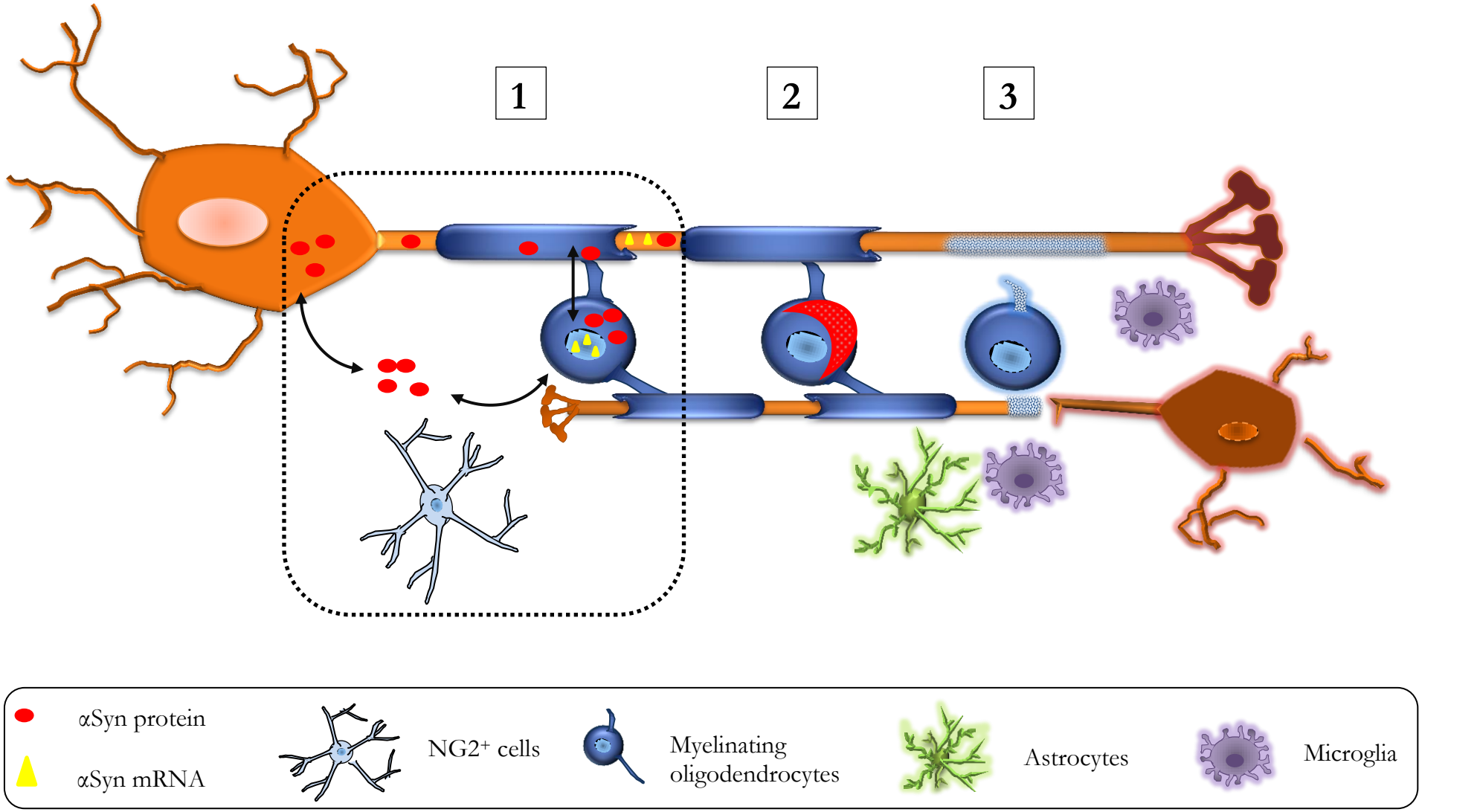
1
2
3
αSyn protein
αSyn mRNA
NG2+ cells
Myelinating oligodendrocytes
Astrocytes
Microglia

Figure 7.1. Hypothesised molecular pathogenesis of MSA

1) αSyn is found in mature myelinating oligodendrocytes but not in precursor cells ($NG2^+$ cells). The origin of αsyn in mature oligodendrocytes may be due to a combination of *de novo* production and internalization through cell-to-cell transfer. A possible role for αsyn in oligodendrocytes is interaction with myelin and the microtubule network. **2)** Overexpression of *SNCA* mRNA, uptake of extracellular αsyn, aberrant interaction with myelin, microtubules and MAPs and inefficient degradation of the protein may lead to formation of GCIs. **3)** As a consequence, there is disruption of the oligodendroglial-myelin-axon-neuron axis leading to myelin loss, axonal damage, synaptic dysfunction and neuronal death which are exacerbated by inflammatory cues.

7.3. CONCLUSIONS AND FUTURE DIRECTIONS

Establishing the step-by-step mechanisms by which GCIs form in oligodendrocytes in MSA is important to understanding the molecular pathogenesis of the disease. Future directions may focus on the role of cellular *SNCA* overexpression and its impact on inclusion formation and cell survival. Analysing *SNCA* expression in LCM-isolated neurons and oligodendrocytes in affected and unaffected brain regions in long duration, minimal change and typical MSA may help to elucidate the selective vulnerability of StrN and OPC regions and provide further insight into the role of *SNCA* mRNA expression on clinical outcome. Furthermore, comparing cellular *SNCA* expression among different α-synucleinopathies may elucidate the preferential accumulation of αsyn in oligodendrocytes in MSA and neurons in PD and DLB.

Despite a common protein culprit, the different pathological and clinical outcomes of members of the α-synucleinopathy group of diseases suggest that there are differences in the properties of αsyn at the transcriptional or posttranscriptional level. Different conformational and structural properties of αsyn have been demonstrated (Bousset et al.; Guo et al., 2013), therefore, investigating the properties of αsyn in these MSA, PD and DLB may provide further insight into reasons behind their different clinico-pathological profiles.

In addition, research into the role of αsyn in oligodendrocytes is warranted. It is important to better understand the ultrastructural localisation of αsyn in oligodendrocytes and its interaction with components of myelin and the microtubule network. Microtubule-polymerizing activity of αsyn has been

demonstrated in COS-1 cultured cells in addition to loss of polymerizing potential by the αsyn mutants A30P and A53T (Alim et al., 2004). Loss of αsyn microtubule assembly activity induces tubulin aggregation and tubulin oligomers act as seeds for αsyn fibrillogenesis creating a cycle for inclusion formation that may be triggered or exacerbated by αsyn or tubulin (Alim et al., 2002, 2004). The role of αsyn as a microtubule-associated protein and the consequences of loss of this activity need to be further investigated in oligodendrocytes. Co-culture systems using microfluidic chambers which separate neuronal cell body in one compartment and axons and oligodendrocytes in another may provide a platform to study the effect of blocking αsyn microtubule-polymerization on the integrity of myelin, axon and cell body (Taylor et al., 2005; Park et al., 2009). Therefore, it may be hypothesized that disruption in αsyn microtubule-polymerization activity in oligodendrocytes may lead to destabilization and oligomerisation of microtubules which seed αsyn aggregation leading to inclusion formation and myelin damage. A clearer view of the role of αsyn in oligodendrocyte is essential to building the step-by-step mechanisms by which GCIs form and cause myelin disruption, therefore, coming closer to unravelling "the nature of the beast" (Quinn, 1989).

PUBLICATIONS

Asi, Y.T, Simpson, J.E., Heath, P.R., Wharton, S.B., Lees, A.J., Revesz, T, Houlden, H, Holton, J.L. 2014. *Alpha-synuclein mRNA expression in oligodendrocytes in MSA*. Glia, , doi: 10.1002/glia.22653. [Epub ahead of print].

Kiely, A., **Asi, Y.T.**, Kara, E., Limousin, P., Ling, H., Lewis, P., Proukakis, C., Quinn, N., Lees, A.J., Hardy, J., Revesz, T., Houlden, H. and Holton, J.L. 2013. *α-Synucleinopathy associated with G51D SNCA mutation: a link between Parkinson's disease and multiple system atrophy?* Acta neuropathologica, 125(5), pp.753–769.

Ahmed, Z., **Asi, Y.T.**, Lees, A.J., Revesz, T. and Holton, J.L., 2013. *Identification and quantification of oligodendrocyte precursor cells in multiple system atrophy, progressive supranuclear palsy and Parkinson's disease*. Brain pathology, 23(3), pp.263–273.

Ahmed, Z., **Asi, Y.T.**, Sailer, A., Lees, A.J., Houlden, H., Revesz, T. and Holton, J.L. 2012. *The neuropathology, pathophysiology and genetics of multiple system atrophy*. Neuropathology and applied neurobiology, 38(1), pp.4–24.

Petrovic, I.N., Ling, H., **Asi, Y.**, Ahmed, Z., Prashanth, L.K.., Hazrati, L.-N., Lang, A.E., Revesz, T., Holton, J.L. and Lees, A.J., 2012. *Multiple system atrophy-parkinsonism with slow progression and prolonged survival: a diagnostic catch*. Mov. Disord. 27, 1186–1190.

Asi, Y.T.*, Ling H*, Ahmed, Z, Lees, A.J., Revesz, T, Holton, J.L. *Pathological changes in multiple system atrophy with cognitive impairment*. Submitted.

Asi, Y.T., Ling, H. *, Petrovic, I.N. *, Ahmed, Z., Prashanth, L.K.., Hazrati, L.-N., Nishizawa, M, Ozawa, T, Lang, A.E., Lees, A.J., Revesz, T. and Holton, J.L. *Long duration and minimal change MSA: benign and aggressive variants?* Submitted.

REFERENCES

Aguzzi A, Heikenwalder M, Polymenidou M. 2007. Insights into prion strains and neurotoxicity. Nat Rev Mol Cell Biol 8:552–561.

Ahmed Z, Asi YT, Lees AJ, Revesz T, Holton JL. 2012. Identification and Quantification of Oligodendrocyte Precursor Cells in Multiple System Atrophy, Progressive Supranuclear Palsy and Parkinson's Disease. Brain Pathol 23(3): 263-273.

Alim MA, Hossain MS, Arima K, Takeda K, Izumiyama Y, Nakamura M, Kaji H, Shinoda T, Hisanaga S, Uéda K. 2002. Tubulin Seeds α-Synuclein Fibril Formation. J Biol Chem 277:2112–2117.

Alim MA, Ma Q-L, Takeda K, Aizawa T, Matsubara M, Nakamura M, Asada A, Saito T, Kaji H, Yoshii M, Hisanaga S, Uéda K. 2004. Demonstration of a role for alpha-synuclein as a functional microtubule-associated protein. J Alzheimers Dis 6:435–449.

Alisky JM. 2006. Neurotransmitter depletion may be a cause of dementia pathology rather than an effect. Med Hypotheses 67:556–560.

Angot E, Brundin P. 2009. Dissecting the potential molecular mechanisms underlying alpha-synuclein cell-to-cell transfer in Parkinson's disease. Parkinsonism Relat Disord 15 Suppl 3:S143–147.

Armstrong RA, Cairns NJ, Lantos PL. 2004. A quantitative study of the pathological changes in ten patients with multiple system atrophy (MSA). J Neural Transm 111:485–495.

Armstrong RA, Cairns NJ, Lantos PL. 2006. Multiple system atrophy (MSA): topographic distribution of the alpha-synuclein-associated pathological changes. Parkinsonism Relat Disord 12:356–362.

Armstrong RA, Cairns NJ, Lantos PL. 2007. A quantitative study of the pathological changes in white matter in multiple system atrophy. Neuropathology 27:221–227.

Athanassiadou A, Voutsinas G, Psiouri L, Leroy E, Polymeropoulos MH, Ilias A, Maniatis GM, Papapetropoulos T. 1999. Genetic analysis of families with Parkinson disease that carry the Ala53Thr mutation in the gene encoding alpha-synuclein. Am J Hum Genet 65:555–558.

Back SA, Luo NL, Borenstein NS, Levine JM, Volpe JJ, Kinney HC. 2001. Late Oligodendrocyte Progenitors Coincide with the Developmental Window of Vulnerability for Human Perinatal White Matter Injury. J Neurosci 21:1302–1312.

Badiola N, de Oliveira RM, Herrera F, Guardia-Laguarta C, Gonçalves SA, Pera M, Suárez-Calvet M, Clarimon J, Outeiro TF, Lleó A. 2011. Tau enhances α-synuclein aggregation and toxicity in cellular models of synucleinopathy. PLoS ONE 6:e26609.

Bak TH, Rogers TT, Crawford LM, Hearn VC, Mathuranath PS, Hodges JR. 2005. Cognitive bedside assessment in atypical parkinsonian syndromes. J Neurol Neurosurg Psychiatr 76:420–422.

Bartels T, Choi JG, Selkoe DJ. 2011. α-Synuclein occurs physiologically as a helically folded tetramer that resists aggregation. Nature 477:107–110.

Bate C, Gentleman S, Williams A. 2010. alpha-synuclein induced synapse damage is enhanced by amyloid-beta1-42. Mol Neurodegener 5:55.

Baumann N, Pham-Dinh D. 2001. Biology of oligodendrocyte and myelin in the mammalian central nervous system. Physiol Rev 81:871.

Benarroch EE, Schmeichel AM, Low PA, Parisi JE. 2004. Involvement of medullary serotonergic groups in multiple system atrophy. Ann Neurol 55:418–422.

Benarroch EE, Schmeichel AM, Parisi JE. 2001. Depletion of cholinergic neurons of the medullary arcuate nucleus in multiple system atrophy. Auton Neurosci 87:293–299.

Benarroch EE, Schmeichel AM, Parisi JE. 2002. Depletion of mesopontine cholinergic and sparing of raphe neurons in multiple system atrophy. Neurology 59:944–946.

Benarroch EE, Smithson IL, Low PA, Parisi JE. 1998. Depletion of catecholaminergic neurons of the rostral ventrolateral medulla in multiple systems atrophy with autonomic failure. Ann Neurol 43:156–163.

Berent S, Giordani B, Gilman S, Trask CL, Little RJA, Johanns JR, Junck L, Kluin KJ, Heumann M, Koeppe RA. 2002. Patterns of neuropsychological performance in multiple system atrophy compared to sporadic and hereditary olivopontocerebellar atrophy. Brain Cogn 50:194–206.

Berry M, Hubbard P, Butt AM. 2002. Cytology and lineage of NG2-positive glia. J Neurocytol 31:457–467.

Beyer K, Domingo-Sàbat M, Humbert J, Carrato C, Ferrer I, Ariza A. 2008a. Differential expression of alpha-synuclein, parkin, and synphilin-1 isoforms in Lewy body disease. Neurogenetics 9:163–172.

Beyer K, Domingo-Sábat M, Lao JI, Carrato C, Ferrer I, Ariza A. 2008b. Identification and characterization of a new alpha-synuclein isoform and its role in Lewy body diseases. Neurogenetics 9:15–23.

Beyer K. 2006. α-Synuclein structure, posttranslational modification and alternative splicing as aggregation enhancers. Acta Neuropathologica 112:237–251.

Blanpied T, Ehlers M. 2004. Microanatomy of dendritic spines: Emerging principles of synaptic pathology in psychiatric and neurological disease. Biol Psychiatry 55:1121–1127.

Borlikova GG, Trejo M, Mably AJ, Mc Donald JM, Sala Frigerio C, Regan CM, Murphy KJ, Masliah E, Walsh DM. 2013. Alzheimer brain-derived amyloid β-protein impairs synaptic remodeling and memory consolidation. Neurobiol Aging 34:1315–1327.

Bousset L, Pieri L, Ruiz-Arlandis G, Gath J, Jensen PH, Habenstein B, Madiona K, Olieric V, Böckmann A, Meier BH, Melki R. Structural and functional characterization of two alpha-synuclein strains. Nat Commun 4:2575.

Braak H, Alafuzoff I, Arzberger T, Kretzschmar H, Del Tredici K. 2006. Staging of Alzheimer disease-associated neurofibrillary pathology using paraffin sections and immunocytochemistry. Acta Neuropathol 112:389–404.

Braak H, Del Tredici K, Rüb U, de Vos RAI, Jansen Steur ENH, Braak E. 2003. Staging of brain pathology related to sporadic Parkinson's disease. Neurobiol Aging 24:197–211.

Bradl M, Lassmann H. 2010. Oligodendrocytes: biology and pathology. Acta Neuropathol 119:37–53.

Brown RG, Lacomblez L, Landwehrmeyer BG, Bak T, Uttner I, Dubois B, Agid Y, Ludolph A, Bensimon G, Payan C, Leigh NP. 2010. Cognitive impairment in patients with multiple system atrophy and progressive supranuclear palsy. Brain 133:2382–2393.

Buchet D, Baron-Van Evercooren A. 2009. In search of human oligodendroglia for myelin repair. Neurosci Lett 456:112–119.

Burn DJ, Jaros E. 2001. Multiple system atrophy: cellular and molecular pathology. Mol Pathol 54:419.

Burré J, Sharma M, Tsetsenis T, Buchman V, Etherton MR, Südhof TC. 2010. Alpha-synuclein promotes SNARE-complex assembly in vivo and in vitro. Science 329:1663–1667.

Bussell R Jr, Ramlall TF, Eliezer D. 2005. Helix periodicity, topology, and dynamics of membrane-associated alpha-synuclein. Protein Sci 14:862–872.

Butt AM, Kiff J, Hubbard P, Berry M. 2002. Synantocytes: new functions for novel NG2 expressing glia. J Neurocytol 31:551–565.

Cajigas IJ, Tushev G, Will TJ, tom Dieck S, Fuerst N, Schuman EM. 2012. The local transcriptome in the synaptic neuropil revealed by deep sequencing and high-resolution imaging. Neuron 74:453–466.

Campbell BC., McLean CA, Culvenor JG, Gai WP, Blumbergs PC, Jäkälä P, Beyreuther K, Masters CL, Li QX. 2001. The solubility of alpha-synuclein in multiple system atrophy differs from that of dementia with Lewy bodies and Parkinson's disease. J Neurochem 76:87–96.

Campion D, Martin C, Heilig R, Charbonnier F, Moreau V, Flaman JM, Petit JL, Hannequin D, Brice A, Frebourg T. 1995. The NACP/synuclein gene: chromosomal assignment and screening for alterations in Alzheimer disease. Genomics 26:254–257.

Carson JH, Worboys K, Ainger K, Barbarese E. 1997. Translocation of myelin basic protein mRNA in oligodendrocytes requires microtubules and kinesin. Cell Motil Cytoskeleton 38:318–328.

Castellani R. 1998. Multiple system atrophy: clues from inclusions. Am J Pathol 153:671–676.

Al-Chalabi A, Dürr A, Wood NW, Parkinson MH, Camuzat A, Hulot J-S, Morrison KE, Renton A, Sussmuth SD, Landwehrmeyer BG, Ludolph A, Agid Y, Brice A, Leigh PN, Bensimon G. 2009. Genetic variants of the alpha-synuclein gene SNCA are associated with multiple system atrophy. PLoS ONE 4:e7114.

Chandra S, Fornai F, Kwon H-B, Yazdani U, Atasoy D, Liu X, Hammer RE, Battaglia G, German DC, Castillo PE, Südhof TC. 2004. Double-knockout mice for alpha- and beta-synucleins: effect on synaptic functions. Proc Natl Acad Sci USA 101:14966–14971.

Chandra S, Gallardo G, Fernández-Chacón R, Schlüter OM, Südhof TC. 2005. Alpha-synuclein cooperates with CSPalpha in preventing neurodegeneration. Cell 123:383–396.

Chang CC, Chang YY, Chang WN, Lee YC, Wang YL, Lui CC, Huang CW, Liu WL. 2009. Cognitive deficits in multiple system atrophy correlate with frontal atrophy and disease duration. Eur J Neurol 16:1144–1150.

Chiba Y, Takei S, Kawamura N, Kawaguchi Y, Sasaki K, Hasegawa-Ishii S, Furukawa A, Hosokawa M, Shimada A. 2012. Immunohistochemical

localization of aggresomal proteins in glial cytoplasmic inclusions in multiple system atrophy. Neuropathol Appl Neurobiol 38:559–571.

Clinton LK, Blurton-Jones M, Myczek K, Trojanowski JQ, LaFerla FM. 2010. Synergistic Interactions between Abeta, tau, and alpha-synuclein: acceleration of neuropathology and cognitive decline. J Neurosci 30:7281–7289.

Colosimo C, Morgante L, Antonini A, Barone P, Avarello TP, Bottacchi E, Cannas A, Ceravolo MG, Ceravolo R, Cicarelli G, Gaglio RM, Giglia L, Iemolo F, Manfredi M, Meco G, Nicoletti A, Pederzoli M, Petrone A, Pisani A, Pontieri FE, Quatrale R, Ramat S, Scala R, Volpe G, Zappulla S, Bentivoglio AR, Stocchi F, Trianni G, Del Dotto P, Simoni L, Marconi R. 2010. Non-motor symptoms in atypical and secondary parkinsonism: the PRIAMO study. J Neurol 257:5–14.

Compta Y, Parkkinen L, Kempster P, Selikhova M, Lashley T, Holton JL, Lees AJ, Revesz T. 2013. The Significance of α-Synuclein, Amyloid-β and Tau Pathologies in Parkinson's Disease Progression and Related Dementia. Neurodegener Dis.

Compta Y, Parkkinen L, O'Sullivan SS, Vandrovcova J, Holton JL, Collins C, Lashley T, Kallis C, Williams DR, de Silva R, Lees AJ, Revesz T. 2011. Lewy- and Alzheimer-type pathologies in Parkinson's disease dementia: which is more important? Brain 134:1493–1505.

Cookson MR. 2009. alpha-Synuclein and neuronal cell death. Mol Neurodegener 4:9.

Coulson DT, Brockbank S, Quinn JG, Murphy S, Ravid R, Irvine GB, Johnston JA. 2008. Identification of valid reference genes for the normalization of RT qPCR gene expression data in human brain tissue. BMC Mol Biol 9:46.

Court JA, Perry EK. 2003. Neurotransmitter abnormalities in vascular dementia. Int Psychogeriatr 15 Suppl 1:81–87.

Culvenor JG, Rietze RL, Bartlett PF, Masters CL, Li Q-X. 2002. Oligodendrocytes from neural stem cells express alpha-synuclein: increased numbers from presenilin 1 deficient mice. Neuroreport 13:1305–1308.

Cutillo V, Montagnese P, Gremo F, Casola L, Giuditta A. 1983. Origin of axoplasmic RNA in the squid giant fiber. Neurochem Res 8:1621–1634.

Dammer EB, Duong DM, Diner I, Gearing M, Feng Y, Lah JJ, Levey AI, Seyfried NT. 2013. Neuron Enriched Nuclear Proteome Isolated from Human Brain. J Proteome Res 12:3193–3206.

Dawson MRL, Polito A, Levine JM, Reynolds R. 2003. NG2-expressing glial progenitor cells: an abundant and widespread population of cycling cells in the adult rat CNS. Mol Cell Neurosci 24:476–488.

Deglincerti A, Jaffrey SR. 2012. Insights into the roles of local translation from the axonal transcriptome. Open Biol [Internet] 2. Available from: http://rsob.royalsocietypublishing.org/content/2/6/120079

Desplats P, Lee H-J, Bae E-J, Patrick C, Rockenstein E, Crews L, Spencer B, Masliah E, Lee S-J. 2009. Inclusion formation and neuronal cell death through neuron-to-neuron transmission of α-synuclein. Proc Natl Acad Sci U S A 106:13010–13015.

Eliezer D, Kutluay E, Bussell R Jr, Browne G. 2001. Conformational properties of alpha-synuclein in its free and lipid-associated states. J Mol Biol 307:1061–1073.

Espinosa-Jeffrey A, Wakeman DR, Kim SU, Snyder EY, de Vellis J. 2009. Culture system for rodent and human oligodendrocyte specification, lineage progression, and maturation. Curr Protoc Stem Cell Biol Chapter 2:Unit 2D.4.

Exner N, Lutz AK, Haass C, Winklhofer KF. 2012. Mitochondrial dysfunction in Parkinson's disease: molecular mechanisms and pathophysiological consequences. EMBO J 31:3038–3062.

Fearnley JM, Lees AJ. 1990. Striatonigral degeneration. A clinicopathological study. Brain 113 (Pt 6):1823–1842.

Fellner L, Jellinger K, Wenning G, Stefanova N. 2011a. Glial dysfunction in the pathogenesis of alpha-synucleinopathies: emerging concepts. Acta Neuropathol 121:675–693.

Fellner L, Jellinger KA, Wenning GK, Stefanova N. 2011b. Glial dysfunction in the pathogenesis of α-synucleinopathies: emerging concepts. Acta Neuropathol 121:675–693.

Franklin RJM, ffrench-Constant C. 2008. Remyelination in the CNS: from biology to therapy. Nat Rev Neurosci 9:839–855.

Franklin RJM. 2002. Why does remyelination fail in multiple sclerosis? Nat Rev Neurosci 3:705–714.

Fuchs J, Nilsson C, Kachergus J, Munz M, Larsson E-M, Schüle B, Langston JW, Middleton FA, Ross OA, Hulihan M, Gasser T, Farrer MJ. 2007. Phenotypic variation in a large Swedish pedigree due to SNCA duplication and triplication. Neurology 68:916–922.

Fujishiro H, Ahn T-B, Frigerio R, DelleDonne A, Josephs KA, Parisi JE, Eric Ahlskog J, Dickson DW. 2008. Glial cytoplasmic inclusions in neurologically normal elderly: prodromal multiple system atrophy? Acta Neuropathologica 116:269–275.

Gai WP, Pountney DL, Power JHT, Li QX, Culvenor JG, McLean CA, Jensen PH, Blumbergs PC. 2003. alpha-Synuclein fibrils constitute the central core of oligodendroglial inclusion filaments in multiple system atrophy. Exp Neurol 181:68–78.

Gai WP, Power JH, Blumbergs PC, Blessing WW. 1998. Multiple-system atrophy: a new alpha-synuclein disease? Lancet 352:547–548.

Gai WP, Power JH, Blumbergs PC, Culvenor JG, Jensen PH. 1999. Alpha-synuclein immunoisolation of glial inclusions from multiple system atrophy brain tissue reveals multiprotein components. J Neurochem 73:2093–2100.

Giasson BI, Murray IV, Trojanowski JQ, Lee VM. 2001. A hydrophobic stretch of 12 amino acid residues in the middle of alpha-synuclein is essential for filament assembly. J Biol Chem 276:2380–2386.

Gilman S, Koeppe RA, Junck L, Kluin KJ, Lohman M, St Laurent RT. 1994. Patterns of cerebral glucose metabolism detected with positron emission tomography differ in multiple system atrophy and olivopontocerebellar atrophy. Ann Neurol 36:166–175.

Gilman S, Wenning GK, Low PA, Brooks DJ, Mathias CJ, Trojanowski JQ, Wood NW, Colosimo C, Dürr A, Fowler CJ, Kaufmann H, Klockgether T, Lees A, Poewe W, Quinn N, Revesz T, Robertson D, Sandroni P, Seppi K, Vidailhet M. 2008. Second consensus statement on the diagnosis of multiple system atrophy. Neurology 71:670 –676.

Giuditta A, Chun JT, Eyman M, Cefaliello C, Bruno AP, Crispino M. 2008. Local Gene Expression in Axons and Nerve Endings: The Glia-Neuron Unit. Physiol Rev 88:515–555.

Goedert M. 2001. Alpha-synuclein and neurodegenerative diseases. Nat Rev Neurosci 2:492–501.

Goers J, Manning-Bog AB, McCormack AL, Millett IS, Doniach S, Di Monte DA, Uversky VN, Fink AL. 2003. Nuclear localization of alpha-synuclein and its interaction with histones. Biochemistry 42:8465–8471.

Gouras G, Tampellini D, Takahashi R, Capetillo-Zarate E. 2010. Intraneuronal beta-amyloid accumulation and synapse pathology in Alzheimer's disease. Acta Neuropathol 119:523–541.

Graham JG, Oppenheimer DR. 1969. Orthostatic hypotension and nicotine sensitivity in a case of multiple system atrophy. J Neurol Neurosurg Psychiatry 32:28 –34.

Greenfield J. 2008. Greenfield's neuropathology. 8th ed. London: Hodder Arnold.

Guo JL, Covell DJ, Daniels JP, Iba M, Stieber A, Zhang B, Riddle DM, Kwong LK, Xu Y, Trojanowski JQ, Lee VMY. 2013. Distinct α-Synuclein Strains Differentially Promote Tau Inclusions in Neurons. Cell 154:103–117.

Hansen C, Angot E, Bergström A-L, Steiner JA, Pieri L, Paul G, Outeiro TF, Melki R, Kallunki P, Fog K, Li J-Y, Brundin P. 2011. α-Synuclein propagates from mouse brain to grafted dopaminergic neurons and seeds aggregation in cultured human cells. J Clin Invest 121:715–725.

Hara K, Momose Y, Tokiguchi S, Shimohata M, Terajima K, Onodera O, Kakita A, Yamada M, Takahashi H, Hirasawa M, Mizuno Y, Ogata K, Goto J, Kanazawa I, Nishizawa M, Tsuji S. 2007. Multiplex families with multiple system atrophy. Arch Neurol 64:545–551.

Harte RA, Farrell CM, Loveland JE, Suner M-M, Wilming L, Aken B, Barrell D, Frankish A, Wallin C, Searle S, Diekhans M, Harrow J, Pruitt KD. 2012. Tracking and coordinating an international curation effort for the CCDS Project. Database (Oxford) 2012:bas008.

Hasegawa M, Houdou S, Mito T, Takashima S, Asanuma K, Ohno T. 1992. Development of myelination in the human fetal and infant cerebrum: A myelin basic protein immunohistochemical study. Brain and Development 14:1–6.

Hawrylycz MJ, Lein ES, Guillozet-Bongaarts AL, Shen EH, Ng L, Miller JA, van de Lagemaat LN, Smith KA, Ebbert A, Riley ZL, Abajian C, Beckmann CF, Bernard A, Bertagnolli D, Boe AF, Cartagena PM, Chakravarty MM, Chapin M, Chong J, Dalley RA, Daly BD, Dang C, Datta S, Dee N, Dolbeare TA, Faber V, Feng D, Fowler DR, Goldy J, Gregor BW, Haradon Z, Haynor DR, Hohmann JG, Horvath S, Howard RE, Jeromin A, Jochim JM, Kinnunen M, Lau C, Lazarz ET, Lee C, Lemon TA, Li L, Li Y, Morris JA, Overly CC, Parker PD, Parry SE, Reding M, Royall JJ, Schulkin J, Sequeira PA, Slaughterbeck CR, Smith SC, Sodt AJ, Sunkin SM, Swanson BE, Vawter MP, Williams D, Wohnoutka P, Zielke HR, Geschwind DH, Hof PR, Smith SM, Koch C, Grant SGN, Jones AR. 2012. An anatomically comprehensive atlas of the adult human brain transcriptome. Nature 489:391–399.

Hirano S, Shinotoh H, Eidelberg D. 2012. Functional brain imaging of cognitive dysfunction in Parkinson's disease. J Neurol Neurosurg Psychiatry 83:963–969.

Huang Y, Garrick R, Cook R, O'Sullivan D, Morris J, Halliday GM. 2005. Pallidal stimulation reduces treatment-induced dyskinesias in "minimal-change" multiple system atrophy. Mov Disord 20:1042–1047.

Inoue M, Yagishita S, Ryo M, Hasegawa K, Amano N, Matsushita M. 1997. The distribution and dynamic density of oligodendroglial cytoplasmic inclusions (GCIs) in multiple system atrophy: a correlation between the density of GCIs and the degree of involvement of striatonigral and olivopontocerebellar systems. Acta Neuropathol 93:585–591.

Isozaki E, Naito A, Horiguchi S, Kawamura R, Hayashida T, Tanabe H. 1996. Early diagnosis and stage classification of vocal cord abductor paralysis in patients with multiple system atrophy. J Neurol Neurosurg Psychiatry 60:399–402.

Iwai A, Masliah E, Yoshimoto M, Ge N, Flanagan L, de Silva HA, Kittel A, Saitoh T. 1995. The precursor protein of non-A beta component of Alzheimer's disease amyloid is a presynaptic protein of the central nervous system. Neuron 14:467–475.

Jakovcevski I, Filipovic R, Mo Z, Rakic S, Zecevic N. 2009. Oligodendrocyte Development and the Onset of Myelination in the Human Fetal Brain. Front Neuroanat 3:5.

Jao CC, Der-Sarkissian A, Chen J, Langen R. 2004. Structure of membrane-bound alpha-synuclein studied by site-directed spin labeling. Proc Natl Acad Sci USA 101:8331–8336.

Jellinger KA, Lantos PL. 2010. Papp–Lantos inclusions and the pathogenesis of multiple system atrophy: an update. Acta Neuropathol 119:657–667.

Jellinger KA, Seppi K, Wenning GK. 2005. Grading of neuropathology in multiple system atrophy: proposal for a novel scale. Mov Disord 20 Suppl 12:S29–36.

Jin H, Ishikawa K, Tsunemi T, Ishiguro T, Amino T, Mizusawa H. 2008. Analyses of copy number and mRNA expression level of the alpha-synuclein gene in multiple system atrophy. J Med Dent Sci 55:145–153.

Jo E, McLaurin J, Yip CM, St. George-Hyslop P, Fraser PE. 2000. α-Synuclein Membrane Interactions and Lipid Specificity. J Biol Chem 275:34328 – 34334.

Kahle PJ, Neumann M, Ozmen L, Haass C. 2000. Physiology and pathophysiology of alpha-synuclein. Cell culture and transgenic animal models based on a Parkinson's disease-associated protein. Ann N Y Acad Sci 920:33–41.

Kane MD, Lipinski WJ, Callahan MJ, Bian F, Durham RA, Schwarz RD, Roher AE, Walker LC. 2000. Evidence for seeding of beta-amyloid by intracerebral infusion of Alzheimer brain extracts in beta-amyloid precursor protein-transgenic mice. J Neurosci 20:3606–3611.

Kao AW, Racine CA, Quitania LC, Kramer JH, Christine CW, Miller BL. 2009. Cognitive and neuropsychiatric profile of the synucleinopathies: Parkinson disease, dementia with Lewy bodies, and multiple system atrophy. Alzheimer Dis Assoc Disord 23:365–370.

Kato S, Oda M, Hayashi H, Shimizu T, Hayashi M, Kawata A, Tanabe H. 1995. Decrease of medullary catecholaminergic neurons in multiple system atrophy and Parkinson's disease and their preservation in amyotrophic lateral sclerosis. J Neurol Sci 132:216–221.

Kawai Y, Suenaga M, Takeda A, Ito M, Watanabe H, Tanaka F, Kato K, Fukatsu H, Naganawa S, Kato T, Ito K, Sobue G. 2008. Cognitive impairments in multiple system atrophy. Neurology 70:1390 –1396.

Kawamoto Y, Akiguchi I, Nakamura S, Budka H. 2002. Accumulation of 14-3-3 proteins in glial cytoplasmic inclusions in multiple system atrophy. Ann Neurol 52:722–731.

Kawamoto Y, Akiguchi I, Shirakashi Y, Honjo Y, Tomimoto H, Takahashi R, Budka H. 2007. Accumulation of Hsc70 and Hsp70 in glial cytoplasmic inclusions in patients with multiple system atrophy. Brain Res 1136:219–227.

Kiely AP, Asi YT, Kara E, Limousin P, Ling H, Lewis P, Proukakis C, Quinn N, Lees AJ, Hardy J, Revesz T, Houlden H, Holton JL. 2013. α-Synucleinopathy associated with G51D SNCA mutation: a link between Parkinson's disease and multiple system atrophy? Acta Neuropathol 125:753–769.

Kisos H, Pukaß K, Ben-Hur T, Richter-Landsberg C, Sharon R. 2012. Increased Neuronal α-Synuclein Pathology Associates with Its Accumulation in Oligodendrocytes in Mice Modeling α-Synucleinopathies. PLoS ONE 7:e46817.

Kitayama M, Wada-Isoe K, Irizawa Y, Nakashima K. 2009. Assessment of dementia in patients with multiple system atrophy. Eur J Neurol 16:589–594.

Kon T, Mori F, Tanji K, Miki Y, Wakabayashi K. 2013. An autopsy case of preclinical multiple system atrophy (MSA-C). Neuropathology 33:667–672.

Konagaya M, Sakai M, Matsuoka Y, Konagaya Y, Hashizume Y. 1999. Multiple system atrophy with remarkable frontal lobe atrophy. Acta Neuropathol 97:423–428.

Konno M, Hasegawa T, Baba T, Miura E, Sugeno N, Kikuchi A, Fiesel FC, Sasaki T, Aoki M, Itoyama Y, Takeda A. 2012. Suppression of dynamin GTPase decreases α-synuclein uptake by neuronal and oligodendroglial cells: a potent therapeutic target for synucleinopathy. Mol Neurodegener 7:38.

Kordower JH, Chu Y, Hauser RA, Freeman TB, Olanow CW. 2008. Lewy body-like pathology in long-term embryonic nigral transplants in Parkinson's disease. Nat Med 14:504–506.

Krishnan S, Mathuranath PS, Sarma S, Kishore A. 2006. Neuropsychological functions in progressive supranuclear palsy, multiple system atrophy and Parkinson's disease. Neurol India 54:268–272.

Krüger R, Kuhn W, Müller T, Woitalla D, Graeber M, Kösel S, Przuntek H, Epplen JT, Schöls L, Riess O. 1998. Ala30Pro mutation in the gene encoding alpha-synuclein in Parkinson's disease. Nat Genet 18:106–108.

Krüger R, Müller T, Riess O. 2000. Involvement of alpha-synuclein in Parkinson's disease and other neurodegenerative disorders. J Neural Transm 107:31–40.

Lange KW, Tucha O, Alders GL, Preier M, Csoti I, Merz B, Mark G, Herting B, Fornadi F, Reichmann H, Vieregge P, Reiners K, Becker G, Naumann M. 2003. Differentiation of parkinsonian syndromes according to differences in executive functions. J Neural Transm 110:983–995.

Langerveld AJ, Mihalko D, DeLong C, Walburn J, Ide CF. 2007. Gene expression changes in postmortem tissue from the rostral pons of multiple system atrophy patients. Mov Disord 22:766–777.

Lashley T, Holton JL, Gray E, Kirkham K, O'Sullivan SS, Hilbig A, Wood NW, Lees AJ, Revesz T. 2008. Cortical α-synuclein load is associated with amyloid-β plaque burden in a subset of Parkinson's disease patients. Acta Neuropathol 115:417–425.

De Laureto PP, Tosatto L, Frare E, Marin O, Uversky VN, Fontana A. 2006. Conformational properties of the SDS-bound state of alpha-synuclein probed by limited proteolysis: unexpected rigidity of the acidic C-terminal tail. Biochemistry 45:11523–11531.

Lee H, Suk J, Patrick C, Bae E, Cho J, Rho S, Hwang D, Masliah E, Lee S. 2010. Direct Transfer of alpha-Synuclein from Neuron to Astroglia Causes Inflammatory Responses in Synucleinopathies. J Biol Chem 285:9262–9272.

Lee H-J, Suk J-E, Bae E-J, Lee S-J. 2008a. Clearance and deposition of extracellular alpha-synuclein aggregates in microglia. Biochem Biophys Res Commun 372:423–428.

Lee PH, An Y-S, Yong SW, Yoon SN. 2008b. Cortical metabolic changes in the cerebellar variant of multiple system atrophy: a voxel-based FDG-PET study in 41 patients. Neuroimage 40:796–801.

Levine JM, Stincone F, Lee YS. 1993. Development and differentiation of glial precursor cells in the rat cerebellum. Glia 7:307–321.

Li J-Y, Englund E, Holton JL, Soulet D, Hagell P, Lees AJ, Lashley T, Quinn NP, Rehncrona S, Björklund A, Widner H, Revesz T, Lindvall O, Brundin P. 2008. Lewy bodies in grafted neurons in subjects with Parkinson's disease suggest host-to-graft disease propagation. Nat Med 14:501–503.

Lincoln SJ, Ross OA, Milkovic NM, Dickson DW, Rajput A, Robinson CA, Papapetropoulos S, Mash DC, Farrer MJ. 2007. Quantitative PCR-based screening of alpha-synuclein multiplication in multiple system atrophy. Parkinsonism Relat Disord 13:340–342.

Lopez MN, Charter RA, Mostafavi B, Nibut LP, Smith WE. 2005. Psychometric properties of the Folstein Mini-Mental State Examination. Assessment 12:137–144.

LoPresti P, Szuchet S, Papasozomenos SC, Zinkowski RP, Binder LI. 1995. Functional implications for the microtubule-associated protein tau: localization in oligodendrocytes. Proc Natl Acad Sci U S A 92:10369–10373.

Lowe R, Pountney DL, Jensen PH, Gai WP, Voelcker NH. 2004. Calcium(II) selectively induces α-synuclein annular oligomers via interaction with the C-terminal domain. Protein Sci 13:3245–3252.

Ltic S, Perovic M, Mladenovic A, Raicevic N, Ruzdijic S, Rakic L, Kanazir S. 2004. Alpha-synuclein is expressed in different tissues during human fetal development. J Mol Neurosci 22:199–204.

Lu J-Q, Fan Y, Mitha AP, Bell R, Metz L, Moore GRW, Yong VW. 2009. Association of alpha-synuclein immunoreactivity with inflammatory activity in multiple sclerosis lesions. J Neuropathol Exp Neurol 68:179–189.

Luk KC, Kehm V, Carroll J, Zhang B, O'Brien P, Trojanowski JQ, Lee VM-Y. 2012a. Pathological α-synuclein transmission initiates Parkinson-like neurodegeneration in nontransgenic mice. Science 338:949–953.

Luk KC, Kehm VM, Zhang B, O'Brien P, Trojanowski JQ, Lee VMY. 2012b. Intracerebral inoculation of pathological α-synuclein initiates a rapidly

progressive neurodegenerative α-synucleinopathy in mice. J Exp Med 209:975–986.

Mackenzie IRA, Neumann M, Baborie A, Sampathu DM, Du Plessis D, Jaros E, Perry RH, Trojanowski JQ, Mann DMA, Lee VMY. 2011. A harmonized classification system for FTLD-TDP pathology. Acta Neuropathol 122:111–113.

Mackenzie IRA, Neumann M, Bigio EH, Cairns NJ, Alafuzoff I, Kril J, Kovacs GG, Ghetti B, Halliday G, Holm IE, Ince PG, Kamphorst W, Revesz T, Rozemuller AJM, Kumar-Singh S, Akiyama H, Baborie A, Spina S, Dickson DW, Trojanowski JQ, Mann DMA. 2010. Nomenclature and nosology for neuropathologic subtypes of frontotemporal lobar degeneration: an update. Acta Neuropathol 119:1–4.

Makioka K, Yamazaki T, Fujita Y, Takatama M, Nakazato Y, Okamoto K. 2010. Involvement of endoplasmic reticulum stress defined by activated unfolded protein response in multiple system atrophy. J Neurol Sci 297:60–65.

Mallon BS, Shick HE, Kidd GJ, Macklin WB. 2002. Proteolipid promoter activity distinguishes two populations of NG2-positive cells throughout neonatal cortical development. J Neurosci 22:876–885.

Masliah E, Rockenstein E, Veinbergs I, Sagara Y, Mallory M, Hashimoto M, Mucke L. 2001. β-Amyloid peptides enhance α-synuclein accumulation and neuronal deficits in a transgenic mouse model linking Alzheimer's disease and Parkinson's disease. Proc Natl Acad Sci USA 98:12245–12250.

Masuda-Suzukake M, Nonaka T, Hosokawa M, Oikawa T, Arai T, Akiyama H, Mann DMA, Hasegawa M. 2013. Prion-like spreading of pathological α-synuclein in brain. Brain 136:1128–1138.

Masui K, Nakata Y, Fujii N, Iwaki T. 2011. Extensive distribution of glial cytoplasmic inclusions in an autopsied case of multiple system atrophy with a prolonged 18-year clinical course. Neuropathology: Official Journal of the Japanese Society of Neuropathology 32:69–76.

Meco G, Gasparini M, Doricchi F. 1996. Attentional functions in multiple system atrophy and Parkinson's disease. J Neurol Neurosurg Psychiatr 60:393–398.

Miake H, Mizusawa H, Iwatsubo T, Hasegawa M. 2002. Biochemical characterization of the core structure of alpha-synuclein filaments. J Biol Chem 277:19213–19219.

Michell AW, Barker RA, Raha SK, Raha-Chowdhury R. 2005. A case of late onset sporadic Parkinson's disease with an A53T mutation in alpha-synuclein. J Neurol Neurosurg Psychiatr 76:596–597.

Miller DW, Johnson JM, Solano SM, Hollingsworth ZR, Standaert DG, Young AB. 2005. Absence of α-synuclein mRNA expression in normal and multiple system atrophy oligodendroglia. J Neural Transm 112:1613–1624.

Mirra SS, Heyman A, McKeel D, Sumi SM, Crain BJ, Brownlee LM, Vogel FS, Hughes JP, Belle G van, Berg L, participating CERAD neuropathologists. 1991. The Consortium to Establish a Registry for Alzheimer's Disease (CERAD). Neurology 41:479.

Mitchell AJ. 2009. A meta-analysis of the accuracy of the mini-mental state examination in the detection of dementia and mild cognitive impairment. J Psychiatr Res 43:411–431.

Mori F, Tanji K, Yoshimoto M, Takahashi H, Wakabayashi K. 2002. Demonstration of [alpha]-Synuclein Immunoreactivity in Neuronal and Glial Cytoplasm in Normal Human Brain Tissue Using Proteinase K and Formic Acid Pretreatment. Exp Neurol 176:98–104.

Mori F, Tanji K, Yoshimoto M, Takahashi H, Wakabayashi K. 2003. Widespread expression of alpha-synuclein in neuronal cytoplasm and glial cells in the central and peripheral nervous systems in human. In: Satoh K, Suzuki S, Matsunaga M, editors. Advances in Brain Research: Cerebrovascular Disorders and Neurodegeneration. Vol. 1251. Amsterdam: Elsevier Science Bv. p 165–171.

Morrow M, Donaldson J. 2011. Nanostring's nCounter--A True Digital Target Profiling Technology. PDA J Pharm Sci Technol 65:692.

Müller R, Heinrich M, Heck S, Blohm D, Richter-Landsberg C. 1997. Expression of microtubule-associated proteins MAP2 and tau in cultured rat brain oligodendrocytes. Cell Tissue Res 288:239–249.

Multiple-System Atrophy Research Collaboration. 2013. Mutations in COQ2 in familial and sporadic multiple-system atrophy. N Engl J Med 369:233–244.

Munschauer FE, Loh L, Bannister R, Newsom-Davis J. 1990. Abnormal respiration and sudden death during sleep in multiple system atrophy with autonomic failure. Neurology 40:677–679.

Muntane G, Dalfo E, Martinez A, Ferrer I. 2008. Phosphorylation of tau and alpha-synuclein in synaptic-enriched fractions of the frontal cortex in Alzheimer's disease, and in Parkinson's disease and related alpha-synucleinopathies. Neurosci 152:913–923.

Nakamura S, Kawamoto Y, Nakano S, Akiguchi I. 2000. Expression of the endocytosis regulatory proteins Rab5 and Rabaptin-5 in glial cytoplasmic inclusions from brains with multiple system atrophy. Clin Neuropathol 19:51–56.

Nave K-A. 2010. Myelination and the trophic support of long axons. Nat Rev Neurosci 11:275–283.

Nielsen JA, Maric D, Lau P, Barker JL, Hudson LD. 2006. Identification of a Novel Oligodendrocyte Cell Adhesion Protein Using Gene Expression Profiling. J Neurosci 26:9881–9891.

Nielsen MS, Vorum H, Lindersson E, Jensen PH. 2001. Ca2+ Binding to A-Synuclein Regulates Ligand Binding and Oligomerization. J Biol Chem 276:22680–22684.

Nieuwenhuis-Mark RE. 2010. The Death Knoll for the MMSE: Has It Outlived Its Purpose? J Geriatr Psychiatry Neurol 23:151–157.

Nishie M, Mori F, Yoshimoto M, Takahashi H, Wakabayashi K. 2004. A quantitative investigation of neuronal cytoplasmic and intranuclear inclusions in the pontine and inferior olivary nuclei in multiple system atrophy. Neuropathol Appl Neurobiol 30:546–554.

Nishiyama A, Komitova M, Suzuki R, Zhu X. 2009. Polydendrocytes (NG2 cells): multifunctional cells with lineage plasticity. Nat Rev Neurosci 10:9–22.

Northcott PA, Shih DJH, Remke M, Cho Y-J, Kool M, Hawkins C, Eberhart CG, Dubuc A, Guettouche T, Cardentey Y, Bouffet E, Pomeroy SL, Marra M, Malkin D, Rutka JT, Korshunov A, Pfister S, Taylor MD. 2012. Rapid, reliable, and reproducible molecular sub-grouping of clinical medulloblastoma samples. Acta Neuropathol 123:615–626.

O'Sullivan SS, Massey LA, Williams DR, Silveira-Moriyama L, Kempster PA, Holton JL, Revesz T, Lees AJ. 2008. Clinical outcomes of progressive supranuclear palsy and multiple system atrophy. Brain 131:1362 –1372.

Olah M, Raj D, Brouwer N, De Haas AH, Eggen BJL, Den Dunnen WFA, Biber KPH, Boddeke HWGM. 2012. An optimized protocol for the acute isolation of human microglia from autopsy brain samples. Glia 60:96–111.

Otsuka M, Ichiya Y, Kuwabara Y, Hosokawa S, Sasaki M, Yoshida T, Fukumura T, Kato M, Masuda K. 1996. Glucose metabolism in the cortical and subcortical brain structures in multiple system atrophy and Parkinson's disease: a positron emission tomographic study. J Neurol Sci 144:77–83.

Ozawa T, Okuizumi K, Ikeuchi T, Wakabayashi K, Takahashi H, Tsuji S. 2001. Analysis of the expression level of alpha-synuclein mRNA using

postmortem brain samples from pathologically confirmed cases of multiple system atrophy. Acta Neuropathol 102:188–190.

Ozawa T, Paviour D, Quinn NP, Josephs KA, Sangha H, Kilford L, Healy DG, Wood NW, Lees AJ, Holton JL, Revesz T. 2004. The spectrum of pathological involvement of the striatonigral and olivopontocerebellar systems in multiple system atrophy: clinicopathological correlations. Brain 127:2657 –2671.

Ozawa T, Takano H, Onodera O, Kobayashi H, Ikeuchi T, Koide R, Okuizumi K, Shimohata T, Wakabayashi K, Takahashi H, Tsuji S. 1999. No mutation in the entire coding region of the α-synuclein gene in pathologically confirmed cases of multiple system atrophy. Neurosci Lett 270:110–112.

Papadopoulos D, Ewans L, Pham-Dinh D, Knott J, Reynolds R. 2006. Upregulation of alpha-synuclein in neurons and glia in inflammatory demyelinating disease. Mol Cell Neurosci 31:597–612.

Papapetropoulos S, Tuchman A, Laufer D, Papatsoris AG, Papapetropoulos N, Mash DC. 2007. Causes of death in multiple system atrophy. J Neurol Neurosurg Psychiatry 78:327–329.

Papp MI, Kahn JE, Lantos PL. 1989. Glial cytoplasmic inclusions in the CNS of patients with multiple system atrophy (striatonigral degeneration, olivopontocerebellar atrophy and Shy-Drager syndrome). J Neurol Sci 94:79–100.

Papp MI, Lantos PL. 1994. The distribution of oligodendroglial inclusions in multiple system atrophy and its relevance to clinical symptomatology. Brain 117 (Pt 2):235–243.

Park J, Koito H, Li J, Han A. 2009. Microfluidic compartmentalized co-culture platform for CNS axon myelination research. Biomed Microdevices 11:1145–1153.

Parkkinen L, Hartikainen P, Alafuzoff I. 2007. Abundant glial alpha-synuclein pathology in a case without overt clinical symptoms. Clin Neuropathol 26:276–283.

Perry RH, Perry EK, Smith CJ, Xuereb JH, Irving D, Whitford CA, Candy JM, Cross AJ. 1987. Cortical neuropathological and neurochemical substrates of Alzheimer's and Parkinson's diseases. J Neural Transm Suppl 24:131–136.

Petrovic IN, Ling H, Asi Y, Ahmed Z, Kukkle PL, Hazrati L-N, Lang AE, Revesz T, Holton JL, Lees AJ. 2012. Multiple system atrophy-parkinsonism with slow progression and prolonged survival: a diagnostic catch. Mov Disord 27:1186–1190.

Pettersen EF, Goddard TD, Huang CC, Couch GS, Greenblatt DM, Meng EC, Ferrin TE. 2004. UCSF Chimera--a visualization system for exploratory research and analysis. J Comput Chem 25:1605–1612.

Pfeiffer SE, Warrington AE, Bansal R. 1993. The oligodendrocyte and its many cellular processes. Trends Cell Biol 3:191–197.

Piao YS, Hayashi S, Hasegawa M, Wakabayashi K, Yamada M, Yoshimoto M, Ishikawa A, Iwatsubo T, Takahashi H. 2001. Co-localization of alpha-synuclein and phosphorylated tau in neuronal and glial cytoplasmic inclusions in a patient with multiple system atrophy of long duration. Acta Neuropathol 101:285–293.

Polymeropoulos MH, Higgins JJ, Golbe LI, Johnson WG, Ide SE, Di Iorio G, Sanges G, Stenroos ES, Pho LT, Schaffer AA, Lazzarini AM, Nussbaum RL, Duvoisin RC. 1996. Mapping of a gene for Parkinson's disease to chromosome 4q21-q23. Science 274:1197–1199.

Pountney DL, Dickson TC, Power JHT, Vickers JC, West AJ, Gai WP. 2011. Association of Metallothionein-III with Oligodendroglial Cytoplasmic Inclusions in Multiple System Atrophy. Neurotox Res 19:115–122.

Prasad K, Tarasewicz E, Strickland PAO, O'Neill M, Mitchell SN, Merchant K, Tep S, Hilton K, Datwani A, Buttini M, Mueller-Steiner S, Richfield EK. 2011. Biochemical and morphological consequences of human α-synuclein expression in a mouse α-synuclein null background. Eur J Neurosci 33:642–656.

Pruitt KD, Harrow J, Harte RA, Wallin C, Diekhans M, Maglott DR, Searle S, Farrell CM, Loveland JE, Ruef BJ, Hart E, Suner M-M, Landrum MJ, Aken B, Ayling S, Baertsch R, Fernandez-Banet J, Cherry JL, Curwen V, Dicuccio M, Kellis M, Lee J, Lin MF, Schuster M, Shkeda A, Amid C, Brown G, Dukhanina O, Frankish A, Hart J, Maidak BL, Mudge J, Murphy MR, Murphy T, Rajan J, Rajput B, Riddick LD, Snow C, Steward C, Webb D, Weber JA, Wilming L, Wu W, Birney E, Haussler D, Hubbard T, Ostell J, Durbin R, Lipman D. 2009. The consensus coding sequence (CCDS) project: Identifying a common protein-coding gene set for the human and mouse genomes. Genome Res 19:1316–1323.

Quinn N. 1989. Multiple system atrophy--the nature of the beast. J Neurol Neurosurg Psychiatr Suppl:78–89.

Ransom BR, Sontheimer H. 1992. The neurophysiology of glial cells. J Clin Neurophysiol 9:224–251.

Reynolds NP, Soragni A, Rabe M, Verdes D, Liverani E, Handschin S, Riek R, Seeger S. 2011. Mechanism of membrane interaction and disruption by α-synuclein. J Am Chem Soc 133:19366–19375.

Richter-Landsberg C, Gorath M, Trojanowski JQ, Lee VM. 2000. alpha-synuclein is developmentally expressed in cultured rat brain oligodendrocytes. J Neurosci Res 62:9–14.

Richter-Landsberg C. 2000. The oligodendroglia cytoskeleton in health and disease. J Neurosci Res 59:11–18.

Riedel M, Goldbaum O, Richter-Landsberg C. 2009. alpha-Synuclein promotes the recruitment of tau to protein inclusions in oligodendroglial cells: effects of oxidative and proteolytic stress. J Mol Neurosci 39:226–234.

Ririe KM, Rasmussen RP, Wittwer CT. 1997. Product differentiation by analysis of DNA melting curves during the polymerase chain reaction. Anal Biochem 245:154–160.

Robbins TW, James M, Lange KW, Owen AM, Quinn NP, Marsden CD. 1992. Cognitive performance in multiple system atrophy. Brain 115 Pt 1:271–291.

Robbins TW, James M, Owen AM, Lange KW, Lees AJ, Leigh PN, Marsden CD, Quinn NP, Summers BA. 1994. Cognitive deficits in progressive supranuclear palsy, Parkinson's disease, and multiple system atrophy in tests sensitive to frontal lobe dysfunction. J Neurol Neurosurg Psychiatr 57:79–88.

Rodriguez-Diehl R, Rey MJ, Gironell A, Martinez-Saez E, Ferrer I, Sánchez-Valle R, Jagüe J, Nos C, Gelpi E. 2012. "Preclinical" MSA in definite Creutzfeldt-Jakob disease. Neuropathology 32:158–163.

Ross OA, Braithwaite AT, Skipper LM, Kachergus J, Hulihan MM, Middleton FA, Nishioka K, Fuchs J, Gasser T, Maraganore DM, Adler CH, Larvor L, Chartier-Harlin M-C, Nilsson C, Langston JW, Gwinn K, Hattori N, Farrer MJ. 2008. Genomic investigation of alpha-synuclein multiplication and parkinsonism. Ann Neurol 63:743–750.

Ross OA, Vilariño-Güell C, Wszolek ZK, Farrer MJ, Dickson DW. 2010. Reply to: SNCA variants are associated with increased risk of multiple system atrophy. Ann Neurol 67:414–415.

Rowitch DH, Lu QR, Kessaris N, Richardson WD. 2002. An "oligarchy" rules neural development. Trends Neurosci 25:417–422.

Sadaoka T, Kakitsuba N, Fujiwara Y, Kanai R, Takahashi H. 1996. Sleep-related breathing disorders in patients with multiple system atrophy and vocal fold palsy. Sleep 19:479–484.

Scholz P, Bauer NG, Thiel G, Richter-Landsberg C. 2007. Transient overexpression of alpha-Synuclein in OLN-93 oligodendroglial cells is not cytotoxic and not affected by HSP70. BMC Neurosci 8:P11.

Scholz SW, Houlden H, Schulte C, Sharma M, Li A, Berg D, Melchers A, Paudel R, Gibbs JR, Simon-Sanchez J, Paisan-Ruiz C, Bras J, Ding J, Chen H, Traynor BJ, Arepalli S, Zonozi RR, Revesz T, Holton J, Wood N, Lees A, Oertel W, Wüllner U, Goldwurm S, Pellecchia MT, Illig T, Riess O, Fernandez HH, Rodriguez RL, Okun MS, Poewe W, Wenning GK, Hardy JA, Singleton AB, Del Sorbo F, Schneider S, Bhatia KP, Gasser T. 2009. SNCA variants are associated with increased risk for multiple system atrophy. Ann Neurol 65:610–614.

Schrag A, Wenning GK, Quinn N, Ben-Shlomo Y. 2008. Survival in multiple system atrophy. Mov Disord 23:294–296.

Schulz-Schaeffer WJ. 2010. The synaptic pathology of alpha-synuclein aggregation in dementia with Lewy bodies, Parkinson's disease and Parkinson's disease dementia. Acta Neuropathol 120:131–143.

Schwartz PH, Bryant PJ, Fuja TJ, Su H, O'Dowd DK, Klassen H. 2003. Isolation and characterization of neural progenitor cells from post-mortem human cortex. J Neurosci Res 74:838–851.

Schwarz L, Goldbaum O, Bergmann M, Probst-Cousin S, Richter-Landsberg C. 2012. Involvement of Macroautophagy in Multiple System Atrophy and Protein Aggregate Formation in Oligodendrocytes. J Mol Neurosci 47:256–266.

Scott D, Tabarean I, Tang Y, Cartier A, Masliah E, Roy S. 2010. A Pathologic Cascade Leading to Synaptic Dysfunction in alpha-Synuclein-Induced Neurodegeneration. J Neurosci 30:8083–8095.

Shibuya K, Nagatomo H, Iwabuchi K, Inoue M, Yagishita S, Itoh Y. 2000. Asymmetrical temporal lobe atrophy with massive neuronal inclusions in multiple system atrophy. J Neurol Sci 179:50–58.

Shimohata T, Ozawa T, Nakayama H, Tomita M, Shinoda H, Nishizawa M. 2008. Frequency of nocturnal sudden death in patients with multiple system atrophy. J Neurol 255:1483–1485.

Ben-Shlomo Y, Wenning GK, Tison F, Quinn NP. 1997. Survival of patients with pathologically proven multiple system atrophy. Neurology 48:384 – 393.

Silber MH, Levine S. 2000. Stridor and death in multiple system atrophy. Mov Disord 15:699–704.

Silva BA, Breydo L, Uversky VN. 2013. Targeting the Chameleon: a Focused Look at α-Synuclein and Its Roles in Neurodegeneration. Mol Neurobiol 47:446–459.

Siri C, Duerr S, Canesi M, Delazer M, Esselink R, Bloem BR, Gurevich T, Balas M, Giladi N, Santacruz P, Marti F, Tolosa E, Rubino A, Meco G, Poewe W, Pezzoli G, Wenning G, Antonini A. 2013. A cross-sectional multicenter study of cognitive and behavioural features in multiple system atrophy patients of the parkinsonian and cerebellar type. J Neural Transm 120:613–618.

Solano SM, Miller DW, Augood SJ, Young AB, Penney JB. 2000. Expression of alpha-synuclein, parkin, and ubiquitin carboxy-terminal hydrolase L1 mRNA in human brain: genes associated with familial Parkinson's disease. Ann Neurol 47:201–210.

Soliveri P, Monza D, Paridi D, Carella F, Genitrini S, Testa D, Girotti F. 2000. Neuropsychological follow up in patients with Parkinson's disease, striatonigral degeneration-type multisystem atrophy, and progressive supranuclear palsy. J Neurol Neurosurg Psychiatr 69:313–318.

Soma H, Yabe I, Takei A, Fujiki N, Yanagihara T, Sasaki H. 2006. Heredity in multiple system atrophy. J Neurol Sci 240:107–110.

Specht CG, Schoepfer R. 2001. Deletion of the alpha-synuclein locus in a subpopulation of C57BL/6J inbred mice. BMC Neurosci 2:11.

Spillantini MG, Divane A, Goedert M. 1995. Assignment of Human α-Synuclein (SNCA) and β-Synuclein (SNCB) Genes to Chromosomes 4q21 and 5q35. Genomics 27:379–381.

Van Spronsen M, Hoogenraad C. 2010. Synapse Pathology in Psychiatric and Neurologic Disease. Curr Neurol Neurosci Rep 10:207–214.

Stefanova N, Bücke P, Duerr S, Wenning GK. 2009. Multiple system atrophy: an update. The Lancet Neurology 8:1172–1178.

Stefanova N, Klimaschewski L, Poewe W, Wenning GK, Reindl M. 2001. Glial cell death induced by overexpression of alpha-synuclein. J Neurosci Res 65:432–438.

Stefanova N, Reindl M, Neumann M, Haass C, Poewe W, Kahle PJ, Wenning GK. 2005a. Oxidative stress in transgenic mice with oligodendroglial alpha-synuclein overexpression replicates the characteristic neuropathology of multiple system atrophy. Am J Pathol 166:869–876.

Stefanova N, Reindl M, Poewe W, Wenning GK. 2005b. In vitro models of multiple system atrophy. Mov Disord 20:S53–S56.

Steiner JA, Angot E, Brundin P. 2011. A deadly spread: cellular mechanisms of [alpha]-synuclein transfer. Cell Death Differ 18:1425–1433.

Tada M, Kakita A, Toyoshima Y, Onodera O, Ozawa T, Morita T, Nishizawa M, Takahashi H. 2009. Depletion of medullary serotonergic neurons in patients with multiple system atrophy who succumbed to sudden death. Brain 132:1810–1819.

Tamo W, Imaizumi T, Tanji K, Yoshida H, Mori F, Yoshimoto M, Takahashi H, Fukuda I, Wakabayashi K, Satoh K. 2002. Expression of α-synuclein, the precursor of non-amyloid β component of Alzheimer's disease amyloid, in human cerebral blood vessels. Neurosci Lett 326:5–8.

Tanikawa S, Mori F, Tanji K, Kakita A, Takahashi H, Wakabayashi K. 2012. Endosomal sorting related protein CHMP2B is localized in Lewy bodies and glial cytoplasmic inclusions in alpha-synucleinopathy. Neurosci Lett 527:16–21.

Tanji K, Imaizumi T, Yoshida H, Mori F, Yoshimoto M, Satoh K, Wakabayashi K. 2001. Expression of α-synuclein in a human glioma cell line and its up-regulation by interleukin-1β. NeuroReport 12:1909–1912.

Tanji K, Odagiri S, Maruyama A, Mori F, Kakita A, Takahashi H, Wakabayashi K. 2013. Alteration of autophagosomal proteins in the brain of multiple system atrophy. Neurobiol Dis 49:190–198.

Taylor AM, Blurton-Jones M, Rhee SW, Cribbs DH, Cotman CW, Jeon NL. 2005. A microfluidic culture platform for CNS axonal injury, regeneration and transport. Nat Meth 2:599–605.

Testa D, Fetoni V, Soliveri P, Musicco M, Palazzini E, Girotti F. 1993. Cognitive and motor performance in multiple system atrophy and Parkinson's disease compared. Neuropsychologia 31:207–210.

Tong J, Wong H, Guttman M, Ang LC, Forno LS, Shimadzu M, Rajput AH, Muenter MD, Kish SJ, Hornykiewicz O, Furukawa Y. 2010. Brain alpha-synuclein accumulation in multiple system atrophy, Parkinson's disease and progressive supranuclear palsy: a comparative investigation. Brain 133:172–188.

Trabzuni D, Ryten M, Walker R, Smith C, Imran S, Ramasamy A, Weale ME, Hardy J. 2011. Quality control parameters on a large dataset of regionally dissected human control brains for whole genome expression studies. J Neurochem 119:275–282.

Tu PH, Galvin JE, Baba M, Giasson B, Tomita T, Leight S, Nakajo S, Iwatsubo T, Trojanowski JQ, Lee VM. 1998. Glial cytoplasmic inclusions in white matter oligodendrocytes of multiple system atrophy brains contain insoluble alpha-synuclein. Ann Neurol 44:415–422.

Ubhi K, Low P, Masliah E. 2011. Multiple system atrophy: a clinical and neuropathological perspective. Trends Neurosci 34:581–590.

Uéda K, Saitoh T, Mori H. 1994. Tissue-dependent alternative splicing of mRNA for NACP, the precursor of non-A beta component of Alzheimer's disease amyloid. Biochem Biophys Res Commun 205:1366–1372.

Uversky VN, Li J, Fink AL. 2001. Metal-triggered structural transformations, aggregation, and fibrillation of human α-synuclein a possible molecular link between parkinson's disease and heavy metal exposure. J Biol Chem 276:44284–44296.

Uversky VN. 2007. Neuropathology, biochemistry, and biophysics of alpha-synuclein aggregation. J Neurochem 103:17–37.

Vandesompele J, De Preter K, Pattyn F, Poppe B, Van Roy N, De Paepe A, Speleman F. 2002. Accurate normalization of real-time quantitative RT-PCR data by geometric averaging of multiple internal control genes. Genome Biol 3:RESEARCH0034.

De Volder AG, Francart J, Laterre C, Dooms G, Bol A, Michel C, Goffinet AM. 1989. Decreased glucose utilization in the striatum and frontal lobe in probable striatonigral degeneration. Ann Neurol 26:239–247.

Wakabayashi K, Ikeuchi T, Ishikawa A, Takahashi H. 1998. Multiple system atrophy with severe involvement of the motor cortical areas and cerebral white matter. J Neurol Sci 156:114–117.

Wakabayashi K, Mori F, Nishie M, Oyama Y, Kurihara A, Yoshimoto M, Kuroda N. 2005. An autopsy case of early ("minimal change") olivopontocerebellar atrophy (multiple system atrophy-cerebellar). Acta Neuropathol 110:185–190.

Wakabayashi K, Takahashi H. 2006. Cellular pathology in multiple system atrophy. Neuropathology 26:338–345.

Waller R, Woodroofe MN, Francese S, Heath PR, Wharton SB, Ince PG, Sharrack B, Simpson JE. 2012. Isolation of enriched glial populations from post-mortem human CNS material by immuno-laser capture microdissection. J Neurosci Methods 208:108–113.

Wang W, Perovic I, Chittuluru J, Kaganovich A, Nguyen LTT, Liao J, Auclair JR, Johnson D, Landeru A, Simorellis AK, Ju S, Cookson MR, Asturias FJ, Agar JN, Webb BN, Kang C, Ringe D, Petsko GA, Pochapsky TC, Hoang QQ. 2011. A soluble α-synuclein construct forms a dynamic tetramer. Proc Natl Acad Sci USA 108:17797–17802.

Wang Y, Lü C, Ye Z. 2002. Alpha-synuclein immunoreactivity and ultrastructural study of glial cytoplasmic inclusions in multiple system atrophy. Chin Med J 115:1491–1495.

Watanabe H, Saito Y, Terao S, Ando T, Kachi T, Mukai E, Aiba I, Abe Y, Tamakoshi A, Doyu M, Hirayama M, Sobue G. 2002. Progression and prognosis in multiple system atrophy: an analysis of 230 Japanese patients. Brain 125:1070–1083.

Weinreb PH, Zhen W, Poon AW, Conway KA, Lansbury PT Jr. 1996. NACP, a protein implicated in Alzheimer's disease and learning, is natively unfolded. Biochemistry 35:13709–13715.

Wenning GK, Quinn N, Magalhães M, Mathias C, Daniel SE. 1994a. "Minimal change" multiple system atrophy. Mov Disord 9:161–166.

Wenning GK, Seppi K, Tison F, Jellinger K. 2002. A novel grading scale for striatonigral degeneration (multiple system atrophy). J Neural Transm 109:307–320.

Wenning GK, Ben-Shlomo Y, Hughes A, Daniel SE, Lees A, Quinn NP. 2000. What clinical features are most useful to distinguish definite multiple system atrophy from Parkinson's disease? J Neurol Neurosurg Psychiatry 68:434 –440.

Wenning GK, Shlomo YB, Magalhães M, Danie SE, Quinn NP. 1994b. Clinical features and natural history of multiple system atrophy. Brain 117:835 – 845.

Wenning GK, Stefanova N, Jellinger KA, Poewe W, Schlossmacher MG. 2008. Multiple system atrophy: A primary oligodendrogliopathy. Ann Neurol 64:239–246.

Wenning GK, Tison F, Ben Shlomo Y, Daniel SE, Quinn NP. 1997. Multiple system atrophy: a review of 203 pathologically proven cases. Mov Disord 12:133–147.

Williams DR, Holton JL, Strand C, Pittman A, de Silva R, Lees AJ, Revesz T. 2007. Pathological tau burden and distribution distinguishes progressive supranuclear palsy-parkinsonism from Richardson's syndrome. Brain 130:1566 –1576.

Withers GS, George JM, Banker GA, Clayton DF. 1997. Delayed localization of synelfin (synuclein, NACP) to presynaptic terminals in cultured rat hippocampal neurons. Dev Brain Res 99:87–94.

Wullner U, Abele M, Schmitz-Huebsch T, Wilhelm K, Benecke R, Deuschl G, Klockgether T. 2004. Probable multiple system atrophy in a German family. J Neurol Neurosurg Psychiatry 75:924–925.

Yokoyama T, Kusunoki JI, Hasegawa K, Sakai H, Yagishita S. 2001. Distribution and dynamic process of neuronal cytoplasmic inclusion (NCI) in MSA:

correlation of the density of NCI and the degree of involvement of the pontine nuclei. Neuropathology 21:145–154.

Yoshida M. 2007. Multiple system atrophy: alpha-synuclein and neuronal degeneration. Neuropathology 27:484–493.

Zarranz JJ, Alegre J, Gómez-Esteban JC, Lezcano E, Ros R, Ampuero I, Vidal L, Hoenicka J, Rodriguez O, Atarés B, Llorens V, Gomez Tortosa E, del Ser T, Muñoz DG, de Yebenes JG. 2004. The new mutation, E46K, of alpha-synuclein causes Parkinson and Lewy body dementia. Ann Neurol 55:164–173.

Zhang SC. 2001. Defining glial cells during CNS development. Nat Rev Neurosci 2:840–843.

Zhou J, Broe M, Huang Y, Anderson JP, Gai W-P, Milward EA, Porritt M, Howells D, Hughes AJ, Wang X, Halliday GM. 2011. Changes in the solubility and phosphorylation of alpha-synuclein over the course of Parkinson's disease. Acta Neuropathol 121:695–704.

Zhu M, Li J, Fink AL. 2003. The association of alpha-synuclein with membranes affects bilayer structure, stability, and fibril formation. J Biol Chem 278:40186–40197.